

# A.S.T.R.O.COM.

Advanced Solar Tracking and Rover Observation Communication

12/05/2023

## Authors:

Alex Fiset	Pedro Kasprzykowski	Stephen Martin	Binh Pham
<i>Electrical Engineering</i>	<i>Computer Engineering</i>	<i>Computer Engineering</i>	<i>Computer Engineering</i>

## Sponsor:

Mike Conroy	<i>FSI</i>	<i>Engineering Support</i>
-------------	------------	----------------------------

## Reviewer Committee:

Dr. Mike Borowczak	<i>ECE</i>	<i>Associate Professor</i>
Dr. Mingjie Lin	<i>ECE</i>	<i>Associate Professor</i>
Dr. Saleem Sahawneh	<i>ECE</i>	<i>Lecturer</i>
Mike Conroy	<i>FSI</i>	<i>Engineering Support</i>

## Mentor:

Dr. Chung Yong Chan



# Table of Contents

List of Figures .....	iv
List of Tables .....	vi
List of Equations .....	vii
<b>Chapter 1 - Executive Summary .....</b>	1
<b>Chapter 2 - Project Description .....</b>	1
2.1 Project Background and Motivation .....	1
2.2 Current Commercial Technologies and Existing Projects.....	2
2.2.1 Heliostaat DIY Kit .....	2
2.2.2 FSI Rover and App .....	3
2.2.3 Summary .....	5
2.3 Objective and Goals.....	6
2.3.1 Hardware .....	6
2.3.1.1 Reflector – Basic Goal:.....	6
2.3.1.2 Wireless Charging/Docking Station – Stretch Goal: .....	7
2.3.2 Software .....	7
2.3.2.1 Basic Goals .....	7
2.3.2.2 Peer to Peer Networking – Stretch Goal:.....	8
2.4 Required Specifications .....	10
2.5 House of Quality.....	13
<b>Chapter 3 - Research .....</b>	14
3.1 Technologies .....	14
3.1.1 MCU.....	14
3.1.1.1 MCU vs FPGA.....	14
3.1.1.2 Why microcontrollers? .....	15
3.1.1.3 Raspberry Pi.....	16
3.1.1.4 Raspberry Pi Zero.....	16
3.1.1.5 Raspberry Pi Pico .....	16
3.1.1.6 Arduino MKR 1000.....	17
3.1.1.7 Arduino MKR WAN 1300 .....	17
3.1.1.8 ESP32 .....	17
3.1.1.9 CC13xx .....	18
3.1.1.10 CC26xx .....	18
3.1.2 Solar Panels .....	20
3.1.2.1 Monocrystalline.....	20
3.1.2.2 Polycrystalline.....	20
3.1.2.3 Thin Film .....	20
3.1.3 Voltage Regulation .....	21
3.1.3.1 Linear Regulators .....	22
3.1.3.2 Switching Regulators.....	22
3.1.4 Charge Controller.....	23
3.1.4.1 PWM .....	23
3.1.4.2 MPPT.....	23
3.1.5 Reflectors.....	24
3.1.5.1 Norway’s Mirror for Artificial Sunlight.....	24
3.1.5.2 James Webb’s Telescope’s Mirror .....	25

3.1.6 Vectoring and Positioning / Solar Tracking Algorithm.....	30
3.1.6.1 Heliostat's Algorithm.....	31
3.1.7 Motors .....	33
3.1.8 Motor Controllers.....	37
3.1.9 Sensor.....	39
3.1.9.1 Photodiodes.....	39
3.1.9.2 Phototransistors .....	40
3.1.9.3 Complementary Metal Oxide Semiconductor (CMOS) .....	41
3.1.9.4 Light-Emitting Diode (LED) .....	42
3.1.9.5 TSL2561 Ambient Light Sensor.....	43
3.1.9.6 BH1750 Ambient Light Sensor.....	44
3.1.9.7 MAX 44009 Ambient Light Sensor .....	45
3.1.9.8 TSL2572 Ambient Light Sensor.....	46
3.1.9.9 AP3216 Ambient Light Sensor:.....	46
3.1.9.10 VL6180X TOF Proximity sensor and Ambient Light Sensor: .....	47
3.1.9.11 APDS-9960 Ambient Light Sensor:.....	48
3.1.9.12 SI1145 Ambient Light Sensor: .....	48
3.1.9.13 VEML7700 Ambient Light Sensor.....	49
3.1.10 Communication technologies.....	51
3.1.10.1 ZigBee .....	51
3.1.10.2 Z-Wave .....	52
3.1.10.3 LoRaWAN .....	52
3.1.10.4 6LoWPAN.....	53
3.1.10.5 Bluetooth.....	53
3.1.10.6 Wi-Fi.....	54
3.1.11 Batteries .....	54
3.1.11.1 Lithium Batteries .....	55
3.1.11.2 Lead Acid .....	56
3.1.12 Development Environment: Languages and Repositories .....	57
3.1.12.1 C .....	57
3.1.12.2 Java.....	57
3.1.12.3 Python.....	57
3.1.12.4 GitHub .....	58
3.1.12.5 Bitbucket.....	58
3.1.13 Antenna .....	58
3.1.13.1 Dipole .....	59
3.1.13.2 Patch .....	60
3.1.13.3 Parabolic Reflector .....	60
3.1.13.4 Yagi-Uda .....	61
3.1.13.5 Helical.....	61
3.1.13.6 Horn.....	62
3.1.13.7 Antenna type selection.....	63
3.1.13.8 PC140.07.0100A .....	64
3.1.13.9 WPC.25.A.07.0150C .....	64
3.1.13.10 FXP74.07.0100A.....	64
3.1.13.11 PC17.07.0070A .....	65
3.1.13.12 FXP70.07.0053A.....	65

3.2 Part Selection.....	66
3.2.1 MCU.....	67
3.2.2 Solar Panels .....	67
3.2.3 Voltage Regulation .....	69
3.2.4 Charge Controller.....	70
3.2.5 Reflectors.....	71
3.2.6 Vectoring and Positioning / Solar Tracking Algorithm.....	72
3.2.7 Motors .....	72
3.2.8 Motor Controllers.....	72
3.2.9 Sensor.....	73
3.2.10 Communication technologies.....	73
3.2.11 Batteries.....	74
3.2.12 Development Environment: Languages and Repositories.....	75
3.2.13 Antenna .....	75
<b>Chapter 4 - Related Standards and Design Constraints .....</b>	<b>77</b>
4.1 Industrial Standards.....	77
4.1.1 PCB Design Standards.....	77
4.1.2 I2C Protocol Standards .....	78
4.1.3 ZigBee Protocol Standards .....	80
4.1.4 Motor Controls.....	81
4.2 Practical Constraints.....	84
4.2.1 Time.....	84
4.2.2 Economic.....	85
4.2.3 Environmental.....	86
4.2.4 Remaining Constraints .....	87
4.2.4.1 Sustainability.....	87
4.2.4.2 Political.....	87
4.2.4.3 Ethical.....	88
4.2.4.4 Health and Safety .....	88
4.2.4.5 Manufacturability .....	88
<b>Chapter 5 - ChatGPT .....</b>	<b>89</b>
<b>Chapter 6 - System Hardware Design.....</b>	<b>96</b>
6.1 Power Delivery/ Electrical Power System .....	96
6.2 Motor Controls .....	98
6.2.1 Stepper Motor Controls .....	98
6.2.2 Servo Motor Controls.....	100
6.3 Lower-Level Subsystem.....	102
6.4 Overall Schematic.....	103
<b>Chapter 7 - System Software Design.....</b>	<b>110</b>
7.1 Motor positioning of Reflector based on light intensity algorithm.....	112
7.2 Power Control Algorithm.....	113
<b>Chapter 8 - System Fabrication .....</b>	<b>114</b>
8.1 PCB.....	114
8.2 Reflector.....	117
8.3 Reflector Tower.....	117
8.4 Communication Tower .....	119
<b>Chapter 9 - Prototype and System Testing.....</b>	<b>121</b>

9.1 Hardware Testing.....	121
9.1.1 ESP32-C6.....	121
9.1.2 MicroSD card adapter .....	121
9.1.3 VEML7700.....	121
9.1.4 TCA9548A I2C Multiplexer.....	121
9.1.5 Motors .....	121
9.1.6 Antenna .....	121
9.1.7 PCB Simulation .....	122
9.1.8 Charge Controller.....	122
9.1.9 Solar Panel.....	122
9.2 Software Testing.....	122
9.2.1 ESP32-C6.....	122
9.2.2 MicroSD card adapter .....	124
9.2.3 VEML7700.....	124
9.2.4 TCA9548A I2C Multiplexer.....	125
9.2.5 Motors .....	125
9.2.6 Antenna .....	126
9.2.7 Use of Interrupts .....	126
9.2.8 Integration of Systems.....	126
9.2.8.1 Integration of the Servo Motor with the Sensors.....	126
9.2.8.2 Integration of the Stepper Motor with the Sensors.....	127
9.2.8.3 Integration of the Servo Motor for the Vertical Movement of the Mirror.....	127
9.2.8.4 Integration of the Servo Motor for the Horizontal Movement of the Mirror .....	128
9.2.8.4 Integration of Zigbee to the Changing of Targets.....	128
<b>Chapter 10 - Administrative Content .....</b>	<b>128</b>
10.1 Budget.....	128
10.2 Bill of Materials .....	129
10.3 Distribution of Worktable .....	130
10.4 Milestones .....	131
<b>Chapter 11 - Conclusion.....</b>	<b>132</b>
<b>Appendix A - Copyright Permissions' Requested .....</b>	<b>133</b>
<b>Appendix B - Copyright Permissions' Granted.....</b>	<b>139</b>
<b>Appendix C - References .....</b>	<b>142</b>
<b>Appendix D - Codes.....</b>	<b>148</b>

## List of Figures

<b>Figure 2.1.</b> FSI Rover and App from previous project.....	<b>3</b>
<b>Figure 2.2.</b> Network Diagram .....	<b>9</b>
<b>Figure 2.3.</b> Hardware Diagram .....	<b>11</b>
<b>Figure 2.4.</b> Software Flowchart .....	<b>12</b>
<b>Figure 2.5.</b> House of Quality .....	<b>13</b>
<b>Figure 3.1.</b> Plot of the best research cell efficiencies.....	<b>21</b>
<b>Figure 3.2.</b> Common Charge Controller/Regulator Designs .....	<b>22</b>
<b>Figure 3.3.</b> The output characteristic curves for a generic PV module for no shading conditions. (a) Current-Voltage correlation curves and (b) Power-Voltage correlation curves.....	<b>24</b>

<b>Figure 3.4.</b> Norway's mirror for artificial sunlight .....	25
<b>Figure 3.5.</b> Power absorption of silicon based on spectral irradiance and wavelength.....	27
<b>Figure 3.6.</b> Spectral reflectivity of perfectly smooth metal surfaces .....	28
<b>Figure 3.7.</b> Solar radiation vs. efficiency for silicon solar cells .....	29
<b>Figure 3.8.</b> Mylar reflectivity.....	30
<b>Figure 3.9.</b> Heliostat reflection mechanism.....	31
<b>Figure 3.10.</b> Reflection of light's diagram from instructible.....	32
<b>Figure 3.11.</b> Rotation of reflector at three different axes, X, Y, and W.....	33
<b>Figure 3.12.</b> (1) Bipolar and (2) Unipolar drivers of stepper motor .....	36
<b>Figure 3.13.</b> Division of full rotation .....	36
<b>Figure 3.14.</b> Photodiode Diagram.....	39
<b>Figure 3.15.</b> Phototransistor Diagram .....	40
<b>Figure 3.16.</b> CMOS Diagram.....	41
<b>Figure 3.17.</b> LED Diagram.....	43
<b>Figure 3.18.</b> An image of the Constant Current (CC) and Constant Voltage (CV) charging method of Li-ion batteries.....	56
<b>Figure 3.19.</b> A plot of the Renology Panel's IV curve. ....	69
<b>Figure 3.20.</b> PC140 average gain versus frequency .....	76
<b>Figure 3.21.</b> PC140 axial ratio .....	76
<b>Figure 3.22.</b> PC140 radiation pattern .....	76
<b>Figure 4.1.</b> Hierarchy of IPC Design Specifications.....	77
<b>Figure 4.2.</b> Basic I2C Block Diagram.....	79
<b>Figure 4.3.</b> I2C Multi-Slave Diagram .....	79
<b>Figure 4.4.</b> I2C Protocol Diagram.....	80
<b>Figure 4.5.</b> Load Torque ad speed between different motor designs .....	82
<b>Figure 5.1.</b> Results for case study #4, .....	94
<b>Figure 6.1.</b> The schematics for the 5V regulator (top) and the 3.3V regulator (bottom) .....	97
<b>Figure 6.2.</b> A schematic of the status LED circuit .....	97
<b>Figure 6.3.</b> Stepper Motor Schematic.....	99
<b>Figure 6.4.</b> Servos and Motor Controller Schematic with information by Limor Fried/Ladyada from Adafruit Industries.....	101
<b>Figure 6.5.</b> Lower-Level (Sensor and Antenna) Connection to MCU .....	102
<b>Figure 6.6.</b> Overall Schematic of All components.....	109
<b>Figure 7.1.</b> Software Use Case Diagram .....	110
<b>Figure 7.2.</b> Software Activity Diagram .....	111
<b>Figure 7.3.</b> Motor positioning base on light intensity flowchart .....	112
<b>Figure 7.4.</b> Sensors and Motor control .....	113
<b>Figure 8.1.</b> Stepper PCB V1 .....	115
<b>Figure 8.2.</b> Stepper PCB V1 .....	115
<b>Figure 8.3.</b> Sensor PCB V1.....	116
<b>Figure 8.4.</b> MCU Servo V1.....	116
<b>Figure 8.5.</b> Reflector Fabrication Step Diagram.....	117
<b>Figure 8.6.</b> Motors Placements on Reflector Tower .....	118

<b>Figure 8.7.</b> Complete 3D model of reflector tower and L-piece with CAD.....	119
<b>Figure 8.8.</b> CAD model of Communication Tower .....	120
<b>Figure 9.1.</b> TI Webench Regulators Simulations.....	122
<b>Figure 9.2.</b> Flashing of hello_world.c example program .....	123
<b>Figure 9.3.</b> Flashing of blink.c example program .....	124
<b>Figure 9.4.</b> Flashing of VEML7700 ALS.....	125

## List of Tables

<b>Table 2.1.</b> Specification of Towers .....	10
<b>Table 3.1</b> Comparison between MCU and FPGA.....	15
<b>Table 3.2.</b> Part 1 MCU Comparison.....	18
<b>Table 3.3.</b> Part 2 MCU Comparison.....	19
<b>Table 3.4.</b> A Table comparing the different solar technologies and the relevant factors.....	21
<b>Table 3.5.</b> A comparison of common regulator designs.....	23
<b>Table 3.6.</b> Existing Reflector Technologies.....	26
<b>Table 3.7.</b> Materials comparison for reflector.....	26
<b>Table 3.8.</b> Comparation between solar tracking algorithms .....	30
<b>Table 3.9.</b> Types of Motors.....	33
<b>Table 3.10.</b> Stepper Motors Comparation.....	34
<b>Table 3.11.</b> Servo Motors Comparation .....	35
<b>Table 3.12.</b> Stepper Motor Controller Comparison.....	37
<b>Table 3.13.</b> Servo Motor comparation.....	39
<b>Table 3.14.</b> Comparison of Light Sensor Technology .....	42
<b>Table 3.15.</b> Part 1 ALS Comparison .....	50
<b>Table 3.16.</b> Part 2 ALS Comparison .....	50
<b>Table 3.17.</b> Communication technologies Comparaisons .....	51
<b>Table 3.18.</b> A table describing the characteristics of common secondary batteries. (Battery University, n.d.) .....	54
<b>Table 3.19.</b> Advantages and Disadvantages of Li-ion cells and batteries for spacecraft applications.....	56
<b>Table 3.20.</b> table with the summary of antenna types discussed. ....	62
<b>Table 3.21.</b> A table with a summary of the antenna products discussed. ....	66
<b>Table 3.22.</b> A table describing the peak power needs from each device.....	66
<b>Table 3.23.</b> A table comparing the different panels to be considered for the heliostat (mirror) tower. ....	68
<b>Table 3.24.</b> A table comparing voltage regulators. ....	69
<b>Table 3.25.</b> A table comparing charge controllers. ....	70
<b>Table 3.26.</b> A table comparing different batteries.....	74
<b>Table 4.1.</b> Output Equivalence between IEC and NEMA Standard .....	83
<b>Table 7.1.</b> A table describing essential systems in low power operation. ....	114
<b>Table 10.1.</b> The Budget allocation for the various parts of the project .....	129
<b>Table 10.2.</b> An Itemized Bill of Materials .....	129

<b>Table 10.3.</b> The distribution of worktable .....	130
<b>Table 10.4.</b> Project Initialization Milestone.....	131
<b>Table 10.5.</b> Project Fabrication Milestone.....	131

## List of Equations

(1) Optical distance law.....	28
(2) Heliostat light angles .....	31
(3) Heliostat's distance ratio .....	32
(4) Phase calculation .....	36

# **Chapter 1 - Executive Summary**

The lunar surface is the next unexplored frontier. NASA's Artemis missions aim to use the Moon as a testbed for future Martian missions. As part of these lunar missions, NASA plans to explore large craters near the south pole, many of which are permanently shaded from the sun. This is problematic when attempting to utilize solar powered assets. To alleviate this issue, the ASTROCOM was developed in partnership with FSI, the Florida Space Institute. The ASTROCOM is designed and assembled entirely by engineering students at the University of Central Florida. The project is composed of two types of towers, designed to be used in a network to transmit power and information wirelessly to and from rovers or other devices within and around these craters.

*Heliosstat:* The first tower is a heliosstat tower, which incorporates a reflector to redirect light from the rim of a crater or vantage, down into the shaded regions of the crater. The reflector is intended to power solar assets from a distance and illuminate permanently shaded areas. The tower also has communication hardware to which regions are illuminated and form a telecommunication network. Designed to be fixed infrastructure, it is designed to sustain itself for long-term usage.

*Communication Beacon:* The second tower is a portable communication beacon, designed to be transported and planted by lunar rovers. This tower would provide a network between the heliosstat tower and rover enabling communication over hills or other obstacles for a set period of time, after which the tower may be collected, recharged, and reused.

The towers are intended to be used in conjunction with the rover. The system would be composed of the three components working together: a rover (developed by another group) that would explore permanently shaded craters, a communication beacon enabling a network to be formed over crater walls, and a heliosstat illuminating the rover's work area or other assets based on commands received over the network. These components working together will enable the exploration of areas of the moon that have never been researched extensively previously.

This document is a record of the ASTROCOM's design process, including the fundamental theories and technologies, part selection, the implementation process, and limitations. The context surrounding ASTROCOM is discussed first, followed by key technologies that enable its implementation. The parts that comprise these towers and the design philosophy used to select these components are discussed next. After that, the standards and constraints used within the design as well as the schematics for how these components will be implemented into complete systems are provided. Following that is the documentation regarding the system fabrication, prototyping, and administrative content. Final Conclusions are presented, followed by appendixes containing references and copyright permissions.

# **Chapter 2 - Project Description**

## **2.1 Project Background and Motivation**

In the vast expanse of space exploration, where humanity's curiosity knows no bounds, our senior design project endeavors to tackle the intricate challenges surrounding rover communication systems and heliosstat light reflection. As we venture into uncharted territories, we confront the

fundamental hurdle of establishing robust and reliable communication networks between rovers and their human counterparts, bridging the vast distances that separate us. Simultaneously, we grapple with the complexities of harnessing the power of heliostat light reflection, leveraging this innovative technology to illuminate unexplored regions and unravel the mysteries hidden within. With unwavering determination and pioneering spirit, our project aims to revolutionize the way we explore and educate others, pushing the boundaries of engineering and innovation to forge a path towards the stars.

In our academia, the senior design project is a great way for undergraduate students to learn to work in teams to achieve a common goal. As a group, we must learn to overcome challenges to brainstorm, innovate, and design a functional project with multiple pieces of software and hardware. Using these factors, we decided that we wanted to pick a project that would not only challenge us but also motivate and inspire us to make change. Because of this, we decided that we wanted to think big for our project.

Our group was approached by a sponsor, Mike Conroy from Florida Space Institute (FSI) Student Design Projects. Mike is a well-respected mentor who has over 35 years of experience working with the National Aeronautics and Space Administration (NASA) as an engineer, team leader, and now senior design mentor. We knew we had an unbelievable opportunity to have a great mentor and idea for a project. A recommendation from our sponsor resulted in a project idea as we were brainstorming different topics and ideas to build an engaging and challenging senior design project. This recommendation was a project to build a mesh communication network with a set of rovers through a main communication tower along with a reflection system to give a target light when they need it.

## **2.2 Current Commercial Technologies and Existing Projects**

### **2.2.1 Heliostaat DIY Kit**

The Heliostaat DIY kit is a commercially available product that uses a mirror to reflect sunlight at a specified location at all times. It does not use any light sensors to achieve this result. It uses a combination of GPS and calculations to determine its positioning. It uses two motors to move the mirror into position. The system is made to last for years even in the event of power failure. The Heliostaat can operate in two modes. The first mode of the product is to be a lamp that is on all day while reducing waste and space from a conventional lamp. The other mode is tracking the sun to maximize output for a solar panel.

The Heliostaat is meant to be low power and is controlled by a remote control. It uses a 12/24 V adapter to power and averages 430 mW. The remote control operates at 433 MHz with a maximum range of 50 meters when in an open area. It is unspecified what motors are used in the product but they are normally used for dish antennas. The software and hardware are both highly accurate with 0.01 degrees of accuracy for the software and 0.0125 degrees for the hardware. The internal processor runs at 48 MHz and the system has an LCD display with information on date, time and positioning on it. It's possible to modify the firmware if desired as well as use your own motors and add a wind sensor.

Heliostaat shares many similarities and differences with ASTROCOM. Both projects seek to track the sun and reflect sunlight using motors as the main idea. Both projects are controlled in some

form with a remote control. The biggest differences lie within the use cases and how that end result will be achieved. For ASTROCOM the possibility using GPS does not exist as it will be used on the moon. This is the largest difference between the method of the two as ASTROCOM will require light sensors, Heliostaat does not. Both, naturally, will need to use calculations to determine any positioning but ASTROCOM cannot take can any action without the light sensors.

Another difference is the reliance on a mesh network hosted by a communications tower so that information can be transmitted between the reflector and one or more targets that need light reflected to their location. Heliostaat doesn't handle changing positions on demand for moving objects. It does calculations by knowing its own position through GPS and everything else falls into place as that will reveal where the sun rises and where the sun sets for every day of the year. For ASTROCOM all positioning calculations are reliant on information being sent through the mesh network so that such calculations can be performed and light can be reflected to the given target.

Overall, the very similar core ideas show that Heliostaat is one of the most similar products on the market to ASTROCOM. That said, it is only the reflector tower part of the project and doesn't involve anything to do with the moon or rovers. The integration of a scalable mesh network with a movable communications tower to coordinate sunlight positioning makes ASTROCOM more complex and wider in scope.

## 2.2.2 FSI Rover and App

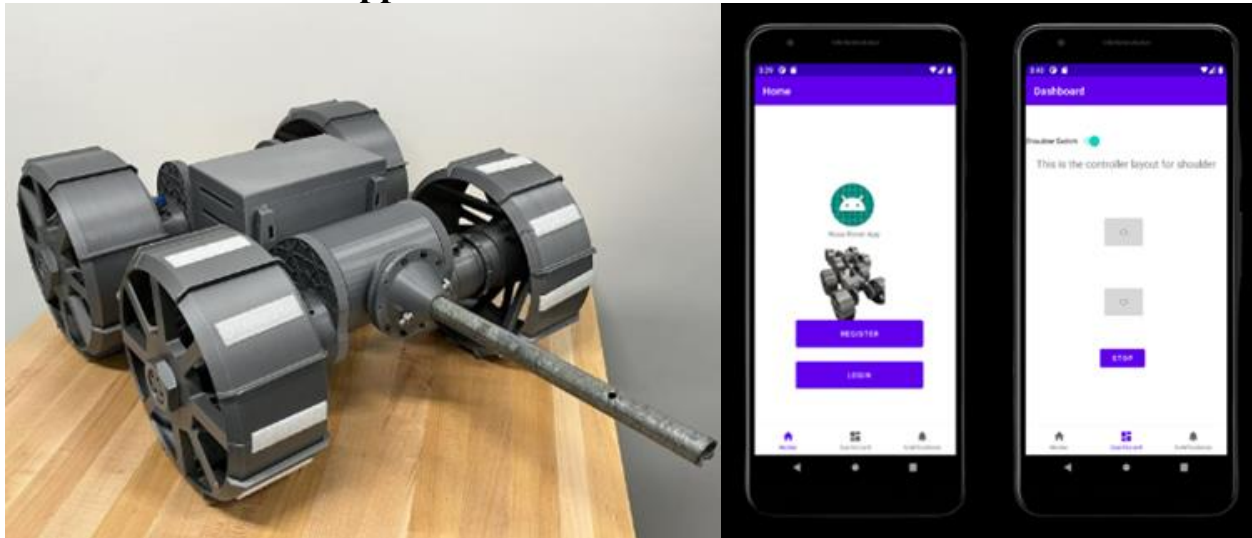


*Figure 2.1. FSI Rover and App from previous project.*

This was a congregation of previous projects that have been built for multiple years and universities, and we would be next in line to improve the rover project. Other schools had built this rover to be fully operational and able to be remotely operated through an app using Raspberry Pi Wi-Fi. Although the rover had been significantly upgraded, the communication aspect and the

electrical components of the rover were lacking. This was a unique challenge for us to be the next group to take the rover project to the next step.

We decided to take this challenge head on. At the time, the group that was constructed had eight people total and we decided to split the groups into a “rover group” and a “tower group” to effectively break this project up into two senior design projects that coincide together. We picked our groups that gave us the best chance to build two successful projects that would work together using the advice and guidance from our mentor professor, Dr. Chan. We brainstormed ideas of the functionalities early on and got a head start on our project, beginning planning and constructing diagrams as early as Spring 2023.

For this project, the main goal of this would be an education source for elementary and middle school kids and a proof of concept to a company such as NASA that they could build off, rather than something that would be put on the moon. FSI would supply us with a budget that would allow little to no cost for this project if we stayed within the boundary of \$750.00. This gave us an unbelievable opportunity to build an interesting senior design project that would be fully funded by a sponsor company while also being a contribution to children’s education in space exploration and communication systems.

As we started brainstorming how we wanted to attack this project, we did not think it would be feasible to have both communication and light reflection on the same tower since it would be too heavy and hard to balance the power draw from the microcontroller. We decided it would be best to break up the communication and mirror reflection into two separate towers to ease the power draw and make it simpler to divide the work among our group. The first tower, which will be the bulkier tower because of the motors and large mirror to reflect light to targets, is the “mirror tower”. The other tower is the “communication tower”, which will be light and compact, and theoretically can be picked up by the rover and placed somewhere else.

From here we started picking team roles and areas we wanted to work with based on undergraduate majors and personal preferences. We have three computer engineers in our group and one electrical engineer, so we based our roles mostly on these parameters. Binh was selected to be the project manager and to be in charge of the motors and mirror reflection. He is a computer engineer studying the Digital VLSI Circuits track at UCF which focuses on hardware-software co-design, making him the right person for the job. Alex, the electrical engineer, would oversee the power supply unit (PSU) in both the mirror and communication tower for the project, as he has the most experience with this field. Rounding up the group working on the mirror tower is Stephen, who is managing the microcontroller and light sensing algorithm for the mirror tower. He is a computer engineer so creating this algorithm relies heavily on coding and computer science resources to do this. Lastly, the person captaining the communication tower is Pedro, who is the last computer engineer of the group, and will be using network protocols and computer science algorithms to create the mesh network communication system with the rovers through the antenna. From here, we started working on our research and project specifications that will be laid out in this project report.

As our main motivation for this project, it is to complete the senior design program, which serves as the capstone program for the College of Engineering and Computer Science at UCF, and to meet the needs of our sponsor, FSI, as they will be the ones funding the project. As we meet these

necessary requirements, there are some internal motivations as well. Each group member wants to use this project as an opportunity to complete a team project with different roles to achieve a common goal, which will be incredibly prevalent as we enter the workforce in the industry after our graduation. On top of this being a great resume booster for any job application, this project will allow us to build necessary skills that will be used in the industry in the real world. These factors will be extremely important for early success by using these skills will allow us to make good first impressions and move up quickly with our respective companies.

Another piece of motivation for this project is to use this as a great opportunity to build a project full of innovative hardware and software to help with education for elementary and middle school students to teach and inspire them to learn about math and science to be the engineers of the future. On top of this, this could be an inspiration for an organization such as NASA to build upon this to create a more advanced system that could be used for future space exploration. This extra motivation keeps our group motivated, on pace, and thinking outside the box to inspire a future generation.

### **2.2.3 Summary**

Overall, looking into currently available commercial technologies and past projects that relate to our current product gives a lot of insight into where we can take this project, how we can match what exists and build upon it in a new direction. Not only that but learning about real existing solutions that are related helps with setting down constraints and understanding practical requirements that must be met for a successful project.

In the special case of our sponsored project, we are actively building upon FSI's rovers with new ideas that will work with them. It's integral to our new project to understand the constraints placed on the rover's design off the bat. Our main concerns are the addition of a reflector tower and a communications tower that are both integrated with the rover through a mesh network.

The reflector tower is completely separate from the rover and the communications tower aside from their communication through the network. The communications tower needs to be small and light enough so that it could potentially be transported by the rover. The rover must also be modified to be able to communicate with our network design.

By looking at the DIY Heliostaat kit, there was a lot to learn about creating an effective reflector. While the context was completely different, locating the sun and reflecting its light to a given point is how both our project seeks to function and how Heliostaat functions. It evidenced how we could not use GPS when we are on the moon and must rely on sensors to get the desired result.

The commercially available kit also showcases price points that we would hope to match or go lower in comparison. Budgeting from our sponsor is a major concern for our project and having an idea of the cost for something similar helps to gauge expectations and goals, as well as understanding what parts are more expensive or what parts deserve more budget allocation.

In conclusion, this less formal and less technical part of researching for the project was important for many reasons. Seeing currently available and past complete projects affects where we want to take our decision making and goals. Special attention goes to the FSI rovers as they are an integral part of our intended complete system within our project.

## 2.3 Objective and Goals

The main idea of this project is to build a communication tower and mirror tower to supply the rovers with a mesh communication network and sunlight for solar charging. Some of the main goals and objectives are listed below.

### Overall Goals

- Build a tower to handle rover communication.
- Build a tower to handle sunlight diversion to targets.

These goals can be narrowed into the objectives of both the mirror and communication tower to successfully create the project.

### Mirror Tower Objectives

- Identify optimal sun location based on lux value from sensor.
- Receive requests from communication tower using protocols.
- Create a heliostat algorithm to orient towards the target with motors.
- Create a self-sustainable power supply using solar and battery power.

### Communication Tower Objectives

- Receive requests from target through mesh network protocols.
- Relay requests to mirror tower using communication protocols.
- Create a small and portable tower that can be moved by rovers.

### Stretch Goals

- Peer to Peer Networking for communication and mirror tower with rovers.
- Wireless charging and/or docking station for communication tower.

### 2.3.1 Hardware

#### 2.3.1.1 Reflector – Basic Goal:

The ASTROCOM's reflector tower's primary function is to redirect sunlight to a specific location as facilities requested when the elements are obstructed by shadow. The facilities use redirected sunlight as replacement energy directly from the sun. The reflector needs to be able to traverse through the range of the sun's path and find the highest amount of sunlight possible to reflect. The reflector tower utilized diode ambient light sensors to measure the amount of lumen. Lumen's data is fed to the microcontroller and calculated by an algorithm to get the light's direction vectors. A motor controls the whole tower from the vectors to get the maximum light for reflecting and charging the attached solar panel.

Various conditions cannot be tested due to environmental constraints such that the testing needs to be done in the earth's surface environment rather than the moon. Certain environmental constraints, such as high temperature, must be adjusted when fabricated for the space environment.

The material used can be less durable because of the earth's atmosphere. Some parts used in the project must be considered in industrial form and alternative.

The moon has specific movement and hence has a different sun's path. Such a constraint needed to be placed. The tower position needed to be strategically placed for the sun to have the highest reflection and reduce the amount of overhead cross path. On the earth's surface, the tower needed to be placed on the North-South axis and at an elevation higher than the targets and facilities. This facilitates the most amount of light, and there is no overhead path.

The mountains and craters on the moon are significantly higher than any elevation on the earth's surface. Hence, the light path effectiveness must be scaled to appropriate intensity when fabricated for the space's environment. An offset can be accounted for due to the minimal atmosphere interference on the moon. The project needed to consider lumen loss and changes in the light path in the earth's atmosphere. The battery needs to be able to last two weeks without sun. This needs to be the case for maximum sustainability for the mirror tower. This will allow for less reliance on the solar panels for charging by having a larger battery.

#### ***2.3.1.2 Wireless Charging/Docking Station – Stretch Goal:***

For power, the main stretch goal for the communication tower would be a wireless charging component possibly with a docking station to allow for easier charging of the rover on the smaller tower that might have less capabilities for self-sustainability in terms of power. This would be a big boost for the accessibility of the rovers so that it could be operated remotely to be able to pick up the tower and bring it to a charging station. With this goal, it would disregard the need for cables to be plugged in or just relying on solar panels.

### **2.3.2 Software**

#### ***2.3.2.1 Basic Goals***

ASTROCOM must carry out multiple goals that comprise of electrical and computer science components. The main goal of the project is to be able to effectively reflect sunlight to a target that might need sunlight or extra light to charge. To be able to do this, ASTROCOM must be able to communicate with these targets using communication protocols to relay the message to the sensor and microcontroller to start this process. Our other main goal is to keep these two features, which are the mirror tower and the communication tower, separate from each other for functionality and mobility.

The main point of these two components being separate is so that the communication tower can be picked up and moved by a rover. This means that another one of our main goals is to have the communication tower be compact to the point that one of the rovers can theoretically pick it up and move it to a new location. Because of this, the communication tower must be able to relay the message to the mirror tower using communication protocols to send the target requests over. This can only be done by hosting a network, which is the primary goal of the communication tower.

In terms of light reflection, the first of the main goals for ASTROCOM are to identify the sun's location by using algorithms with the light sensor and microcontroller to determine the optimal location for most light intensity. From here, ASTROCOM needs to calculate a vector for light

trajectory to provide to the hardware's movements with the motors. This movement of the motors will have to correspond with the specific coordinates of the target in need of light.

For power, the main goals of ASTROCOM are to be sustainable and self-sufficient so that the towers can run on battery and solar power. From here, the towers will need to effectively deliver power to each component using a calculation software to determine which components are most important or in need of power on the towers. These power goals are critical for the functionality of ASTROCOM.

### ***2.3.2.2 Peer to Peer Networking – Stretch Goal:***

In the communication tower, there is a main stretch goal that is on the table if time permits. For the networking aspect, having a peer-to-peer network for each of the towers and to the rovers would be ideal to create a seamless communication system. The peer-to-peer networking system would allow for complete decentralization so there is no single point of failure between the rovers and communication tower. This would also allow for easy scalability for future additions to this project. Lastly, the peer-to-peer networking would add some extra security with no need for intermediary nodes.

The mesh network is designed in such a way that it is scalable for more rovers and communication towers. Using the Zigbee protocol the network can be extended infinitely, theoretically. Within a Zigbee network, all nodes function as repeaters. Every element in the network will essentially function as a “client” and a “host”.

Targets are able to request light from the communication tower by providing their latitude and longitude in relation to the reflector, which is always stationary. Keeping track of all of its own movements and providing this information to the reflector also serves as auxiliary info for determining where to reflect light.

For the basic use case of a single reflector tower, a single communication tower and a single rover the communication tower acts primarily as a repeater. The rover is able to move the communication tower by itself, allowing for a much wider range of communication to the reflector.

If more rovers are added into the system and the rovers are always in range of each other, an infinitely far away rover may still request light from the reflector.

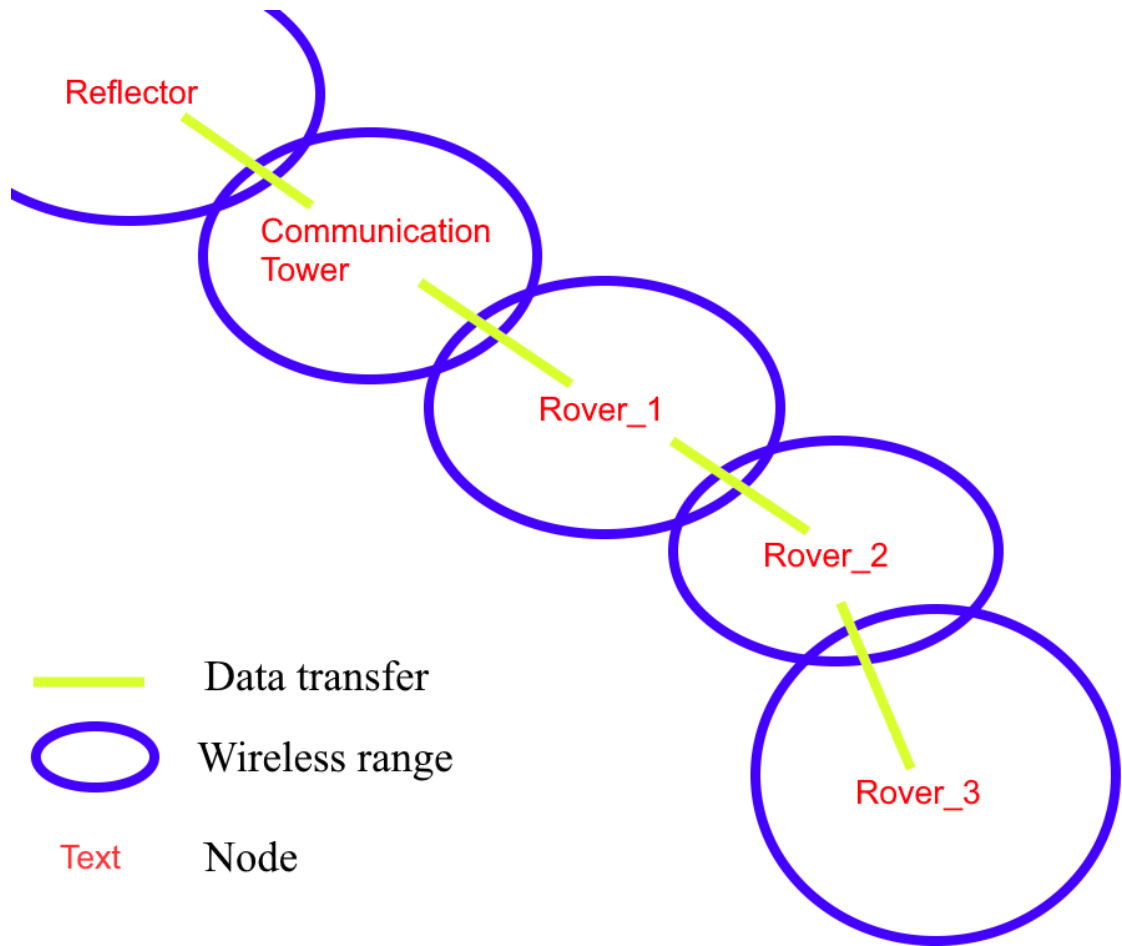


*Figure 2.2. Network Diagram*

## 2.4 Required Specifications

In consideration of objectives and constraints, specifications are required:

**Table 2.1.** Specification of Towers

<b>Heliosstat Tower</b>	
Minimum Temperature	-40°C
Reflector	
Minimum size	1ft diameter
Maximum size	5ft diameter
Maximum Weight	9kgs
Minimum Reflectivity	98%
Response Time	3 minutes
Tower Frame	
Maximum total weight	27kgs
Minimum Weight Capacity	10kgs
Solar Panel	
Minimum Power	30W during sunlight hours
Maximum Voltage	24V
Battery	
Minimum Lifespan	2 weeks without sun
<b>Communication Tower</b>	
Minimum Enclosure Volume	6.5"x6.5"x5"
Maximum Weight	2kg
Minimum Network Range	20m
Communication Rate	2400MHz
Voltage input	3.3V or 5V
Maximum Current Draw	500mA
Minimum Temperature	-40°C
Latency	1 second
Maximum Power	5W

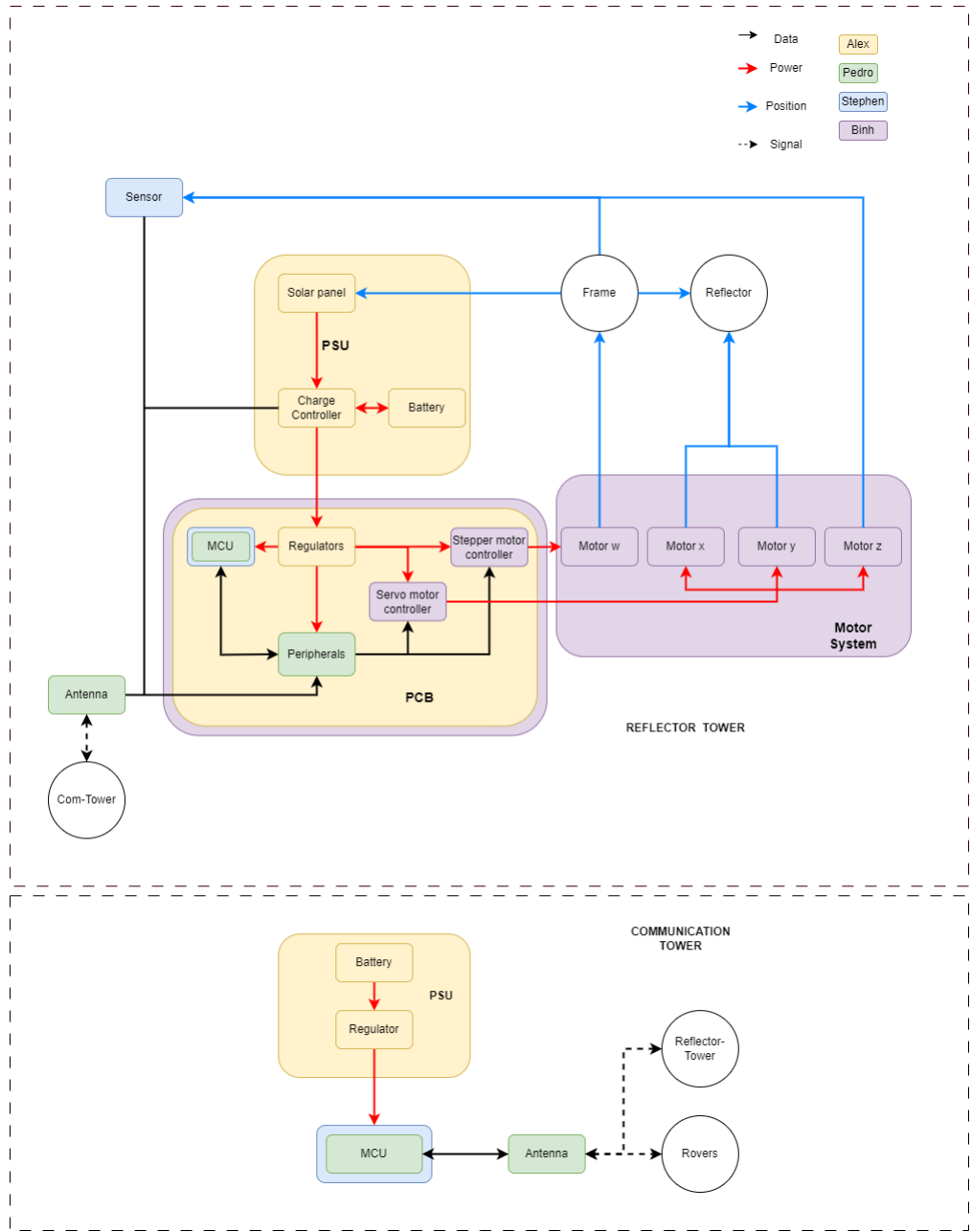


**Figure 2.3. Hardware Diagram  
by Authors**

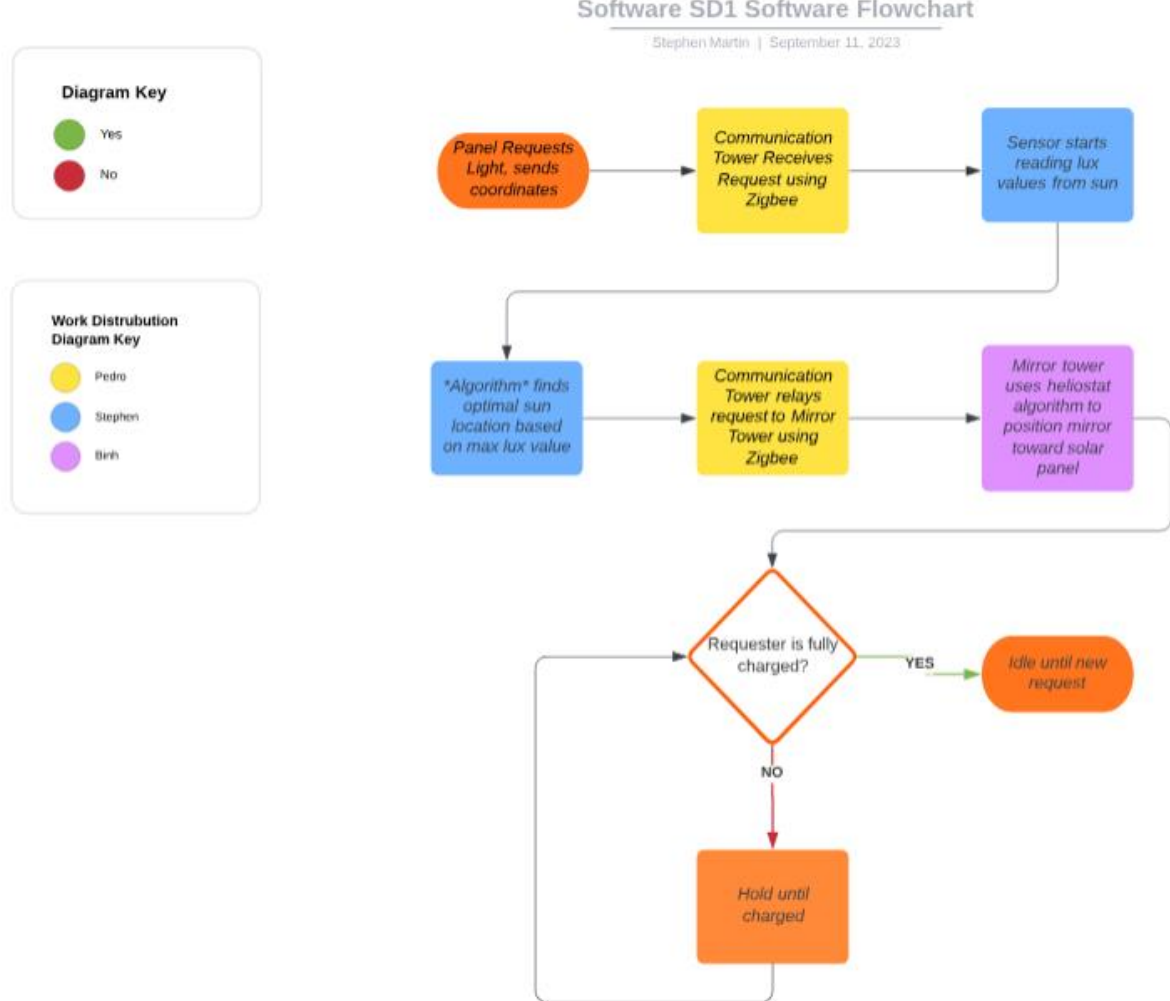


**Figure 2.4.** Software Flowchart  
by Authors

## 2.5 House of Quality

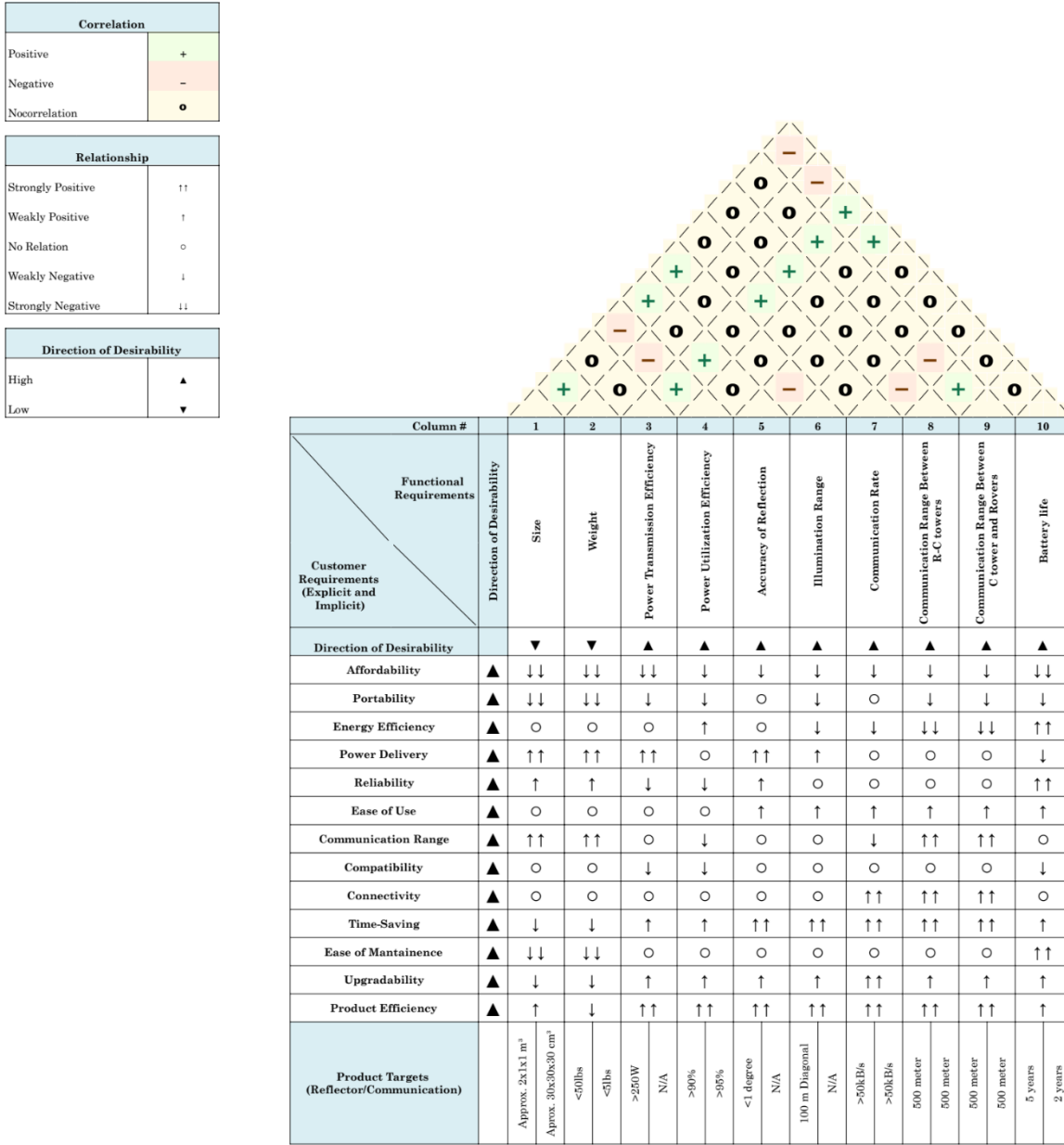


Figure 2.5. House of Quality

# Chapter 3 - Research

## 3.1 Technologies

### 3.1.1 MCU

#### 3.1.1.1 MCU vs FPGA

For the embedded systems in our project there is a choice between going for a microcontroller unit or a field-programmable gate array. There are pros and cons to each, for example, FPGAs are much more powerful and precise compared to MCUs. They aren't going to tolerate a large margin of error and are highly specialized for the task they are programmed and designed to do. That comes with several drawbacks for the FPGA, in many cases it is a higher cost option and consumes a lot more power than a microcontroller would.

FPGAs consume a lot more power due to their increased processing capabilities and typically having applications in parallel processing. Microcontrollers are geared towards being low power devices, often having many different customizable low power modes out of the box. FPGAs are also missing out on being user friendly as they have complex programmable hardware to be geared towards niche industry applications. FPGAs also use hardware description programming languages like Verilog and VHDL, making them more difficult to work with. In a similar vein, in terms of peripherals, FPGAs will require external components to integrate things like analog-to-digital converters or communication interfaces such as UART and I2C.

MCUs usually have most of these features already present, if not all. This makes a microcontroller development board extremely user friendly in comparison. They have tons of easy-to-use documentation and online resources available, from manufacturers and hobbyists alike. They have standardized architectures while also being a very established field. MCUs usually have their own IDEs with dedicated support and updates. They also use common programming languages with desktop programming like C, Python and other similar languages or variations. This aspect also makes it so debugging is not as large of a concern when working with microcontrollers compared to FPGAs. Familiar tools will make debugging a breeze while it would take much more effort on an FPGA due to their complex nature, documentation is often hardware centric and more difficult to parse. Due to the non-standardized nature of the hardware it's common for documentation to wildly differ between vendors as well.

After being familiarized with working with microcontrollers, the barrier of entry is significantly lower when using products of a new board family or manufacturer, the same cannot be said when working with FPGAs. In terms of design and implementation it's already easy to think of a way to do anything with a microcontroller as we are essentially using desktop programming on a smaller scale, a development board that has required features is all that would be needed, everything else would fall into place. Microcontrollers usually have built in error handling and similar features to ensure stability.

The thought process and implementation for FPGAs is not as straightforward as there are many more considerations when designing hardware and a much more specialized set of knowledge is required. Error handling would generally need to be a newly created and customized feature and not something available out of the box. On the flipside this has a big advantage for the FPGA, it's very scalable and won't be as limited as a microcontroller in needing more processing power for

future upgrades to a system. The last point to talk about is environmental robustness. Microcontrollers tend to be more robust out of the box and usually include features like temperature sensors and watchdog timers so they can ensure stable operation. FPGAs are more sensitive to environmental factors like temperature and electromagnetic interference and may need some sort of special enclosure to ensure proper operation.

### **3.1.1.2 Why microcontrollers?**

We will be using our embedded systems in the project primarily for sensors and wireless communications. We probably want to use the same board in multiple locations for ease of use, they will all likely need to be connected to the network we're setting up. With this in mind we may want some equipment that can handle both networks and sensors. It'll also use pre-existing open source software to accomplish it. There are many options for microcontrollers that can potentially fit the bill here, including even boards that run operating systems. We need to be able to pick and choose the software we're working with and the selected hardware just needs to be compatible.

FPGAs can pack considerably more processing power if we were to select one but for our needs it would be overkill. An FPGA would provide us a lot of deeper ways to customize the hardware for our specific application but because we are not looking to design our own mesh network, communication protocols and sensor system, a microcontroller will suit the design better. We want something that ticks all the boxes for: low power consumption, easy to use and implement, broad in its applications, has useful features out of the box and is cost effective.

The right microcontroller development board selection will be capable of doing everything we want out of our embedded system as well as make development user friendly. Standardized documentation within the established ecosystem of microcontrollers also significantly eases development and design. Most aspects that make FPGAs attractive options for projects would go completely wasted for our use case and in many cases make implementation more difficult while also consuming unnecessary power. These are the reasons why a microcontroller is the best option for our design over an FPGA.

**Table 3.1 Comparison between MCU and FPGA**

Criteria	Microcontroller	FPGA
<b>Environmental robustness</b>	✓	
<b>Low power consumption</b>	✓	
<b>Parallel processing</b>		✓
<b>Ease of use</b>	✓	
<b>Processing power</b>		✓
<b>Cost</b>	✓	
<b>Scalability</b>		✓
<b>Integration/Peripherals</b>	✓	
<b>Documentation</b>	✓	

### **3.1.1.3 Raspberry Pi**

The traditional Raspberry Pi series presents many potential benefits for this project but it also has plenty of downsides to counteract them. This model teeters the line of being an embedded system and a full desktop computer, as it is a complete Linux machine, just a very small one. This will allow us to very easily work with the software and debug any problems we may have with the mesh network and/or the sensors. It also opens up the doors to using any programming language we want.

The 1.8 GHz quad-core CPU is more than enough for our purposes, it is almost certainly overkill. This Pi also has at least 1 GB of RAM and at least 32 GB of storage capacity which is more than we'll ever need for this project which essentially eliminates the memory constraint that other embedded systems options have. These have 2.4 and 5 GHz 802.11ac wireless, Bluetooth and Bluetooth Low Energy built in which may be useful to us. On the other hand we can add additional peripherals through its USB 3.0 ports.

It needs 5 V and minimum 3 A to power which is a lot of power compared to traditional microcontroller boards. It cannot operate under moon temperatures. It is capable of UART, SPI and I2C protocols through the 40-pin header GPIO pins. It does not have an ADC or DAC by default which is an important aspect to consider depending on how the network is handled. It is more on the expensive side compared to more bare metal boards. We can potentially incur a lot of overhead from running our software on a Pi since it is a full desktop computer running an operating system and not something that's made to fill a small set of niches like other options.

### **3.1.1.4 Raspberry Pi Zero**

Raspberry Pi has other options besides their main series like the Raspberry Pi Zero series which is largely similar but has more in the way of networking capabilities that may prove more enticing. There are less features we may find superfluous on this board such as the GPIO pins being unpopulated and less memory. It also needs less power, the manufacturer recommends 1.2 A but it can run with less, especially for our purposes. The Zero has 2.4 GHz bgn wireless lan and an onboard antenna that makes it different from the traditional series while still having the Bluetooth and Bluetooth Low Energy options. The processor is weaker at 1 GHz quad-core and half as much RAM at 512 MB but this is a much cheaper board with the main benefits remaining intact. Overall the traditional Pi and the Zero are fantastic choices for making our software development very efficient and giving us the most options to work with and very few limitations. The largest downsides are a lack of ADC, DAC and other communication options like Zigbee aside from using a lot more power, even if we're talking about the Zero.

### **3.1.1.5 Raspberry Pi Pico**

The last products to consider from Raspberry Pi are their microcontrollers, the Raspberry Pi Pico series boards that use their own chip, the RP2040. These boards, being typical microcontrollers, are much more in line with all other embedded systems options we have laid out for this project, the previous Pis being outliers.

We'll lose all the software benefits that a Linux environment provides but these boards require much less power. They are limited to C/C++ and MicroPython for programming languages. These

boards can use 1.8-5.5 V and average 38 mA. They have plenty of GPIO pins that include UART, SPI, I2C, ADC and PWM totaling 26 pins. The Pico has ADC but does not have DAC which is a big downside if we want to do our own signal modulation with an external antenna.

The Pico W models have 2.4 GHz 802.11n wireless. It also supports WPA3 for security and can be used as a soft access point which are features that greatly fit our use case. These MCUs are more standard in their processing power and memory running at 133 MHz with a dual core processor and 264 KB of RAM with at least 2 MB of flash memory. Their operating temperatures are not suitable for the moon. These boards are very cheap, starting at \$4. Overall, the Pico series is a solid option due to its low power consumption and wireless capabilities out of the box coupled with its very low cost.

### **3.1.1.6 Arduino MKR 1000**

Arduino has Wi-Fi and LoRaWAN board families available that may fit our use case well. The MKR Wi-Fi 1000 series boards use a standard 5 V power supply and operate at 3.3 V while only using 7 mA per pin used. This is very low power consumption, and it also supports using a rechargeable battery without any modifications and will charge while on a power supply automatically.

These boards include UART, SPI, I2C, PWM, ADC and DAC, everything we would need to set up a custom radio front end while also having 2.4 GHz 802.11 bgn Wi-Fi, Bluetooth and Bluetooth Low Energy out of the box. With 256 KB of flash memory, 32 KB of RAM and a 48 MHz processor it's up to standards for other MCU offerings and servers our needs just right. At around \$40 USD, it is a very expensive board. Its operating temperatures are not suitable for the moon.

### **3.1.17 Arduino MKR WAN 1300**

The other option from Arduino is their WAN series boards that use LoRa and LoRaWAN for networking. These are largely similar to the Wi-Fi boards with the main difference being using LoRaWAN over Wi-Fi and having a bundled pentaband antenna with 2 dB of gain.

Another advantage these boards have are ultra low power modes that are usable on battery power using as low as 104 uA. LoRaWAN allows for this low power consumption and also has a longer range than the Wi-Fi option. These also won't work with moon temperatures. For any Arduino board there is some flexibility with programming languages but the Arduino language is preferred. These boards are the most expensive under consideration at \$46 USD but have enough upsides to try justify it. Overall the options offered by Arduino are on the expensive side but packed with useful features for our use case that make them options to consider.

### **3.1.1.8 ESP32**

The ESP32 series boards from ESPRESSIF are focused on networking applications and are packed with Wi-Fi, Bluetooth and Zigbee features. These have antennas included and at least 4 MB of flash memory. The processor is above average running a dual-core at 240 MHz and lots of SRAM at 520 KB, the processor speed can be lowered to a minimum of 80 MHz for power purposes.

The ESP32's operating temperatures are the closest to being able to operate on the moon. The power supply uses less voltage than usual with a minimum of 3 V. It has all the peripherals we would ever need on board like UART, SPI, I2C, PWM, ADC, DAC and more over its 26 GPIO pins. These dev boards are also ultra low power, needing a minimum of 28 mA current draw and peaking at 379 mA for transmitting. They are also one of the cheapest boards from our options at \$10 USD. The ESP32 series boards are very specialized for our purpose of creating a mesh network, their low power consumption and low price point make them one of the best options on the market.

### **3.1.1.9 CC13xx**

Texas Instruments has a couple of networking focused boards that also have a lot of sensor specific features so they can be of great use within our project scope. One of these boards is the CC13xx series. This series is a low power board with Wi-Fi, Zigbee, Bluetooth and 6LoWPAN available out of the box. They need 1.8-3.8 V to operate and have a fairly low current draw at barely 100 mA on average. It can be as low as 30 uA if used only for sensors.

The CC13xx series is more capable than a lot of boards in its wireless features while also having lots of peripherals with their GPIO pins like UART, SPI, I2C, ADC and DAC but no PWM. 80 KB of RAM is plenty. They have a very usual clock frequency of 48 MHz. There are many tools and software available for development including for configuring the radio front end. It has plentiful flash memory at 352 KB. They also have operating temperatures that are fairly close to working on the moon. This is a fairly expensive development board at a price of \$29 USD.

### **3.1.1.10 CC26xx**

The CC26xx series is a lower end version of the CC13xx series from Texas Instruments. It has many of the same benefits as the CC13xx series while missing some features and generally just being weaker. It's also listed at a higher price costing around \$40 USD for a development kit which makes it a very questionable choice. It lacks the Wi-Fi and 6LoWPAN capabilities of the CC13xx while also having less than half the flash memory at 128 KB and a quarter of the RAM at 20 KB. It maintains the same clock speed, peripheral operating temperatures, size and power requirements as the CC13xx. Overall, the TI boards are very expensive but do have a lot of useful features that are worth considering.

**Table 3.2. Part 1 MCU Comparison  
by Authors**

	<b>ESP32</b>	<b>MSP430</b>	<b>Raspberry Pi 0</b>	<b>Arduino MKR1310</b>	<b>Arduino MK1010</b>
<b>Cost - Processor &amp; DevKit (USD)</b>	9.18	20	15	46	38.6
<b>Wi-Fi</b>	Yes	No	Yes	No	Yes
<b>Bluetooth</b>	Yes	No	Yes	No	Yes
<b>Zigbee</b>	Yes	No	Yes	No	No
<b>Z-Wave</b>	No	No	Yes	No	No

<b>LoRaWAN</b>	No	No	Yes	Yes	No
<b>6LoWPAN</b>	No	No	Yes	No	No
<b>UART</b>	Yes	Yes	Yes	Yes	Yes
<b>I2C</b>	Yes	Yes	Yes	Yes	Yes
<b>SPI</b>	Yes	Yes	Yes	Yes	Yes
<b>PWM</b>	Yes	Yes	Yes	Yes	Yes
<b>ADC</b>	Yes	Yes	Yes	Yes	Yes
<b>DAC</b>	Yes	Yes	No	Yes	Yes
<b>Flash Memory</b>	4 MB	128 KB	None	256 KB	256 KB
<b>RAM</b>	520 KB	2 KB	512 MB	32 KB	32 KB
<b>Operating Voltage (V)</b>	3.6	5	5	3.3	3.3
<b>Current Draw (A)</b>	0.379	0.2	2.5	0.154	0.154
<b>Power Consumption (W)</b>	1.3644	1	12.5	0.5082	0.5082

**Table 3.3. Part 2 MCU Comparison by Authors**

	Raspberry Pi Pico	Raspberry Pi	CC13XX	CC26XX
<b>Cost - Processor &amp; DevKit (USD)</b>	5	35	29	39.99
<b>Wi-Fi</b>	Yes	Yes	Yes	No
<b>Bluetooth</b>	Yes	Yes	Yes	Yes
<b>Zigbee</b>	Yes	Yes	Yes	Yes
<b>Z-Wave</b>	No	Yes	No	No
<b>LoRaWAN</b>	No	Yes	No	No
<b>6LoWPAN</b>	No	Yes	Yes	No
<b>UART</b>	Yes	Yes	Yes	Yes
<b>I2C</b>	Yes	Yes	Yes	Yes
<b>SPI</b>	Yes	Yes	Yes	Yes
<b>PWM</b>	Yes	Yes	No	No
<b>ADC</b>	Yes	No	Yes	Yes
<b>DAC</b>	No	No	Yes	Yes
<b>Flash Memory</b>	2 MB	32 GB*	352 KB	128 KB
<b>RAM</b>	264 KB	1 GB	80 KB	20 KB
<b>Operating Voltage (V)</b>	5	5	3.8	3.8
<b>Current Draw (A)</b>	0.038	3	0.1092	0.1092

<b>Power Consumption (W)</b>	0.19	15	0.41496	0.41496
<b>Operating Temperature (C)</b>	[-20 - 85]	[0 - 50] C	[-40 - 105]	[-40 - 85]
<b>Processing Power</b>	133 MHz	1.8 GHz	48 MHz	48 MHz
<b>Processing Cores</b>	2	4	1	1
<b>WPA3 Encryption</b>	Yes	No	No	No

### 3.1.2 Solar Panels

There are three commercially available solar cell technologies, Monocrystalline Polycrystalline, and Thin Film. The solar panel to be used must be able to withstand cold temperatures of 80-300K and produce enough energy to sustain the mirror tower for 10+ years unaided. Solar panels do degrade over time, historically ~1% per year. This is unavoidable but can be accounted for. A sufficiently oversized panel should be used, such that years of degradation on the panel will not significantly affect operations. Important considerations to make when discussing solar panels in this context are temperature tolerance, maintenance requirements, efficiency, low-light performance, and of course, cost and availability.

#### 3.1.2.1 Monocrystalline

As the name suggests, this type of solar cell is made of a single silicon crystal (mono c-Si) and is the most popular solar cell. This is due to their material parameters being better than other options. Originally mono c-Si cells were more expensive due to the slow and controlled manufacturing process. As manufacturing processes were refined, the cost of monocrystalline cells decreased significantly. This is the most commercially viable option for use.

#### 3.1.2.2 Polycrystalline

Polycrystalline (poly c-Si) solar cells are typically cheaper, due to the simpler manufacturing processes. They are less popular however due to the performance lost between the grains of crystals. Poly c-Si panels do suffer from reduced low-light efficiency when compared to monocrystalline panels, in conjunction to their reduced efficiency requires a larger sized panel for the same power output a monocrystalline panel would provide.

#### 3.1.2.3 Thin Film

Thin Film solar cells are specialized cells. Typically made from heavy metals, they are significantly thinner than traditional c-Si solar cells. This makes them the best choice for semi-transparent or flexible solar cells. This also makes them lighter and more adaptable, which is an important consideration when designing space applications. The commercially available thin-film solar modules are less efficient than similarly sized c-Si modules and tend to degrade faster than comparable mono c-Si panels.

**Table 3.4.** A Table comparing the different solar technologies and the relevant factors.

Solar Panel Technology	Efficiency	Low-Light Performance	Temperature Tolerance	Radiation Resistance	Degradation	Weight & Size
Monocrystalline	High	Excellent	Good	Good	Low	Relatively heavier
Polycrystalline	Moderate	Good	Good	Good	Low to Moderate	Moderate
Thin-Film	Low	Varies	Good	Varies	Moderate to High	Lightweight & Flexible

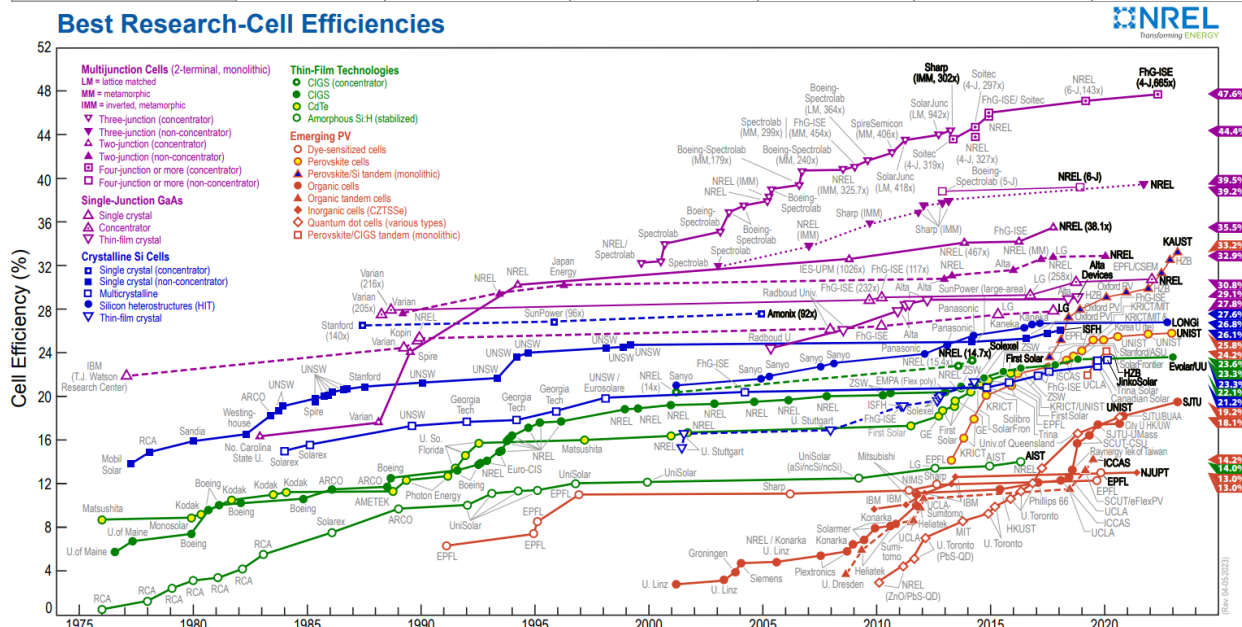


**Figure 3.1.** Plot of the best research cell efficiencies.

(National Renewable Energy Laboratory, n.d.)

### 3.1.3 Voltage Regulation

Voltage regulation is also required due to the varied voltage requirements of the other systems involved. This would be placed in line with the loads that require a specific line voltage. Ensuring that the voltage regulator can continuously support the power requirements of connected devices is essential to proper functionality. The two primary types of voltage regulator are linear and switching regulators. Linear voltage regulators are less efficient, less flexible, and larger than switching regulators. Linear regulators are, however, easier to design, dependable and cost-efficient. Special attention must be given to loads that require sudden, high currents like motor controllers and drivers. The DC/DC converter handling these systems must be able to quickly respond to these dramatic changes in demand.

### 3.1.3.1 Linear Regulators

It is important to note that linear regulators can only step-down voltages. Any excess voltage will be dissipated as heat, making it a less efficient regulator. The two forms of linear regulators are series and shunt regulators. Like their names imply they are placed either in series or in parallel with the lines they are intended to regulate. Shunt controllers work by shorting the PV module and would have a constant short-circuit current across the shunt element. For this reason, shunt regulators are less common and limited to systems less than 20 amps. The more common series regulator opens and closes a switch to the PV module to charge or discharge the battery. Both designs incorporate low voltage disconnects (LVD) to disconnect the load when the battery is critically low, promoting the long-term health of the chosen battery. (Dunlop, 1997)

Low-Dropout (LDO) regulators are a common form of series voltage regulator. They are named Low-Dropout due to their low drop in voltage between input and output. LDO regulators are typically used locally to supply ICs or components with a precise level of low-noise voltage. An LDO regulator can also be used for a simple and inexpensive solar charge controller, reducing the output voltage of a typical 50W 24Voc solar panel to a stable 12V, however this would be energy inefficient and lacks control over precise power delivery.

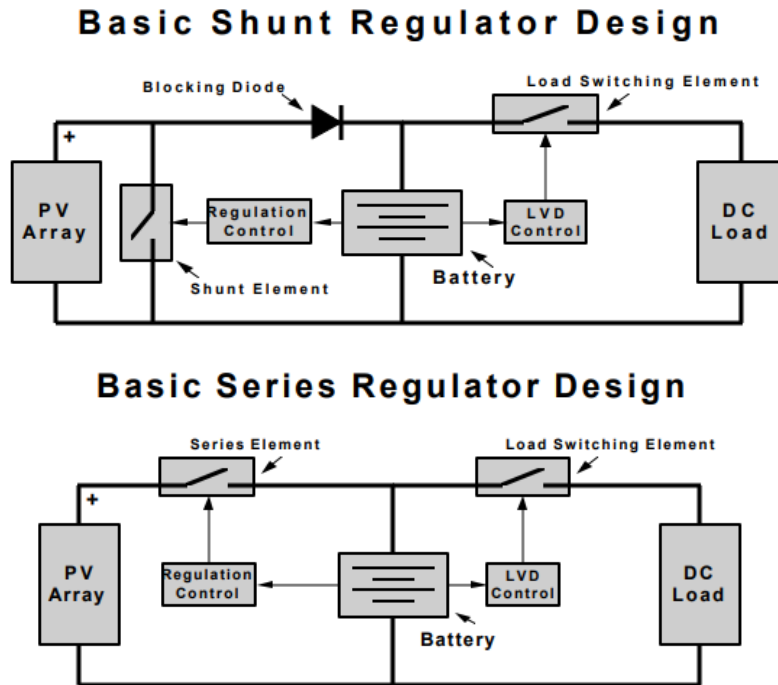


**Figure 3.2. Common Charge Controller/Regulator Designs**  
(Dunlop, 1997)

### 3.1.3.2 Switching Regulators

Switching regulators are regulators that rapidly switch the input voltage on and off using PWM to achieve the desired output voltage. The modulated signal is then pushed through an inductor-

capacitor circuit to power the load continuously. Various ICs exist that enable a wide range of duty cycles, and therefore a wide range of flexibility in design. This enables them to efficiently step-up or step-down the output voltage depending on the design. The common switching DC/DC converters for voltage regulation are Buck, Boost, Buck-Boost, and Cuk Converters. An important consideration to keep in mind when choosing components is that the ripple voltage seen as a result of equivalent series resistance of the output capacitors increases as temperature is reduced.

**Table 3.5.** A comparison of common regulator designs.

Specifications	Linear Regulators	Switching Regulators		
		Buck	Boost	Buck-Boost
<b>Efficiency</b>	Moderate		High	
<b>Heat</b>	Moderate		Low	
<b>Voltage Output (relative to input)</b>	Step-Down	Step-Down	Step-Up	Up or Down
<b>Output Ripple</b>	Low	Low	High	Low
<b>Complexity</b>	Low	Moderate	Moderate	High
<b>Cost</b>	Low	Moderate	Moderate	High

### 3.1.4 Charge Controller

A charge controller is necessary when using a solar panel to charge batteries. The charge controller ensures that the batteries are charged safely, preventing overcharging and over-discharging. Charge controllers may also regulate voltages and current to connected loads. Setting voltage and current regulation parameters is essential to an effective charge control system. This would be the key component in ensuring the power system operates reliably. There are two ways to control the charge provided from a solar panel, PWM and MPPT. These methods would be used in conjunction with voltage and current regulators to effectively and safely power components and batteries.

#### 3.1.4.1 PWM

Pulse-Width Modulation (PWM) Controllers rapidly connect and disconnect the PV module to the battery, enabling fine control over the rate of charge of the battery. This enables the utilization of batteries with strict charging requirements and reduces the risk of thermal runaway. PWM is rather inexpensive and there are many COTS solutions available. They are common for smaller scale systems due to their simplicity and low design cost.

#### 3.1.4.2 MPPT

Maximum Power point tracking (MPPT) refers to a technique of maximizing the power generated by variable power sources, in this case a solar panel. Typically incorporated in a charge controller, an MPPT device aims to alter the operating current and voltage for peak power. Shading of solar cells in modules with bypass diodes cause multiple local power points to form, forcing more complicated methods of finding the global MPP (GMPP). (Mohammadmehdi Seyedmahmoudian, 2013) In this work, the panel sized targeted typically only has one bypass diode(if any), therefore these complexities can be avoided. There are various methods of MPPT that operate differently,

however the same basic principle applies to all: find the maximum power output and hold that point. Charge controllers that incorporate MPPT tend to be more expensive than those that do not offer very little benefit in this specific use-case. There are some commercially available ICs that can manage MPPT, however these may be more expensive and require more design complexity compared to basic PWM charge controllers.

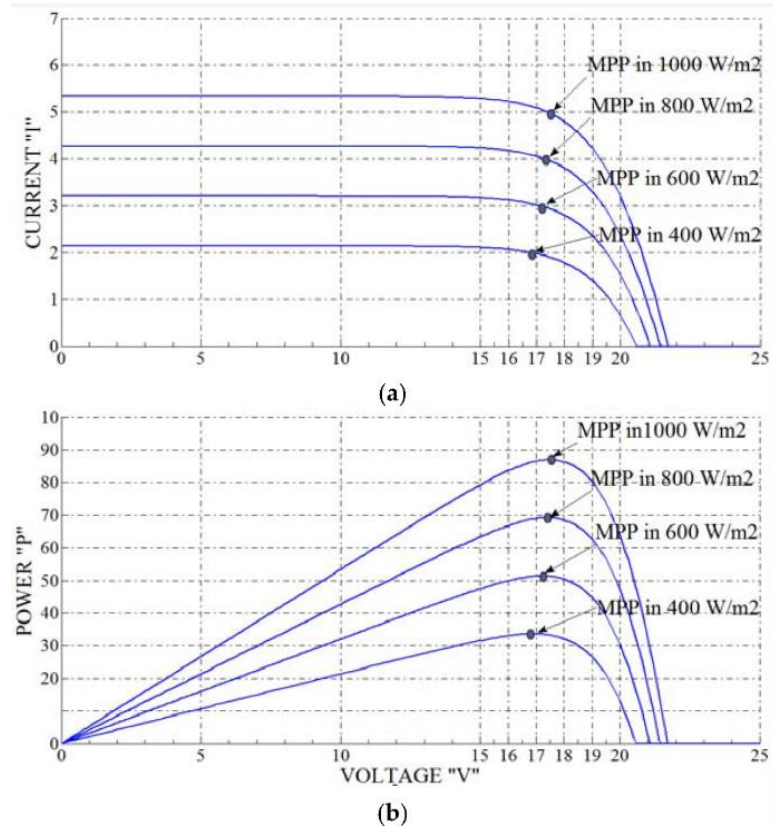


**Figure 3.3.** The output characteristic curves for a generic PV module for no shading conditions.  
(a) Current-Voltage correlation curves and (b) Power-Voltage correlation curves.

### 3.1.5 Reflectors

#### 3.1.5.1 Norway's Mirror for Artificial Sunlight

In Norway, Rjukan, a town, has a similar environment to the moon of a low valley with limited light. A mirror system was built on top of the mountain to redirect sunlight to a fixed location in the valley. The distance between the reflector and the redirected site is about 450 meters. There are three square mirrors with a surface area of 17m<sup>2</sup>. The mirrors are made to rotate to face the sun for the highest reflectivity, which has an efficiency of 80 to 100% reflectivity. Motors are used to track the sun's movement by using heliostat mechanisms and computer algorithms. The mirrors are standard glass-coated metal mirrors. The light reflected a 600m<sup>2</sup> eclipse shape area. Twelve non-moving solar panels collect energy for the mirror's rotation. The total area of the mechanism is approximately 51m<sup>2</sup>. The cost of the project is \$849,300.

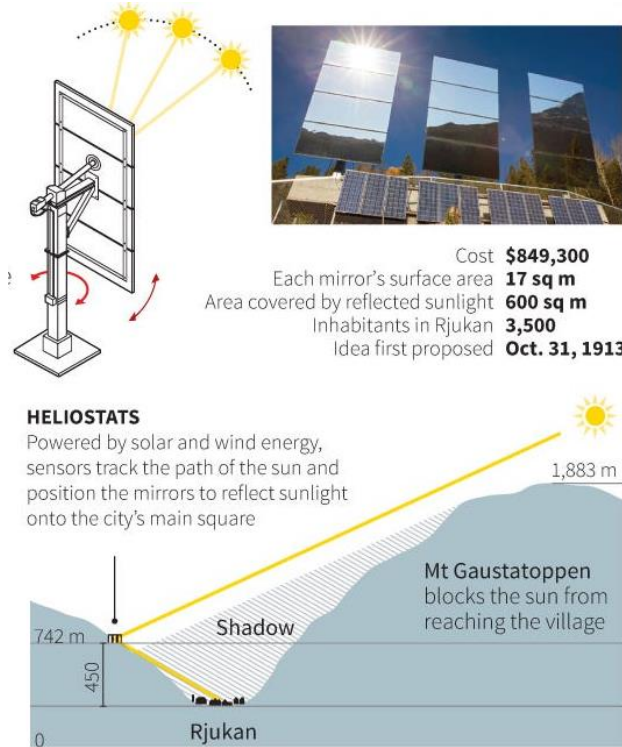


**Figure 3.4.** Norway's mirror for artificial sunlight  
by Norsk Telegrambyra AS

Norway's mirror for artificial sunlight has a much higher expected cost than the “Tower’s” project’s requirements. The environments have similar aspects in provision. The conditions on the moon’s surface impeded many parts of Norway’s mirror project, as this project is built for earth environments. The mirror’s materials are not viable considering the extreme environment. Maintenance is more difficult when brought into consideration by the moon’s reflector.

Some technologies that can be utilized are the heliostat system for tracking the sun and the specification of size for the reflector. The reflector needs to be able to track the sun to have the best angle to reflect sunlight efficiently. The motor movements and algorithms can be replicated to move the reflector. The mirror can be scaled to be smaller as the destination area only needs to be covered by a small solar panels field.

### 3.1.5.2 James Webb’s Telescope’s Mirror

James Webb’s telescope has a large reflector that enhances astronomical observation in detail. The reflector improves light sensitivity and image quality through high-quality reflected light. The telescope is needed to travel in space. Hence, a minimal surface area is required, such that the reflector is designed to be compact by folding in with hexagonal segments. There are 18 segments with a 1.32-meter diameter per segment. The material used for the mirrors is beryllium with polished gold coating. Berylliums are lightweight and durable. At the same time, gold has high heat conductivity and reflectivity. The weight of each mirror segment is approximately 20 kilograms.

Mirror folding makes a compact structure for more accessible transportation. Mirror with a coating of highly reflective material with a solid base metal can be used instead of glass coating. The disadvantages of James Webb's telescope's mirror are the high cost of materials, complex assembly, the algorithm needed to assemble mirror structure, and toxic materials handling.

**Table 3.6. Existing Reflector Technologies**  
by Authors with information from Business Insider/ REUTERS and NASA

Reflector's technologies	Financial cost (USD)	Weight	Size	Materials	Efficiency	Temperature Durability
<b>Norway's Mirror</b>	\$849,300	Very heavy (fixed location )	17m <sup>2</sup> /panel . 51m <sup>2</sup> total	Glass coated metal	80-100% reflectivity on earth's environment	Approx. (-25°C to 45°)
<b>James Webb's telescope Mirror (per segment)</b>	Approx. \$77 million	20kg	1.13m <sup>2</sup>	Polished gold coated beryllium	High efficiency in space	Withstand -240°C

**Table 3.7. Materials comparison for reflector**  
by Authors with Information from dailymetalprice, roofonline and Evaluation of reflectivity of metal parts by a thermo-camera

Materials	Financial cost (USD)	Weight (kg/m <sup>3</sup> )	Spectral reflectivity (%) at 10 <sup>3</sup> nm	Temperature Durability	Malleability
<b>Metals</b>					
<b>Aluminum</b>	\$2.237/kg	2,700	95-100%	High	High
<b>Titanium</b>	\$6.75/kg	4,500	60-70%	High	Medium
<b>Copper</b>	\$8.527/kg	9,000	95-100%	High	High
<b>Gold</b>	\$67,020/kg	19,300	98-100%	High	High
<b>Beryllium</b>	\$1,200/kg	1,850	Low	High	Medium-Low
<b>Silver</b>	\$ 844/kg	10,490	95-100%	High	High
<b>Tungsten</b>	\$7.165/kg	19,300	50-100%	High	High
<b>Coating</b>					
<b>Tempered glass</b>	\$10-55/ft <sup>2</sup>	2500	99-100%	Low	Low
<b>Mylar</b>	\$3/kg	1.85	99-100%	High	High

In essence, reflectors are reflective surfaces coined into a device, i.e., a mirror. In this project, the reflection of light intensity is of particular interest rather than a collection of images. The reflector is expected to reflect light directly from the sun, as it is placed at the highest altitude, to a specific location requested by a facility. A concave mirror can increase light intensity by combining reflective rays of the incident ray to a focal point. The focal point depends on the center of curvature, which requires a high flexibility of the reflector. A flat reflector has the advantage of

evenly distributed reflecting light and reduces a requirement variable of flexibility. The target locations for light delivery, changes based on the request, have various distances. A flat reflector is better than a concave mirror due to cost and complexity.

The purpose of the tower's reflector requires a high amount of lumen to be distributed to the solar panel for the highest performance efficiency. Reflectors' features must be considered to maximize delivered energy to the solar panel material and its reflectivity. Silicon photovoltaic cells absorb the most power in the visible light spectrum, with wavelengths of approximately 300nm to 700nm, as shown in Figure 3.5.

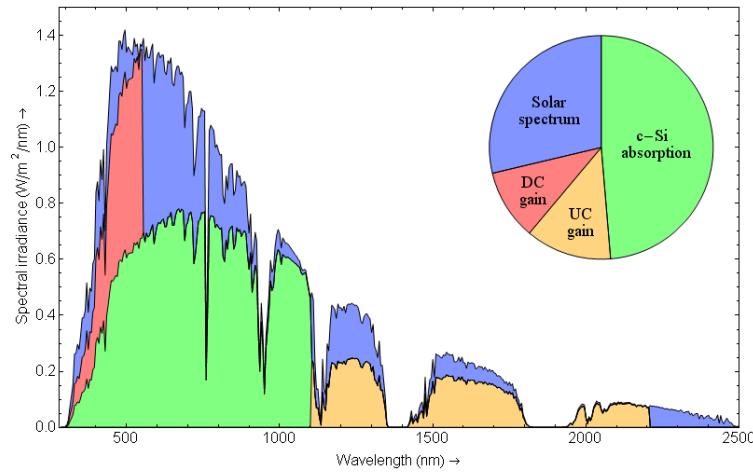


**Figure 3.5.** Power absorption of silicon based on spectral irradiance and wavelength.  
from W.G.J.H.M. van Sark, A. Meijerink, and R.E.I. Schropp, "Solar Spectrum Conversion for Photovoltaics Using Nanoparticles," Third Generation Photovoltaics, DOI: 10.5772/39213

Additionally, a glass-coated reflector would increase the percentage of reflectance by approximately ten percent along with the metal reflectance. Glass coating also provides rigidity for the mirror. However, rigidity can harm transportation efficiency when placing reflector towers. The moon's temperature in the daytime is  $120^{\circ}\text{C}$  and night-time is  $-130^{\circ}\text{C}$ . The temperature fluctuation of  $210^{\circ}\text{C}$  requires the reflector's material to handle extreme high-temperature change. Glass adds weight and can't withstand high-temperature oscillation of the moon since glass has poor temperature conduction. Under stress, the glass surface can crack and impede surface reflectivity. Glass coating increases the cost of maintenance and transportation. The tradeoff is that glass coating is not a viable option for the reflector.

A consideration to most solar cells' light absorption range is from 500~750nm, gold, silver, aluminum, and copper, based on Figure 3.6. as the material for the reflector since the spectral reflectivity is shown the highest in the  $10^3\text{nm}$  wavelength. A few aspects must be considered when choosing metals as reflector materials, such as cost and flexibility. The flexibility of metal decreases weight and reduces cost when transportation, along with increasing the durability of the reflector. Tungsten has the highest heat absorption and durability, however, have very low reflectivity. Gold would have the highest malleability and high thermal conductivity. The tradeoff of gold is lower durability and much higher cost. Aluminum and copper would be most efficient with both cost and high spectrum reflectivity. Aluminum has 60 to 70 percent reflectance of light with lightweight, much lower cost, and high-temperature conductivity. The metal can be in foil

form to reduce weight and increase flexibility. The durability can be reinforced using other metals as a base and polished high-reflective metal as a coating.

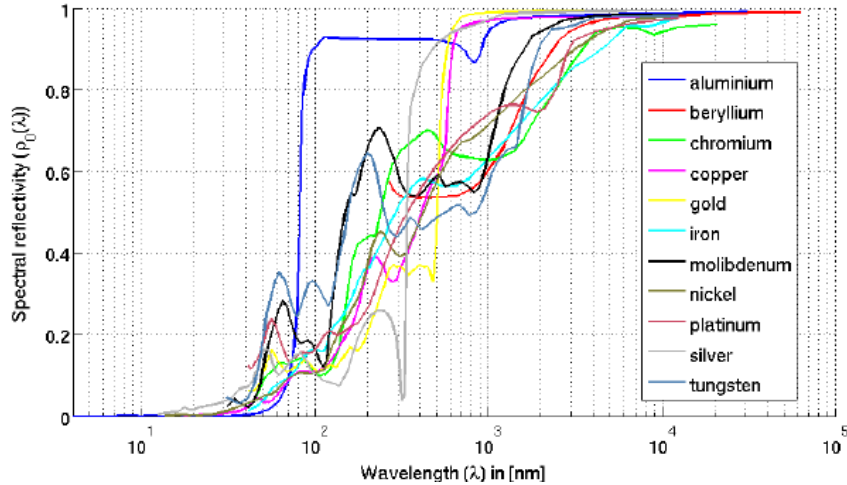


**Figure 3.6.** Spectral reflectivity of perfectly smooth metal surfaces  
from Sárosi, Zoltán & Knapp, Wolfgang & Kunz, Andreas & Wegener, Konrad. (2010).  
Evaluation of reflectivity of metal parts by a thermo-camera

The amount of light delivered to the solar panel depends on two factors: the reflectance of the reflector and the distance of the light source to the intended location. Optical distance law, as shown in (1) the light intensity, illumination ( $E$ ) (lux, lumen/m<sup>2</sup>) is the quantity of light from the source ( $\phi$ ) (lumen) over the square of the distance from the light source.

$$E = \frac{\phi}{d^2}; E_1 d_1^2 = E_2 d_2^2; \frac{E_1}{E_2} = \frac{d_2^2}{d_1^2}$$

(1) Optical distance law

Illumination is inverse to the distance from the reflector to the target location. An expected efficiency needed to have approximately 96,000 or 800 W/m<sup>2</sup> solar irradiance at the solar panel, which the mirror is likely to reflect at least 80 to 90 percent of sunlight to meet expectations.

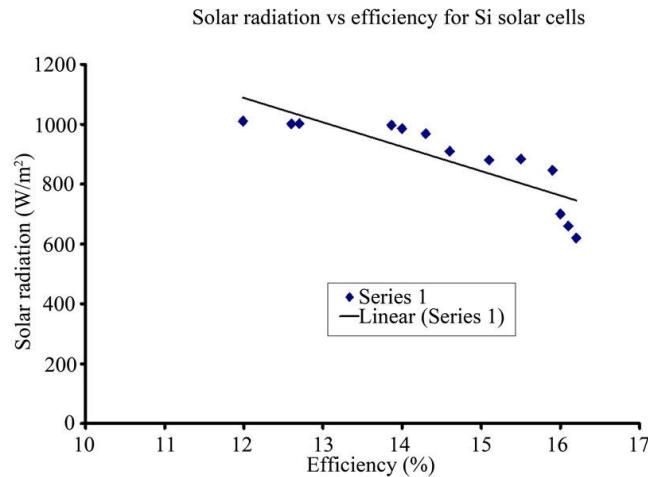


**Figure 3.7.** Solar radiation vs. efficiency for silicon solar cells  
from Accreditation A. Ibrahim, "Analysis of Electrical Characteristics of Photovoltaic Single Crystal Silicon Solar Cells at Outdoor Measurements," Smart Grid and Renewable Energy, Vol. 2 No. 2, 2011

The size of the mirror also needs to be efficiently large to cover an area of solar panels. As stated, there is a loss of illumination when there is a long distance. According to previous technologies, a mirror with a surface area of  $17 \text{ m}^2$  can redirect a light area of approximately  $200 \text{ m}^2$ . An efficient field of solar panels can be used based on the size of most common solar panels. The area is proportional to weight. Hence, the reflector must minimize weight by utilizing the most efficient size.

Other materials, such as Mylar, beryllium, or Titanium, can be considered. Mylar, or BoPET (biaxially oriented polyethylene terephthalate), is a polyester film rather than metal. Mylar is inexpensive compared to glass, with lightweight, high durability, and high reflectivity. Mylar's flexibility can be folded into smaller area configurations for transport, shown below in Figure 3.8. Mylar reflectivity is around 90 percent. Mylar can be fabricated as a coating to reinforce a chosen metal. A disadvantage is that the fabrication process can be complicated to coat the metal with mylar.

The size of the mirror also needs to be efficiently large to cover an area of solar panels. As stated, there is a loss of illumination when there is a long distance. According to previous technologies, a mirror with a surface area of  $17 \text{ m}^2$  can redirect a light area of approximately  $200 \text{ m}^2$ . An efficient field of solar panels can be used based on the size of most common solar panels. The area is proportional to weight. Hence, the reflector must minimize weight by utilizing the most efficient size.

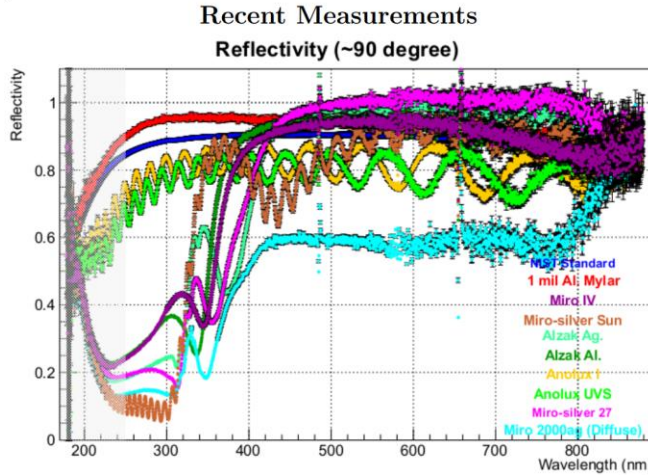


**Figure 3.8.** Mylar reflectivity  
by Dustin McNulty, “Reflectivity Measurements,” Idaho State University

James Webb's telescope shows that Beryllium is an effective metal for fabricating mirrors for space environments. Beryllium is a durable and lightweight material that can be used as a base to increase durability. This material can be expensive and require special handling due to the toxic nature of beryllium dust. Titanium has high durability, and heat conductivity, which can be used to fabricate the backing of mirrors. Titanium is one of a few paramagnetic materials which can improve maintenance. Due to this property, an electric current can remove lunar dust.

### 3.1.6 Vectoring and Positioning / Solar Tracking Algorithm

**Table 3.8.** Comparation between solar tracking algorithms

by Authors with ChatGPT and Google Scholar

Algorithms	Heliostat	Kalman Filtering	Skyview Factor	Ray Tracing	Two-axis Solar Tracking System	Sun tracking Photodiode
<b>Financial Cost</b>	Open Source	Ambiguous	Open Source	Not available	Open Source	No available
<b>Sensor</b>	Ambient Light	Ambient Light	Ambient Light	Ambient Light	Ambient Light	Photodiode
<b>Algorithm code library</b>	Available on GitHub	Available in python	Available on GitHub	Available in Research paper	Available in GitHub	Not available
<b>Efficiency</b>	High	Low	Medium	Medium	High	High
<b>MCU compatibility</b>	Good (C Language)	Fair (Python)	Bad (R Script)	Good (C Language)	Good (C Language)	Bad (No code)
<b>Additional Requirements</b>	Change to an algorithm to change light	Compass Reading or gyroscopic data				

	measuring location					
--	--------------------	--	--	--	--	--

### 3.1.6.1 Heliostat's Algorithm

Heliostat is a mechanism of redirecting sunlight to a specific target using a mirror. The target is a camera as a digital input to read in light intensity at a particular hour of the day, such that the sun's location can be determined. The light's trajectory from the sun can be used to calculate the best angle to reflect the sunlight to a specific area, as requested by the facility. A basic heliostat structure can be seen in Figure 3.9. camera C is looking into mirror H as an anchor, and based on the direction of the reflected line of light c, the mirror angle of a can be calculated to point toward point A.

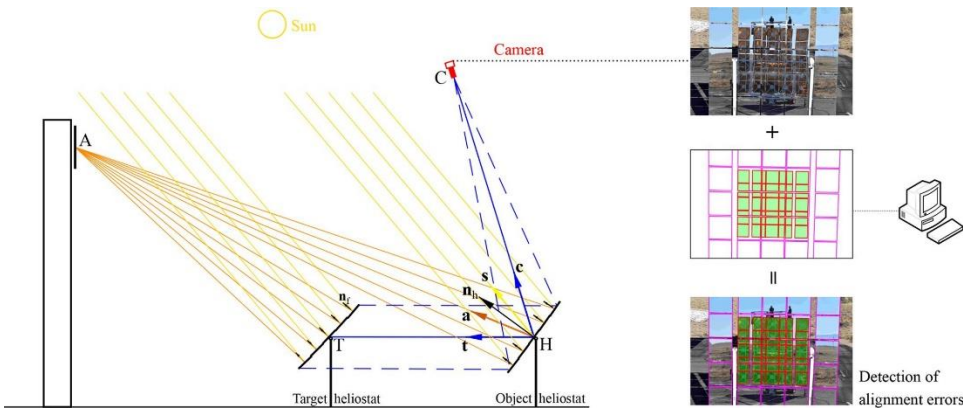


**Figure 3.9. Heliostat reflection mechanism**

by Alberto Sánchez-González, Julius Yellowhair, "Reflections between heliostats: Model to detect alignment errors," Solar Energy, Volume 201, 2020, Pages 373-386, ISSN 0038-092X, <https://doi.org/10.1016/j.solener.2020.03>.

The heliostat can be calculated using an algorithm; according to Figure 3.10, we can realize an equation (2) such that:

$$\frac{d}{r} = \frac{\sin(\theta)}{\sin(2\theta - \phi)}$$

(2) *Heliostat light angles*

This is based on the law of sine to calculate the angle, TCB at the center of the reflection circle,  $\phi$  is the rotation origin, and T is the target location. The angle variable  $\theta$  is unknown and can be calculated using geometry such that  $\frac{\phi}{2}$  is the limit of an iterative process.

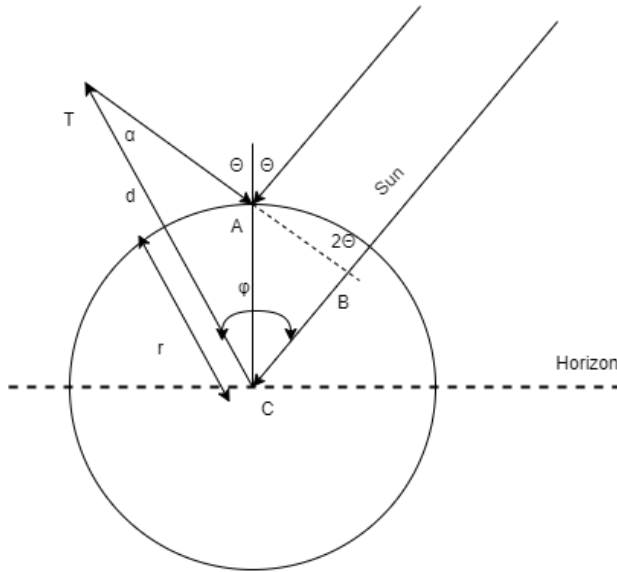


**Figure 3.10.** Reflection of light's diagram from instructible by Authors

An algorithm can be realized as equation (3), with  $n$  being the rotating process iteration. This algorithm is the base to find the highest angle of the lumen to the reflector. However, the mirror needs to be rotated in 2 different axes based on incoming requests rather than automatically shine to a fixed position—an additional algorithm based on the grid network to pinpoint a location.

$$\frac{d}{r} = \left| \frac{\sin\left(\left(\frac{x}{2^n} + 2\right)\phi\right)}{\sin\left(\left(\frac{x - 2^n + 1}{2^n + 1}\right)\phi\right)} \right|$$

(3) Heliostat's distance ratio

An additional algorithm of rotation needs to be used to control the reflector. The horizontal axis W of the whole tower will rotate according to the sun's position. An additional motor must turn the mirror to control the X and Y axis to point to a pre-determined location based on the network algorithm.

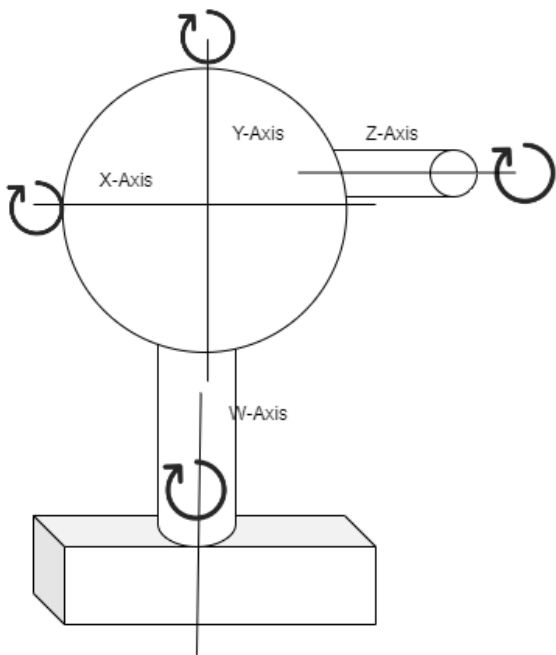


**Figure 3.11.** Rotation of reflector at three different axes, X, Y, Z, and W.  
by Authors

### 3.1.7 Motors

**Table 3.9.** Types of Motors

by Authors with Assistant of ChatGPT and Google Search

Types of Motors	DC Brush	DC Brushless	AC	Stepper	Servo
<b>Financial Cost</b>	Small: \$5-\$50 Medium: \$20-\$100	Small: \$10-\$100 Medium: \$100-\$500	Small: \$50- \$200 Medium: \$200-\$2,000	Small: \$10-\$50 Medium: \$50-\$200	Small: \$50-\$200 Medium: \$200-\$1000
<b>Size</b>	~8mm-35mm	~13mm-35cm	~10cm-30cm	~0.4cm-20cm	~0.4cm-10cm
<b>Torque</b>	0.36-160 nNm	4-400 nNm	203000Ncm-610000Ncm	10-10000Ncm	10-1000Ncm
<b>Speed</b>	5,000 to 14,000 rpm	100,000 rpm	1800-3600 rmp	Low	High
<b>Voltages requirement</b>	4.5V/4.5V/7.0V	4-24V	115V/208V/230V	3V-100V	3V-100V
<b>Durability</b>	High	High	High	High	Low
<b>Weight</b>	0.5-160g	10-1000g	750g	150-5000g	

AC motors have high speed and high torque, which are out of the needed constraints. Additionally, this type of motor requires an AC power supply, which is not compatible and inefficient with the planned power source setting of solar charging. The voltage rating and price for this type of motor

also exceed the expected financial and power budget. Even though DC motors with both brushless and brush needed a DC power supply, required a higher voltage rating than the rest of the motor types. DC motor might provide high speed and high torque. The project, however, does not require these properties.

Servo motors are inexpensive, small, and lightweight coupled with high torque. However, with low durability, generic brands can be used but need to be replaced with industrial grade to meet extreme environmental conditions of the moon's surface. The torque required for the w to move the whole tower can be done by servo and stepper motors. However, between these two motor types, a stepper motor is more cost-effective and has higher durability at the specific weight requirement.

Only sizes Small and medium are considered due to the limited torque needed in addition to size, weight, and voltage constraints. The motor speed and acceleration are minimal due to the speed of change in the sun's movements. Three motors must be chosen for axes x, y, and w. In the x and y axis, the torque required is only affected by the weight of a  $2ft^2$  reflector which is 9lbs. Hence, the chosen motor type would be servo to save on financial costs. On the other hand, the torque of the w axis is much higher due to the whole tower's weight and solar panel, which is subject to a more efficient motor and still in low-speed rotation such as a stepper motor. This project uses inexpensive and generic motors due to limited budgets. However, the extreme environment of the moon required more industrial-grade motors, so generic servo motors could not be met.

**Table 3.10. Stepper Motors Comparation  
by Authors with Assistant of ChatGPT and Osmtec's prices**

Motors	Nema 17	Nema 23	Nema 34	Spur Gearbox	Moon's AM Hybrid
<b>Financial Cost (USD)</b>	\$12.33-\$22.29	\$21.89-\$49.51	\$59.93-\$140.70	\$69.48-\$200.63	\$30-\$746
<b>Holding Torque (N*cm)</b>	11-65	55-300	220-1300	500-4000	8-10000
<b>Step Angle</b>	0.9-1.8	0.9-1.8	1.8	1.8	0.9-1.2-1.8
<b>Dimension (mm<sup>3</sup>)</b>	$42 \times 42 \times (21 - 60)$	$57 \times 57 \times (42 - 114)$	$86 \times 86 \times (66 - 151.5)$	$23 \times 23 \times 110; 34 \times 34 \times 169$	$86 \times 86 \times (20 - 177)$
<b>Current Rating(A)</b>	0.31-2.1	0.44-5.66	2.0-5.5	2.8-4.0	0.35-6.3
<b>Wiring Configuration</b>	Bipolar /Unipolar	Bipolar /Unipolar	Bipolar /Unipolar	Bipolar	Bipolar /Unipolar
<b>Torque</b>	High	High	High	High	High
<b>Accuracy</b>	High	High	High	70-90%	High
<b>Acceleration</b>	High	High	High	Low	Low-High
<b>Speed</b>	High	High	High	Low	Low-High
<b>Durability</b>	Medium	Medium	Medium	High	Low-High
<b>Weight (g)</b>	150-500	500-1600	1700-5450	1500-5000	400-4400

Stepper Motors come in a variety; the range of financial costs to fit the project's budget is \$12 to \$389. Additionally, the stepper motors in this range are adequate for w-axis rotation. Due to the heavyweight, the Torque needed to rotate the tower at least 1000 Nema. Hence the stepper motor needs to be at least in the model Nema 34 and above. The spur gearbox was not chosen due to negligible constraints on Earth. The speed and accuracy are low compared to other stepper motors, which can still fit in the declared constraints. Hence, the chosen motor for the two axes is Nema 23. Spur Gearbox would be preferable to operate in the moon environment.

**Table 3.11. Servo Motors Comparation  
by Authors with Information from Amazon and Osmtec's prices**

Motors	MG996R Servo Motor	DS3225 25KG Digital Servo	Brushless industrial Servo
<b>Financial Cost (USD)</b>	\$5	\$17.5	\$279-\$389
<b>Holding Torque (N*cm)</b>	186	205-245	15.5- 1013.33
<b>Dimension (mm<sup>3</sup>)</b>	40 × 19 × 43	120 × 96 × 35	57 × 57 × 70; 86 × 86 × 108
<b>Current Rating(A)</b>	3	2-2.45	~11
<b>Wiring Configuration</b>	Power/Ground/ Signal	Power/Ground/ Signal	Bipolar
<b>Torque</b>	Moderate	High	High
<b>Accuracy</b>	High	High	High
<b>Acceleration</b>	High	High	High
<b>Speed</b>	High	High	High
<b>Durability</b>	Low	Low	High
<b>Weight (g)</b>	55	167	~3000

Stepper motors are precise motors controlled by electrical pulse without needing feedback to sense position. The angles are switched by the current applied to the motor. The motor angles are divided in 360° full rotation with equal steps. Most motors in the current market are hybrid, combining a permanent magnet and variable reluctance. There are two types of windings for two-phase stepper motors, bipolar and unipolar, represented by Figure 3.12.1,2. Bipolar motors offer higher torque and performance but require more complex wiring and motor drivers. Unipolar motors are simpler to wire but may have slightly lower performance. Since the reflector is heavy, high torque is preferable and bipolar motors are more suitable.

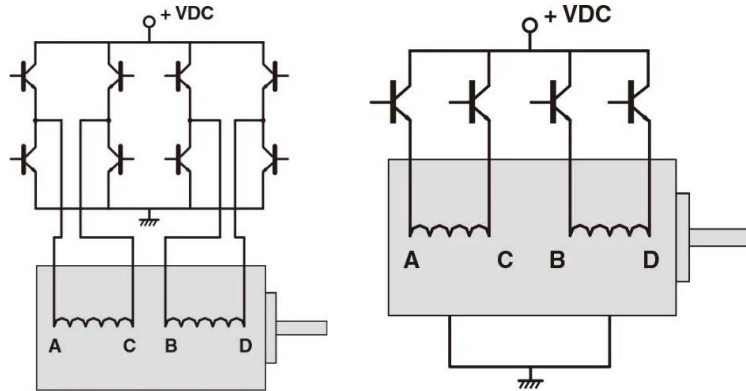


**Figure 3.12.** (1) Bipolar and (2) Unipolar drivers of stepper motor by moonsindustries

The rotation length is related to the number of pulse A, as shown in equation 4. The step angles ( $\theta_s$ ) the angular distance each motor step covers. Most common stepper motors have a step angle of 1.8 degrees per step or 0.9 degrees per step (half-step mode). Smaller step angles provide finer resolution and better positioning accuracy, but typically result in lower torque. The total angle  $\theta$  can be divided into many different steps, shown in Figure 3.13. Consider the required accuracy and resolution for the reflector and tower rotation. Smaller step angles and higher resolution can provide finer positioning, but factors like mechanical play and system limitations can affect the overall accuracy. The w-axis needs less precision due to the sun's wide range of light intake. However, due to distance correction, the precision of the reflector's x and y axis needed to be high for accurate calculation.

$$\theta = \theta_s \times A; N = \frac{\theta_s}{360} f$$

(4) Phase calculation

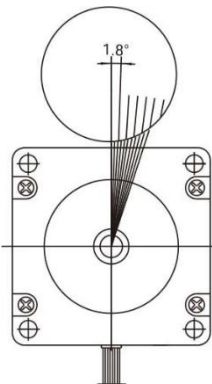


**Figure 3.13.** Division of full rotation  
By moonsindustries

The frequency fluctuation can be used to determine the motor's required rotational speed and acceleration capabilities. Stepper motors have a maximum speed and acceleration limit, so ensure the chosen motor can meet your desired performance requirements. Such a relation can be calculated using equation 5; the higher frequency (f) oscillates, the higher the speed. The speed of

the motor is less of a concern since the rate of the sun is fixed and travels relatively slowly. Only a few urgent situations must be considered at a high rotation speed, such as critical energy requirements for facilities when requested. However, these are out of scope consideration and only applicable for the x and y axis of rotation.

Stepper motors have a torque rating, which indicates the rotational force they can exert. The torque requirement for the tower's x and y axis mostly depends on the load of the reflector, which would be around 15 lbs, as the chosen material for the reflector would be an aluminum sheet, backing, and a coating of mylar. The distance from the rotation axis is relatively short, approximately 30 cm. The w-axis motor's torque must be higher because the distance from the rotation axis can be up to 6m. However, the weight direction of the load is slightly less than the x and y-axis. Additional forces or friction can be considered, increasing the torque rating by approximately 0.01NM. Holding torque refers to the torque the motor produces when it is not rotating and is actively holding a position. The most effective axis that would need to be considered for holding torque would be the y-axis. Nonetheless, the two other axes also need minimal holding torque. Holding torque has minimal impact when considering motor options.

Most stepper motors' physical dimensions and mounting options can be overlooked since the reflector tower's relative size is much more significant. Still, for the most efficiency, the smallest possible measure is preferable—additionally, the weight of the motors needed to be minimal to reduce complications upon transport.

Stepper motors require a specific current to operate correctly. Overdriving or under-driving the motor can lead to performance issues or even motor damage. Stepper motors have a voltage rating that should be compatible with your power supply. Make sure the motor's voltage rating matches the voltage output of your driver or power source. These ratings must match the motor controller, the main MCU, and the power supplies, either the solar panel or the implementing battery.

### 3.1.8 Motor Controllers

The motor controller needs to be compatible with the motors chosen. Hence, the Stepper motor controller is selected to control the w-axis motor, and the Servo Motor controller is considered for the x and y motors. Stepper controllers are preferable due to their lower cost and current rate.

**Table 3.12. Stepper Motor Controller Comparison**  
by Authors with assistant of ChatGPT and pololu Robotics and Electronics.

Controller Models	Pololu A4988	MP6500, Digital CC	DRV8834 Low-Voltage Stepper Motor	DRV8434S, 2A Max.	TB6560	High-Power Stepper Motor Driver 36v4	Gecko Drive G540
Financial cost (USD)	\$13.95-\$14.95	\$6.95	\$7.95	\$12.95	\$11.39	\$29.95	\$289
Max continuous current (A)	1-1.2	2	2	1.2	3.5	4	3.5

<b>Micro stepping</b>	1/16	1/8	1/4-1/32	1/256	1,1/2,1/8,1/16	1/256	2000 PPR
<b>Min-Max Operating Voltage (V)</b>	8-35	4.5-35	2.5-10.8	4.5-48	10-35	8-50	18-50
<b>Special feature</b>	-	digital current control	-	SPI control, stall detection, 8 decay mode options	Able to handle 2A current pull from Nema23	extra-high current, high max voltage, SPI interface, 1/256 micro-stepping, back EMF feedback, stall detection	Operating at 0°C ~ 70°C,

The stepper motor must be directed since it is not dependent on feedback. Motor controllers are devices that are used to coordinate the motor's angles. The controller must be compatible with the type of stepper motor, whether bipolar or unipolar. The motor's voltage and current ratings to ensure they match the controller's specifications. The maximum current rating of the controller should provide enough current to drive your stepper motor without overheating or causing performance issues.

The desired step resolution for the tower application is lower than the regular usage of the stepper motor. Stepper motor controllers offer different levels of micro-stepping, allowing for smoother motion and finer control. The tower only needs a lower range of step resolution to save energy and improve torque. The communication interface supported by the controller needs to match the MCU. Standard interfaces include parallel, USB, serial (such as UART or RS-485), and digital interfaces like SPI or I2C. Depending on the chosen MCU, the motor controller can be adjusted to the correct interface. Different controllers offer various motor control modes, such as full-step, half-step, or micro-stepping. The rotation axis does not need to be high precision and high speed. Hence, a whole step is preferable; a half-step is necessary for the x and y axis because these motors require a slightly higher precision.

Protection features in the controller are desired, such as overcurrent protection, thermal shutdown, and reverse voltage protection. These features help protect the controller and motor from damage and improve system reliability. Additionally, the controller will encase with the microcontroller to avoid extreme weather conditions on the moon's surface.

The software and configuration options are available with the controller. Some controllers come with user-friendly software tools that allow you to configure motor parameters, motion profiles, and control settings conveniently.

**Table 3.13.** Servo Motor comparation  
by Authors with Information from Amazon

Controller Models	WWZMDiB PCA9685	HiLetgo PCA9685	Maker Focus PWM Servo Motor Driver IIC	DEVMO 2PCS PCA9685 PWM Servo Motor Driver
<b>Financial cost (USD)</b>	\$9	\$9	\$18	\$21.99
<b>Max continuous current (A)</b>	3A	3A	3A	3A
<b>Communication</b>	I2C	I2C	I2C	I2C
<b>Min-Max Operating Voltage (V)</b>	5-10	5-10	3.3-5	5

### 3.1.9 Sensor

#### 3.1.9.1 Photodiodes

Photodiodes are semiconductor devices renowned for their ability to convert incident light energy into electrical current, operating based on the principle of the internal photoelectric effect. As particles of light, photons, impinge upon the photodiode's surface, they transmit energy to electrons within the semiconductor material, propelling them to higher energy levels. This extraordinary process spawns electron-hole pairs, where the excited electrons roam freely, while positively charged holes remain behind.

The photodiode boasts a sophisticated p-n junction architecture comprising p-type and n-type semiconductor regions. The p-type region carries an excess of positive charge carriers, or holes, whereas the n-type region brims with negative charge carriers, or electrons. Absorbed photons trigger the formation of electron-hole pairs within this junction. The p-n junction's intrinsic electric field drives electrons towards the n-side and holes towards the p-side, culminating in a potential difference or voltage across the diode.

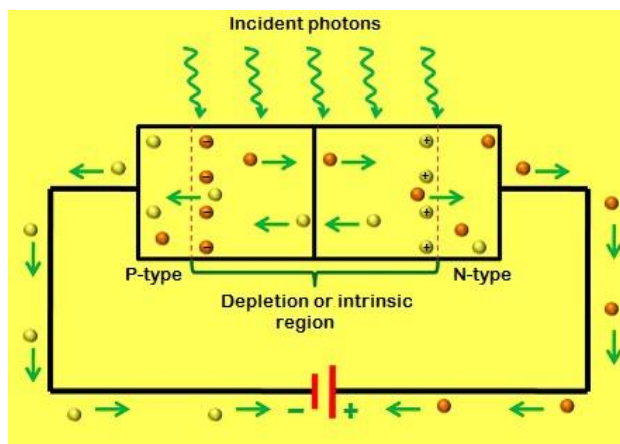


**Figure 3.14.** Photodiode Diagram

*From Image Source: <https://www.electronicshub.org/photodiode-working-characteristics-applications/>*

Linking the photodiode to an external circuit, such as a load resistor, enables the measurement of generated photocurrent as a voltage drop across the resistor. The magnitude of the current is directly proportional to the intensity of the incident light. Photodiodes, renowned for their heightened sensitivity to light, find extensive application in diverse domains, but will be specifically used for light sensors in this project.

Photodiodes are an ideal choice for ambient light sensors due to their exceptional sensitivity and rapid response to changes in light levels. They offer an extensive dynamic range, facilitating the detection of even the most subtle fluctuations in light levels across diverse environments. Moreover, photodiodes can be engineered to operate across a wide spectrum, encompassing visible, infrared, and ultraviolet regions, making them versatile for a multitude of applications. Their compact form factor, low power requirements, and compatibility with electronic circuits make them highly suitable for integration into compact and energy-efficient ambient light sensor devices. By delivering reliable and prompt performance, photodiodes play a pivotal role in ensuring accurate assessment of ambient light conditions, thereby enhancing the functionality and usability of ambient light sensors.

### 3.1.9.2 Phototransistors

Phototransistors, combining the principles of photodiodes and transistors, excel at detecting and amplifying light signals. Similar to photodiodes, they generate electron-hole pairs when exposed to light due to their semiconductor material. However, phototransistors utilize a different semiconductor type, transistors instead of diodes, and differ in how they harness these pairs to control current flow. Most of the time, the phototransistors are made from bi-polar transistors with either n-p-n or p-n-p types.

Comprising three layers (base, emitter, and collector), a phototransistor allows a fraction of light-generated electrons to reach the base-collector junction, creating a current flow from collector to emitter, which can be amplified through transistor action. These pairs can move freely within the semiconductor. In a phototransistor, the thin and lightly doped base region allows a small fraction of light-generated electrons to reach the base-collector junction, creating a current flow from collector to emitter. This current can be amplified through the transistor action of the device.

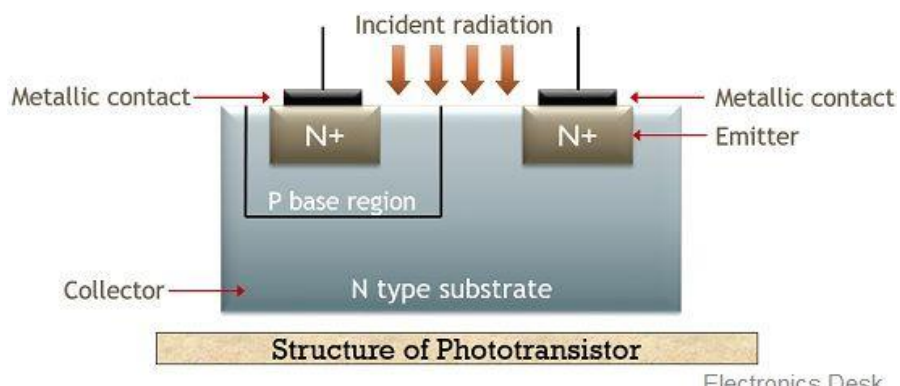


**Figure 3.15. Phototransistor Diagram**  
by Image Source: <https://electronicsdesk.com/phototransistor.html>

Phototransistors boast higher sensitivity and gain compared to photodiodes, thanks to the significant amplification of small photocurrents achieved through transistor amplification. Additionally, their fast response times make them suitable for applications necessitating swift detection of light changes. Nevertheless, for ambient light sensors primarily focused on measuring overall light intensity rather than detecting and amplifying light signals, phototransistors might be considered “overkill” due to their heightened complexity and amplification capabilities, potentially increasing costs without providing necessary benefits for this project.

### **3.1.9.3 Complementary Metal Oxide Semiconductor (CMOS)**

Complementary Metal-Oxide-Semiconductor (CMOS) is another type of transistor-styled approach to this technology, but instead of using the bi-polar transistors, CMOS uses MOSFETs. This comprises of a gate, source, and drain. The MOSFET operates by regulating the current flow between the source and drain regions using an electric field generated by the gate. In CMOS, two types of MOSFETs come into play: nMOS (n-type) and pMOS (p-type). The nMOS transistor conducts current when a voltage exceeding the threshold voltage is applied to the gate, while the pMOS transistor conducts current when a voltage below the threshold voltage is applied. By combining these transistor types, CMOS circuits can implement logic gates and perform a wide range of digital operations.

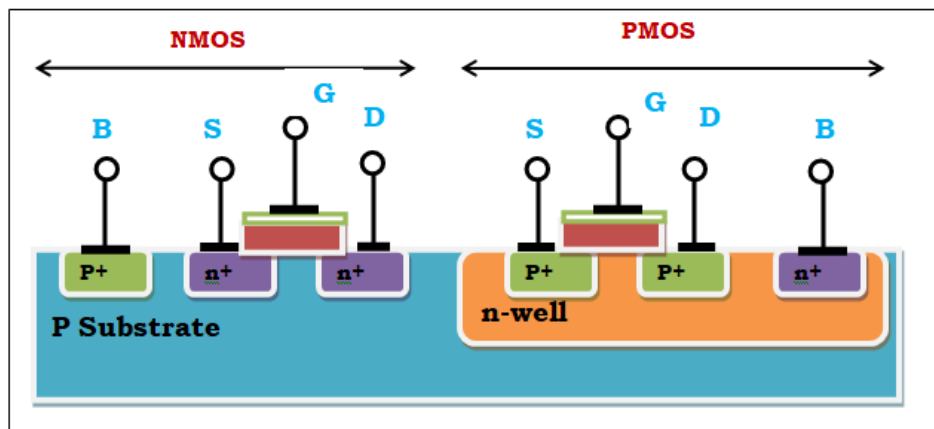


**Figure 3.16. CMOS Diagram**

by Image Source: <https://www.learnelectronicswithme.com/2021/10/cmos-logic-and-their-characteristics.html>

In a light sensor, CMOS technology can be used to create a highly efficient and sensitive device. The CMOS light sensor typically consists of an array of photodiodes, which are integrated with CMOS circuitry on the same chip. Each photodiode operates based on the principles of photodiodes discussed earlier, converting incident light into electrical current.

CMOS technology boasts several notable advantages. It excels in power efficiency, minimizing power dissipation by only consuming energy during switching, making it an excellent choice for portable and battery-powered devices. Furthermore, CMOS circuits demonstrate remarkable noise immunity, operating reliably even in noisy environments. The wide operating voltage range of CMOS devices allows them to function seamlessly with various supply voltages, enhancing their versatility across diverse applications. Overall, CMOS technology has significantly transformed

the semiconductor industry and stands as a fundamental pillar in the realm of modern electronic devices.

CMOS technology, while versatile and powerful, may be considered overkill for an ambient light sensor due to several factors. Ambient light sensors primarily focus on measuring the overall light intensity in an environment rather than detecting and processing complex light signals. CMOS technology, with its extensive integration capabilities and advanced circuitry, is better suited for applications that require high precision, extensive signal processing, and complex functionality.

### **3.1.9.4 Light-Emitting Diode (LED)**

Light-emitting diodes, commonly known as LEDs, are semiconductor devices that can convert electrical energy into light energy. This process, called electroluminescence, occurs when a voltage is applied across the LED, causing current to flow through the device. The layers of semiconductor materials within the LED, typically consisting of a p-type and an n-type layer, enable the release of energy in the form of photons as electrons from the n-type layer combine with holes from the p-type layer at the junction.

LEDs are primarily used as light emitters, but they can also operate in a mode called "photodiode mode" or "LED reverse bias mode," allowing them to function as light sensors. In this mode, the LED is set up in reverse bias, similar to a photodiode. When light shines on the LED in reverse bias, it generates a small current known as the photovoltaic effect.

To utilize an LED as a light sensor, it needs to be connected in reverse bias to a circuit that measures current. The current generated by the LED is directly proportional to the intensity of the incident light, enabling the LED to provide information about the light intensity. However, it's worth noting that LEDs are primarily designed for light emission rather than detection, so their sensitivity in this mode is generally lower compared to dedicated photodiodes.

While it is possible to use an LED as a light sensor, it is not as common or efficient as using dedicated photodiodes. Dedicated photodiodes are purpose-built for light detection, offering higher sensitivity and accuracy. Nonetheless, in certain low-cost or basic applications, utilizing LEDs as light sensors can provide a straightforward and cost-effective solution.

**Table 3.14. Comparison of Light Sensor Technology by Authors**

	<b>Photodiodes</b>	<b>Phototransistors</b>	<b>CMOS Sensors</b>	<b>LEDs</b>
<b>Technology Used</b>	Diode	Bi-polar Transistor	MOSFET	Diode
<b>Response Speed</b>	Very Fast	Slow	Slow	Fast
<b>Produces Current</b>	Yes	Yes	Yes	Yes
<b>Produces Voltage</b>	Yes	No	Yes	Yes
<b>Amplification</b>	No	Yes	Yes	No
<b>Sensitivity</b>	No	Yes	Yes	No

<b>Biassing</b>	Forward & Reverse	Forward	Forward	Reverse
<b>Cost</b>	Low	High	Low	Low

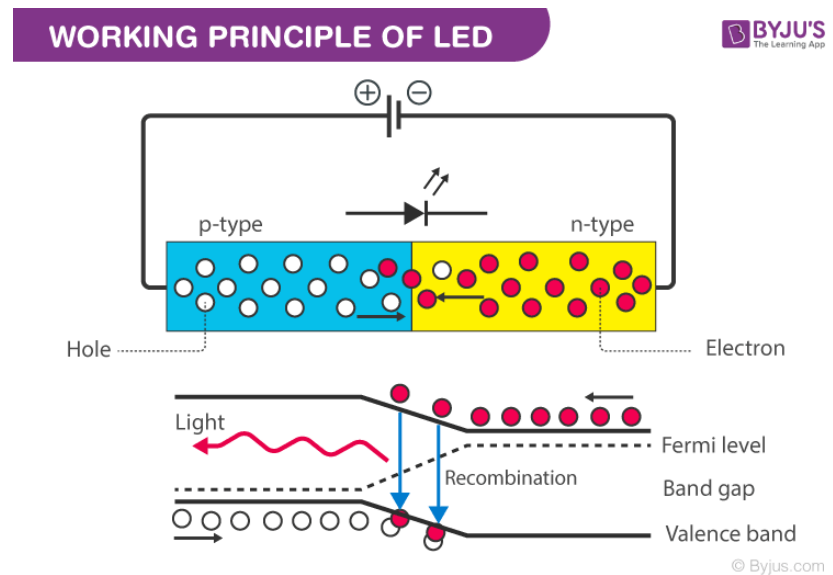


**Figure 3.17. LED Diagram**

by Image Source: <https://byjus.com/physics/light-emitting-diode/>

### 3.1.9.5 TSL2561 Ambient Light Sensor

The TSL2561 is a highly acclaimed digital ambient light sensor developed by Texas Instruments, known for its exceptional performance, seamless integration capabilities, and extensive feature set, making it a top choice for a wide range of applications. Its standout feature is its precise measurement of visible and infrared light levels, ensuring accurate illuminance readings across diverse lighting conditions. With its wide dynamic range, the TSL2561 effectively handles environments with both low and high light intensities, delivering consistent measurements in various scenarios. This adaptability enables the sensor to provide precise results in any lighting condition. Additionally, the TSL2561 simplifies interfacing with microcontrollers or digital systems by incorporating an analog-to-digital converter, streamlining data exchange and configuration.

The TSL2561 seamlessly integrates into projects through its digital output, simplifying the development process. Its digital interface enables smooth data transfer and configuration, facilitating easy integration with microcontrollers. The sensor's programmable interrupt capabilities allow users to define specific light level thresholds that trigger alerts or actions, making it ideal for applications requiring precise light control. Despite its powerful capabilities, the TSL2561 maintains a compact size and low power consumption, making it well-suited for battery-powered devices and space-constrained applications. Its small form factor ensures easy integration into compact designs without compromising performance, while its energy-efficient nature extends device battery life.

The TSL2561 ambient light sensor offers seamless integration with microcontrollers, providing a convenient option for projects requiring light sensing capabilities. Its digital output interface allows for communication with microcontrollers using standard digital protocols like I2C or SMBus, eliminating the need for complex analog circuitry. This simplifies the connection process and enables seamless data transfer between the sensor and the microcontroller. Additionally, the TSL2561 incorporates built-in functionalities that enhance usability. By integrating an analog-to-digital converter, the sensor eliminates the need for external ADCs, enabling direct reading of digital illuminance values. This significantly reduces circuit design complexity and streamlines integration. Moreover, the TSL2561 provides programmable interrupt functionality, allowing users to set light level thresholds that trigger interrupts on the microcontroller. This simplifies the implementation of light-based triggering or control systems by offering a straightforward approach to respond to changes in light levels.

The TSL2561 ambient light sensor delivers cost-effective benefits for projects requiring light sensing capabilities. Firstly, it combines the functionality of a photodiode, amplifier, and analog-to-digital converter into a single chip, reducing the need for additional components and simplifying circuit design, leading to cost savings. The elimination of extra components reduces material and manufacturing costs, making the TSL2561 an economical choice for system development. Additionally, the widespread adoption and popularity of the TSL2561 result in economies of scale, enabling higher production volumes and competitive pricing, further enhancing cost-effectiveness. The sensor's low power consumption minimizes energy requirements, prolonging the battery life of portable or battery-powered devices.

### **3.1.9.6 BH1750 Ambient Light Sensor**

The BH1750 is a widely used ambient light sensor renowned for its accuracy, reliability, and user-friendly features. Developed by ROHM Semiconductor, this sensor employs a digital light intensity sensing method, eliminating the need for complex analog circuitry. It incorporates a built-in analog-to-digital converter (ADC), enabling direct digital output of light intensity values. This simplifies integration and ensures precise measurements. The BH1750 seamlessly interfaces with microcontrollers and digital systems through standard protocols like I2C or SMBus, facilitating effortless integration into existing designs.

For our project, the BH1750 ambient light sensor offers significant advantages, particularly its low power consumption and compact size. In a senior design project where energy efficiency and space optimization are crucial, the BH1750's low power consumption ensures efficient operation without excessive power drain. This is particularly beneficial for battery-powered devices or long-term operating systems. Furthermore, the sensor's compact size allows seamless integration into our project design without occupying excessive space. This is particularly valuable as senior design projects often involve multiple components and sensors within limited physical constraints. By incorporating the BH1750, our project can leverage its energy-efficient performance and compact form factor, enabling the development of innovative solutions within the project's technical and design limitations. On top of this, the BH1750 is one of the cheapest options on the market, cheaper than almost every other ambient light sensor in the table above.

Among the sensors listed in the table above, the BH1750 ambient light sensor stands out with its highest current draw. This technical characteristic has implications for power-sensitive

applications that require necessary power management. The higher current draw of the BH1750 sensor necessitates careful consideration of power budgets, battery life, and power supply sizing. While the BH1750 sensor excels in providing accurate light intensity measurements and seamless integration capabilities, its higher current draw mandates diligent power optimization strategies to achieve optimal energy consumption and meet power constraints.

### ***3.1.9.7 MAX 44009 Ambient Light Sensor***

The MAX44009 ambient light sensor, developed by Maxim Integrated, is a highly acclaimed component renowned for its exceptional performance and versatility in light intensity measurement. This sensor employs a digital light sensing methodology, eliminating the complexities associated with analog circuitry. It integrates a photodiode, amplifiers, analog-to-digital converter (ADC), and a digital interface into a single chip, streamlining system design and ensuring accurate and precise measurements.

The MAX44009 ambient light sensor stands out from the others in the table above due to its significantly higher lux range, providing exceptional light intensity measurement capabilities across a wide spectrum of illumination levels. With a lux range that surpasses that of comparable sensors, the MAX44009 excels in accurately capturing and quantifying light levels in environments with both extremely low and high lux values. By surpassing the lux range capabilities of its competitors, the MAX44009 establishes itself as the preferred choice for capturing and interpreting light data across diverse and challenging lighting conditions, ensuring optimal performance and reliability in demanding environments, such as the moon.

Among the sensors listed in the table above, the MAX44009 ambient light sensor distinguishes itself with its exceptional feature of having the lowest current draw. This attribute positions the MAX44009 as an ideal choice for power-constrained applications and energy-conscious designs. With its remarkably low current draw, the MAX44009 operates with optimal efficiency while consuming minimal power, making it highly suitable for battery-powered devices and power-sensitive systems. Despite its low power consumption, the MAX44009 delivers outstanding performance, providing precise and reliable light intensity measurements across a wide range of illumination levels.

With its compact form factor, the MAX44009 can be easily incorporated into space-constrained designs without compromising performance. Its small size allows for flexible placement and integration into various projects. Leveraging its high level of integration, accuracy, and low power consumption, the MAX44009 is extensively utilized in applications such as automatic lighting control, display brightness adjustment, and energy management systems.

In summary, the MAX44009 ambient light sensor offers exceptional performance and versatility in light intensity measurement. Its digital light sensing methodology, wide dynamic range, digital interface with I2C compatibility, low power consumption, and compact form factor position it as a preferred choice for developers and engineers seeking a reliable and high-quality ambient light sensing solution.

### **3.1.9.8 TSL2572 Ambient Light Sensor**

The TSL2572 ambient light sensor, developed by Texas Instruments, is an exceptional device engineered for precise and reliable light level measurements across diverse applications. It integrates a cutting-edge photodiode array, analog-to-digital converter (ADC), and digital interface into a single chip, enabling seamless integration and simplifying circuit design complexities. With an impressive dynamic range, the TSL2572 surpasses expectations by accurately capturing light intensities across a wide spectrum, ranging from ultra-low to extremely high levels, while maintaining unparalleled accuracy and linearity.

Incorporating dual photodiodes for both infrared and visible light, this sensor delivers unparalleled versatility and adaptability in light sensing applications. Leveraging advanced digital signal processing techniques, the TSL2572 effectively suppresses noise and enhances sensitivity, ensuring consistent and reliable readings even in challenging environments. Its adjustable gain control feature empowers users to optimize sensor performance for specific lighting conditions, offering unmatched customization.

The TSL2572 ambient light sensor distinguishes itself with its exceptionally low current draw, making it an outstanding choice for applications with stringent power constraints. In comparison to the other sensors in the table above, the TSL2572 showcases remarkable efficiency in power consumption. This ultra-low power operation is especially beneficial in battery-powered devices and energy-efficient systems, where maximizing battery life is of paramount importance. By operating on minimal power, the TSL2572 enables extended operational durations and minimizes the frequency of battery replacements or recharging. With its low current draw, the TSL2572 establishes itself as a top-tier solution for applications that demand both energy efficiency and long-lasting performance.

The TSL2572 ambient light sensor outshines its counterparts in the table above with its significantly smaller form factor, making it a superior choice for this project where space optimization is critical. Compared to the other sensors, the TSL2572 boasts a compact design that minimizes its footprint without compromising its performance capabilities. This compact size allows for seamless integration into space-constrained designs, making it particularly advantageous in limited physical dimensions. The TSL2572's smaller size enables greater flexibility in design layouts and facilitates the development of sleek and compact devices without sacrificing functionality. With its superior small size, the TSL2572 sets itself apart as the preferred solution for this project that demand both high-performance ambient light sensing and efficient use of space.

Employing a standard I2C digital interface, the TSL2572 facilitates seamless communication with microcontrollers and digital systems, elevating convenience, and compatibility. Overall, the TSL2572 ambient light sensor stands as a robust solution, equipped with a comprehensive feature set, unrivaled accuracy, and effortless integration, making it an ideal choice for a broad range of applications requiring precise light sensing capabilities.

### **3.1.9.9 AP3216 Ambient Light Sensor:**

The AP3216 is an advanced ambient light sensor developed by Diodes Incorporated. It incorporates a dual-channel analog-to-digital converter (ADC) for accurate and high-resolution

conversion of light signals into digital data. The AP3216 has a wide dynamic range and exceptional sensitivity that allows for precise capturing with subtle variations in light intensity, ensuring reliable readings across diverse lighting conditions. It is very small in comparison to other ambient light sensors and ranks third on the table for smallest size. Its low power consumption makes it well-suited for integration into space-constrained and energy-efficient electronic devices and systems.

The AP3216 is a highly space-efficient ambient light sensor that ranks as the third smallest sensor among those listed in the table. Its compact size allows for seamless integration into electronic devices and systems with limited space. Despite its small footprint, the AP3216 maintains high-performance capabilities, offering accurate and reliable ambient light measurements. This makes it an ideal choice for applications where space optimization is crucial, enabling us to incorporate ambient light sensing functionality without sacrificing valuable real estate on our PCBs. The AP3216's compact form factor combined with its advanced light sensing capabilities makes it a versatile solution for various space-constrained applications.

The AP3216 exhibits the lowest maximum lux value compared to the other sensors listed in the table. While it still provides accurate and reliable measurements within its operating range, the lower lux value may limit its effectiveness in scenarios where higher levels of illumination need to be detected or measured. This characteristic makes the AP3216 less advantageous for this project that require sensing in extremely bright or high-intensity lighting conditions on the moon. However, in environments where lower lux levels are sufficient, the AP3216 can still offer reliable performance and precise ambient light sensing capabilities.

The AP3216 is a standout choice when it comes to cost-effective ambient light sensors in the table. Its competitive pricing provides an attractive option for our project with a limited budget, while still ensuring essential features and reliable performance. We are particularly drawn to its affordability, as it aligns well with our project's cost constraints. Moreover, the AP3216 maintains its effectiveness by delivering accurate ambient light sensing capabilities across various lighting conditions. Its compact design and low power consumption further enhance its value, making it a valuable asset for our specific project requirements.

### ***3.1.9.10 VL6180X TOF Proximity sensor and Ambient Light Sensor:***

The VL6180X sensor, developed by STMicroelectronics, is an advanced proximity and ambient light sensing solution that incorporates Time-of-Flight (ToF) principles for accurate distance measurements and ambient light level detection. The sensor utilizes a combination of an infrared emitter, a photodiode array, and integrated digital signal processing to achieve high-precision proximity sensing in various environmental conditions.

One downside of this product is that it has proximity sensing, which will not be needed for this project and is extra resource which is unnecessary. While its proximity sensing feature will not be needed for this specific project, the sensor's ambient light detection functionality can still be highly beneficial. The VL6180X offers accurate and reliable ambient light level measurements, allowing you to gather valuable data about the surrounding light conditions. This information can be utilized for tasks such as adjusting display brightness, implementing energy-saving strategies, or optimizing lighting control systems.

Among the sensors listed in the table, the VL6180X stands out with its impressive max lux value, ranking third highest. This sensor offers accurate ambient light level measurements across a wide range of lighting conditions. With its advanced photodiode array and integrated digital signal processing, the VL6180X provides reliable lux readings, enabling precise assessment of light intensity. This high lux value is particularly advantageous for this project where accurate ambient light detection is critical.

### ***3.1.9.11 APDS-9960 Ambient Light Sensor:***

The APDS-9960 is an ambient light and proximity sensor developed by Broadcom. It integrates multiple sensing capabilities into a single compact module, making it suitable for various applications. The sensor utilizes integrated IR LED and photodiodes to accurately measure ambient light levels while also incorporating proximity sensing functionality, allowing detection and proximity measurements of objects near the sensor. Its digital output interface simplifies integration with microcontrollers, while its low power consumption ensures efficient operation in battery-powered devices.

While the APDS-9960 is a highly capable ambient light and proximity sensor, its inclusion of proximity sensing functionality makes it a disadvantage for this project. The project requirements do not involve proximity detection or the need for proximity measurements. Therefore, the inclusion of this feature adds unnecessary complexity and potentially increases the cost of the sensor. In this context, a sensor without proximity sensing capabilities would be more suitable, as it would better align with the specific needs of the project, ensuring a more streamlined and cost-effective solution.

The APDS-9960 ambient light and proximity sensor presents a clear disadvantage when compared to the other products listed in the table due to its lowest maximum lux value. With its limited lux range, the APDS-9960 may not be suitable for this project that requires accurate light measurements in high-intensity lighting conditions while looking at the sun. This drawback restricts its effectiveness and versatility, particularly in environments with bright illumination. Other sensors in the table offer higher lux ranges, enabling more comprehensive light sensing capabilities and providing more accurate readings across a wider range of lighting scenarios.

The APDS-9960 ambient light and proximity sensor stands out as a drawback among the other products in the table due to its highest cost. The elevated price of the APDS-9960 may pose a challenge for projects with budget constraints, as it requires a greater investment compared to the other sensors. On top of this, this ambient light sensor offers the lowest lux value for the highest price, showing it to be unreasonable for this project.

### ***3.1.9.12 SI1145 Ambient Light Sensor:***

The SI1145 ambient light sensor, developed by Silicon Laboratories, is a highly capable and versatile sensor designed for precise measurement of ambient light levels. Its advanced architecture integrates multiple sensing channels, including infrared, visible, and ultraviolet light, enabling accurate detection and characterization of different light sources. The SI1145 sensor utilizes sophisticated algorithms and signal processing techniques to deliver reliable and high-resolution light intensity measurements. Its comprehensive feature set, including programmable

LED drivers and an I2C interface, further enhances its flexibility and ease of use in various electronic systems, such as microcontrollers.

The SI1145 ambient light sensor distinguishes itself with its impressive maximum lux value, ranking as the second highest among the sensors listed in the table. This exceptional lux range enables the SI1145 to accurately measure and monitor a wide spectrum of light intensities, making it an advantageous choice for our application where precise illuminance readings are crucial. Its ability to capture even subtle variations in light intensity makes it an asset for this project requiring accurate and versatile ambient light sensing capabilities.

The SI1145 offers a diverse range of sensing capabilities, making it an excellent choice for our project. With its ambient light sensing, IR sensing, and UV sensing capabilities, the SI1145 provides a comprehensive solution for capturing and analyzing various types of light. Its ambient light sensing feature allows for accurate measurement and monitoring of light levels in different environments. The IR sensing capability enables the detection of infrared light, which can be useful in applications such as proximity sensing or gesture recognition. Additionally, the UV sensing functionality allows for the measurement of ultraviolet light levels, enabling applications that require monitoring of UV radiation exposure. The SI1145's versatility in detecting multiple types of light makes it a valuable and flexible option for our project's requirements.

### ***3.1.9.13 VEML7700 Ambient Light Sensor:***

The VEML7700 is an ambient light sensor and proximity sensor that was developed by Vishay Semiconductors is newer and capable light sensor that is being considered for this project. The VEML7700 has very advanced spectral responsiveness which mimics the likeness of a human eye. This allows the sensor to have measurements that accurately represent that of a human. The VEML7700 uses both I2C and ADC which are very important to relay numbers to the microcontroller in an organized and standardized method.

One part of this sensor that is not necessary is the fact that it has a proximity sensor attached to it. This will not be necessary for our project. Even though the proximity sensing is not necessary for this project, the ambient light sensing for this product is very helpful to the project because it still has a high lux value compared to some other products without sacrificing on price. Even with it having the proximity sensing, this sensor is still one of the cheapest options on the tables below.

Another reason that this light sensor is very good is because it can easily be fabricated on our PCB for the project. Unlike some other light sensors, this can be placed on our PCB much easier than some other products because of its pinout and mounting holes. Its small form factor ensures it can be seamlessly integrated into PCB designs, making it suitable for space-constrained applications. Its size is another advantage because it will save space for other peripherals for the project altogether.

An advantage of the VEML7700 ambient light sensor is its low operating current. The low operating current allows for power saving on the mirror tower which will have battery and solar charging. With its low operating current, it allows for other peripherals on the tower to have longer lasting and sustained power, which keeps the tower operating longer. On top of this, it also gives off less heat which allows it to be more environmentally friendly and efficient for the project.

Lastly, the VEML7700 is great for this project because of its broad range of lux values that it can measure. Because of this range, it can accurately measure different levels of sunlight to accurately determine the best position for the mirror to operate. If the lux value was lower, it might cut off the best possible position for the mirror to operate at, which would not be a complete and fully functioning mirror reflection.

**Table 3.15. Part 1 ALS Comparison**

from TSL2561: <https://www.mouser.com/datasheet/2/737/tsl2561-932888.pdf>,

BH1750: <https://cdn-learn.adafruit.com/downloads/pdf/adafruit-bh1750-ambient-light-sensor.pdf>,

MAX44009: <https://www.analog.com/media/en/technical-documentat>,

TSL2572: [https://ams.com/documents/20143/36005/TSL2572\\_DS000178\\_5-00.pdf](https://ams.com/documents/20143/36005/TSL2572_DS000178_5-00.pdf),

and AP3216: <http://www.datasheet-pdf.com/PDF/AP3216C-Datasheet-LITE-ON-1016217>

	<b>TSL2561</b>	<b>BH1750</b>	<b>MAX44009</b>	<b>TSL2572</b>	<b>AP3216</b>
<b>Cost (USD)</b>	\$5.95	\$2.90	\$5.96	\$14.95	\$2.30
<b>Measuring Principle</b>	Photodiodes	Photodiode	Photodiode	Photodiode	Photodiodes / IR-LED
<b>Max Lux</b>	40000	65000	188000	60000	23000
<b>Ambient Light Sensing</b>	Yes	Yes	Yes	Yes	Yes
<b>IR Sensing</b>	Yes	No	No	Yes	Yes
<b>UV Sensing</b>	No	No	No	No	No
<b>Operating Voltage (V)</b>	3.6	4.5	3.6	3.8	4.5
<b>Operating Current (mA)</b>	0.5	7	0.0003	0.25	0.7
<b>I2C</b>	Yes	Yes	Yes	Yes	Yes
<b>SMBus</b>	No	No	Yes	Yes	No
<b>ADC</b>	Yes	Yes	Yes	Yes	Yes
<b>Size (mm^2)</b>	240.24	257.15	4	4	9.84
<b>Operating Temperature ( C )</b>	[-30 - 70]	[-40 - 85]	[-40 - 85]	[-30 - 70]	[-40 - 85]
<b>C/C++ Libraries</b>	Yes	Yes	Yes	Yes	Yes

**Table 3.16. Part 2 ALS Comparison**

from VL6180X: <https://www.st.com/resource/en/datasheet/vl6180x.pdf>,

APDS-9960: [https://cdn.sparkfun.com/assets/learn\\_tutorials/3/2/1/Avago-APDS-9960-datasheet.pdf](https://cdn.sparkfun.com/assets/learn_tutorials/3/2/1/Avago-APDS-9960-datasheet.pdf),

SI1145: <https://cdn-shop.adafruit.com/datasheets/Si1145-46-47.pdf>, and

VEML7700 : <https://www.vishay.com/docs/84286/veml7700.pdf>

	<b>VL6180X</b>	<b>APDS-9960</b>	<b>SI1145</b>	<b>VEML7700</b>
<b>Cost (USD)</b>	\$14.49	\$16.50	\$9.95	\$4.95

Measuring Principle	TOF/IR Laser Photodiode	IR-LED, Photodiodes	IR-LED Photodiode	Photodiode
<b>Max Lux</b>	100000	20000	128000	120000
<b>Ambient Light Sensing</b>	Yes	Yes	Yes	Yes
<b>IR Sensing</b>	No	No	Yes	No
<b>UV Sensing</b>	No	No	Yes (extrapolated)	No
<b>Operating Voltage (V)</b>	3	3.8	3.6	3.6
<b>Operating Current (mA)</b>	0.3	0.25	7	0.045
<b>I2C</b>	Yes	Yes	Yes	Yes
<b>SMBus</b>	No	No	No	No
<b>ADC</b>	Yes	Yes	Yes	Yes
<b>Size (mm<sup>2</sup>)</b>	234	9.2984	360	15.98
<b>Operating Temperature ( C )</b>	[-20 - 70]	[-40 - 85]	[-40 - 85]	[-25 – 85]
<b>C/C++ Libraries</b>	Yes	Yes	Yes	Yes

### 3.1.10 Communication technologies

Table 3.17. Communication technologies Comparaisons

Criteria	Wi-Fi	LoRaWAN	Bluetooth	6LoWPAN	Zigbee	Z-Wave
<b>Range (m)</b>	45	15000	10	100	980	800
<b>Data rate</b>	54 Mbps	50 Kbps	1 Mbps	250 Kbps	250 Kbps	100 Kbps
<b>Power consumption</b>	30 uA-250 mA	1 uA-16 mA	9 uA-39 mA	0.3 uA-35 mA	12 uA- 54 mA	1 uA-23 mA
<b>Max devices</b>	255	120	3-4	100	100	232
<b>Scalability</b>	✓	✓	✗	✓	✓	✓
<b>Frequency</b>	2.4/5/6 GHz	902.3-914.9 MHz	2.4 GHz	2.4 GHz	915 MHz/2.4 GHz	908-916 MHz

#### 3.1.10.1 ZigBee

ZigBee is a low-cost, low-power wireless communication standard that works on the 900 MHz and 2.4 GHz frequency bands developed by the ZigBee Alliance. Being based on the IEEE 802.15.4 standard, ZigBee has a low throughput rate, reaching a maximum of 250 kbps; this however allows it to have a peak current consumption of 54 mA; this same standard gives ZigBee built in security through AES128 encryption.

ZigBee has a maximum range of 100 m and is highly scalable, being capable of handling over 64000 nodes per network, moreover, network coordinators may be linked to expand this even further. This is of particularly great use given its popularity (with companies like Texas Instruments and Atmel providing IEEE 802.15.4 compatible chips) as interoperability between certified ZigBee devices is guaranteed.

Working on the 2.4 GHz band is accompanied by a high probability of interference due to its crowdedness, ZigBee looks to alleviate this by utilizing 16 different 5 MHz channels within the band as well as a CSMA-CA protocol.

ZigBee devices are capable of reducing their energy consumption by sleeping, only activating to communicate with other ZigBee devices. Some typical operation times can be seen in the following list.

- New slave enumeration: 30 ms
- Sleep slave to active: 15 ms
- Active slave channel access: 15 ms

These times allow for minimal battery usage, making ZigBee devices a great choice for long-lived applications in areas where a constant power supply may not be guaranteed.

### **3.1.10.2 Z-Wave**

Z-Wave is a proprietary wireless network low bandwidth protocol. Designed for reliable communication in a low cost control network, Z-Wave devices are capable of outputting data at a rate of 40 kbps using 1 mW of power with a maximum possible rate of 100 kbps; these rates are lower than that of other protocols such as ZigBee, which makes Z-Wave inadequate for tasks such as the transfer of a large amount of data or applications where timing is of the essence; another possible flaw may be found within its range, as Z-Wave devices have a max communication range indoors of 50 m.

These faults, however, are offset by the protocol's capacity to transfer a message between nodes, effectively extending the operational range; Z-Wave also operates in a frequency range that avoids Wi-Fi and Bluetooth systems operating on the 2.4 GHz, thus preventing interferences with devices which utilize those protocols.

Being a proprietary protocol, Z-Wave devices are limited to interoperability with products designed around it, moreover, the frequency at which the protocol works differs based on each country's standards (ranging from 865.20 MHz to 921.40 MHz), thus, any two products must work at the same frequency for interoperability between them to exist and any design must be modified should plans for deployment in several regions exist.

### **3.1.10.3 LoRaWAN**

LoRaWAN is a wireless communications protocol designed for long range, low power applications. Its capabilities and properties such as baud rate (0.3 to 50 kbps) and power consumption (up to 50 mW) depend on the device's class of which the following three exist:

1. Class A: The lowest power system, each uplink transmission by the end device is followed by two short downlink reception windows which makes this class useful only in applications that exclusively require downlink communication from a server a short time after the device has sent an uplink transmission as any other transmission will not be received until the end device initiates a new uplink transmission.

2. Class B: These devices add extra reception windows at pre scheduled times on top of Class A's windows, this is controlled by the gateway in order to allow the server to know when the device is listening. This class consumes a greater amount of power than Class A, but is nonetheless suitable for battery powered devices.
3. Class C: This class is capable of receiving downlink transmissions nearly all the time, only closing the windows during an uplink transmission, granting it the lowest latency out of all three classes. This however also makes it the most power hungry, making this class unsuitable for battery powered devices except for irregular tasks such as firmware updates where a temporary switch between classes may be used to maintain a steady connection.

Its operational range goes from 5 km in urban areas to 15 km in rural areas. LoRaWAN is capable of operating in conjunction with other protocols such as Wi-Fi or Bluetooth in order to leverage existing networks, increase range, improve battery life, etc. enabling the use of several protocols to delegate tasks.

In a similar manner to other protocols, the frequency band at which devices are allowed to operate changes based on the country and plan being used, with the allowed frequencies ranging from 433 to 928 MHz, as such, special care must be taken when designing devices which may be deployed in areas with different plans.

#### **3.1.10.4 6LoWPAN**

Developed by the Internet Engineering Task Force (IETF) 6LoWPAN is an adaptation layer for the IEEE 802.15.4 standard focused on optimizing the transmission of IPV6 packets over low power (peak current consumption of ~20-35 mA), low throughput networks (usually limited to 250 kbps) that work in the 2.4 GHz band, this is accomplished via stateless or shared-context compression which can reduce header sizes to, in the best case scenario, 4 bytes.

Its operational range is that of 10-100 m when working under the 2.4 GHz band and a theoretical maximum of several km on the sub-G (900 MHz) band. Link layer security is ensured via the Advanced Encryption Standard (AES) protocol while end-to-end security is attained by means of an adapted IPSec protocol on the network layer and Datagram Transport Layer Security (DTLS) on the application layer.

Being an adaptation layer, 6LoWPAN is capable of operating with external IPv6 networks such as Wi-Fi, allowing interaction with a large number of devices.

#### **3.1.10.5 Bluetooth**

Bluetooth Low Energy is a WPAN technology meant for devices operating at a very low power. Its capable of outputting data at rates from 125 kps all the way to 2 Mbps while having a theoretical outdoors range of over 2000 m when utilizing the maximum possible transmit power of 100 mW, this however comes at the cost of increased power consumption which must be taken into account should a battery powered device be designed.

Contrary to other standards, Bluetooth LE works in the 2.4 GHz frequency band, transmitting data using 40 channels, this improves interoperability with other Bluetooth devices and reduces part of

the burden of design as devices will use the same band worldwide, this however makes it susceptible to interference from other devices utilizing the same band such as microwave ovens or Wi-Fi enabled devices; Bluetooth attempts to remedy this by utilizing frequency-hopping spread spectrum transmission to change between a set narrowband frequencies on the fly.

### 3.1.10.6 Wi-Fi

Wi-Fi is a family of network protocols based on the IEEE 802.11 series of standards, of which IEEE 802.11ax, dubbed Wi-Fi 6 by the Wi-Fi Alliance, is currently in force. It is worth noting that this is not the latest standard, as it is set to be replaced by IEEE 802.11be (Wi-Fi 7) in early 2024, however this section will be focused on Wi-Fi 6 due to the possibility of changes in Wi-Fi 7 between the writing of this document and the date of the standard's release.

Capable of operating with the 2.4 GHz or 5 GHz frequencies and having a theoretical maximum data rate of 2.4 Gbps when utilizing 2 spatial streams with 1024-QAM modulation, Wi-Fi 6 is by far the fastest protocol analyzed here, however, this comes with a lack of range (with a best case scenario reaching a mere 45 m) as well as a large current draw (max ~ 250 mA), making this protocol inefficient in battery powered applications where longevity is imperative. Moreover, the highest data rates are obtained when working in the 5 GHz frequency band, however, the higher frequency causes the waves to have trouble when penetrating solid objects, further reducing its range.

Having been adopted worldwide, Wi-Fi is capable of operating alongside a wide range of devices, making it capable of dealing with a variety of tasks; but its reliance on the crowded 2.4 and 5 GHz bands make interference a likely problem.

### 3.1.11 Batteries

Before delving into the benefits of various battery technologies, first a distinction must be made in the types of battery used. Primary batteries are batteries that are intended for one-time use and not intended to be recharged or cannot be recharged. Secondary batteries are batteries intended to be recharged and maintained over prolonged periods. (Flowers, 2023) For this project, both the batteries for the Mirror Tower and Communication tower should be secondary batteries. The Mirror Tower should be able to sustain itself over sun-less periods. The communication tower should be able to be collected and recharged after its mission for reuse.

Secondary Batteries have many properties that are important to consider. Among them are specific energy, cycle life, charging profile, maintenance requirements, cost, and charge/discharge temperatures. Of particular importance is charge/discharge temperatures and specific energy. Traditionally Nickel-Cadmium (NiCd) or Nickle-Hydrogen (NIH<sub>2</sub>) batteries were used by NASA for spaceflight, however, more recently there has been a transition to Lithium-ion (Li-ion). The transition was mostly driven by higher energy density and relative cycle life improvements offered by Li-ion. (Garcia, 2021) (Leon, 2004) (Halpert, 1986)

**Table 3.18.** A table describing the characteristics of common secondary batteries. (Battery University, n.d.)

Specifications	Lead Acid	NiCd	NiMH	Li-ion
----------------	-----------	------	------	--------

				Cobalt	Manganese	Phosphate
<b>Specific Energy</b>	30-50	45-60	60-120	150-250	100-150	90-120
<b>Internal Resistance</b>	Very low	Very low	Low	Moderate	Low	Very low
<b>Cycle Life</b>	200-300	1000	300-500	500-1000	500-1000	1000-2000
<b>Self-Discharge/month (Room-Temp)</b>	5%	20%	30%	<8%		
<b>Operating Temperatures</b>	-20 to 50 C	0 to 45 C	0 to 45 C	0 to 45 C		
<b>Maintenance Requirements</b>	3-6 Months topping charge	Full discharge every 90 days		Maintenance free		
<b>Safety Requirements</b>	Thermally stable	Thermal stable, fuse protection		Protection circuit mandatory		
<b>Cost</b>	Low	Moderate		High		

Regardless of battery technology utilized, temperature control of the battery is a must. There are no commercially viable batteries that can withstand the Lunar South Pole's 80-300K temperature swings (Mahoney, 2022) without active thermal control.

Another consideration is the type of cycles placed upon the battery. In the intended lunar environment, the sun would be nearly constant, enabling the solar panel to power devices upwards of 85% of the time. (P. Glaser, 2014) This would reduce the number of cycles, and the depth of the cycles significantly.

### **3.1.11.1 Lithium Batteries**

Lithium-Ion (Li-ion) and lithium polymer (LiPo) batteries are attractive due to their high specific energy and are a lightweight commercial-off-the-shelf (COTS) option; however, they suffer from strict charging/discharging requirements due to strict thermal limitations. Li-ion batteries tend to slip into thermal runaway if not carefully monitored and controlled. 18650 cylindrical cells are the standard format for lithium battery cells. There are various types of Li-ion and LiPo batteries with various chemistries, however they tend to have similar characteristics. There are many commonly used ICs to enable the charging of specific models of Li-ion batteries. Li ion batteries require a constant current stage (CC) and a constant voltage (CV) stage of charging. The CC stage is used to raise the State of Charge (SOC) significantly from 0 to 50%, until the CV stage is reached and the current tapers off.

**Table 3.19.** Advantages and Disadvantages of Li-ion cells and batteries for spacecraft applications.  
 (Barrera, 2023)

Advantages	Disadvantages
High specific energy (Wh/kg) and energy density (Wh/L)	Lack of procurement controls on COTS cell suppliers
High coulombic and energy efficiency	Irreversible degradation above +65°C
Long cycle and calendar life characteristics	Cell degradation at high charge rates and low temperatures
Low self-discharge rate	Intolerant to overcharge and overdischarge
Low heat generation during charge and discharge	Added mass and cost due to need for cell-to-cell charge balancing electronics (if required)
High operating cell-level voltage	Added mass and cost due to battery management systems (if required)
SOC can be estimated from cell voltage	Cell and battery safety hazard controls are required
Wide variety of COTS cell designs enables battery design flexibility	Severity and consequences of thermal runaway hazards
Low cost of COTS cell designs	Propagation resistant battery designs add mass, volume, and cost
No need for reconditioning due to no memory effect	Need to comply with Li-ion battery transportation regulations
Various cell geometries enable battery packaging efficiencies	Supply chain risks due to critical raw materials availability
Ability to electrically connect cells in parallel to create a module of higher capacity	
Operating temperature range (-10 to +40°C) reduces thermal management requirements	
Competitive and diverse manufacturing base	

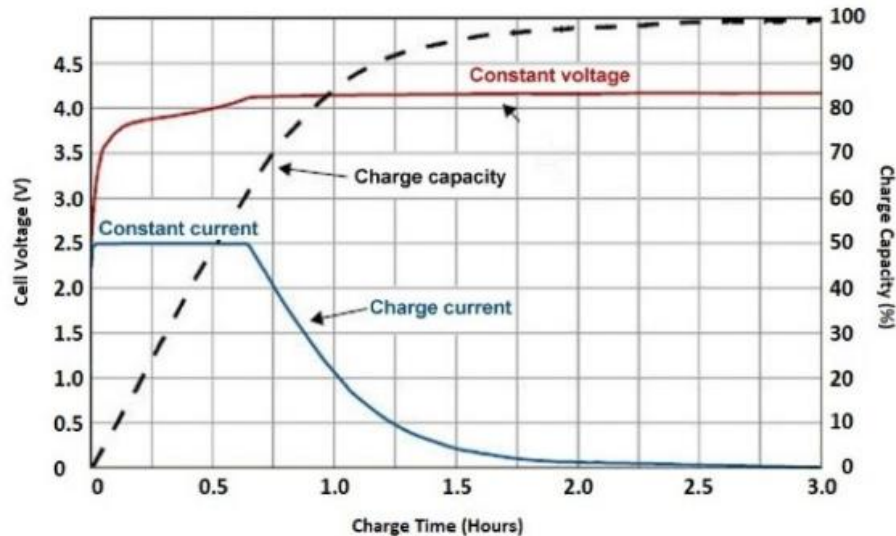


**Figure 3.18.** An image of the Constant Current (CC) and Constant Voltage (CV) charging method of Li-ion batteries

### 3.1.11.2 Lead Acid

Lead acid batteries are an older technology, with plenty of low-cost COTS solutions in various size formats. They are thermally stable and relatively easy to manage, however, they suffer from a low energy density. For the intended purpose of a lunar mission, they do not offer enough weight to performance to be a viable solution. Captive electrolyte lead-acid batteries are particularly attractive due to their low maintenance and the reduced susceptibility to freezing, which is particularly important in the intended application.

### **3.1.12 Development Environment: Languages and Repositories**

#### **3.1.12.1 C**

C is a simple programming language that is very easy to use because it is so simple. C is mostly used for low-level programming and does not have a lot of object-oriented components involved in it. C is mostly used for hardware development and is very popular for embedded and semiconductor programming. The C programming language has many libraries that are written and accessible for anyone using it to solve problems without having to write your own functions. The C language is specifically good for hardware because it allows user to get easy access to the hardware through the language. It is very easy to access registers, memory, and flags using the C language, allowing for users to adjust memory in different hardware that is attached to a C program. C does require compilation so that it can translate high-level language to assembly and then machine code for a computer to execute certain memory operations. Since C is such an old language, it does not have many of the new styles that would be preferred in a project such as object-oriented programming and inheritance. Overall, C is a great option for low level coding and can also be easily used in embedded software, which could be very important for this project which involves multiple microcontrollers.

#### **3.1.12.2 Java**

Java is a programming language with a lot of options for object-oriented and class-based coding. Java is both a programming language and a software platform which makes it very portable and easy to move to different devices. The Java code is compiled to turn it into machine code called Java bytecode which is then run on the machine using the Java development kit (JDK). Unlike C, Java uses object-oriented programming which makes writing code much easier. Key concepts that are included in object-oriented programming that are made easy using Java include, but are not limited to, classes, objects, encapsulation, inheritance, polymorphism, and abstraction. All these processes provide multiple benefits for a team-based project which include code organization, code reusability, scalability, and collaboration. The organization of the code can be kept separate for security reasons but also to make information easy to find. Reusability is important because it allows users to create one object and reuse it multiple times by referencing it after it was written. Scalability is important because it allows programmers to debug easily by testing classes and code independently from one another. Collaboration is the last key advantage of Java because it allows work to be delegated easily by having separate classes and objects between a group of people. Overall, Java seems to be a great option for a programming language because of its portability, built-in software platform, and object-oriented nature.

#### **3.1.12.3 Python**

Python is a high-level programming language that is very powerful because of its capabilities. Python has very simple syntax and is easy to pick up for beginners. Python has many libraries that make it easy to create algorithms by using built-in functions. Python also allows for complex statistical analysis of big data, which make it very useful for machine learning, data science, automation, and software development. Python can also build visual models such as graphs, charts, and 3D plots that are important for data analysis. Another benefit of Python is that it can be used for automation, scripting, and machine learning which can be very beneficial and is very powerful than many other languages cannot provide for. Python allows for object-oriented programming like

Java where you can create classes and objects to keep variables and programming organized. Python includes all the pieces of object-oriented software that includes inheritance, encapsulation, abstraction, polymorphism, classes, and objects. Python also includes important components of object-oriented programming such as method overriding and method overloading which allow for multiple methods of the same name with different arguments. Overall, Python is a very powerful language that would allow for some unique characteristics that other programming languages cannot provide.

#### **3.1.12.4 GitHub**

GitHub is a Git based repository software used to share code between multiple people at the same time. GitHub can be either a private or public, open-source repository. GitHub is a very well-known repository because of its free use for public repositories. GitHub works by using a concept called Version Control, which is where a person in the repository “clones” the code to make changes to it; this process is called branching. When finished with what they want to do, the user then uploads those changes back to the repository for others to see, without affecting whatever was happening before and during the cloning; this process is called merging. This makes collaboration very easy because it allows a group of programmers to edit code as a group but also make individual changes, so they do not get in each other’s way.

#### **3.1.12.5 Bitbucket**

Bitbucket is a Git based repository software that allows a group of people to actively work on a software project together. Like GitHub, a team can own a repository that stores source code and edit it by using Version Control. The big difference between GitHub and Bitbucket is that Bitbucket has Jira and Trello integration built into it. Jira is a tool that actively tracks bugs within a code to allow for easy and simple debugging and creates organization in group-based project management. Jira makes it easy to fix bugs by immediately outlining the issues and prioritizing them in the project. Jira is important for project management because it keeps track of progress and accounts for dependencies within the project. Trello is an interactive software that helps with project management by giving clear and visual representations of team responsibilities and assignments. Trello uses multiple different visual representations such as cards, boards, and lists that make it easy to organize software roles and assignments for certain projects. On top of this, Trello also makes it easy to track members, due dates, attachments, and checklists all in a centralized location to easily manage a project. Even though Bitbucket does include all these benefits, there is a clear downside that it has a cost of use.

### **3.1.13 Antenna**

To ensure optimal functioning of the system, specific attributes are necessary for its antenna. Factors such as directivity, gain, polarization, beamwidth, center frequency, and efficiency play a pivotal role in antenna selection.

In the context of the tower's operations, excessively high directivity is not essential, given the target's variable position in relation to the tower. Consequently, the antenna's capability to both transmit and receive signals in all directions becomes crucial. This accommodates bidirectional communication for both downlink and uplink signals. The concept of gain follows a similar

principle, but now takes potential signal losses into account. When considering the rover's intended use, it's vital to factor in potential signal degradation during transmission.

Linearly polarized antennas may encounter polarization mismatches due to shifts in antenna orientations. To address this concern, circularly polarized antennas offer a more suitable solution. Their inherent resistance to polarization mismatch makes them optimal for scenarios where the rover's antenna orientations may change during movement. Circular polarization maintains consistent polarization characteristics, regardless of the receiving antenna's alignment. This feature ensures dependable communication for a rover in motion, even though it might introduce some added complexity and minor signal losses.

For effective communication between the rover and the tower, a wide beamwidth is essential. It ensures consistent coverage, especially when the rover's exact position might be in flux. This broader beamwidth not only ensures uninterrupted connections but also eases the system's configuration. Using antennas with narrower beamwidths could require continuous tracking mechanisms to maintain a robust link, adding unnecessary complexity.

The antenna's optimal operating frequency should be centered at 2400 MHz to be in sync with the tower's communication frequency. Moreover, efficiency remains paramount. Given the rover's need to operate for long durations without frequent recharges, it's crucial that the antenna operates at peak efficiency. Even the slightest inefficiency could detrimentally affect the rover's overall performance due to power constraints.

### **3.1.13.1 Dipole**

The dipole antenna comes in several variants, each with distinct attributes. The short dipole offers an omnidirectional pattern with a directivity of less than 1.76 dBi. It also boasts a relatively wide beamwidth. While these specifications are desirable, it's important to acknowledge that as directivity increases, the antenna's omnidirectional traits diminish. In most scenarios, an antenna with 3 dBi of directivity is generally considered to retain its omnidirectional quality.

Another concern lies in the linear polarization of the antenna, which could potentially pose challenges during rover movement. Additionally, matching a short dipole antenna proves complex due to its substantial reactance value during load impedance calculations. This can lead to efficiency problems arising from high VSWR (Voltage Standing Wave Ratio). Furthermore, dealing with such high reactance values makes implementing a matching network challenging, resulting in a narrow-band design to uphold signal quality and prevent losses.

Hence, for the project's objectives, the short dipole antenna isn't the optimal choice due to its linear polarization and resulting efficiency concerns. Exploring alternative antennas with higher directivity and more suitable polarization attributes would be preferable to achieve the project's goals and ensure dependable signal transmission.

The dipole antenna has other variations besides the short type. The length of a dipole antenna, whether it's  $\lambda/4$ ,  $\lambda/2$ , or  $\lambda$ , has a direct impact on its directivity. As the antenna approaches a length of 1.25 times its wavelength, there's a notable spike in directivity. Beyond this length, while the directivity still grows, it doesn't do so consistently. When extended, directivity can surge past 1.76 dBi, reaching close to 5.2 dBi. This pronounced rise, in comparison to shorter dipoles, enables the

antenna to direct energy more efficiently. However, the enhanced directivity doesn't automatically make it the best choice for the rover; it might direct excessive energy.

A potential downside is the linear polarization of the antenna, which might not align with the tower communication needs. In terms of impedance, short dipoles are highly capacitive, while half-wave dipoles (just under  $0.5\lambda$ ) resonate, exhibiting zero reactive impedance. This resonance promotes better power radiation (evidenced by low S11 at its resonant frequency) and streamlines the design of the impedance matching network. As a result, the antenna boasts heightened efficiency, only needing to adjust real impedances.

Given the above, the half-wavelength dipole seems most suited for this project, providing an ideal mix of gain and efficiency. Yet, its linear polarization might be a concern for tower communications. In sum, the half-wavelength dipole offers a balanced blend of directivity and efficiency, tailored for the rover's operations.

### **3.1.13.2 Patch**

Patch antennas, also known as microstrip antennas, have the added benefit of being able to be printed directly onto a circuit board. They are known for maintaining a low profile, having a low cost and being very easy to fabricate. Patch antennas usually have a wide range of directivity which enabled a larger flexibility when choosing the most suitable commercially available antenna for the project.

These antennas can be linearly polarized in the horizontal direction but are also available in a circularly polarized form. A circular polarization is suitable for the rover's needs which is a big plus for patch antennas. Patch antennas are known to be narrowband in most cases, generally presenting a bandwidth of 3%. They were also originally designed to operate at 100 MHz, much lower than we are looking to operate at but nowadays there are patch antennas that can operate at higher frequencies like the standard 2400 MHz that the mesh network will operate at. The usual beamwidth of a conventional patch antenna will be 80 degrees in the H-plane and 90 degrees in the E-plane which is not as wide as preferred.

In terms of gain we can reach a maximum of 7-9 dBi when using a patch antenna. Patch antennas have a fairly high efficiency, usually being in the 80-90% range. The center frequency for a patch antenna is calculated in function of its length. There is an inversely proportional relationship between a patch antenna's length and its operating frequency. For the purposes of this project we would be able to reach 2.4 GHz with a patch antenna around 20 cm in length, a fairly practical size.

### **3.1.13.3 Parabolic Reflector**

Parabolic reflector antennas, commonly referred to as satellite dish antennas have very high gain. Being within the 30-40 dB range is common for this type but they can reach over 50 dB in some cases. They also have a sizable bandwidth, this aspect depends greatly on the size of the dish. Most commercial models will have a 5% bandwidth but they can reach wideband levels for huge dishes. Some of the largest can operate from 150 MHz all the way to 1500 MHz. Smaller dishes are generally going to be within the 2000 to 28000 MHz band. This will enable the possibility of an ideal center frequency for the project's operation at 2400 MHz. Efficiency for parabolic reflectors

is average, generally being in the 50-70% range which is acceptable but not great. This type of antenna can have any kind of polarization as it will vary depending on the feed antenna used in the design. If a dish antenna is chosen for the project it can be circularly polarized to suit our needs.

The main advantage of a parabolic reflector antenna is high directivity. The directivity of a parabolic reflector antenna tends to be very high because the entire purpose is to minimize the losses in directivity seen in antenna designs like the dipole by using the dish, the reflector. In theoretical situations the directivity tends towards infinity. An ideal reflector is not possible in a practical situation but directivities within the 30-40 dB range is commonly seen. The drawback to high directivity is having a very narrow beamwidth of approximate 2.6 degrees. When applied to the rover network, this much directivity is not ideal, going too much above 5 dB will do more harm than good. A larger beamwidth is also preferred.

#### **3.1.13.4 Yagi-Uda**

The Yagi-Uda antenna is usually used for high or ultra high frequencies, anywhere from 3 MHz to 3000 MHz. Despite this it has a very low bandwidth which only reaches a few percent of the center frequency, most commonly 2 to 3 percent. The frequencies that Yagi-Uda antennas operate at are suitable for the project that will be operating at 2400 MHz.

Many aspects of the Yagi-Uda antenna are dependent on the number of elements, their lengths and how they are spaced which allows for a lot of flexibility in options if choosing to work with this type of antenna. An advantage of the Yagi-Uda antenna is its high gain, almost always above 10 dB. With the right spacing between directors, these antennas can reach over 16 dB in gain, maxing out at around of 20 dB. For the Yagi-Uda antenna, the gain is inversely proportional to the beamwidth.

Due to usually being used for high gain, the beamwidth is generally lower than other antenna types, a large con in this case because the network should have a wide reach and be able to maintain connections with moving objects. These antennas can be linearly polarized in the horizontal or vertical direction which is a big con of this type of antenna in the case of the project's network functionality, circular polarization will be needed. The directivity will typically be 7-9 dB, much higher than we'd like to see for the rover network. Yagi-Uda antennas with high gain can reach efficiencies of around 75% which is pretty good but not the best we can do.

#### **3.1.13.5 Helical**

Employing a helical antenna with well-defined design parameters can potentially be a great choice for the functionality of the network. Opting for shorter helical antennas characterized by fewer turns and a wider pitch can yield lower directivity. This characteristic renders them more compatible with maintaining an omnidirectional radiation pattern. This will ensure the rover's ability to communicate throughout the network to reach the tower independent of its position.

Helical antennas also bring forth the advantage of polarization diversity. By adjusting the helix's orientation, the antenna can assume either a right-hand circularly polarized (RHCP) or left-hand circularly polarized (LHCP) configuration. This dynamic feature serves to mitigate polarization mismatch and signal fading challenges during tower-rover communication.

Nonetheless, helical antennas do have a limitation in the form of narrower bandwidth compared to certain other antenna types. There needs to be attention to detail when thinking of the tuning and impedance matching of the helical antenna's design to achieve optimal performance and efficiency across the intended frequency spectrum. An advantage that comes with this antenna type is that the input impedance of a helical antenna is primarily real, simplifying impedance matching and potentially leading to heightened efficiency, despite some chance of losses still existing.

For all of the network's applications, a compact helical antenna emerges as a viable choice. It delivers an appropriate level of directivity, provides circular polarization, and facilitates efficiency optimization, all contributing to effective communication between the rover and the reflector tower through the network.

### **3.1.13.6 Horn**

Horn antennas offer high directivity, making precise signal transmission and reception towards and from the tower easier to maintain. However, when dealing with a mobile rover that requires itself to stay connected to the network while exploring the moon, reaching a sweet spot is crucial, too much directivity would be harmful to continuous proper operation of the overall system. There needs to be a balance between being directed enough to reach the target area but also not directed excessively to a point where the area of coverage becomes narrow.

Utilizing a circularly polarized horn antenna proves advantageous for a rover undergoing a lot of movement while exploring dark crevasses around the surface of the moon. Circular polarization guarantees steady signal transmission, ensuring communication reliability with the tower, without having to worry about the rover's erratic movements.

Antenna efficiency is always one of the most important attributes to consider when it comes to the communication system within the project. Horn antennas are renowned for their impressive power radiation efficiency, effectively converting input power into radiated electromagnetic energy. This efficiency holds particular significance for anything that is battery-operated, as it conserves power resources, ultimately prolonging operational durations so that the rover can stay exploring and maintain connection longer.

Overall, the directivity, polarization, and efficiency of the horn antenna would have a large impact on the functionality of the rover-tower communication system's capabilities. An optimized horn antenna that presents a balanced level of directivity, circular polarization, and above average efficiency, would be a great choice to implement. An ideal horn antenna would be great for guaranteeing a strong link between the rover and the network so that it can communicate back and forth with the reflector tower. With all that said, finding a horn antenna on the market with the specific characteristics required is difficult and most likely impractical.

**Table 3.20.** table with the summary of antenna types discussed.

	Dipole	Patch	Reflector (Parabolic )	Yagi – Uda	Helical Antenna	Aperture (Horn)
<b>Gain (dBi)</b>	1.76-7	0.5 -10	10 - 40	5 – 20	3 – 15	10 – 25

Polarization	Linear	Linear/ Circular	Circular	Linear	Circular	Linear/ Circular
Efficiency	High	High	High	High	High	Very High
Bandwidth	Narrowband	Wideband	Narrowband	Narrowband	Wideband	Narrowband
Directivity	Omni - directional	Omni - directional	Highly Directional	Highly Directional	Directional	Highly Directional

### 3.1.13.7 Antenna type selection

After thorough research on the theory of various antenna types, the helical antenna and the patch antenna are definitely the most promising candidates. These two selections align greatly with the needs of the project while also having practical designs and real world products with the wanted criteria beyond being good in theory.

The patch antenna offers a moderate level of directivity, which allows it to have an omnidirectional radiation pattern. This attribute is the most essential for the project, where the rover's position relative to both the communications tower and the reflector tower will vary constantly. Similarly, the helical antenna, while generally associated with higher directivity, can also be tailored to achieve a quasi-omnidirectional radiation pattern through precise adjustments in size, turns, and pitch.

Polarization is an aspect where the helical antenna outperforms the patch antenna. While circularly polarized patch antennas exist on the market, they are less common than their linearly polarized versions. In contrast, helical antennas are innately circularly polarized antennas which aligns more effectively with our intended antenna operation. This consideration is only important because there will be less flexibility in patch antenna options when we delimit our search to only ones with the preferred circular polarization.

Efficiency-wise, both the patch and helical antennas fit the bill. A properly designed patch antenna often maintains a primarily real impedance, streamlining efficient power transfer. Similarly, helical antennas predominantly feature a real impedance component, facilitating efficient conversion of electrical current to electromagnetic waves. Either kind of antenna will have products available with our desired level of efficiency.

The primary edge that the patch antenna holds over the helical antenna is its form factor. Thanks to their planar design, patch antennas boast a slim topology, rendering them more compact and suitable for space-restricted applications. The antenna needs to fit properly within the constraints of at least three different components within the project, the reflector tower, the communications tower and the rover. The space is a concern for the latter two, where the antenna should take up the least space possible. While helical antennas can be found in small sizes, they innately need more space than patch antennas because of their design philosophy.

With all the different aspects to consider in the project's successful operation, choosing the right antenna type is a really important decision. Finding an antenna that meets all mentioned

specifications is a challenge, but they are likely to be found within these two categories. In the search for commercially available antennas to select, they will be the primary candidates.

### **3.1.13.8 PC140.07.0100A**

The PC140 is a low-profile, circularly polarized (RHCP) antenna that operates in the 2.4GHz band. It is designed for applications where the orientation of the antenna to the other device may be unknown, such as the rover in this project. The antenna is made of FR4 and has dimensions of 57 x 57 x 0.97 mm and a weight of 5.7 grams. It includes a 100 mm coaxial cable and IPEX connector for easy installation. The compact size of the antenna makes it a desirable choice for applications where space is limited. The double-sided 3M adhesive ensures easy mounting on non-metal surfaces.

The antenna exhibits a strengthened circular polarization in the 2.4 GHz band, with an axial ratio between 3.2 and 3.75. It provides a peak gain of 2 dBi and typical efficiency of over 60% across Wi-Fi bands, making it suitable for direct mounting on plastic or glass covers on the rover. The antenna's performance characteristics, with an average gain ranging from -1.92 to -1.83 dB and an efficiency between 64% and 65%, and peak gains between 1.67 and 1.54 dBi, are optimal for the omnidirectional communication required by the rover to maintain a stable link with the stationary tower.

The PC140's Voltage Standing Wave Ratio (VSWR) of less than 2 and return loss of less than -10 dB, with an impedance of 50 Ohms, further supporting its use in this application. The antenna is also designed to function within a temperature range of -40°C to +85°C, which aligns well with the expected conditions that all the components of the system using the antenna may encounter.

### **3.1.13.9 WPC.25.A.07.0150C**

The WPC.25A 2.4 GHz Ceramic Patch Antenna with cable is designed to operate in the 2.4 GHz band. It consists of an embedded patch antenna, a mini-coax cable, and an IPEX MHF1 connector. The antenna has its own ground PCB carrier, making it ground independent.

The antenna's electrical characteristics include a frequency band of 2400-2500 MHz, an efficiency of 76.9%, an average gain of -1.14 dB, a peak gain of 5.15 dBi, an impedance of 50 Ω, and an omnidirectional radiation pattern. The maximum input power supported by the antenna is 2 W. It is important to note that this antenna is linearly polarized, which may not be ideal for this application.

The antenna has dimensions of 25 x 25 x 5.5 mm and is connected using a 1.37 mini coaxial cable with a length of 150mm. The antenna is designed to withstand environmental conditions, with a temperature range of -40°C to 85°C and non-condensing humidity up to 95% RH at 65°C.

Overall, the WPC.25A 2.4 GHz Ceramic Patch Antenna with cable offers reliable performance in various wireless communication applications within the 2.4 GHz band.

### **3.1.13.10 FXP74.07.0100A**

The FXP74 Black Diamond antenna is a small, ultra-low-profile antenna that is designed to operate in the 2.4GHz band. It is made from a flexible polymer and has a compact form factor, making it

easy to mount on devices. The antenna supports communication systems such as Bluetooth, Wi-Fi, and Zigbee.

The antenna has an efficiency of 50%, a gain of 4 dBi, a return loss of less than -10 dB, an impedance of  $50 \Omega$ , and a VSWR of  $\leq 2:1$ . It has a linear polarization and can handle up to 5 W of power.

The antenna has dimensions of  $14 * 7.0 * 0.1$  mm and weighs 1.2 grams. It uses an MHFI (U.FL compatible) connector and is connected using a standard mini-coax 1.13mm cable with a length of 100 mm. The antenna is designed to operate within a temperature range of  $-40^{\circ}\text{C}$  to  $+85^{\circ}\text{C}$  and can withstand various environmental conditions.

### **3.1.13.11 PC17.07.0070A**

The PC.17 is an ultra-miniature PCB antenna that is designed for 2.4 GHz band applications, such as Wi-Fi, Bluetooth, and ISM. It has a robust antenna and mini coaxial cable, and it is only  $24 * 11$  mm \* 0.8 mm in size, making it a great choice for applications where space is limited.

The antenna has an efficiency of 44%, a peak gain of 0.9 dBi, and an average gain of -3.6 dBi. It has a return loss of -12 dB, an impedance of  $50 \Omega$ , and a VSWR of  $\leq 1.5:1$ . It features linear polarization and can handle a power of 2 W.

The PC.17 antenna has dimensions of  $10.75 * 24 * 0.8$  mm and uses an MHFI (U.FL compatible) connector and a standard Mini-Coax 1.13mm cable. It can operate within a temperature range of  $-40^{\circ}\text{C}$  to  $+85^{\circ}\text{C}$  for both operation and storage. It is also RoHS compliant.

Overall, the PC.17 antenna is a compact and efficient solution for wireless communication in the 2.4 GHz band. It offers customization options and meets environmental standards.

### **3.1.13.12 FXP70.07.0053A**

The FXP70 Freedom 2.4 GHz Antenna is a versatile antenna that can be used in a variety of applications, including Wi-Fi, ZigBee, Bluetooth, and ISM bands at 2.4 GHz. It is specifically designed to work with different plastic materials, and has been tested using a 2mm thick ABS plastic as a baseline.

The antenna has an efficiency of 63.7% on a 2 mm ABS material and 30.5% in free space. The average gain is -2 dB on 2 mm ABS and -5.2 dB in free space, while the peak gain is 1.1 dBi on 2 mm ABS and -1.9 dBi in free space. It has an impedance of  $50 \Omega$ , linear polarization, an omnidirectional radiation pattern, and a VSWR of  $\leq 1.5:1$ . The antenna can handle a maximum input power of 5W.

The FXP70 antenna is small and lightweight, with dimensions of  $27 \times 25 \times 0.08$  mm and a weight of 1.2g. It uses an MHFI (U.FL compatible) connector and a 53mm Mini-Coax 1.13 mm cable. The antenna is affixed using 3M 467 adhesive.

The FXP70 antenna is designed to operate within a temperature range of  $-40^{\circ}\text{C}$  to  $85^{\circ}\text{C}$ , and can withstand non-condensing humidity levels of up to 95% RH at  $65^{\circ}\text{C}$ .

**Table 3.21.** A table with a summary of the antenna products discussed.

	<b>PC140</b>	<b>WPC.25A</b>	<b>FXP74</b>	<b>PC17</b>	<b>FXP70</b>
<b>Average Gain (dB)</b>	-1.92	-1.14	-2	-3.6	-2
<b>Peak Gain (dBi)</b>	1.67	5.15	4	.9	1.1
<b>Efficiency (%)</b>	64	76.9	50	44	63.7
<b>VSWR</b>	<2	<2	<2	<1.5	<1.5
<b>Polarization</b>	RHCP	Linear	Linear	Linear	Linear
<b>Cost (USD)</b>	\$27.26	\$9.21	\$7.69	\$16.60	\$27.09

## 3.2 Part Selection

Now that other components have been selected, we can begin selecting power delivery components.

**Table 3.22.** A table describing the peak power needs from each device.

<b>Device</b>	<b>Quantity</b>	<b>Voltage (V)</b>	<b>Peak Power (W)</b>
<b>MCU</b>	1	3.3	5
<b>W-axis Stepper Motor</b>	1	3.3	14
<b>X-axis Servo Motor</b>	1	5	10
<b>Y-axis Servo Motor</b>	1	5	10
<b>Stepper Motor Controller</b>	1	5	<1
<b>Servo Motor Controllers</b>	2	5	<1
<b>Sensor</b>	1	3.3	<1
<b>Total</b>			43

Here we can see the total peak power consumption of the heliostat tower is 43 W. This is a very high figure as it is extremely unlikely that the MCU and all motors and motor controllers will be operating at peak power simultaneously. More typical power requirements would be significantly lower. For this reason, we will use a 50W solar panel which will supply less than 50W typically but will be assisted by a battery. This will enable the motors to draw as much power as they need for brief time periods whilst keeping costs low and reducing the footprint. The heliostat tower has peak power requirements of ~22W at 5V and ~20W at 3.3V

We will also require a battery to enable the heliostat tower to send and receive communications during periods of time when the sun is not visible. Assuming a total standby power consumption of 0.125W for two weeks, we will require at minimum a 50WH battery. 12V batteries are very common for marine or motorsport applications and much less expensive than specialty batteries.

12V 4Ah-7Ah batteries are typically small enough to be lightweight and are common enough to fit our use-case perfectly. It should be noted that the thermal operating range of these batteries will need to be considered. Operating on the moon requires the ability to withstand wide temperature swings.

### 3.2.1 MCU

Out of all the options for microcontroller boards that we researched the ESP32 has to take the top spot. It has a great dual-core processor which is way more than we need for our basic set up but that will allow for future scalability of the project.

It has a small form factor compared to all other boards we have researched which makes it easy to fit into our design. It's also one of the cheapest boards available. In a project where we want to use multiple boards the ESP32's price is almost unbeatable. It has great flash memory and RAM that will be more than what we need so we have a lot of wiggle room with what we want to do. It has a very wide range for operating temperature, the best of all boards looked at so it will need the least cushioning to get into moon operating range.

The power consumption is not the best as it is a more powerful board but it's nothing extreme like the Raspberry Pi. With Wi-Fi, Bluetooth and ZigBee on board we can choose from some of the best wireless protocols available to host our network and communicate between devices. It also ticks all the boxes for peripherals, other boards that can do the same are much more expensive and larger.

### 3.2.2 Solar Panels

For the heliostat tower, we require a solar panel of approximately 30-50W. To ensure we are in a power surplus during standard operation 50W panels will be considered.

Brand: Ensuring the manufacturer of the solar panel is reputable, and reliable is essential. Having the appropriate documentation and support for a product makes integration and troubleshooting simpler. It also helps ensure that the solar panel has high-quality cells free from defects or mismatched performance.

Technology: The type of solar cell used within the panel is directly related to how the panel performs under certain conditions and reliability of the panel. Monocrystalline cells have the highest efficiency and best low-light performance. Polycrystalline cells are a close second. Thin-Film cells are flexible and lightweight, although rather expensive, less efficient and are not as common.

Voltage and Current at Maximum Power Point: The maximum power point is the location on the IV curve that results in the highest product of voltage and current. This location is denoted as MPP, comprised of  $V_{mp}$  and  $I_{mp}$ . The maximum power point is related to the open circuit voltage  $V_{oc}$ , and short circuit current  $I_{sc}$ , however is not directly correlated to these measures.

**Table 3.23.** A table comparing the different panels to be considered for the heliostat (mirror) tower.

Model	RNG-50D-SS	HQST-50P-US	SP-52-L
<b>Brand</b>	Renogy	HQST	Solbian
<b>Technology</b>	Monocrystalline	Polycrystalline	Monocrystalline
<b>Price</b>	\$ 59.99	\$ 65.99	\$ 499.00
<b>Pmax at STC</b>	50 W	50 W	52 W
<b>Voc</b>	22.3V	23.3V	10.9V
<b>Vmp</b>	18.6V	19.8V	9.1V
<b>Imp</b>	2.69A	2.53A	5.7A
<b>Isc</b>	2.94A	2.63A	6A
<b>Weight</b>	7.7 lbs	8.4lbs	1.8lbs
<b>Dimensions (inches)</b>	22.9 x 20 x 1.2	25.9 x 18.6 x 1.2	43.7 x 11.49 x 0.1
<b>Temp Coefficient of Pmax (%/degC)</b>	-0.37	-0.37	-0.38

\*Note that the all data above was determined at standard test conditions (STC - Irradiance: 1000W/m<sup>2</sup>, Temperature: 25 C, Air Mass: 1.5)

The thin-film modules available were either much to large in footprint or expensive to include within this document.

Of the options considered, the three in the table above were the most attractive. All three options are rated for similar power outputs, with the Solbian offering more cells in parallel and fewer in series when compared to the other two options, increasing the output current and reducing the output voltage. The Solbian SP52L is the most rugged of the bunch, being designed for marine applications. It is also the lightest and has a footprint that would be best suited for the intended use case. However, it is far too expensive to be used for this project. The HQST-50P-US was another good option; however, the higher weight and price makes the Renogy RNG-50D-SS the better choice for this application. It should be noted that the monocrystalline panel offers marginally less power at the peak power point; although, it has a smaller footprint and reduced weight when compared to the HQST. Typically, monocrystalline panels perform better in low light conditions which would aid in supplying power when most needed. For these reasons the Renogy panel was selected for the heliostat tower.

The RenoCharge py panel has a detailed datasheet available, which cannot be said for the HQST panel. The manufacturers even supplied the IV curve of the panel, providing an easy reference.

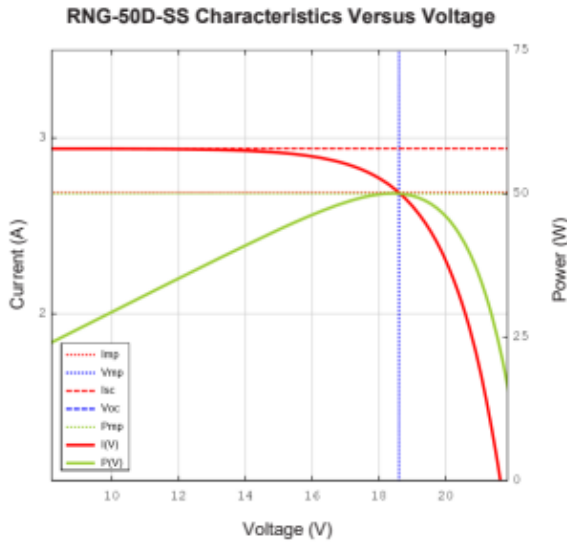


**Figure 3.19.** A plot of the Renogy Panel's IV curve.

### 3.2.3 Voltage Regulation

**Table 3.24.** A table comparing voltage regulators.

Model	LM1085IT-5.0/NOPB	DROK MiniBuck Converter	LM2596	TPS54JA20
<b>Brand</b>	Texas Instruments	DROK	Texas Instruments	Texas Instruments
<b>Input Voltage</b>	2.6-26V	2.5-24V	3-40V	2.7-16V
<b>Output Voltage</b>	3.3 or 5	3.3 or 5	1.5 to 35	0.5 to 5.5V
<b>Output Current</b>	3A	3A	3A	12A
<b>Price</b>	2.19	1.97	1.495	0.65
<b>Type</b>	LDO Buck	Buck	Buck	Buck

Now that a charge controller has been selected to stepdown the solar panel's output to a constant 12V, another step-down regulator is required to step the 12V from the battery and charge controller to the require 5V and 3.3V required for the other components. The components with the largest power draw are the motors themselves. The other components take an insignificant amount of power by comparison so a majority of the voltage regulation will be designed around these components. The stepper motor selected operates at 3.3V and draws a maximum of 2.8A per phase. The selected voltage regulator should be able to tolerate this for brief periods of time. The servo motors selected are rated for 5V with 3A max. Most COTS voltage regulators are limited to 3A or less, individual voltage regulators are required for these high-current draw devices. The MCU and sensor both operate at 3.3V and may use a shared 3.3V regulator. The servo and stepper motor controllers both operate at 5V and may use a shared 5V regulator.

In order to meet these requirements, the TPS54JA20 has been selected to be used as the primary voltage regulator. The TPS54JA20 regulator offers many features over the other products. Primarily, the high current output enables a single regulator to be used for each voltage level required, reducing the number of parts required and design complexity. This voltage regulator also features a soft start feature, which the other regulators do not. The price of this regulator is also cheaper than comparable options. Texas Instruments is a well-known manufacturer and provides good documentation on how to implement this voltage regulator onto a PCB, including tables with individual component values for given design parameters. For these reasons, the TPS54JA20 was selected to be the primary 5V and 3.3V voltage regulator.

### 3.2.4 Charge Controller

*Table 3.25. A table comparing charge controllers.*

Model	BQ25798RQMR	SR11004	Adventurer
<b>Brand</b>	Texas Instruments	SMARAAD	Renogy
<b>Input Voltage</b>	24V max	26V max	50V max
<b>Output Voltage</b>	18.8V max, Programmable	12/24V	12/24V
<b>Output Current</b>	5A	10A	30A
<b>Price</b>	6.25	39.99	59.99
<b>Power</b>	Not Specified	260W	1500W
<b>Type</b>	MPPT	MPPT	PWM
<b>Programming MPPT</b>	I2C	Not Specified	NA
<b>MPPT Type</b>	Sets Voltage to % of Voc	Not Specified	NA
<b>Charge controls</b>	Programmable	Not Specified	Preprogrammed depending on chemistry

Now that a battery has been selected, the heliostat tower requires a charge controller to maintain battery charge. The charge controller needed should be able to sufficiently power devices solely from the solar panel and charge the LiFePO4 battery during sunny periods. It should also have a charging profile designed specifically for a LiFePO4 battery. An MPPT controller is preferred, to maximize power output from the relatively low power solar panel and ensure the system remains in a power surplus for as long as possible. However, a PWM controller may be considered if it offers other attractive features, such as a low price point, a higher degree of configurability, or communications. Three charge controllers are evaluated below.

*Renogy's Adventurer:* This complete charge controller offers a 30A maximum charge current, which is more than sufficient for the needs of the heliostat. It is a PWM charge controller, which is not preferred. However, it does offer pre-programmed charging profiles for a variety of battery chemistries including LiFePO4, however does not distinguish between load and battery outputs, limiting the versatility of this charge controller. The manufacturer is the same as the selected solar panel, which is to say they are reputable. The high price of 59.99, lack of MPPT and high current

rating suggests this controller may be better suited towards larger systems rather than low power systems such as the heliostat.

Texas Instruments' BQ25798: This charge controller is only an IC, requiring a custom PCB and supporting components to operate. This is partially offset by its lower cost of \$6.25, however time spent designing and manufacturing a usable product would make implementing this board impractical. Development boards featuring this chip are upwards of \$150 and too expensive to be reasonably considered. This chip, even if properly implemented, would occasionally be operating near its output current limit during heavy motor usage, and near its input voltage limit as the selected panel's Voc is 93% of this chip's limit. It does have many desirable features, such as being able to configure the device over I2C and a form of MPPT, although not "true" MPPT in the traditional sense. Unfortunately, implementing this chip is impractical due to the constraints imposed by the project, and even if implemented would likely fail due to operating too closely to maximum limits frequently.

SMARAAD's SR11004: This complete 10A charge controller is manufactured by SMARAAD, a Chinese company offering their products on Ali-express and Amazon. They appear to be a quality manufacturer, focusing primarily on renewable power electronics with good reviews on both retail sites. This charge controller also offers an RJ485/RJ45 for communication over MODBUS with a PC, a nice feature for the price. There is also an onboard temperature sensor for temperature compensated MPPT tracking. The exact method of MPPT is unknown, as it is not made publicly available. At the price-point of \$39.99, this option provides the most utility per dollar, despite being less than forthcoming with the MPPT methodology.

Overall, the SMARAAD offering is the best for project. Texas Instrument's BQ25798 has many of the features desired, however the project limitations and chips limitations make it unfeasible. Renogy's Adventure charge controller offers ample margin with high voltage and current limits, being overbuilt for the intended application and resulting in higher costs. The SMARAAD charge controller fits between these quite well, offering more configurability than many of its competitors and exceeding the necessary ratings by a healthy margin, while still retaining a modest price point. For these reasons the SMARAAD SR11004 was selected to be the charge controller for the heliostat tower.

### 3.2.5 Reflectors

Aluminum and Copper would be the most viable metals to use for the fabrication of reflectors. These metals have high reflectivity, durability, and low cost. Mylar can be used to increase aluminum durability. There would be more trade-offs, which is the reduction of efficiency.

Other materials, such as Mylar, beryllium, or Titanium, can be considered. Mylar, or BoPET (biaxially oriented polyethylene terephthalate), is a polyester film rather than metal. Mylar is inexpensive compared to glass, with lightweight, high durability, and high reflectivity. Mylar's flexibility can be folded into smaller area configurations for transport, shown in Figure 3.8. Mylar reflectivity is around 90 percent. Mylar can be fabricated as a coating to reinforce a chosen metal. A disadvantage is that the fabrication process can be complicated to coat the metal with mylar. In this project a substitution of acrylic panel made as a cheaper and lighter alternative to aluminum.

### **3.2.6 Vectoring and Positioning / Solar Tracking Algorithm**

The source code typically has an expensive financial cost, which can be avoidable using open-source codes with modifications to fit the project constraints. Several algorithms can be used to find the position of the sun and calculated into vectors to control the reflector with the most efficiency. Sun tracking photodiode doesn't have an available code library, such that the programming of the algorithm is out of the project scope.

In addition to the available code library, the algorithm also needs to be compatible with the MCU. The chosen MCU for the project is an ESP, which is most compatible with C programming languages and can be ported with Python. Heliostat, Ray Tracing, and Two-Axis Solar tracking systems are the most compatible algorithms. The algorithm must also be compatible with the hardware used to monitor the change in sunlight direction. The chosen input system is an ambient light sensor incompatible with heliostat and sun tracking photodiode. However, heliostat can still use ambient light sensors by switching out the camera input with ambient light sensor input. Sun-tracking photodiodes can give more accurate light vector input. The change in vectors a negligible, which can be omitted.

Ray tracing, however, could be more efficient for consideration of a large amount of code modification due to the original purpose of this algorithm being different from the project. Two-axis solar tracking is a more complicated version of heliostat and goes beyond the project scope, which also requires more modification to the code and excess unused code. Hence, Heliostat is the chosen algorithm for the project with minimal programming modifications and only changes for a camera to ambient light sensing.

### **3.2.7 Motors**

Some environmental factors need to be considered for operating due to the severe environmental impact of the moon's surface. The stepper motor must limit exposure to high temperatures, dust, or moisture. All motors need to be encased when fabricated. Some stepper motors may have additional features like integrated encoders for closed-loop control, motor dampers for reduced vibration, or customized shaft options. These features are an improvement but are optional.

Based on all the considerations above and the financial cost, the motor for the x,y and z-axis of the reflector would be Servo DS3325 motor, which can handle up to 25kg stall torque. The w-axis motor was chosen to be the lowest model of Nema 23 since they don't need to be as precise or required to be at high speed. However, higher torque is needed because the load is far from the rotation axis. Both models have high durability and operate in bipolar wiring configurations. The dimension for the motor is larger than other models but is negligible when compared to the relative size of the tower.

### **3.2.8 Motor Controllers**

Like the stepper motor, the power rating must match the power supply and microcontroller. The controller's physical size and mounting options are also negligible because they are smaller compared to the relative size of the project. However, it is preferable to be smaller than 10 cm to match the microcontroller and save space. Initially, the DRV8834 Low-Voltage Stepper Motor Driver Carrier would be the best fit due to its low cost and meet the current requirement.

Additionally, this motor driver has high precision and a more accessible interface. The voltage rating is optimal and compatible with the chosen MCU. However, The Nema 23 have a current drawn of at least 2A or higher, another substitution is needed. The stepper controller TB6560, have a larger control with higher voltage and amperage rate to be a better fit for the Nema 23 operation,

Since most motor controllers for servos are approximately the same as I2C communications compatible with the MCU, the set of 2 PCA9685 is chosen to control the x and y-axis motors, which draws minimum power from a DC source.

### **3.2.9 Sensor**

The light sensor that we found to be best suited for the project was the VEML7700, which ranked highly in multiple categories against the other light sensors including max lux value, lowest power consumption, and size which were all crucial pieces for our project. The most important piece was the max lux value which would be necessary with the sensor looking directly into the sun. A sensor with a high max lux value can determine the best possible position for the mirror to point at in the sun to give the sensors on the target the best opportunity to charge using solar energy.

All of this comes at a great price point of under \$10.00 and most websites that sell the product even have them for under \$5.00. This gives us the best “bang for our buck” and will allow for best results and a small hit on our budget for the project. On top of this, the VEML7700 was best suited for our project because it can easily be fabricated onto our PCB, which will make for easy hardware design. After some discussion with the group, we were all in agreement that the best light sensor for our project’s success would be the VEML7700 Ambient Light Sensor.

### **3.2.10 Communication technologies**

Zigbee is the preferred choice for this project’s use case. As we will be transmitting data periodically, there is no need for a high power protocol like Wi-Fi that can transmit at much higher speeds. A higher level of precision is not required for what is trying to be achieved. Zigbee also has a much larger maximum range which is something that should be focused on as much as possible.

Due to the long term objective being to use this technology on the moon an even larger range will be achievable than on earth. Zigbee’s maximum theoretical range of 980 meters is perfect. While at a glance LoRaWAN can look very promising, checking most of the same boxes as Zigbee, the associated hardware is more expensive and the much larger range would likely go underutilized, if utilized at all. Bluetooth also seems like it would be a pretty solid option as it is widely used and easy to work with without using too much power. However, Bluetooth’s low range and no possibility of scaling makes it unfavorable.

Another great advantage to Zigbee is the flexibility in frequency that is available compared to other protocols. If this technology is to be used on the moon as part of an attempt to expand our exploration of the satellite, then inevitably there will be more wireless frequencies used as time goes on. These options in frequency allow for future proofing in such a case to avoid interference and maintain the preferred range of operation.

In terms of power consumption all protocols reviewed are low power with the exception of Wi-Fi, making Zigbee a good option in that regard without missing out on any other upsides it presents. The max number of devices also allows for scalability just like a majority of the other protocols. Zigbee is also used in the microcontroller judged to be the best for the project which makes it an even better fit.

### 3.2.11 Batteries

The heliostat and communication tower both require batteries. The heliostat tower requires a battery that will be able to sustain it for a minimum of 2 weeks during sunless periods. As previously discussed, a 5-7 Ah, 12V battery will be more than enough to sustain the battery during these periods. A few other important specifications besides voltage and amp hour, are technology, price, brand, and any charging/discharging requirements.

Technology: The type of cell used within the battery is important to the performance of the cell and operating conditions. Lead acid batteries are easy to work with and inexpensive, however they suffer from low energy density and are typically heavier than other technologies for a given energy capacity. Lithium Iron Phosphate (LiPO4) batteries have the benefit of high energy density and low weight, however, are more expensive and suffer from thermal instability if charging requirements are not met properly.

Charging and Discharging Requirements: As previously mentioned, lead-acid batteries are typically easier to manage, as a constant voltage is the only thing necessary to charge them. A float charge may also be delivered depending on the use case, but again this is comparatively simple. LiPO4 batteries require a more complex charging mechanism as they require a period of constant current then a period of constant voltage in order to safely charge. Discharging LiPO4 batteries also require some thermal regulation, as they are more thermally unstable and may go into thermal runaway if either charging or discharging is done improperly. Lithium-Ion batteries with internal BMS systems to prevent thermal-runaway should be preferred to prevent fire or damage to the cells.

**Table 3.26.** A table comparing different batteries.

Model	ML5-12	HW-4F7	PQ12V/6AH
<b>Brand</b>	Mighty Max Battery	Howell Energy	Power Queen
<b>Voltage</b>	12	12	12.8V
<b>Amp Hour</b>	5	7	6
<b>Technology</b>	SLA AGM	LiFePO4	LiFePO4
<b>Price</b>	16.99	32.99	19.59
<b>Temperature Rating</b>	-20 to 50	-20 to 70	Not Specified
<b>Weight</b>	3lbs	1.9lbs	1.8lbs
<b>Dimensions</b>	3.5 x 2.8 x 4.2	5.9 x 2.6 x 3.7	5.9 x 2.6 x 3.7
<b>Charging Requirements</b>	CV	CC 3.5A, CV 14.6V, Built-in BMS	Not Specified, Built in BMS

### **3.2.12 Development Environment: Languages and Repositories**

For the development environment, the thing that is the most important is familiarity for a group project. Because of this, the best option for us was to keep things as simple as possible so we do not have to learn to “remake the wheel”. What this means is that we do not want to learn a new programming language or a new repository system when we could have used one that everyone in our group already has experience with. This will save us time and “hair-pulling” moments to learn and debug in different programming languages. For this reason, we decided it would be best to use GitHub as our main repository for our development environment. Everyone in our group at least has a bit of experience using GitHub, so this will allow for seamless transition into the project.

As a bonus, GitHub also has a lot of open-source code that will be needed for our heliostat software that we can easily clone into our repository for easy use. Having this was an important piece of our decision because it makes things very simple for file transfer. One thing that GitHub does not have that BitBucket did have built in was team dynamic software such as Trello or Jira, but those can be used separately if need be.

For our programming language, the easiest option to pick was C. The C coding language works best with microcontrollers and is the simplest language to learn and master. As a result of this, everyone has experience with this language and with using microcontrollers with C. This will make it very easy to start building and coding in our project with this foundation. If it is needed, we will also use C++ if more object-oriented programming is required for the calculation-oriented heliostat algorithms. This would not be ideal though because some members of our group do not have experience with this language.

### **3.2.13 Antenna**

Among the antennas at hand, the PC140.07.0100A proves to be the best option, mainly due to its circular polarization attribute. A circular polarization is the most important aspect to maintain network connectivity between the towers and the rover while it is in movement on the moon. While certain alternatives might provide enhanced efficiency or directivity, none present circular polarization. Efficiency and directivity are not as important as being omnidirectional. The PC140 is still a solid choice in terms of efficiency and directivity while also having the most important aspect of all, circular polarization. For this reason, it is the best choice to implement within the project. Due to the project sponsor’s constraints, it was opted to use a similar antenna in the final project. This antenna is the wlaniot 2.4G Wireless Mini PCI PCI-E Antenna which has similar statistics to the PC140 and also has the same connector so that it will integrate seamlessly with the microcontroller connector.

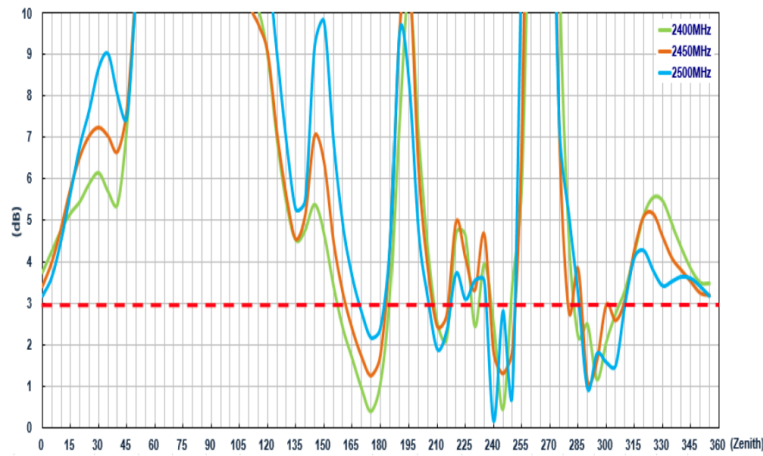


**Figure 3.20.** PC140 average gain versus frequency

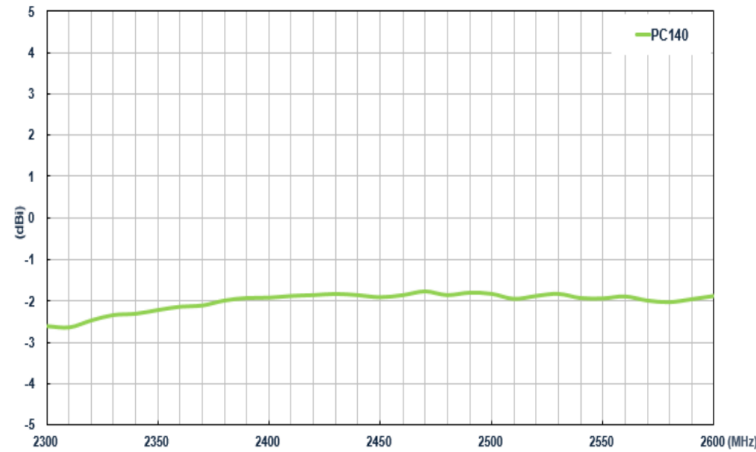


**Figure 3.21.** PC140 axial ratio

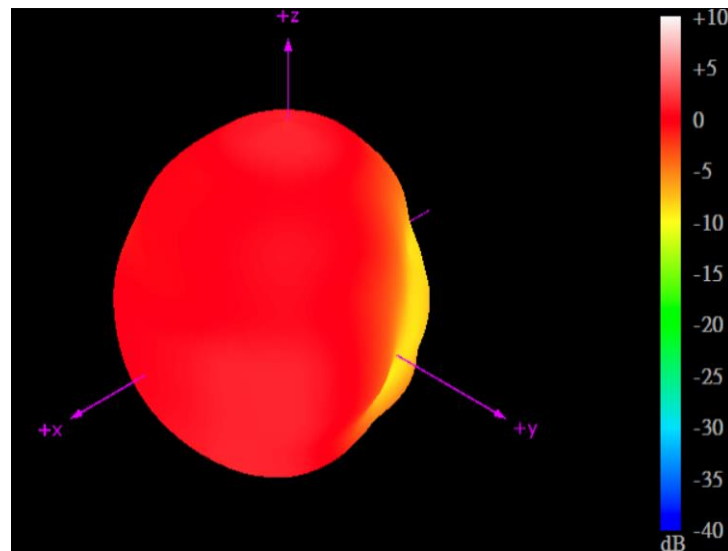


**Figure 3.22.** PC140 radiation pattern

# Chapter 4 - Related Standards and Design Constraints

## 4.1 Industrial Standards

### 4.1.1 PCB Design Standards

PCB design standards are the criteria required for the PCB to be manufacturable, determined by individual manufacturers. In this case, JLC PCB is the designated manufacturer so their standards will be used. Other PCB design standards are in order for the PCB to function properly, such as trace widths for high current applications. Their standards include clearances, maximum and minimum thicknesses and diameters and required file formats.

For the selected manufacturer we are limited to 1 or 2 oz copper for the outer layers for the 2 layer boards to be used. Holes are limited to between 0.3-6.3mm with via sizes limited to a minimum of 0.3mm holes with 0.5mm pads. Clearances are also specified with a minimum of 0.5mm between holes and pads with holes of different nets. Vias need to be placed 0.254mm away from other vias and tracks regardless of net. Pads must be placed 0.127mm away from other pads of different nets and 0.2mm away from tracks. The minimum specified trace width is 0.127mm and tracks must be spaced 0.127mm away from each other. The minimum distance from track to edge of board is 0.3mm.

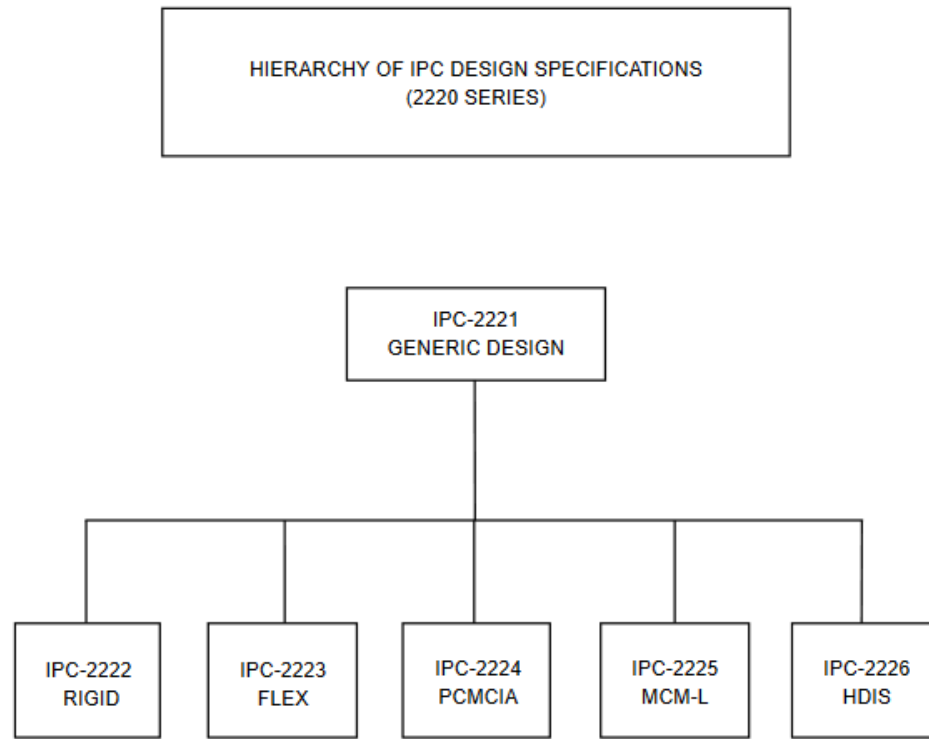


**Figure 4.1.** Hierarchy of IPC Design Specifications

IPC-2221 guidelines and recommendations for the design of PCBs. The standard encompasses a wide range of aspects related to PCB design to ensure the reliability, manufacturability, and performance of PCBs. Some key points that IPC-2221 addresses are:

1. **Design Guidelines:** IPC-2221 offers guidelines for designing PCBs with considerations for parameters such as trace width, spacing, and layers. These guidelines are crucial for achieving proper signal integrity, power distribution, and thermal management on PCBs.
2. **Material Selection:** The standard also provides recommendations on the selection of materials for PCBs, considering factors such as dielectric properties, thermal conductivity, and mechanical strength. Proper material selection is essential for meeting the performance requirements and environmental conditions of the electronic system.
3. **Component Placement:** IPC-2221 additionally includes guidelines for the placement of components on the PCB. It addresses issues related to signal interference, thermal management, and accessibility for assembly and testing. Proper component placement is important for optimizing the overall functionality and reliability of the PCB.
4. **Trace Routing:** The standard provides recommendations for routing traces on the PCB, considering factors like impedance control, signal integrity, and EMC. It outlines best practices for routing high-speed signals and minimizing the potential for signal crosstalk or interference.
5. **Thermal Considerations:** IPC-2221 addresses thermal management in PCB design, offering guidelines for heat dissipation, thermal vias, and the placement of heat-generating components. Proper thermal design is crucial for preventing overheating and ensuring the long-term reliability of electronic devices.
6. **Design for Manufacturability (DFM):** The standard emphasizes the importance of designing PCBs with manufacturability in mind. This includes considerations for ease of fabrication, assembly, and testing. Adhering to DFM guidelines helps reduce the likelihood of manufacturing issues and improves the overall efficiency of the production process.
7. **Quality and Reliability:** IPC-2221 includes sections for ensuring the quality and reliability of PCBs. It outlines testing and inspection criteria that can be employed to verify the integrity of the finished boards and ensure they meet industry standards.

Overall, IPC-2221 serves as a comprehensive guide in PCB design, providing a framework for creating robust and reliable electronic systems. These standards will be utilized to ensure the PCBs designed are manufacturable and function properly at minimal cost.

#### 4.1.2 I2C Protocol Standards

The I2C, which stands for Inter-Integrated Circuit is a two-wire serial bidirectional bus that connects Integrated Circuits (ICs) or boards together. The I2C is a standardized method of serial communication that is used on many types of electronics and is used in this project with the sensor specifically. To understand how the standards are important, the general idea of I2C will be explained below.

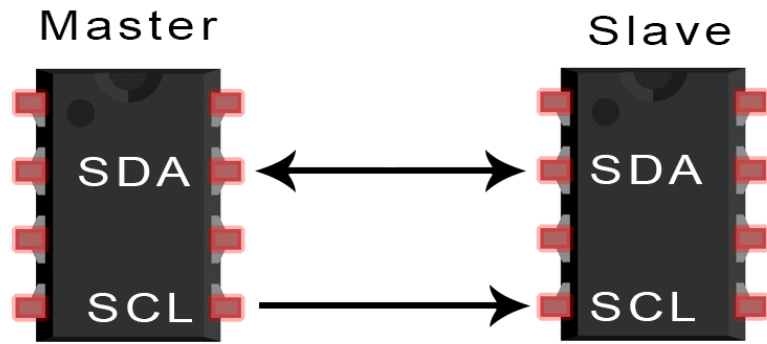


**Figure 4.2.** Basic I2C Block Diagram

by Image Source: <https://www.circuitbasics.com/basics-of-the-i2c-communication-protocol/>

Firstly, the I2C uses a two-line system that uses a clock system which is denoted by Serial Clock (SCL) and a Serial Data (SDA). The Master provides the SCL which gives synchronization for the system, but the master can also start and stop data transfer through the SDA at any point, which can make the system asynchronous. The SDA line is bidirectional which means data can be sent in either direction. The I2C system is an open-drain system, which means that the slave devices in the system cannot pull the devices to high voltage and only slowly drop them to low, hence the draining. For this reason, there are pull-up resistors in the system that can pull the devices back up when no devices are being used. On top of this, multiple slaves can be connected to the master to form a multi-slave configuration where the master manages the bus to ensure no conflicts on the data line.

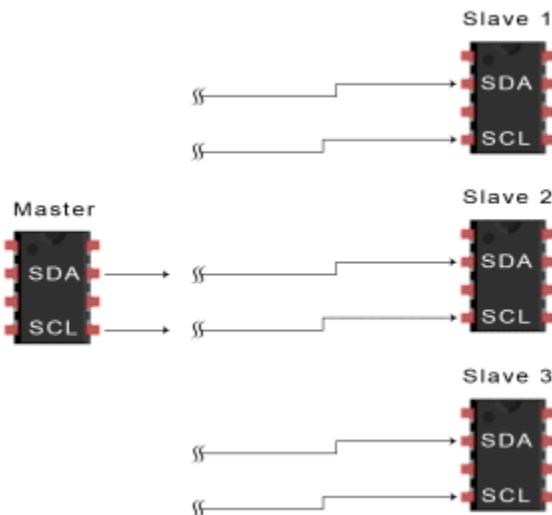


**Figure 4.3.** I2C Multi-Slave Diagram

by Image Source: <https://www.circuitbasics.com/basics-of-the-i2c-communication-protocol/>

For the standardized protocol, the master must commence a data transfer which means the SDA and SCL must be high indicating that the system is currently idle. The start condition of the data transfer is when the SDA line goes from high to low while the SCL line is high; this tells the slave that data transfer is starting. The I2C addressing is mostly used in 7-bit which gives the master 128 slaves to choose from. The master then sends one of those 128 addresses for the place where it wants to send the data. From here, the master will send a register value for the slave to either read the data or write the data to. This process is done bit by bit, with each bit being sent on the synchronized clock starting with the most significant bit (MSB). The devices can send an acknowledgement (ACK) or not acknowledgement (NACK) by pulling the SDA low to confirm if it has received the bit. To end the data transfer, the master will pull the SDA from low to high while the SCL is high to inform the slaves that the data transfer is complete.

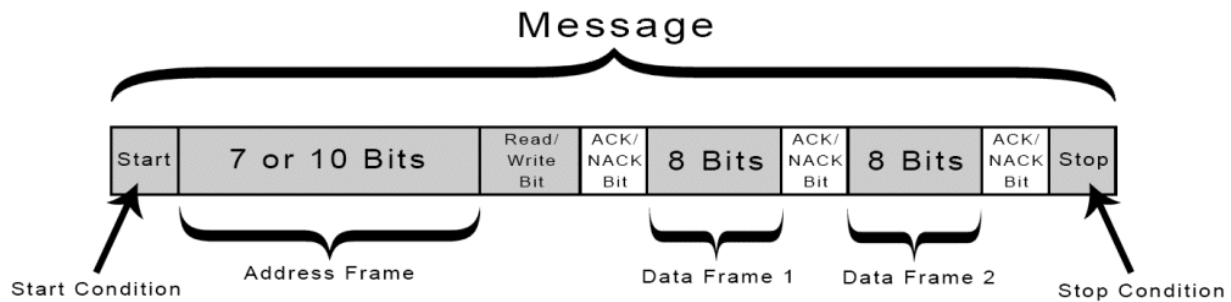


**Figure 4.4. I2C Protocol Diagram**

by Image Source: <https://www.circuitbasics.com/basics-of-the-i2c-communication-protocol/>

There are also other standards in I2C which can be defined by the settings that they run on which is dependent on clock speed. The standard is the most used, which operates at a maximum clock rate of 100kHz. There is also a fast mode, which operates at a maximum frequency of 400kHz. There are other faster versions which are less popular but operate at maximum frequencies of 1MHz and 3.4MHz respectively. One last thing to mention about the standards of I2C is that the maximum speed of the data transfer will only be as fast as the slowest device can handle. These standards are widely used in serial communication using microcontrollers and other ICs.

#### 4.1.3 ZigBee Protocol Standards

According to sub-clause 6.6 of version 1.0 of the ZigBee Base Device Behavior Specification, all ZigBee devices, and as such the project, shall comply with the following series of requirements:

All nodes shall be capable of processing the following service commands:

Service	Input command	Response
ZDO discovery	Active_EP_req, Node_Desc_req, Simple_Desc_req, IEEE_addr_req,	Active_EP_rsp, Node_Desc_rsp, Simple_Desc_rsp, IEEE_addr_rsp,

	NWK_addr_req, Match_Desc_req	NWK_addr_rsp, Match_Desc_rsp
<b>ZDO node manager</b>	Mgmt_Bind_req, Mgmt_Lqi_req	Mgmt_Bind_rsp, Mgmt_Lqi_rsp
<b>ZDO binding table</b>	Bind_req, Unbind_req	Bind_rsp, Unbind_rsp
<b>ZDO network manager</b>	Mgmt_Leave_req	Mgmt_Leave_rsp

After broadcasting an Identify Query command frame during the finding and binding process, a node shall be capable of handling at least one Identify cluster, Identify Query Response command frame. Handling of several Identify Query Response command frames at once, when supported by the node, is implementation specific.

In the case a node supports finding and binding as an initiator, it shall implement a binding table with a number of available entries that is greater than or equal to the sum of the cluster instances supported on each device of the node which are initiators of application transactions. Bindings are configured in the binding table during finding & binding, touchlink or centralized commissioning. The binding table shall be consistent such that its contents can be retrieved via the use of the Mgmt\_bind\_req command, regardless of the commissioning mechanism used to generate the bindings.

A node shall have a default report configuration for every implemented attribute that is specified as mandatory and reportable. This is ruled by sub-clause 6.7 which denotes that a default report configuration is such that in case a binding is created on the node to a given cluster, it shall be capable of sending reports to the binding without requiring the setting of any additional reporting configuration. The default reporting configuration may be overwritten at any point in time and, if this is to be the case, the most up to date configuration shall be used.

Reports shall be generated in accordance with the Maximum Reporting Interval, such that the time elapsed since the previous report is equal to it. Were the Maximum Reporting Interval be set to 0x0000 there will be no periodic reporting, however, change based reporting will still be operational.

Any node that may be the target of an application transaction shall support group addressing of at least eight memberships in the group table.

#### 4.1.4 Motor Controls

In the United States the physical dimensions of stepper motors are defined by National Electrical Manufacturer Association. Based on NEMA ISC 2-1996, part 8 (R2004, R009), the controller, contactor and Overload relays rated limiting to 2000V in alternate current and 750V in Direct Current. In this part, the related devices include ac motor circuits switches rated 600V and assessors such as break and molded-case switches.

A worldwide standard for AC 3-phase motor usually according to the International Electrotechnical Commission. NEMA standards are used in this project for the motor. Hence, some comparation can be used to coordinate between standards. Motor cooling methods such as ODP guard open type comparable to IC 01, TENV totally enclosed non ventilated to IC40, totally enclosed fan cooled to IC41, TEAO totally enclosed air over to IC 48.

The ingress protection used such as open type (IP00), Open type guarded, against contact by a 12 mm probe (IP 20), ODP Open type, Drip-proof (IP 12), WP Weather-proof (IP13), TE Totally Enclosed (IP55), Submersible motor, e.g., pump (IP 68). Some motor design type included NEMA Design B, Normal locked rotor torque and normal locked rotor current., NEMA Design C, High locked rotor torque, normal locked rotor current. NEMA Design D, High locked rotor torque and high slip, NEMA Design A, Normal locked rotor torque, and high locked rotor current.

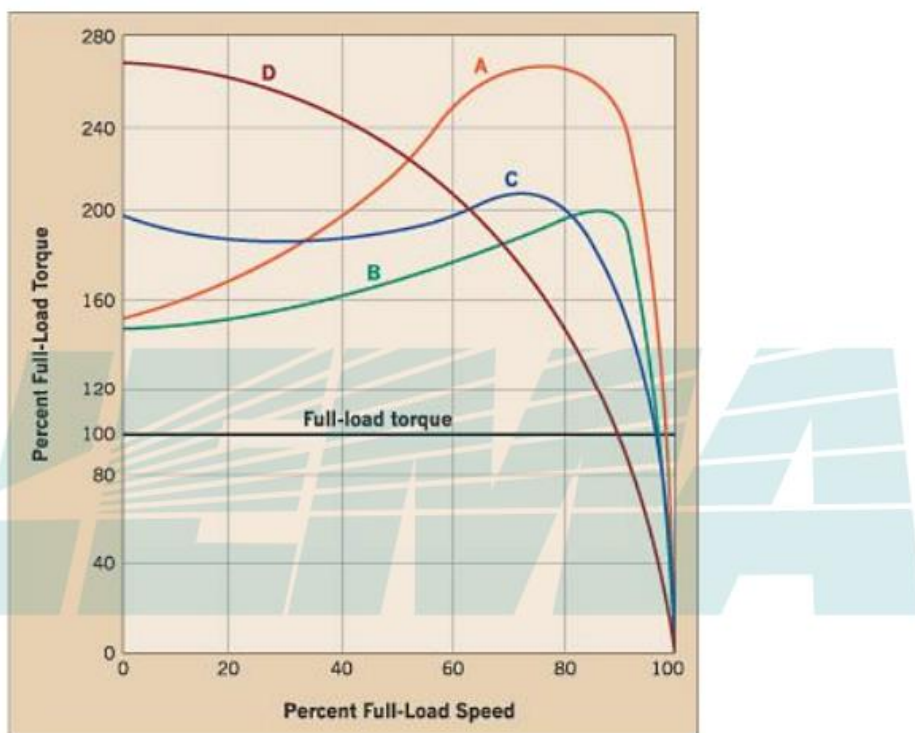


**Figure 4.5.** Load Torque ad speed between different motor designs

IEC also defined motor duty cycle standards into eight rating according to IEC 60034-1:

**S1 Continuous duty:** The motor works at constant load for enough time to reach temperature equilibrium.

**S2 Short-time-duty:** The motor works at constant load, but not long enough to reach temperature equilibrium, and rest periods are long enough for the motor to reach ambient temperature.

**S3 Intermittent periodic duty:** Sequential, identical run and rest cycle with constant load. Temperature equilibrium is never reached. Starting current has little effect on temperature rise.

**S4 Intermittent periodic duty with starting:** Sequential, identical start, run and rest cycles with constant load. Temperature equilibrium is never reached but starting current affects temperature rise.

**S5 Intermittent periodic duty with electric braking:** Sequential, identical cycles of starting, running at constant load, electric braking, and rest. Temperature equilibrium is not reached.

**S6 Continuous operation with intermittent load:** Sequential, identical cycles of running with constant load and running with no load. No rest periods.

**S7 Continuous operation with electric braking:** Sequential, identical cycles of starting, running at constant load, and electric braking. No rest periods.

**S8 Continuous operation with periodic changes in load and speed:** Sequential, identical duty cycles of start, run at constant load and given speed, then run at other constant loads and speeds. No rest.”

An equivalent of horsepower used in NEMA standard instead of kilowatt as of IEC standards. Such that, a comparable rating can be done with IEC 60072-1 document, through full load motor amperes, ac induction motor, four pole, 3ph, (400 v - 50 Hz, 1500 rpm), and (460 v - 60 Hz, 1800 rpm).

**Table 4.1. Output Equivalence between IEC and NEMA Standard**

FLA at 400 vac50Hz	kW Primary Series	kW Secondary Series	HP (746 w)	FLA at 460 vac 60 Hz, (NEC 430-250)
1.1	0.37		½	1.1
1.5	0.55		¾	1.6
1.9	0.75		1	2.1
2.5	1.1		1.5	3.0
		1.8		
4.8	2.2		3	4.8
		3		
6.3	3.7		5	7.6
8.1		4		
11	5.5		7.5	11
		6.3		
14.8	7.5		10	14
		9		
21	11		15	21
28.5	15		20	27

## 4.2 Practical Constraints

### 4.2.1 Time

The main constraint of this project is the time constraint. Doing this project as a senior design only gives us a certain amount of time to fabricate the idea, process, and design which heavily limits how much we can accomplish in such a short amount of time. Due to this, there are some decisions we must make that will help us meet our deadline instead of building a better product.

One of the first general issues as a time constraint is that we are limited to the timeframe of one academic calendar year to make this a fully functional product. Because of this, there are no extensions on the timeframe of the project, which gives us a hard deadline that we must meet to successfully complete the project and pass the class. Luckily, we were able to get a head start on this project by creating our groups, brainstorming, and researching in the Spring and Summer semesters beforehand to mitigate this constraint.

Another general issue of the time constraint is that the group must do extensive testing, debugging, and design in this short time frame. There will be multiple setbacks and errors that must be fixed throughout the course of this project that does not have a lot of room for error. Because of this, the time constraint poses a threat to the success of this project due to the unforeseen errors that might come from the design, construction, and testing of the project.

A general issue from the time constrain that might come into play is the ordering of parts, specifically the PCB. One thing that happens in senior design projects is that the group will order parts and there can be delays because of supply shortages or lack of workers that can cause backup on parts that need to come in. Because of this, the group can be waiting for a part to start designing a certain piece of the project that can waste valuable time on a project with a hard deadline.

An added issue that would be a time constraint to our project is the design and fabrication of the mirror on the mirror tower. This needs to be done before the start of Senior Design 2 so that the part assembly can still be on a continuous schedule. This might be difficult because we need to get the proper aluminium sheet in a circular shape and apply the mylar onto it so that it can properly reflect the light. By doing this early, it will allow us to stay on schedule by designing the mirror tower after this.

The result of these time constraints can lead to a rushed project, which might not give the expected or necessary results, which can cause late changes to our goals and cutting corners to meet the end goal. This can cause us to fail our project and force a retake of the senior design class because of the constraints if we don't take the necessary steps for our project.

Some ways that we can mitigate these constraints is through a multitude of different team values that we have set for each other. Some of these include time management, accountability, productivity, communication, and attendance. Most importantly, if we all abide by the saying in senior design, which is "Do What You Say You Will Do" which is shortened into the acronym, DWYSYWD, the time constraint will not be a factor because we will have good planning so that

even if we hit a roadblock in parts, debugging, or redesigning, we will be able to complete the project and do it well within the time constraint.

#### **4.2.2 Economic**

One of the main constraints that were notable for ASTROCOM were economic constraints. The budget that was given to us by our sponsor FSI was \$750.00. This made it very difficult to make decisions to decide if we wanted a product to be cost-effective or better performance. Specifically, for both of the towers, there was a hard trade-off between efficiency and cost to ensure the project stayed under the budget.

Another piece of this economic constraint is that we are limited by even more than our \$750.00 budget because we must keep some money unused from our original parts to be able to have some backup money in case parts break during testing. By doing this, it allows us to have no worries that we will go over the budget in case parts break. This does make even more of a time constraint though because it limits our spending even more than the original budget given by our sponsor, FSI.

The first of the economic constraints on the mirror tower is that our group was forced to use the Servo motors because of the budget that was placed on us. These motors are cheaper and have limitations to their functionality because of their price. Some of these functionality limitations are speed, torque, and durability, which all factor into our project. With these constraints, we must ensure that we are able to overcome these limitations with our design to avoid the economic constraint for our motors.

Another economic constraint we have in parts selection is in our antenna. Because of our budget, it forces us to select an antenna that is larger and less powerful. This constraint can cause our antenna to have a smaller range and signal strength, which will affect the performance of our communication tower. With a larger budget, we would be able to host a more powerful network. Secondly, a result of a cheaper antenna means it is more likely to come across noise with other electronic devices that could weaken the signal. Furthermore, another factor of a cheaper antenna is bulkier equipment that could have a higher power consumption. This equals a bigger product that will drain power faster. All these factors of a cheaper antenna are a result of our budget with the economic constraint. To avoid these constraints from becoming a big issue in the project, there needs to be good planning and design to create a product that matches the quality of the antenna on the communication tower.

Likewise, to the antenna, another piece of parts selection that results from the economic constraint is the choice for the microcontroller. It would make it very easy to use an Arduino microcontroller that has built-in Wi-Fi to host a network for the communication tower, but that is limited by our budget and necessary requirements for the project. For the job that needs to be done on the communication tower, an Arduino microcontroller would be a waste of money and affect the budget because it has extra tools that are not required for the scope of the project. This means that we would be paying extra on the Arduino for something that the ESP32 already does but saving

time on the workload of the network. Because of this economic constraint, we opted to pick the ESP32 to save money in our budget.

Overall, the economic constraint poses a huge threat to our project because it causes us to pick products that will fit into our budget instead of the best products on the market to achieve our project goals. This means that we will need to overcome these challenges by doing great research, planning, and designing to ensure that our project still meets the goals that we set out to achieve while staying under our budget. We can also do this by giving ourselves some extra money to rebuy products if they break or do not work as expected in the project to stay under the budget that was set by the sponsor for our project.

### **4.2.3 Environmental**

The biggest design constraint that is a factor for this project is the environmental constraint. Because this project is just a proof of concept and we cannot test this on the moon, there are a variety of factors that do not allow us to design and test the way we want to.

The first of these environmental constraints is temperature. The moon endures extreme temperatures and can change drastically throughout the lunar day which can cause equipment to fail in these harsh conditions. This is almost impossible to replicate on earth and therefore this project will be tested as one that operates on earth. To be able to replicate these conditions, we would need a specialized chambers which would be very expensive and unrealistic for this project.

The next factor of the environmental constraints is the lunar dust on the moon. Since this project will only be tested on earth, we cannot recreate the lunar dust that would take place if we were to test this project on the moon. Lunar dust can cause wear and tear on equipment for the project because of its jagged edges and composition of materials that might come from the moon such as silicates and basalts. On top of this, the lunar dust tends to stick to electronic equipment because it can be electrically charged from UV radiation of the sun. This lunar dust can contaminate the equipment but cannot be duplicated on earth for testing.

Another environmental constraint of this project is the difference in solar tracking patterns between the earth and the moon. The average day and night cycle on the moon is equivalent to about 29.5 days on earth, so being able to track that would be much more difficult due to its unorthodox timing compared to the earth. Since this product is being tested on earth, the project will not be able to replicate these environmental factors, and therefore a constraint of this project would be the inability to test solar tracking from the moon.

An environmental constraint that needs to be considered is the topography of the moon. The moon has many craters and mountains that will be very hard to replicate on earth. The moon's tallest mountain is over 18,000 feet tall and the largest crater being over 42,000 feet deep, the topography of the moon is impossible to mimic on earth. Due to this, it is an extreme constraint that we will not be able to recreate for testing on the moon.

One possibility to consider when talking about constraints is the differences in atmosphere between the earth and moon. The moon is almost a complete vacuum, meaning that there is almost no atmospheric pressure. This means the equipment cannot be tested in the same environment than if it were to be tested on the moon. This is one of the factors from the atmospheric constraint of having to test on earth rather than the moon. Other features that the atmosphere effects are the thermal and radiation control that atmosphere has on earth that the moon does not have. The earth's surface is protected from these factors with the atmosphere, but the moon is not.

One last feature of the environmental constraints from the moon, which is quite an obvious one compared to the others, is the lack of networks on the moon. Unlike earth, there are no network towers with connection to cellular or Wi-Fi networks. This means that every network that we have in this project will have to be locally hosted using the microcontrollers and power sources to make them work.

It is hard to mitigate these constraints because we cannot replicate the environment of the moon, but we can attempt to show that we understand the limitations of the moon and give a fair warning for those that try to replicate the project with a larger budget. But, as for our project, we will test on earth and use our resources that we have here to show a proof of concept for both towers to ensure a working project and a guideline for anyone who wants to replicate it.

## **4.2.4 Remaining Constraints**

### ***4.2.4.1 Sustainability***

The sustainability constraint of this project is one that relies on environmental factors. By making a product that will be on the moon means that it must be able to sustain multiple environmental factors that were mentioned above such as lunar dust, radiation, and temperature. These factors will play into the lifespan of the project through deterioration from the environment. We must be very thoughtful in part selection to ensure we pick mechanical products that can sustain up to -40 C of cold weather and enclose technological pieces in polycarbonate to ensure that they do not break down over time.

All rovers and moon equipment will have a shorter lifespan than if they were on earth because of the different factors. Some of the products that could be affected by the environmental factors that cause a sustainability constraint. These products include the solar panels, mirror, batteries, and other structural pieces. Although this project will not physically encounter these constraints because it will be tested on earth, it is still important to note that if this product were to be used on the moon, it would half a much shorter lifespan due to these factors that affect the sustainability.

### ***4.2.4.2 Political***

A lesser constraint but still important is a political constraint. This can be factored into part sourcing and where we order from. It is important to note that this product is sponsored by FSI, which is a branch of NASA, a United States company. We should be careful that we are choosing parts, technology, and other ideas from that of our own country. This is a constraint because we

are being funded by our sponsor, and if this project does not meet their guidelines, specifications, or ulterior motives, it could affect our sponsorship and funding.

We can attempt to lessen this constraint by ensuring that we are getting our parts from reliable sources that our sponsor trusts. This will allow the project to stay within the bounds of the company's liking, and therefore keep us out of any potential disturbances to our project because of it. This constraint is less of a factor than the others but is still important to note because of the sponsor and funding to the project.

#### ***4.2.4.3 Ethical***

Another piece of part sourcing which factors into an ethical constraint is to ensure that the companies we buy from are not outsourcing from countries that use child labor or any type of slavery. This is an ethical constraint to make sure our project does not take advantage of third-world countries that might be exploiting for their work. This is a trade-off between cost and morals, but one that our group decided was important to be aware of.

To make sure this constraint is factored into, our project used parts from trusted companies that have a good track record. This means that our project uses parts from fair businesses that are not exploiting different countries for using unfair labor practices. This means that the ethical constraint is limited by the extra research that was done to ensure that parts are chosen to limit unfair business practices to the best of the group's knowledge.

#### ***4.2.4.4 Health and Safety***

Another constraint that must be factored into this project is the health and safety. Since we are testing on earth with other people that might be present, we must ensure that the product is safe to test around others, especially with the reflection of light. This could pose a problem for people that operate motor vehicles and pedestrians with light possibly being reflected in their area. We can mitigate this constraint by checking for people in the area while testing.

Another piece of this constraint is the safety of the parts while testing. This is especially important for the battery, which could very easily cause problems by exploding if not put under the correct testing environment. Another piece of the safety constraint is the materials used to fabricate the product. This means that we need to use beryllium, which is non-toxic and will ensure the health and safety of those testing and using the product.

#### ***4.2.4.5 Manufacturability***

The final constraint that needs to be considered for this project is the manufacturability, which is constraint for our group as undergraduate students. This group is limited to the lab equipment that is offered by the university, and severely limits how much construction and manufacturing we can do for this project. This constraint impacts the group by keeping the overall design simple enough to design with lab equipment.

One positive of this project is that the group does not have to construct this project by hand and can buy mechanical pieces online to reduce the amount of manufacturing design that is needed for

this project. With this, we can buy products online and then piece them together with different techniques to lessen the mechanical designing of this project. That is one way that we can limit the amount of manufacturing for mechanical products. But, with the electrical components such as the PCB, we will need to manufacture it with lab equipment, which is a factor in the manufacturability constraint.

## Chapter 5 - ChatGPT

ChatGPT is currently still in development and is a partial system with 100% accuracy. On the other hand, ChatGPT can give quick guidance on how to start with research components. However, since the database of ChatGPT is from 2016, the cost of material is drastically different, along with some updated changes. There is a need to be selective when considering the result from ChatGPT.

Most research papers from ChatGPT are randomly generated such that Google will provide a more solid source when doing research. Any mathematical calculation must be done by hand since chat GPT is also unreliable.

### Case study 1: Question “What properties do I need to consider when making a mirror?”

“When making a mirror, several properties need to be considered to ensure its quality and functionality. Here are some important properties to consider:

1. Reflectivity: The primary purpose of a mirror is to reflect light. Reflectivity refers to the ability of the mirror to reflect light effectively. A high-quality mirror should have a high reflectivity, meaning it reflects a significant portion of the incident light.
2. Flatness: The surface of the mirror should be as flat as possible to ensure accurate reflection. Any deviations or distortions in the surface can cause image distortion. The mirror should have a smooth, even surface with minimal warping or irregularities.
3. Optical Coating: Mirrors often have a thin layer of reflective coating applied to the surface. This coating, usually made of materials like aluminum or silver, enhances the mirror's reflectivity. The quality and durability of the optical coating are crucial to ensure long-lasting performance.
4. Durability: Mirrors should be resistant to scratches, corrosion, and other forms of damage. Consider the material used for the mirror substrate, such as glass or acrylic, and choose one that is durable and able to withstand regular cleaning and handling.
5. Size and Shape: The size and shape of the mirror depend on its intended use. Consider the desired dimensions and shape to suit your specific needs. Mirrors can be rectangular, square, circular, or even custom-shaped.
6. Thickness: The thickness of the mirror can affect its weight, durability, and optical performance. Thicker mirrors tend to be sturdier but may be heavier. The thickness should be chosen based on the desired strength and practicality of the mirror.
7. Anti-Reflective Coating (optional): An anti-reflective coating can be applied to the front surface of the mirror to reduce glare and enhance visibility. This is particularly useful in

situations where reflection-free viewing is important, such as in high-end optical systems or displays.

8. Frame or Backing: Consider the type of frame or backing that will support the mirror. This is especially relevant for mirrors intended for hanging or mounting purposes. The frame should complement the mirror's aesthetics and provide stability.

9. Environmental Considerations: If the mirror is exposed to outdoor or harsh environments, it's important to choose materials that can withstand those conditions. Consider factors like humidity, temperature fluctuations, and exposure to chemicals.

By considering these properties, you can ensure that the mirror you create meets the desired quality and functionality for its intended purpose.” (OpenAI, 2023)

In this case, ChatGPT output multiple factors for a glass mirror with a metal coating. Which is not a very good consideration for ASTROCOM’s reflector. The general information can still be extracted, such as the properties listed. ChatGPT also listed the most important property that needs to be considered, reflectivity, as its first point. This is based on the commonality of all reflection devices and is highly related to the ASTROCOM project, which can be expanded by searching with different engines and research papers.

Google can do such cases of extended research. This method results in multiple websites with information on how to make mirrors. The websites can provide additional sources and citations for expanding research. However, the availability of citations could be more consistent depending on the professional indication of each website. With the same question asked, Google’s first results are more catered to the fabrication of glass mirrors and are unproductive to the project. In extension, Google’s newly developed AI in google lab answers differently when provided the same question.

“Here are some properties to consider when making a mirror:

- Flatness: A mirror must be flat so that light hits the mirror at the correct angle, providing an accurate image
- Surface roughness: The surface roughness should be smaller than the wavelength of the light.
- Smoothness: The surface should be smooth and free of blemishes to show a person's reflection more clearly
- Thickness: Thicker mirrors are sturdier and don't cause the reflection to distort
- Silvering: A good mirror should have a thick, high-quality coating of silvering on one side of the glass to make it reflective
- Clarity: The clarity of the glass contributes to a better reflective quality
- Impurities: The glass should be cleaned and polished to remove impurities and contaminants

Modern mirrors are largely produced by the wet deposition of silver or aluminum.” (Google,2023)

Similar to the engine search result, the answers could be more in-depth, and properties are less related to the project, which is less desirable than ChatGPT. However, there are two advantages

to Google AI. There are follow-up prompts generated related to the topic for further research, such as “What are the basic properties of mirrors?”, “What do you need to make a mirror?” and “What makes a good quality mirror?”. These questions provide some guided direction when the previous answers are not sufficient. Additionally, websites and videos with related topics are provided next to the search. This perk is due to the association with existing search engines.

For more extensive research, google also provides a service of google scholar. This method will offer research papers related to mirrors with some selectivity. However, the information is extensive and requires selection by the researcher. The information is more credible compared to ChatGPT and would be more effective for a detailed understanding of each property of mirrors.

**Case study 2:** “Which stepper motor should I use to move a heavy object in precise rotation?”

“To move a heavy object with precise rotation, you would typically require a stepper motor with high torque and accurate positioning capabilities. The specific stepper motor you should use depends on several factors such as the weight of the object, the required rotational speed, the desired accuracy, and the mechanical setup of your system. However, I can provide some general guidance.

1. Determine the torque requirement: Calculate the torque needed to move your heavy object. Consider factors like the weight, the distance from the rotation axis, and any additional forces or friction in the system. Ensure the stepper motor you choose has a torque rating that exceeds this requirement.
2. Consider stepper motor types: There are various types of stepper motors, including:
  - Hybrid Stepper Motors: These motors offer a good balance between torque, accuracy, and cost. They are commonly used for precision applications and are available in different sizes and torque ratings.
  - High-Torque Stepper Motors: If your heavy object requires substantial torque, you might consider using high-torque stepper motors. These motors provide more torque but might be physically larger and more expensive.
3. Determine the motor size: The physical size and weight of the motor can affect your system's mechanical design. Consider the available space and mounting options in your setup.
4. Select the appropriate step angle: Stepper motors rotate in discrete steps, and the step angle determines the angular resolution. Smaller step angles (e.g., 1.8 degrees) provide finer resolution and better accuracy but typically result in lower torque.
5. Consider additional features: Some stepper motors have additional features that can be beneficial for specific applications. For example, closed-loop stepper motors include feedback mechanisms to detect missed steps and provide improved accuracy.
6. Consult motor specifications and manufacturer guidance: Review the specifications provided by the motor manufacturer to ensure the motor meets your requirements. Consider factors such as current rating, voltage requirements, and wiring configuration.

It's important to note that while stepper motors can provide precise positioning, they may not be suitable for high-speed applications due to their inherent step-by-step movement. For high-speed and continuous rotation, other motor types like servo motors may be more appropriate.

Given the complexity of your specific requirements, it is recommended to consult with a knowledgeable supplier or engineer who can assist you in selecting the most suitable stepper" motor for your application." (OpenAI,2023)

Similar to case 1, ChatGPT can give a few properties for the motors to be chosen according to the project's constraints. However, these properties have some conflicting information and require deeper understanding. In this aspect, Google Scholar provides the most accuracy and information regarding each proposed motor. Research papers are peer-reviewed, providing a more credible and informed decision when selecting project parts.

**Case study 3:** "what are some stepper motor models available in the market at this moment?"

"As an AI language model with a knowledge cutoff in September 2021, I don't have real-time access to current market information. However, I can provide you with some popular stepper motor models that were available in the market up until my last update. It's essential to research and verify the availability and suitability of these models for your specific application.

1. NEMA 17 Stepper Motor: NEMA 17 is a widely used stepper motor size with a 1.8-degree step angle. It offers a good balance between size and torque, making it suitable for a range of applications.
2. NEMA 23 Stepper Motor: NEMA 23 is larger than NEMA 17 and provides higher torque output. It is commonly used in applications that require more power, such as CNC machines and 3D printers.
3. NEMA 34 Stepper Motor: NEMA 34 is even larger than NEMA 23, providing even higher torque. It is often used in applications that require substantial power and torque, such as industrial machinery and robotics.
4. Oriental Motor PKP Series: Oriental Motor offers a range of stepper motors in their PKP series, including PKP22, PKP26, PKP33, and PKP42 models. These motors are known for their compact size, high torque, and accuracy.
5. Leadshine DM Series: Leadshine is a well-known manufacturer of stepper motors and drivers. Their DM series includes various models with different torque and step angle options, offering versatility for different applications.
6. Moons' Stepper Motors: Moons' Industries manufactures a variety of stepper motors, including the high-torque MS series and the compact and accurate ML series.
7. Applied Motion Products ST Series: Applied Motion Products offers the ST series stepper motors known for their high torque, accuracy, and durability. They provide options for different frame sizes and torque ratings.

Remember to check with manufacturers, suppliers, or distributors for the most up-to-date information on available models, as the market is continually evolving. It's also important to consider factors like torque, step angle, accuracy, and other specifications to determine which specific model will best suit your application.” (ChatGPT, 2023)

As stated by ChatGPT, the information answered is from a database limited at collection of September 2021. Hence, recent developments may not be considered. In this aspect, ChatGPT only presents options that can be improved through additional real-time research with specific vendors. These motors can still link to vendors with updated information and parts.

In this case, ChatGPT gives adequate starting information. Additional information is needed to have a more accurate and effective representation of part of ASTROCOM’s project. However, Google Scholar can also give additional information with minimal effect to the project.

**Case study 4:** “what are the price range of brushless dc motor?”

“The price range of brushless DC (BLDC) motors can vary depending on various factors such as power rating, size, brand, efficiency, and specific application requirements. Additionally, market fluctuations, technological advancements, and other factors can impact prices. It's important to note that the following price ranges are approximate and can provide a general idea of the cost of brushless DC motors:

1. Small Brushless DC Motors:

- Low-power miniature BLDC motors: \$10 to \$50
- Medium-power BLDC motors for small appliances, drones, or RC vehicles: \$50 to \$200
- High-performance or specialized small BLDC motors: \$200 to \$500 or more

2. Medium-Sized Brushless DC Motors:

- General-purpose medium-sized BLDC motors: \$100 to \$500
- Higher power and performance BLDC motors for industrial applications: \$500 to \$1,000 or more

3. Large Brushless DC Motors:

- Large industrial BLDC motors: \$1,000 to several thousand dollars or more, depending on the power rating, size, and application requirements

It's important to keep in mind that these price ranges are approximate and can vary significantly based on factors such as the specific motor specifications, customization requirements, and supplier or manufacturer pricing policies. To obtain accurate pricing information for the specific brushless DC motor you need, it is recommended to research and consult with motor manufacturers, distributors, or suppliers who can provide detailed quotes based on your specific requirements.” (ChatGPT, 2023)

As per the question, the price is requested for each of the motors given the arbitrary price range. These ranges could be more accurate when compared to vendors. The information is both out of date and is estimated from a database. Price accuracy is more effectively researched through

utilized search engines. Such as Google, as there are multiple vendors' options for price comparison and an accurate price for a bill of material. In this case, Google Scholar is obsoleted due to the nature of the research paper, which focuses more on the functionality of the motors rather than prices. In this aspect, Google AI has a higher advantage than ChatGPT since they have a real-time update and suggest vendors' appropriate motors.

 Generative AI is experimental. Info quality may vary.

Brushless DC motors are more expensive than brushed DC motors because they require a switching controller to sequence the proper charge through the stator coils. However, brushless DC motors have advantages in terms of efficiency, lifespan, and maintenance.

Here are some products to consider:

	<b>FlashHobby D3536 Brushless Motor 750KV...</b> 5.0 ★ (1) Amazon.com - Seller, + more <b>\$19.98</b>	This motor is designed for quads like 10 inch quad frames, and is suitable for RC plane, aircraft, multicopter, helicopter, fixed wing and robotic arm.
	<b>VEVOR Electric Brushless DC Motor 48V 2000W...</b> 5.0 ★ (2) BuildClub <b>\$169.17</b>	This motor has a 100% copper core for low noise operation and high working efficiency. It features an aluminum alloy shell and comes with a complete accessories kit.
	<b>DJI RoboMaster GM6020 Brushless DC Motor</b> DJI Official Store, + more <b>\$179.00</b>	This brushless DC motor has an integrated driver.

**Figure 5.1.** Results for case study #4,  
By Google AI

### Case study 5 - Light Sensor

Using ChatGPT for research was very effective because I was able to get an easy starting point for my research. I knew I was tasked with researching different light sensors for our project, so I had to research the technologies used on the light sensors as well as the available products on the market. As a starting point, I used ChatGPT to generate the most common technologies used in light sensors and ambient light sensors and tried to take the common answers between the two of them. This gave me a good baseline for my research because ChatGPT gave me a one to two sentence summary of how each technology was designed and how it is used in products.

As a result of this first search, ChatGPT gave me “photodiodes, phototransistors, CMOS, and LEDs” as viable technologies to use in the sensor for this project. There were others that were also displayed but were too far out of the scope of the project to even be talked about in the research.

This was a great starting point for me because I was able to find websites that clearly and easily explained how these different technologies worked and how they were to be used in different sensors. I was able to narrow down my searches on Google to more specific lenses to be able to find exactly what I needed to know from a circuitry standpoint and a functionality standpoint.

From this, I was able to use ChatGPT again to search for products on the market that would be suitable for our project. I prompted ChatGPT asking for different products on the market that used photodiodes and phototransistors which is what I determined to be the most suitable technologies for the sensor that would be used in our project. ChatGPT gave many answers in which helped me to lay out my options from a technology standpoint. ChatGPT also gave me brief descriptions of which companies developed these different products which made it much easier to find the details and datasheets of each product.

As a next step, I was able to lay out the different technologies and start searching for the different tech specs of the sensors, which allowed me to easily construct a table to compare the different light sensors. Having a table as a part of the research is crucial because it allows our group to easily pick the most suitable sensor and to display in the research which product is most applicable for the project. Using ChatGPT gives a great baseline for where to start research and to narrow the scope of what to look for on Google and other reputable sources.

Although ChatGPT is a great resource and eases the process of research, it is important to note that it cannot be 100% trusted because it pulls sources from all over the internet and combines them into a summarized message which might not always be accurate. On top of this, ChatGPT uses GPT3 which is the AI software that was last updated in 2021, which means the data that it gives its users is not always up to date and should always be followed with more research to confirm its responses and dive for more information.

## **Case Study – 6**

ChatGPT was an invaluable asset when doing research of any kind for this document. The largest part of the document is research and ChatGPT alleviates a lot of gaps in knowledge one may have when conducting research on subjects to figure out key points to look for and laying out a wide array of resources with valuable information. It's particularly useful when starting out researching a new topic and understanding it.

When researching microcontrollers and FPGAs I already felt very comfortable with the subject but when comparing the two my inexperience started to show. I needed to know what aspects are important when considering one over the other. What strengths and weaknesses are quantifiable on each side that I can generalize two massive fields and compare them with? ChatGPT helped out a lot with figuring out what parameters to weigh in this decision, along with providing many reputable sources of information to read and understand what I was actually comparing to make an educated decision. This resulted in the decision to use a microcontroller over an FPGA that was properly justified and thought out.

ChatGPT didn't help very much when researching available microcontroller choices. Most of the information for this part I already understood well and knew that ChatGPT was feeding me some

incorrect info at times. Doing independent research using what I already knew and asking others with experience in the field proved to be much more helpful and yielded great results.

Where ChatGPT really had a chance to shine was when researching information for the communication protocols and antennas. Firstly, communication protocols are like a whole other dimension where you can put together a solution in infinite ways with whatever protocol. ChatGPT was a great supplement to figure out what the most used and popular protocols were for hosting a network that would be the main use in ASTROCOM. It was also great for finding websites with information on these protocols like the official alliance websites that have a crazy amount of information to dissect and learn from. It was also perfect for figuring out which aspects matter when selecting a protocol. This allowed me to find out exactly which ones matter to the project and what should be represented in the summary table and explanations.

Antennas are where I was most missing knowledge and ChatGPT was most useful when researching antenna types. Deciding which antenna type to use was very complicated, ChatGPT could help with giving examples of important parameters but could not help with quantifying them to specific antenna types so that comparisons could make sense. It also had a lot of incorrect information regarding which parameters matter for what purposes. That's when asking ChatGPT for resources on antenna theory made everything work regarding antenna type selection. With lots of reading and research, ChatGPT could once again be a powerful tool for finding existing antenna products that I could already properly compare.

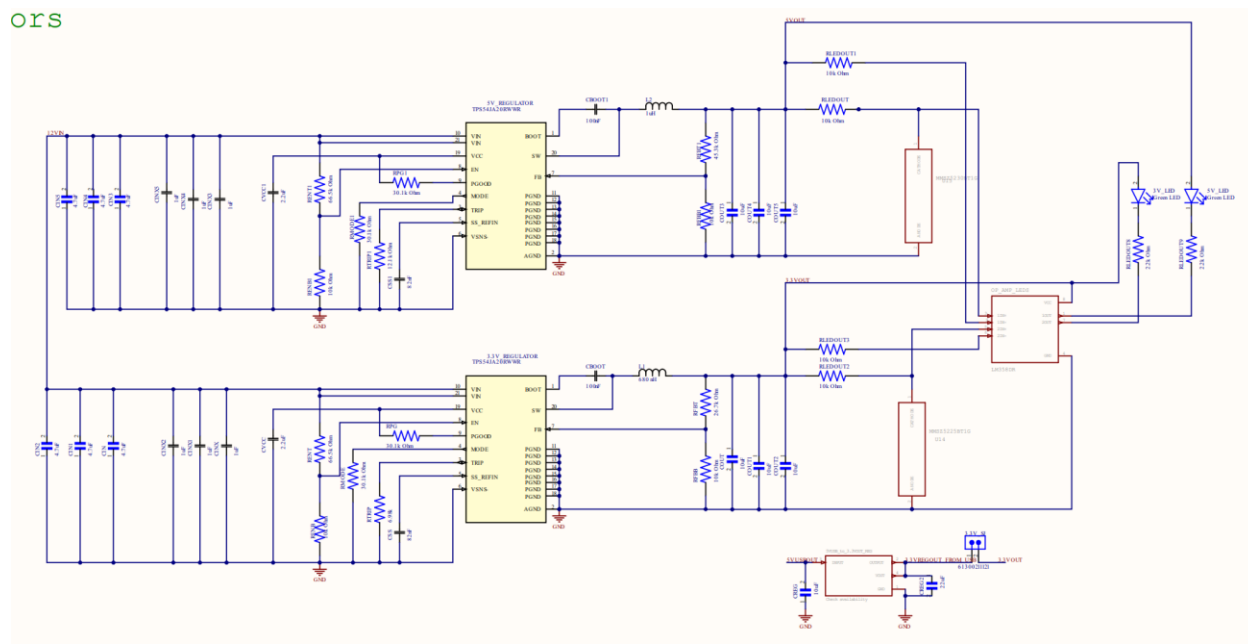
While ChatGPT was generally a huge help in research it also had a lot of downsides. The GPT-3.5 version that is free only contains information from up to 2021 which made it unreliable for many fields within ASTROCOM's scope as technologies are constantly improving and changing and new competitors are plentiful. It is not always correct, which is when reading more tried and true documentation and information from scholarly articles or textbooks comes in handy to make sure the information is good. It was also completely useless for looking for similar commercial technology and past projects. It failed to provide any helpful links or information and dodged the question with vague information. Overall, it provided many more benefits than downsides and conducting research would have been much more difficult without ChatGPT.

## **Chapter 6 - System Hardware Design**

### **6.1 Power Delivery/ Electrical Power System**

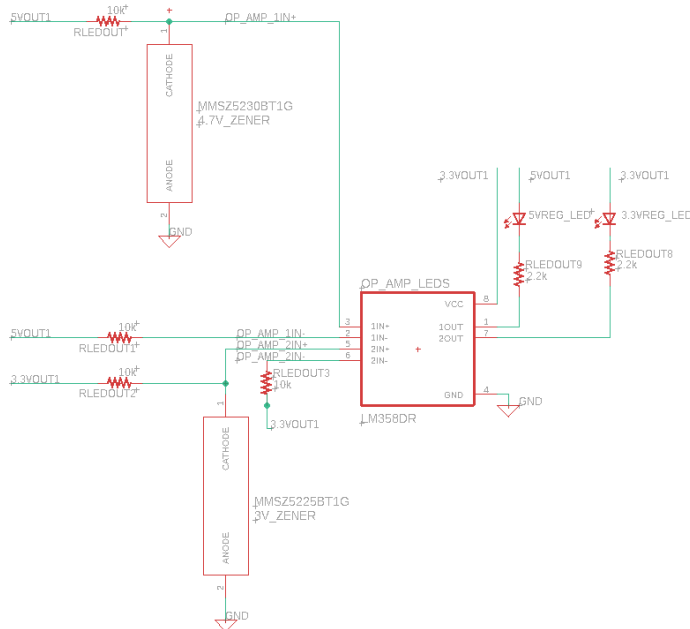
The power delivery system draws power from the solar panel a majority of the time. When solar power is not available the charge controller will automatically switch to drawing power from the battery. This means that we only require one power input into our MCU PCB. The components on the MCU PCB only require 3.3V, however the motors require 5V. A 5V regulator is placed on the PCB to reduce the total number of regulators and to allow the MCU to control whether the motor controllers are powered. Below is a schematic of the 5V and 3.3V regulators. In later revisions, the stepper motor was supplied with 12V from the charge controller directly.

ors



**Figure 6.1.** The schematics for the 5V regulator (top) and the 3.3V regulator (bottom)

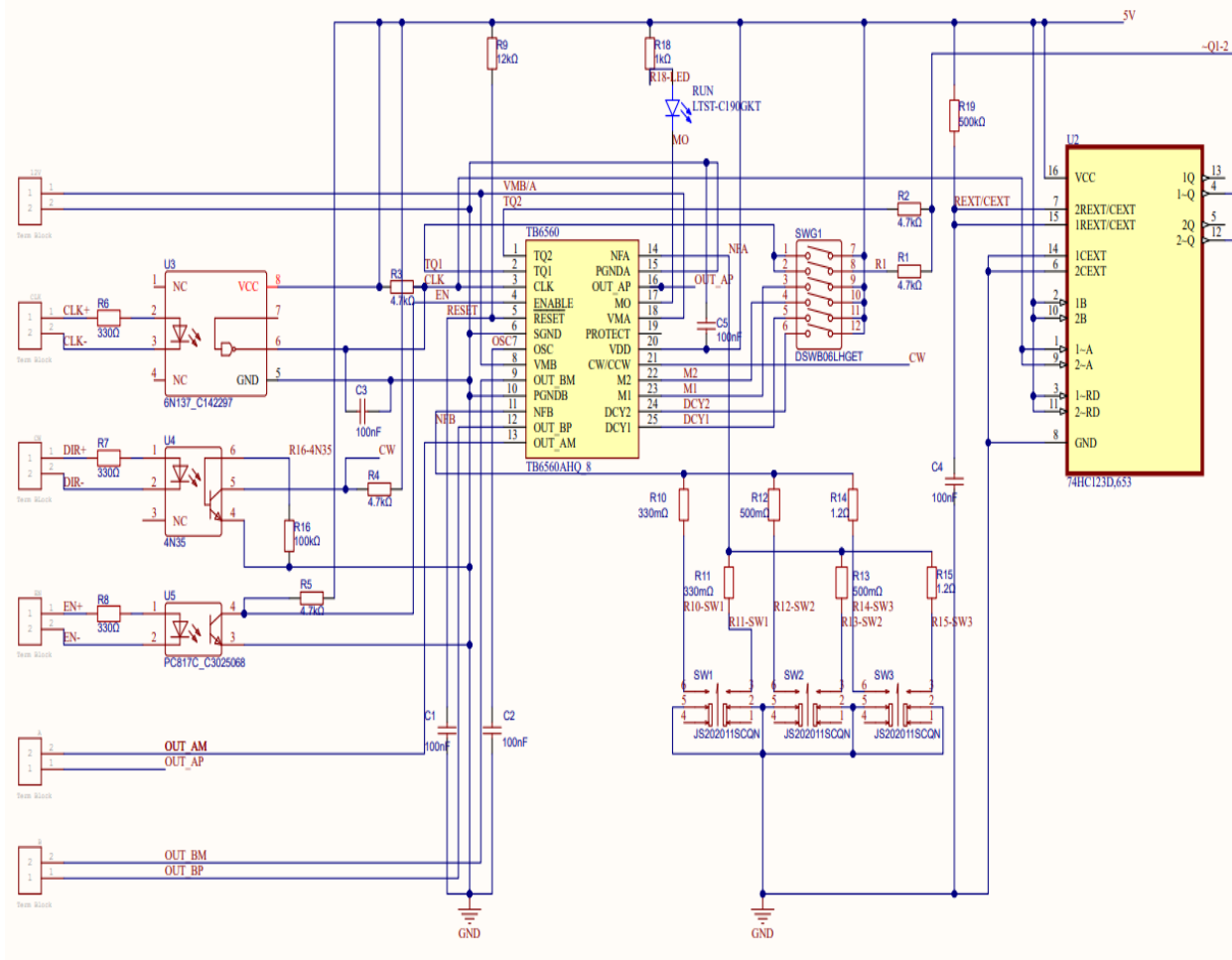
A simple op amp was used to build a status LED circuit for the regulators. This will simplify troubleshooting and reduce confusion whether the board is powered or not. The circuit detects undervoltage conditions for the respective regulator and turns off the status LED during these periods. This is done using Zener diodes with breakdown voltages set to slightly lower than nominal voltages.

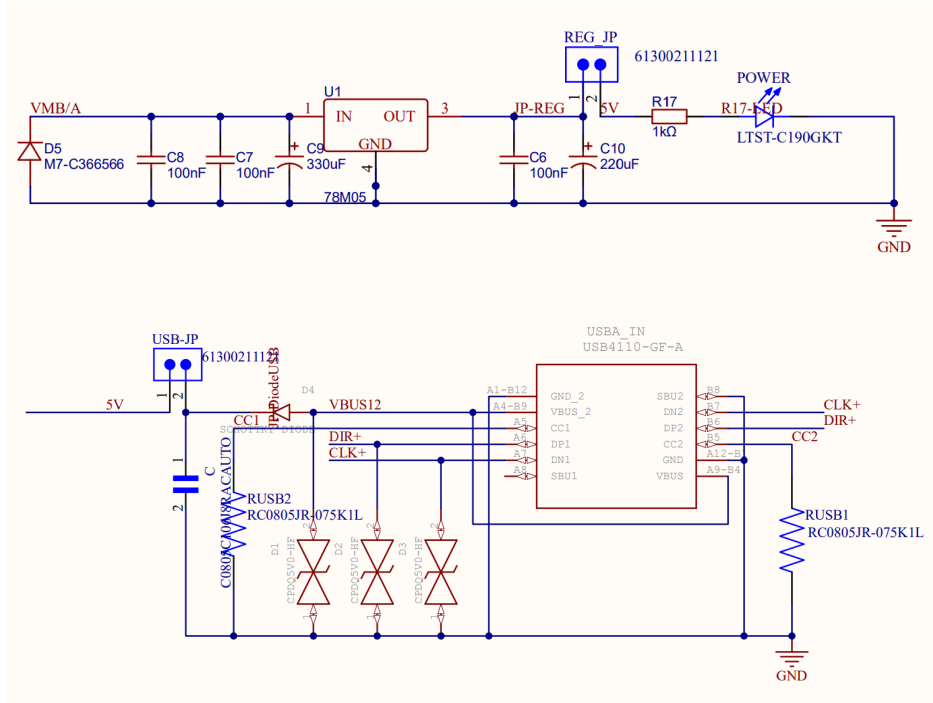


**Figure 6.2.** A schematic of the status LED circuit

## 6.2 Motor Controls

### 6.2.1 Stepper Motor Controls





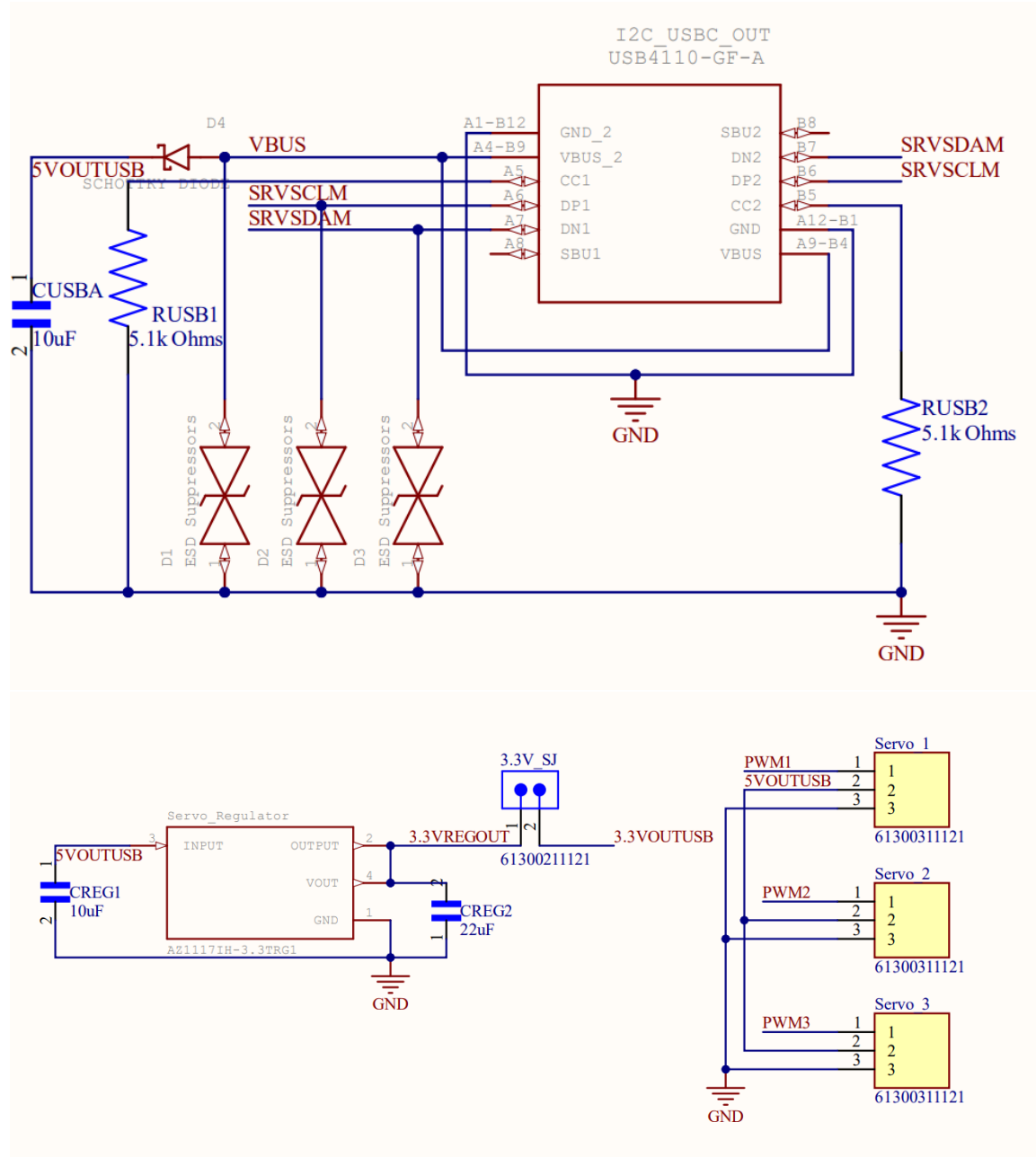
**Figure 6.3. Stepper Motor Schematic**

Figure 6.2 shows the connection of bipolar stepper motor Nema23 and various terminals of stepper motor controller DRV8834. The four terminals of the stepper motor labeled with black, green, red, and blue annotated the color of the wires from the stepper motor, which then connect to A and B out of the stepper motor's controller, respectively. The motor controller is then connected to the logic and motor power supply, which logic power supply for the microcontroller and motor power supply to both the motor controller and the motor. The microcontroller connects to the step and direct terminal for data transfer and control of the stepper motor. The  $100\mu F$  capacitor connect to the motor power supply to regulate the power deliver threshold.

Surface jumper on configuration and voltage reference are using for testing and changing configuration. A potentiometer is implemented to change the reference voltage, which dictate revolution speed of the stepper motor. This can be done by limiting the current input base on the reference voltage. Decays and Enable pin are pull down for active low.

This schematic is a separate PCB's board for a more efficient data transmission between driver and motors. The break board then connected to the MCU using a USB-C connector and cable. A regulator is added to control the 5V in to output 3.3v for the board, while 5V line is used for motors. A LED is implemented for checking connection and signal. The motor shown is a separated component connected to the breakout board.

## 6.2.2 Servo Motor Controls



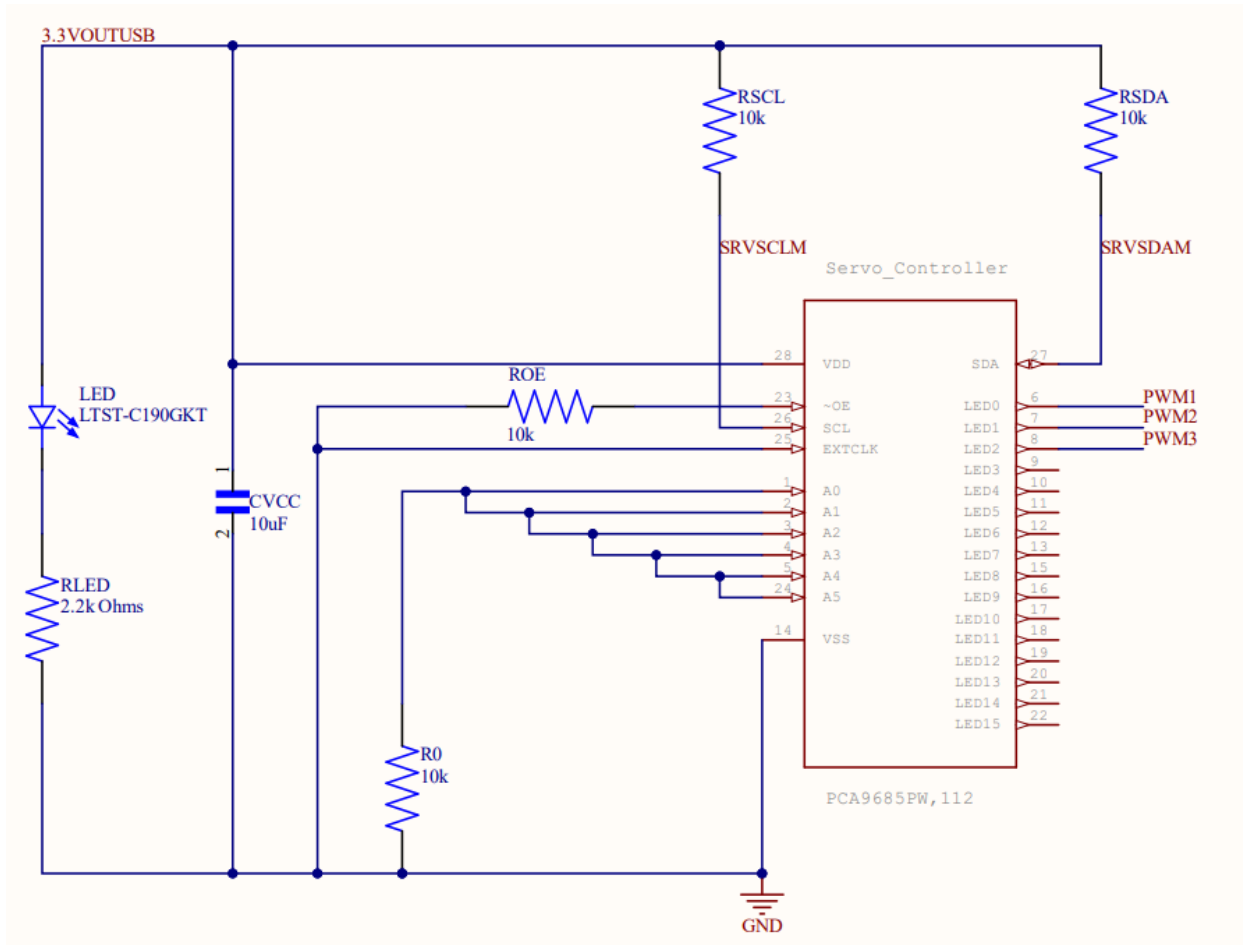


**Figure 6.4.** Servos and Motor Controller Schematic with information by Limor Fried/Ladyada from Adafruit Industries

In figure 6.3, three MG996R servos are connecting to port 0 to port 3 of PCA9685 16-Channel Servo Driver. Each servo controls an axis of x, y and z, which are the rotation of reflector and sensors group. PCA9685 motor controller then connects to microcontroller for data line of terminals SDA and SDL for rotation code to control the servo. The schematic of the board and connection to PCA9685 chips and its peripheral are provided in data sheet as fabricated by Adafruit Industries.

Similarly, to the stepper motor controller breakout board, the servo controller also needs to be in separate PCB due to the line latency from I2C procedure. The PCB board can be brought closer to the servos motor physical location and eliminated the need to wire extension and in turn reduce loss of data and latency. Since there are only 3 servos are needed in the project, only 3 pins are wired to 3 set of pins out. All the address pins are pull down to the ground and established data bit as 00000. a LED is integrated to the controller line instead of power input to check for connection. Power input and data are delivered through an USB-C connector and cable.

## 6.3 Lower-Level Subsystem

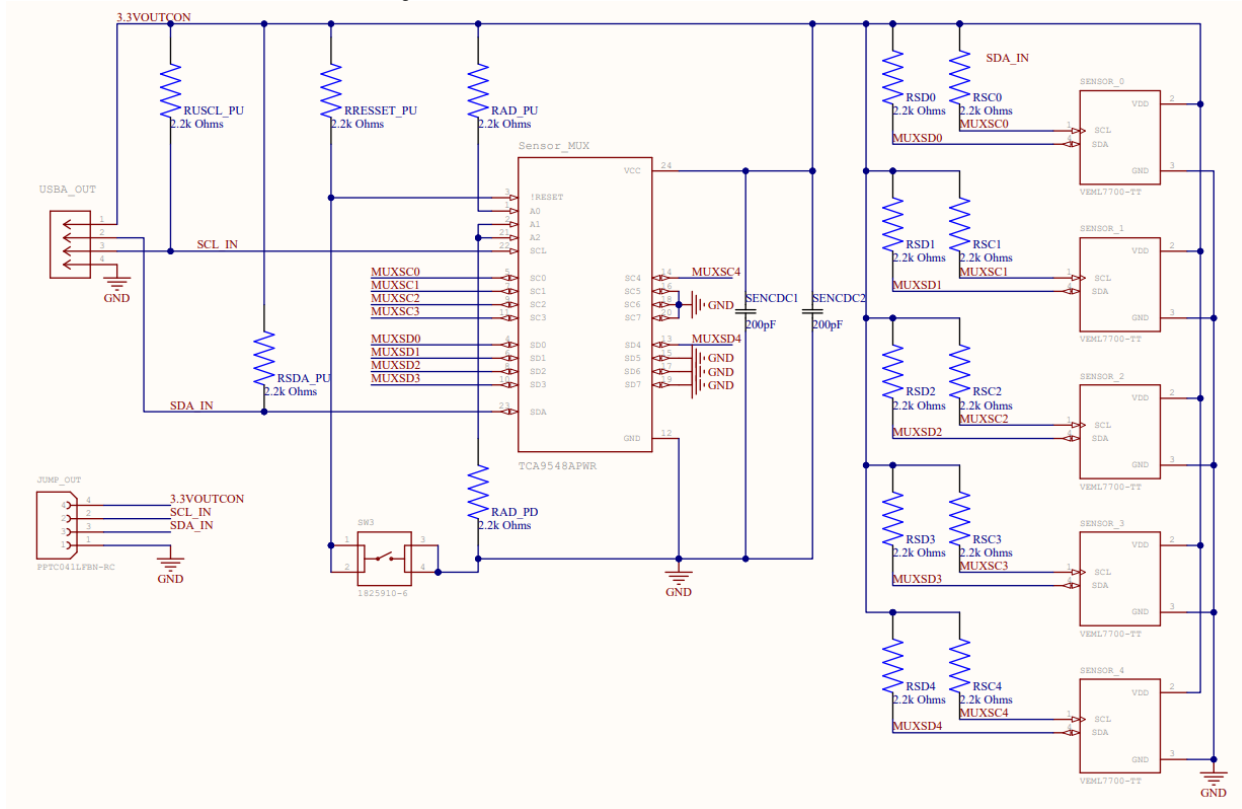


**Figure 6.5. Lower-Level Sensor Connection to MCU through MUX**

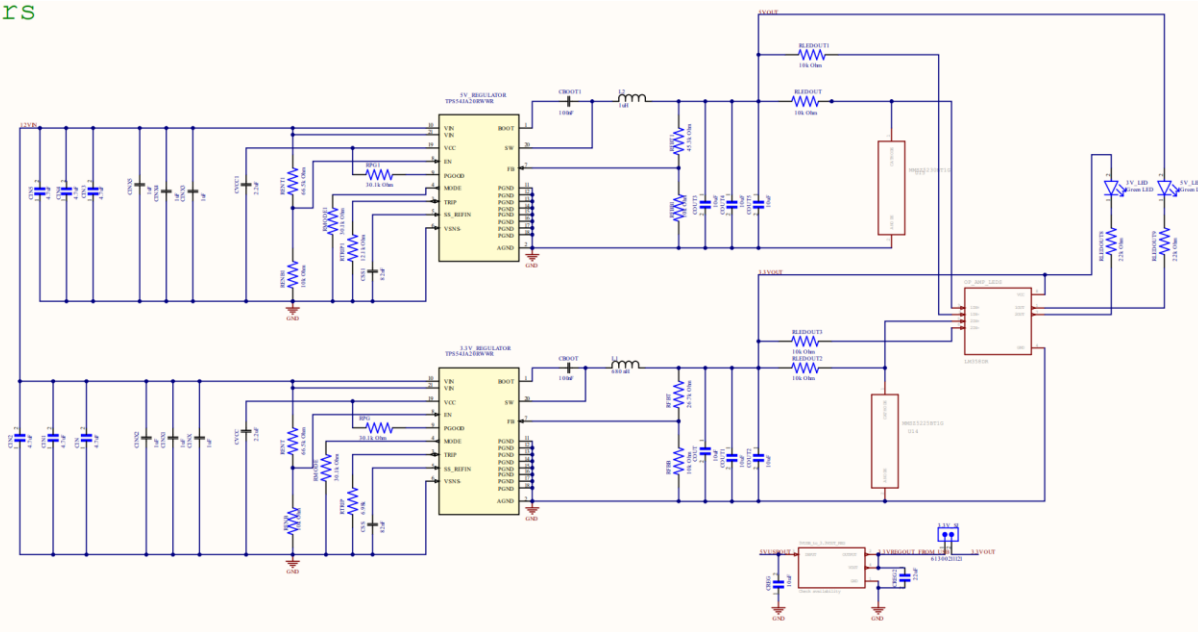
In figure 6.5, the sensor VEML7700 is connect to the MCU in I2C configuration. SDA and SCL is connect to pins 12 and 13 respectively for low power I2C input of ESP32-C6 MCU. Each data transfer pins also connected to Vcc with resistor of 10k Ohm to reduce power. Both the ESP32-C6 board and the sensor are connected to separate regulator to provide 3.3V and 3.7V respectively. A0 and INT pints connect to ground for utilization of low power mode.

Antenna PC140.07.0100A is connect to the dev board ESP-C6's IPEX connector as an external antenna. The dev board will regulate frequencies receptors for compatibility with the external antenna. The MCU chips are the same across two towers. However, communication tower utilizes an integrated dev board due to the existing IPEX connector for the antenna.

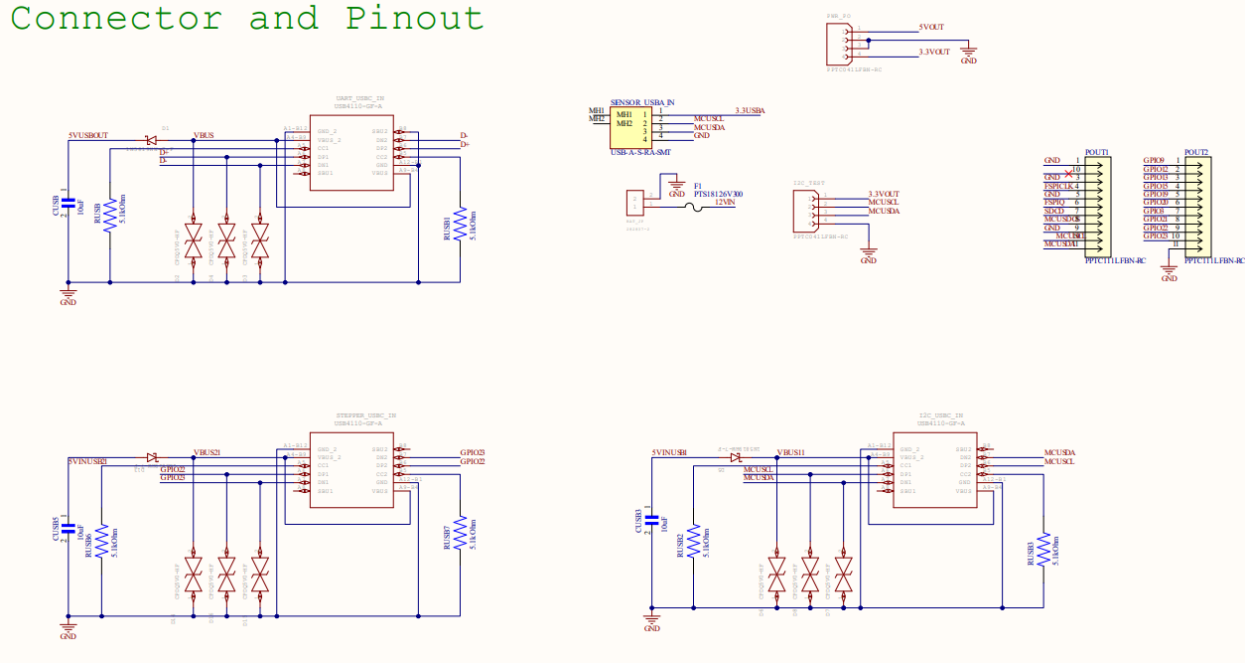
The reflector tower uses a PCB fabricated with MCU ESP32, which housed both the sensors and the external antenna. An additional IPEX port is integrated on the MCU hence the antenna can be directly connected.

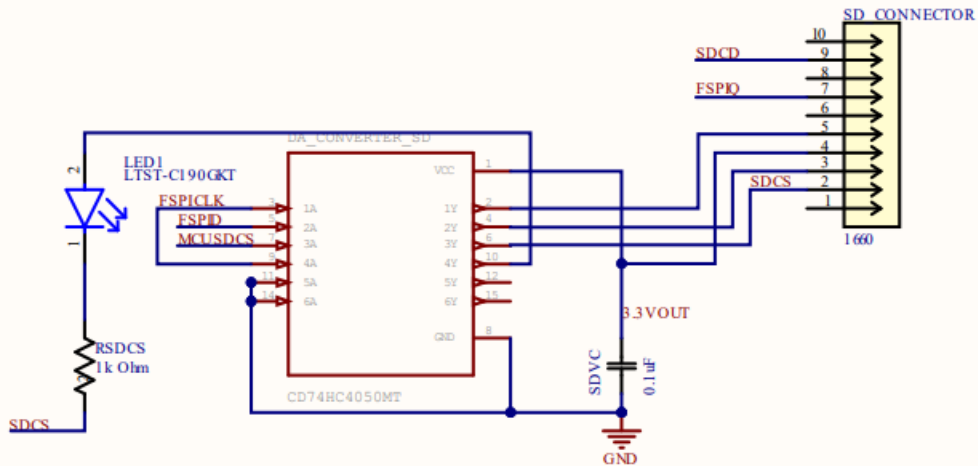
## 6.4 Overall Schematic

ors

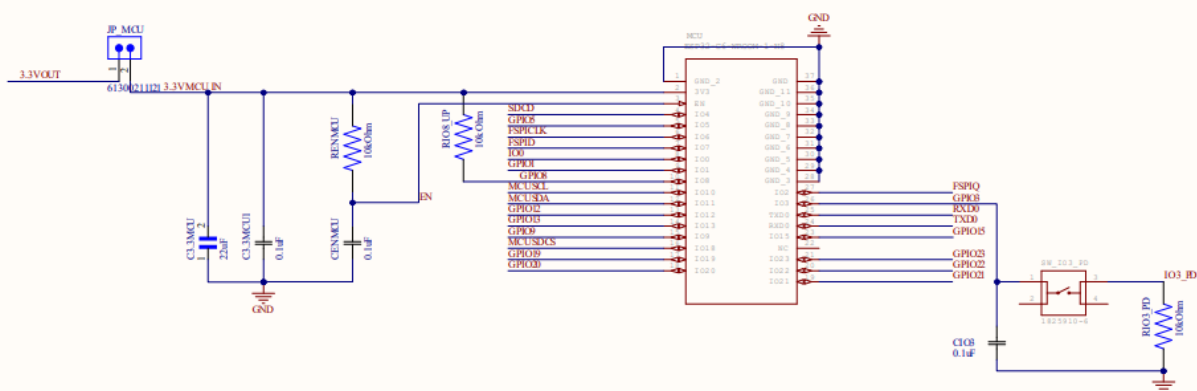


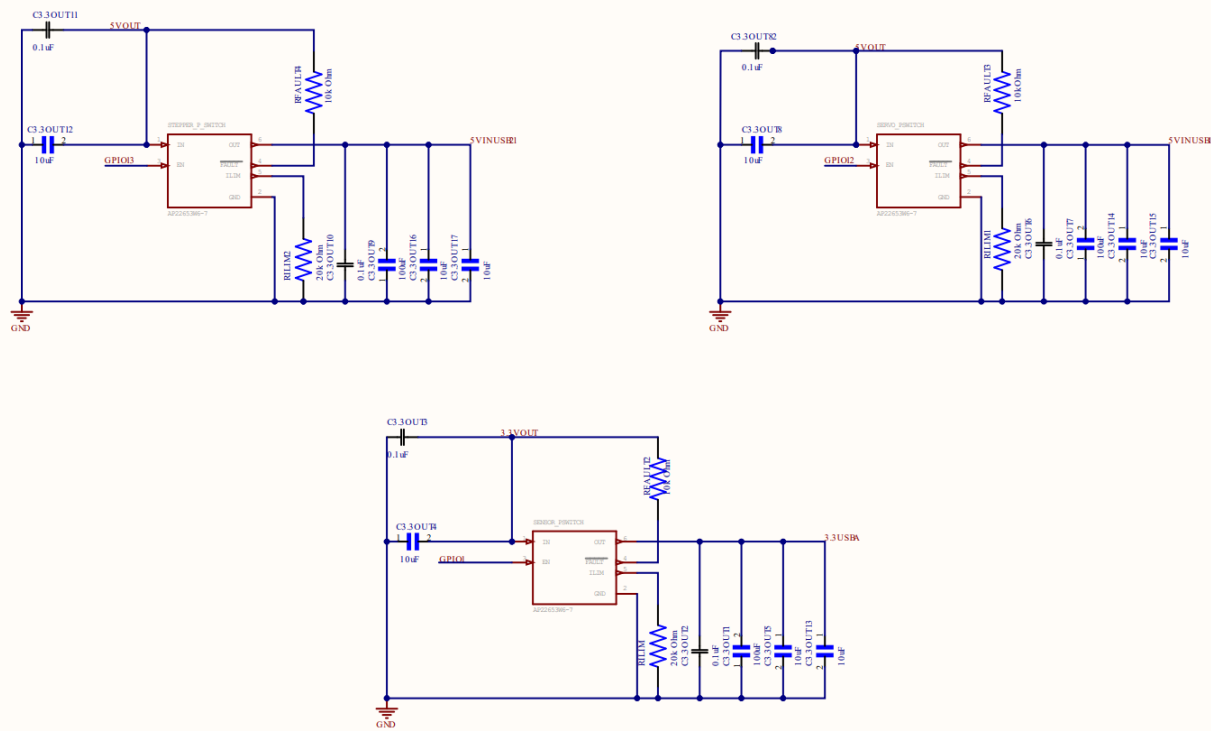
### Connector and Pinout



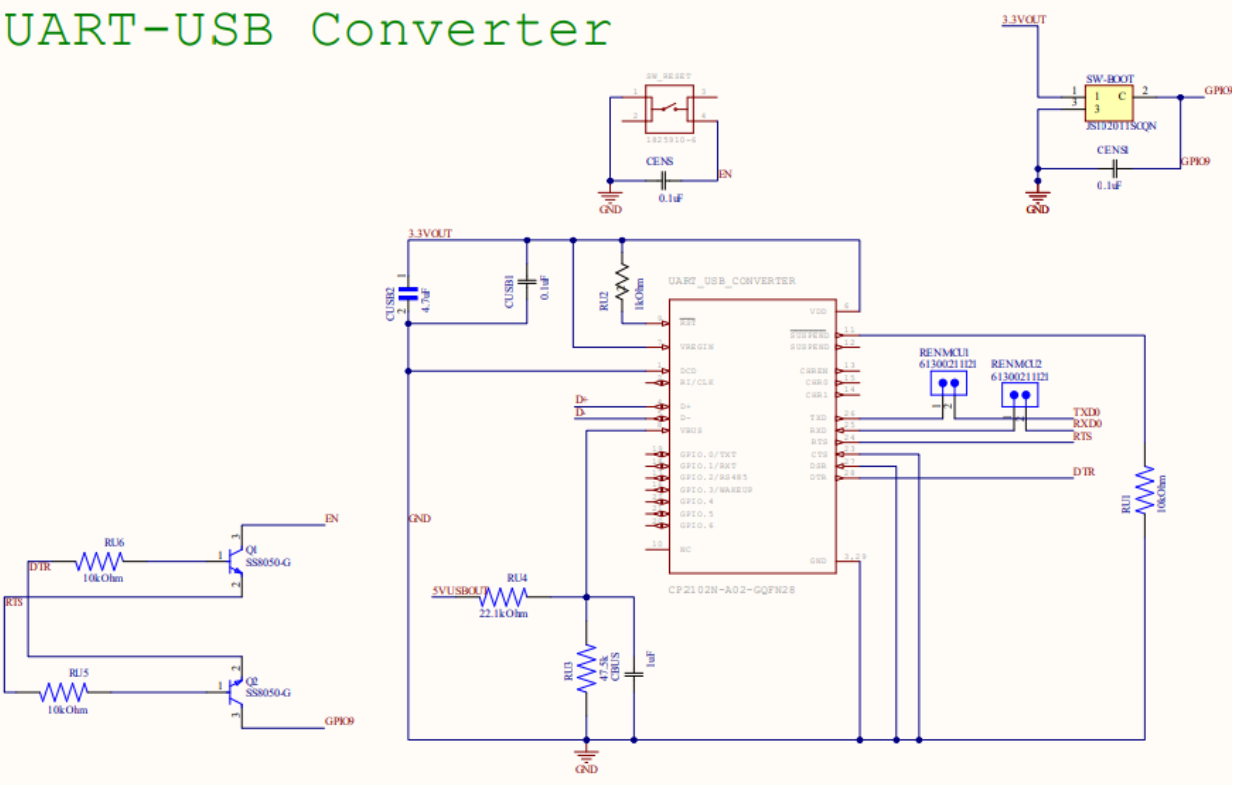


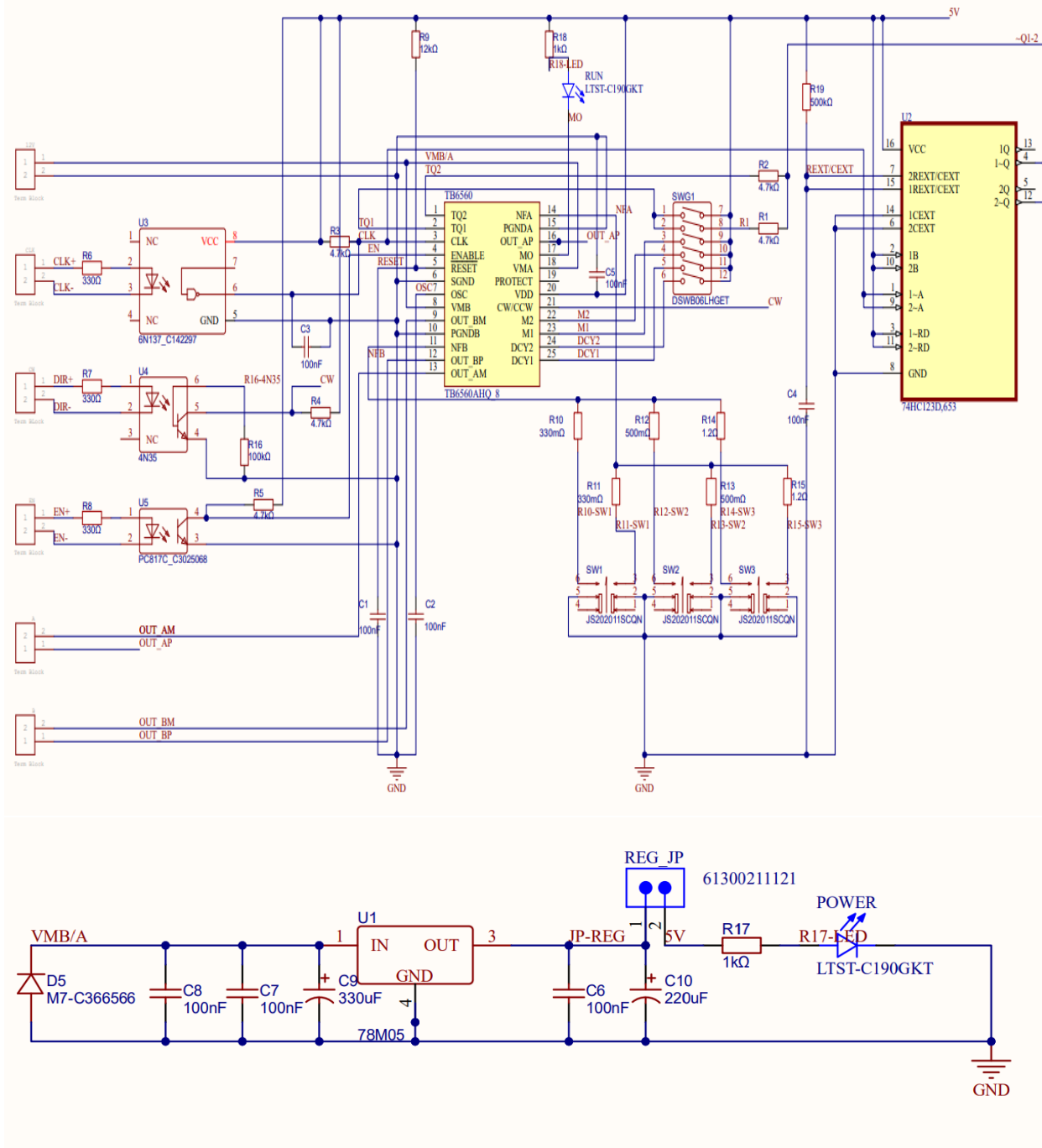
MCU

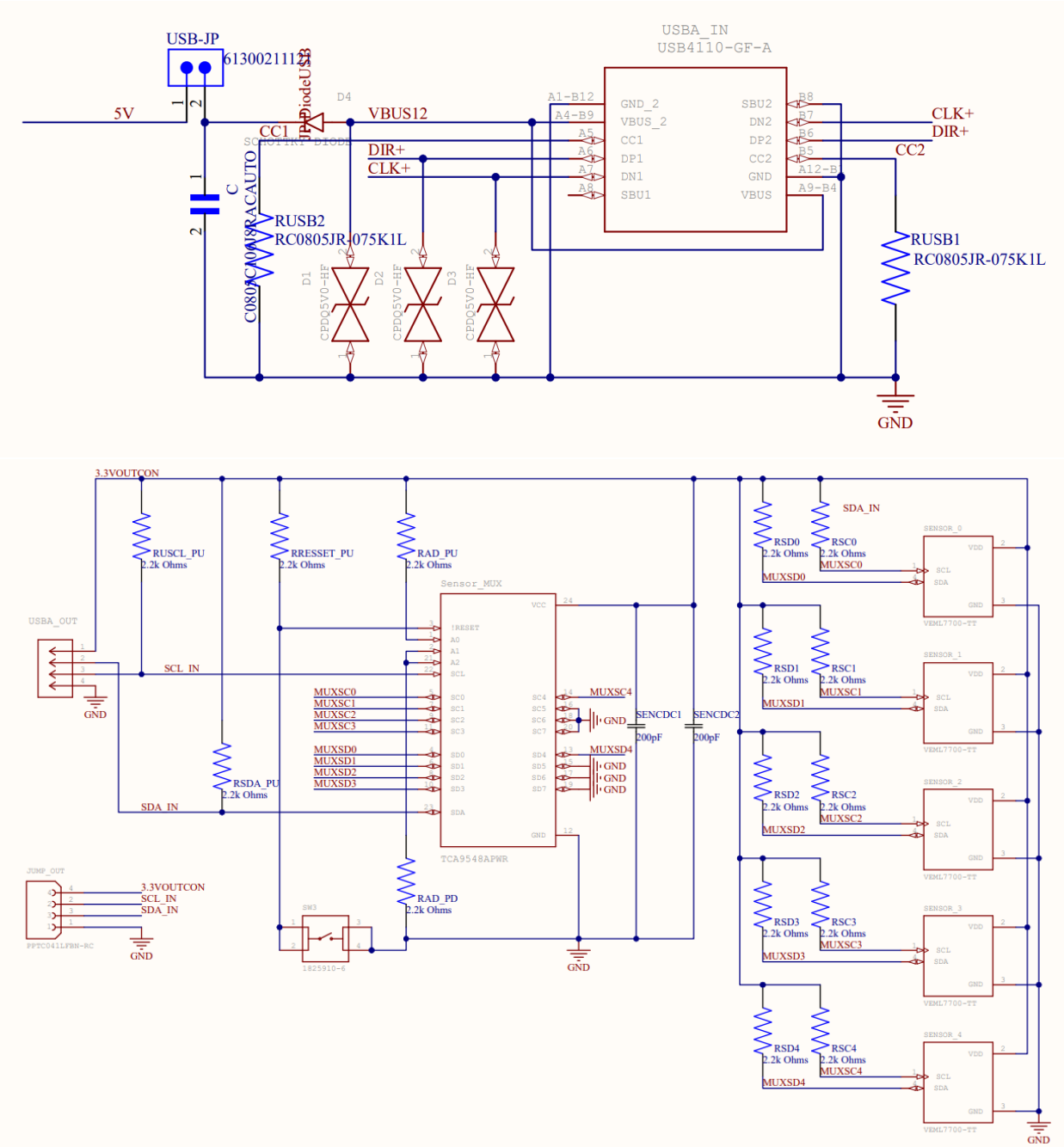


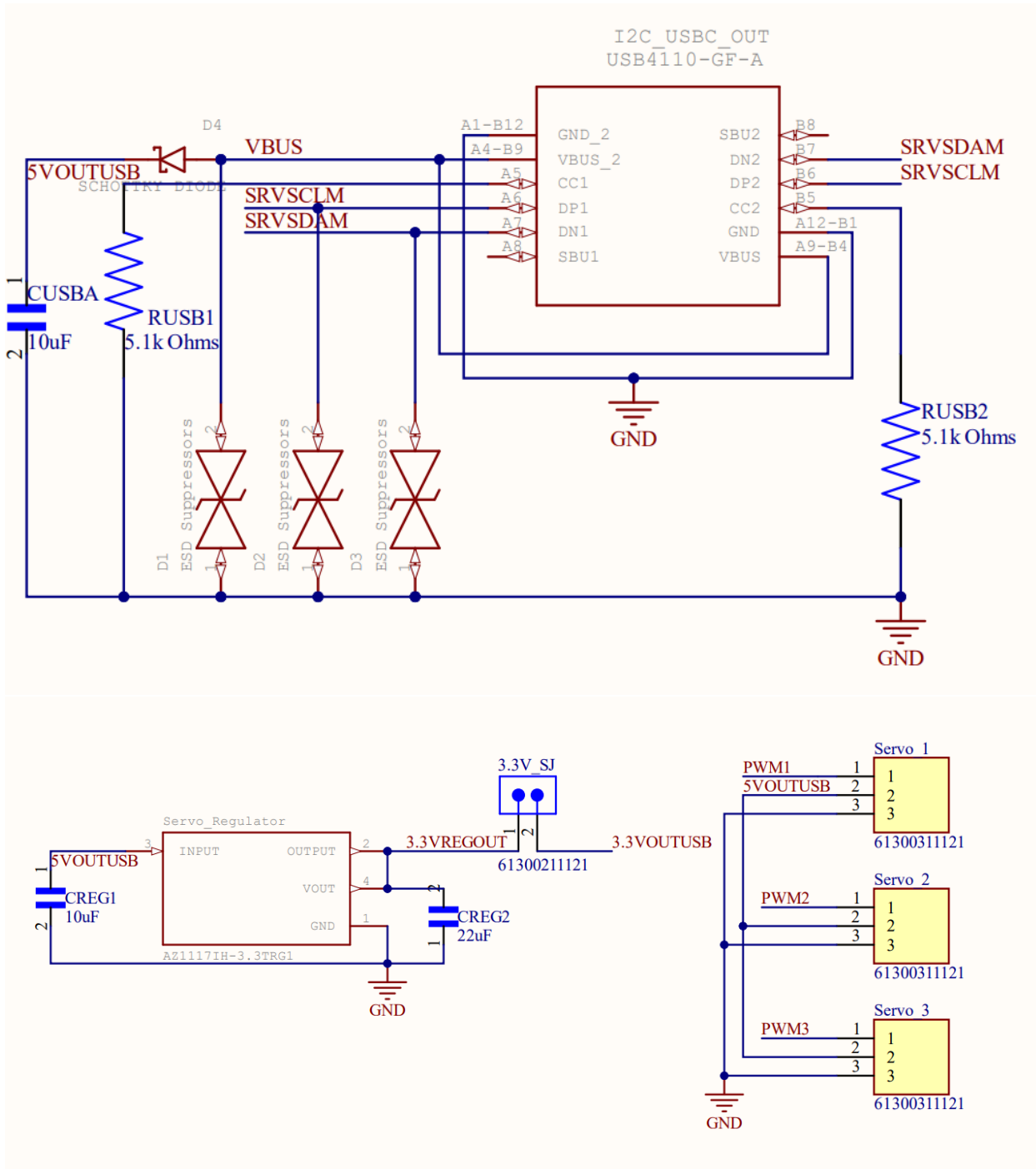


## UART-USB Converter









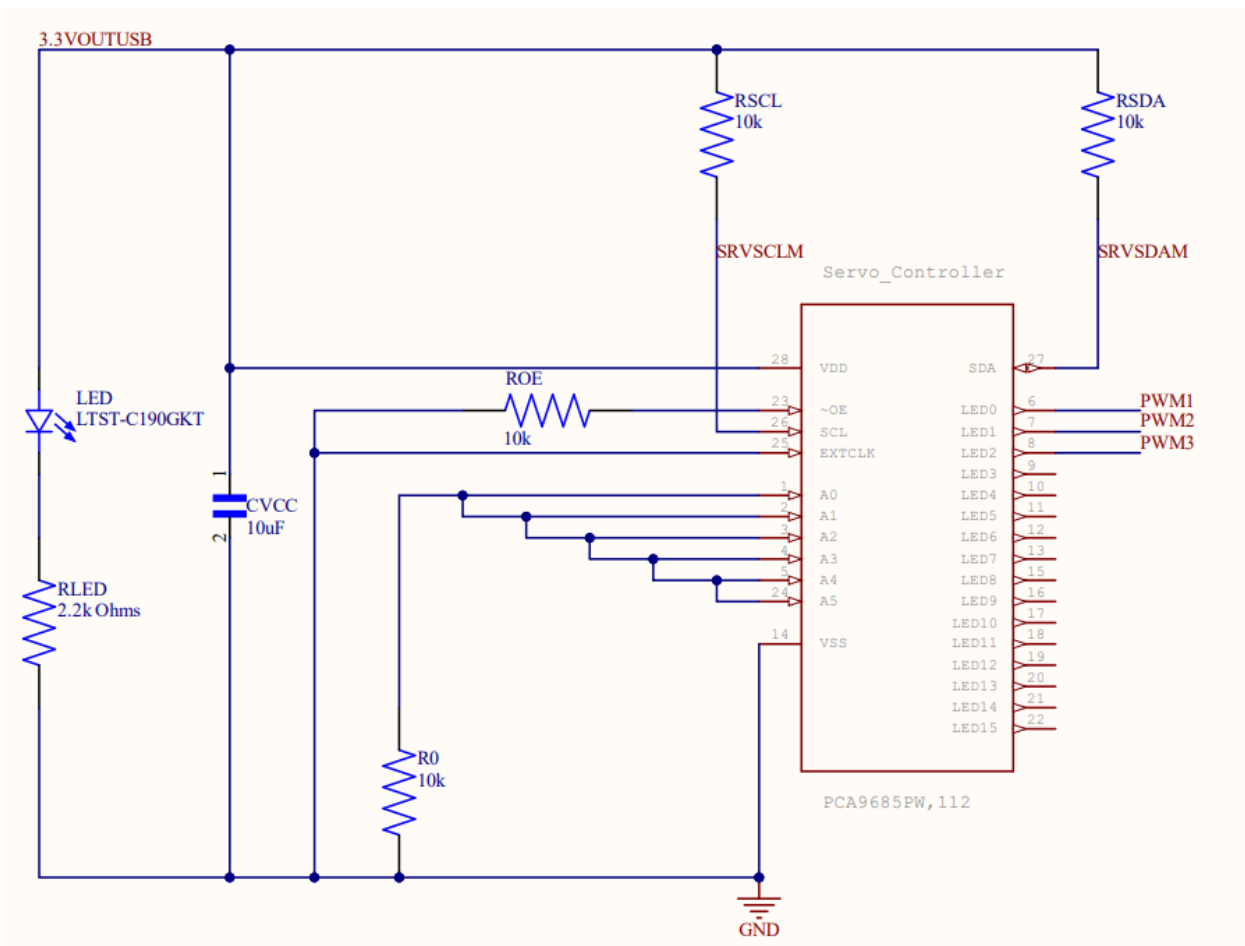


**Figure 6.6.** Overall Schematic of All components  
by Author

# Chapter 7 - System Software Design

SD1 Software Use Case Diagram

Stephen Martin | September 11, 2023

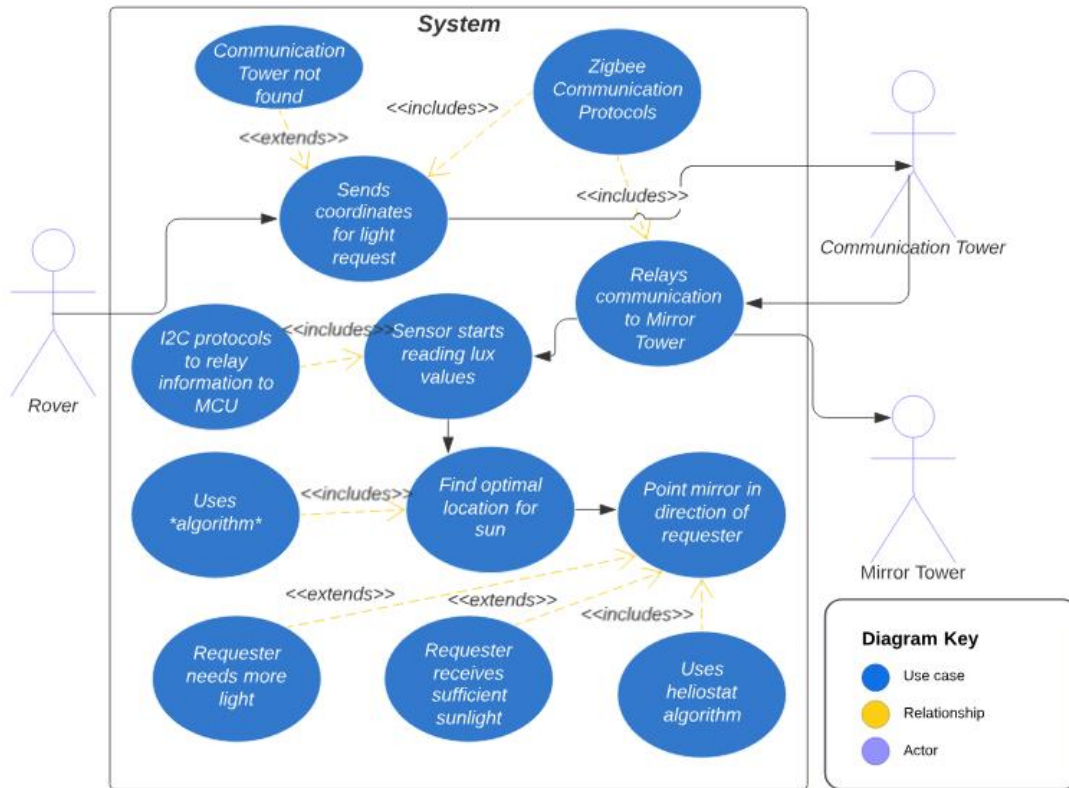


**Figure 7.1.** Software Use Case Diagram  
by Authors

## SD1 Activity Diagram

Stephen Martin | September 11, 2023

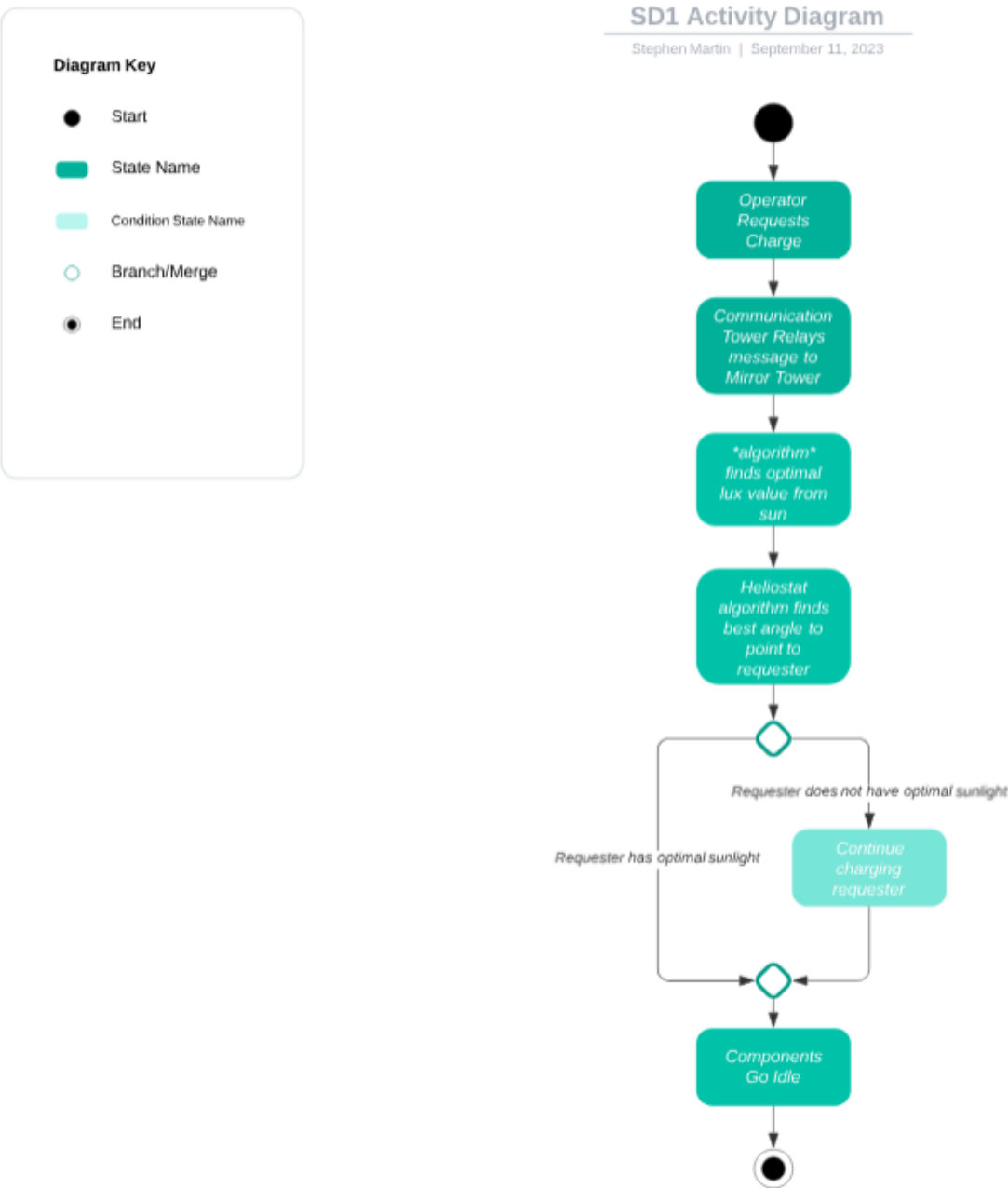


**Figure 7.2.** Software Activity Diagram  
by Authors

## 7.1 Motor positioning of Reflector based on light intensity algorithm.

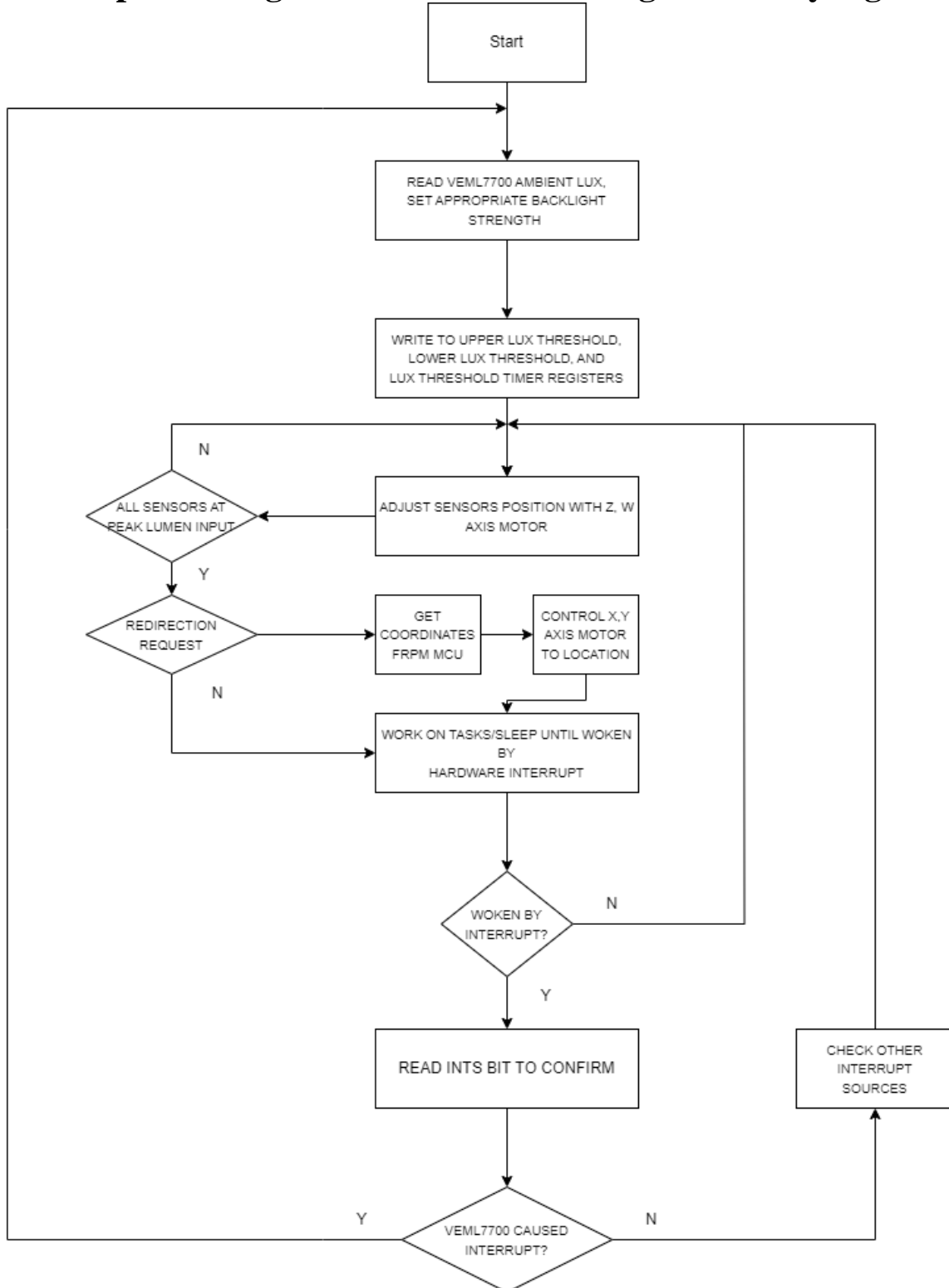


**Figure 7.3.** Motor positioning base on light intensity flowchart with additional information form data sheet.

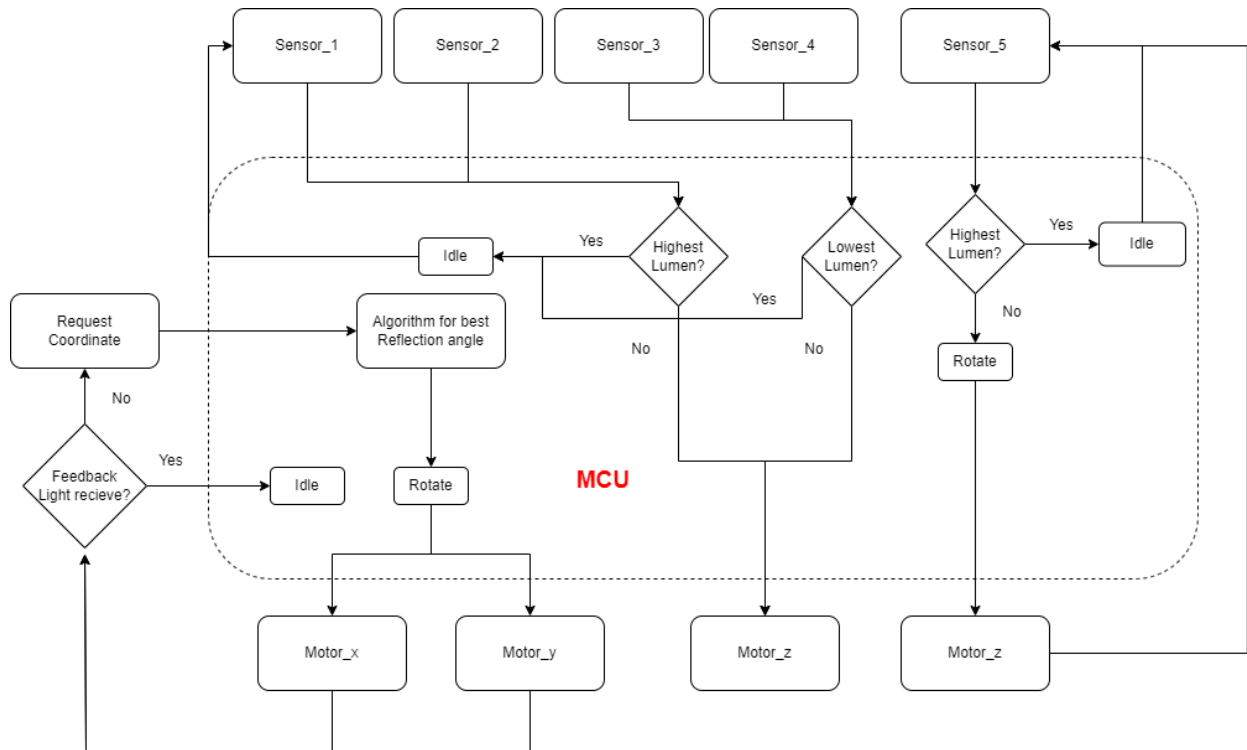


**Figure 7.4. Sensors and Motor control**

Start intake with lumen values through VEML7700. From the intake lumen calculate current maximum sun light position with predetermined threshold. Implement x, y and z term for servos motors. With stepper motor in separate w-axis. Without consider Julian calendar due to different trajectory of the sun on moon's surface, rotate the sensor motor z-axis to get maximum lumen input from all sensors. Rote w-axis motor for both tower frame and sensor at maximum light intake.

The input signal for checking if there exists any request. If there are not an existing request for redirection move on to trigger interrupt. Both motor z and w will rotate along the sun light path for maximum light intake. If a request exists, get coordinate information from MCU provide by antenna intake from grid. x and y-axis motors are rotate to designated coordinate provided. Motors x and y, continuous rotate along with the frame until the request is release. Motor x and y will stop rotating. The interrupt is continuously read throughout redirecting process.

## 7.2 Power Control Algorithm

Power curtailment will be essential for the heliostat's success during the extended sunless periods the south lunar pole experiences. Towards that goal, a power control algorithm is utilized to reduce the current draw from any unnecessary components during sunless periods. All non-essential components will be disabled, and any essential components will be in low-power mode. A table below describes which components are essential and what low-power mode they will be in during sunless periods.

**Table 7.1.** A table describing essential systems in low power operation.

Component	Essential/Non-Essential	Low-Power Considerations
MCU	Essential	Low-Power Mode, only essential functions
Antenna	Essential	Receive only
Sensors	Essential	Sensors will be turned on periodically
Stepper Motor	Non-Essential	
Servo Motors	Non-Essential	

During sunless periods it is essential to keep power consumption low in order to keep the drain on the battery minimal. To this end, the highest power consumption components, such as the motors should not be used during these periods unless necessary. Before the sunsets, the position of the tower should be oriented to where the sun is next expected. This will ensure that when the sunsets, the motors will not need to be used until the sun rises again. To determine when the sun rises again, the sensors will be turned on in order to detect the lux levels; if there is a significant positive change, this will indicate the sun is rising and that more components can be enabled again.

Another important feature of the power control algorithm is the management of the battery. Both the heliostat and the communication beacon require this system. If ever the battery is undervoltage, the algorithm will dictate that all non-essential components are disabled and will wait until the solar-panel and charge controller can restore normal operating voltage to the battery. This will be important during periods of heavy motor or antenna usage, such as during testing or high demand periods.

Other fault conditions, such as over-temperature and over-voltage should be managed internally by the charge controller selected and the BMS within the battery. There will also be redundant precautions, such as shutdown if ever the battery reaches over-temperature or over-voltage.

## Chapter 8 - System Fabrication

### 8.1 PCB

PCBs are designed and placement done by Altium software application. Some adjustments were done such as the trace width of some wiring needed to be adjusted. Inclusion of more features, such as a switch for the strapping pins and more labels were included in the revised MCU board. All PCBs included ground planes and polygon stitching for an efficient connection between layers. Jumpers' pads are connected at several location for easy access and break off for testing. Stepper motor board noise isolation between USBC and Motor Controller by braid cable to GND, tripod body, between ESP and Motor controller. Minimized hanging pin to account for open circuit. Regulators were placed further away from sensitive components to reduce noise from the switching regulators. Capacitors were placed close to relevant devices to reduce the size of current loops. The first designs of the sensor and servo boards worked well and requiring only 1 revision of the MCU board and a reorder of the sensor board (due to mechanical error) was necessary.

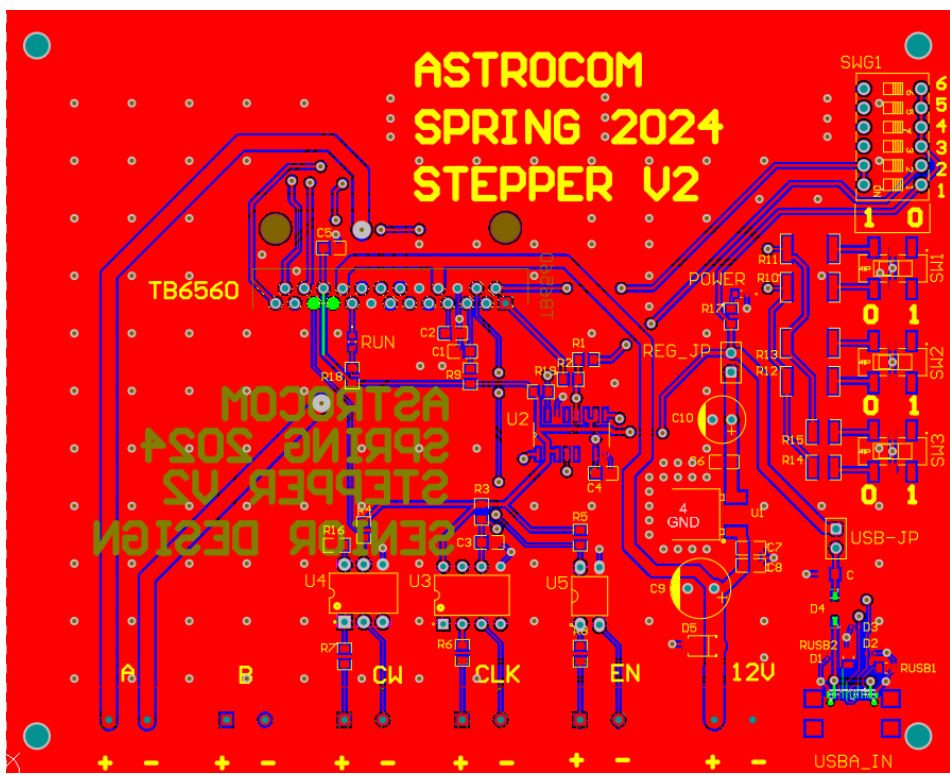


**Figure 8.1.** Stepper PCB VI

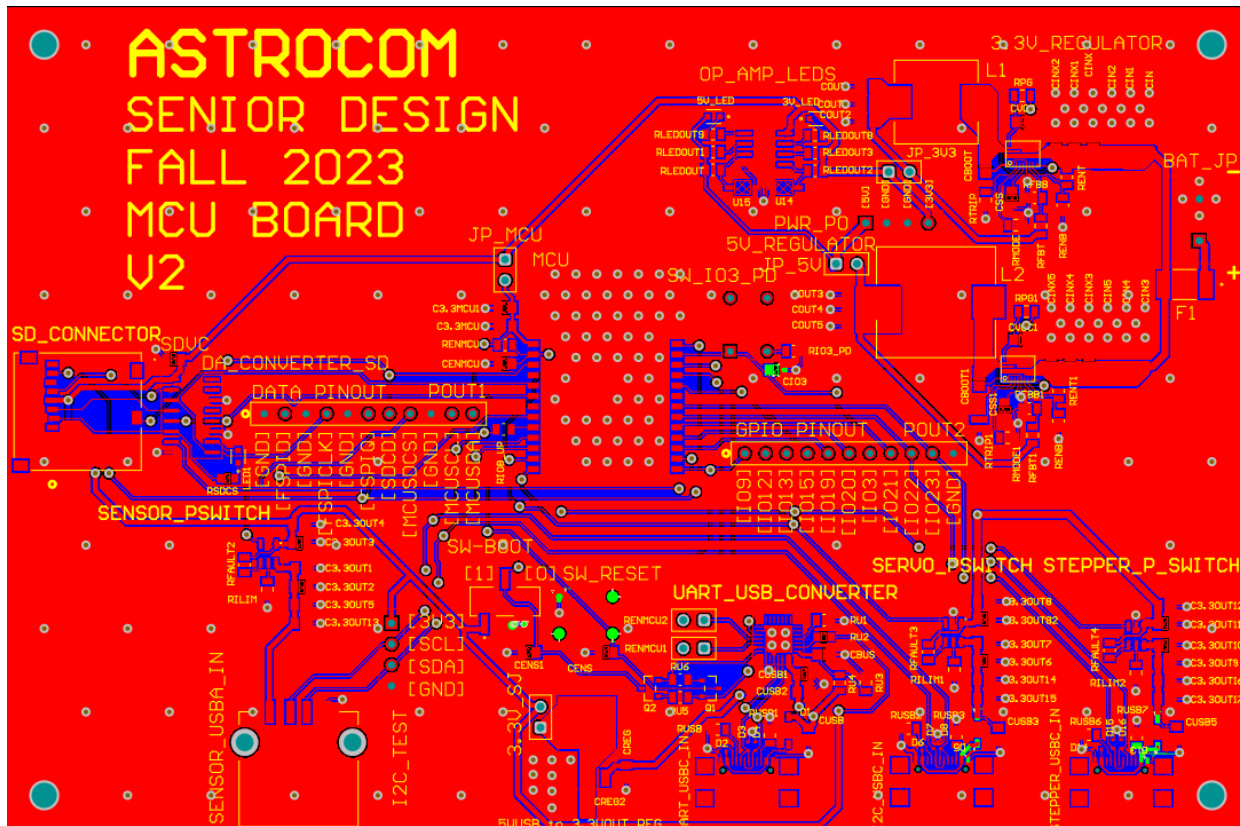


**Figure 8.2.** Stepper PCB VI

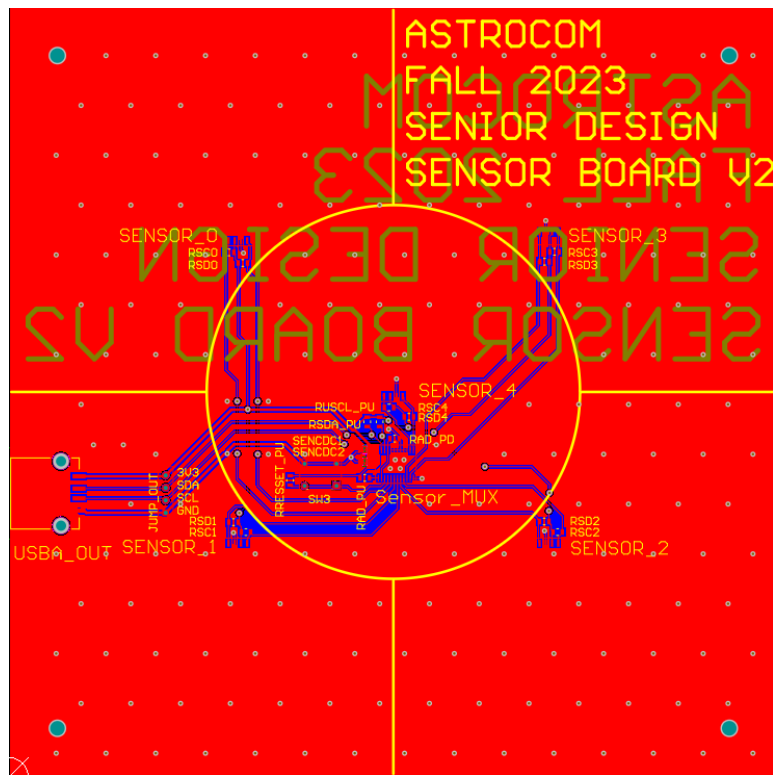


Figure 8.3. Sensor PCB V1

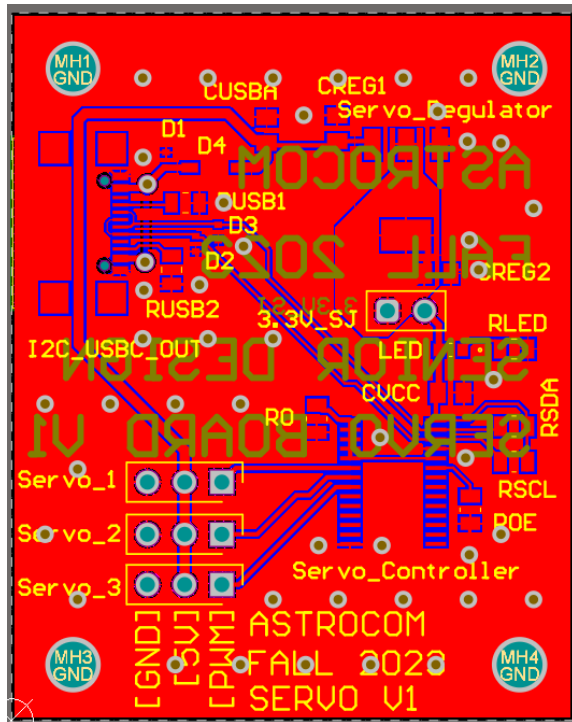
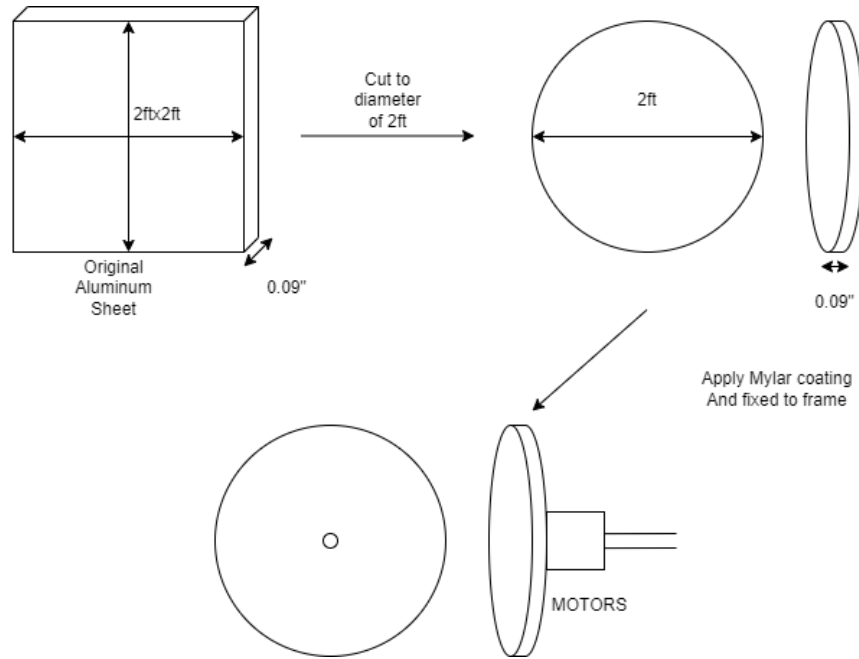


Figure 8.4. MCU Servo V1

## 8.2 Reflector

A 0.09" Aluminum Sheet 5052-H32 in  $2ft \times 2ft$  cut into a circular disc with a diameter of 2ft. The weight calculated after trim could be  $w_t = \frac{w}{2ft^2} \times 1^2\pi ft^2 = \frac{5.04lb\pi}{2} = 7.92lb$ . The disc is then covered by a Mylar sheet which is affixed by adhesive with the most negligible change in surface reflection. To minimize reflection loss, the reflector connects to a frame with a bolt in the middle.



**Figure 8.5. Reflector Fabrication Step Diagram**

by Authors

## 8.3 Reflector Tower

The frame is then connected to the x and y motor. A motor must be placed to control the z-axis, which controls the sensor for the most effective light intake.

Fabrication of the w-axis needs to consider the modification of the frame. The tripod or frame is cut in the middle with a CAD 3D prints mechanical box to implement w-axis rotation using the w-stepper motor. Other parts, which are not purchased, can be fabricated using CAD and 3D printing.

The fabrication of the sensor mechanism accounts for 4 sensors and 1 motor rotating on specified z-axis. The four sensors are set in partition to vary the shadow when first receiving light from the sun. Based on the light intensity intake from the sensors, the motor z moves based on the vectors generated by the matrix algorithm for the maximum light intake from all sensors. The partition and mechanical mechanism are fabricated using CAD to form a 3D model. When the sensors all detect the same amount of light (within some margin) that means they have found the optimal position and the motor position is recorded so that the light reflection angle can be calculated. The construction of the tower can be described as a tripod with the assembly shown in Fig. 8.6 at the top of the tripod. The tripod rests on a turntable with a bearing controlled by the stepper motor.

The stepper motor is housed in a box ensuring it can support the weight of the bearing. The box is made of 3/8ths inch plywood due to cost and convenience. The turntable bearing is supported with accessory roller bearings on the underneath the edge of the turntable, to help support the weight far from the center of the bearing. In future works, further thought should be placed in the mechanical design of the base.

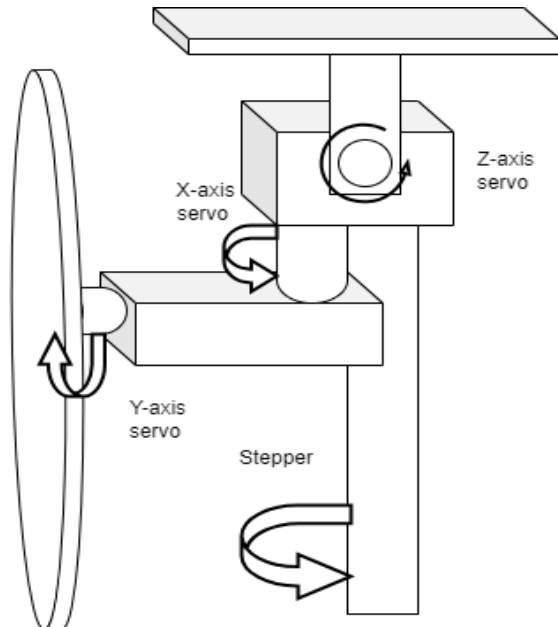


**Figure 8.6. Motors Placements on Reflector Tower**

by Author

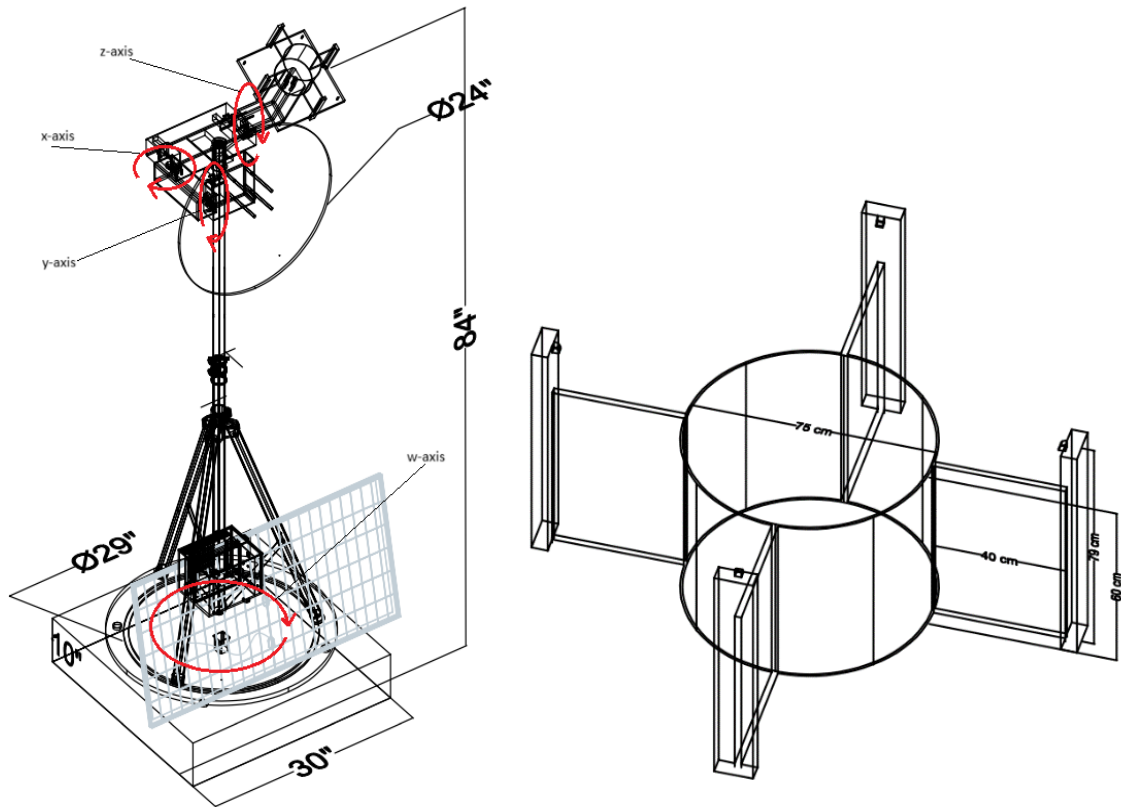


**Figure 8.7.** Complete 3D model of reflector tower and Sensor partition with CAD

by Author

## 8.4 Communication Tower

The communication tower will be in the shape of a small box with dimensions of at least 6.5 in \* 6.5 in \* 5 in. This will be in the form of a commercially available polycarbonate enclosure that will be modified to suit the project's needs. The dimensional constraint ensures that the microcontroller board and battery power can fit inside. There will also be an antenna attached to the microcontroller board.

The enclosure will be modified such that the antenna can peek out and optimal range is ensured. A hole will be drilled at the top of the enclosure for the antenna to peek out. Due to the small size of the antenna, the bottom will have to be padded about 4 in. so that the antenna can peek out of a hole at the top of the enclosure and reduce risk of range interference.

The battery is large and will fit snugly in the enclosure, its bottom will not require any padding, only the microcontroller with the antenna. The final modification is the installation of a small handle to the side of the enclosure. The tower must be as light as possible so that the rover can carry it with the handle. The weight of the handle and interior padding will be negligible.

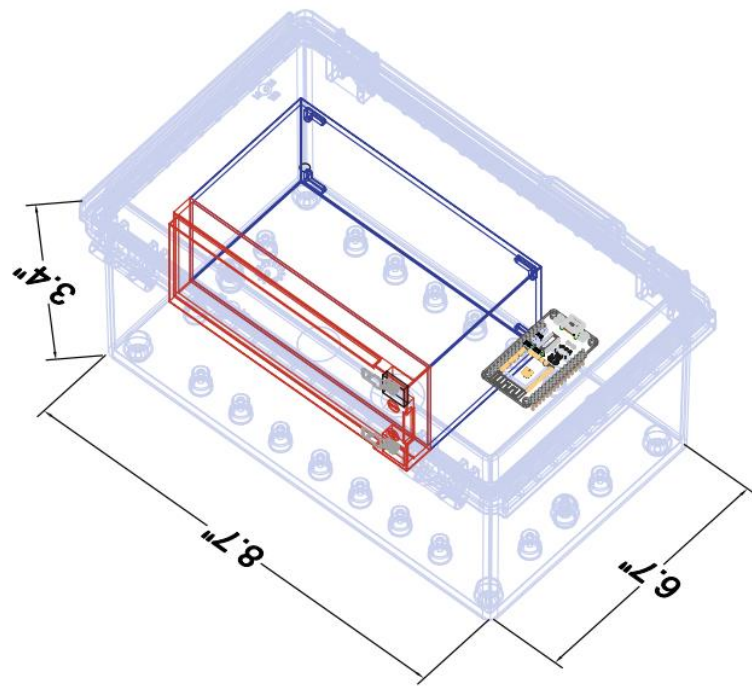


**Figure 8.8.** CAD model of Communication Tower

by Author

# **Chapter 9 - Prototype and System Testing**

## **9.1 Hardware Testing**

### **9.1.1 ESP32-C6**

To test that the ESP32-C6 development boards purchased were working correctly, they were first plugged into power through their USB-C ports. The RGB LED powering on verifies that the device is receiving power. After this, GPIO pin voltages could be verified using a digital multimeter. The reset button functionality could be verified by pushing it.

### **9.1.2 MicroSD card adapter**

To test the AdaFruit MicroSD card breakout board, the breakout board was connected appropriately to the ESP32-C6 using the DO to pin 2, DI to pin 7, CS to pin 18, CLK to pin 6, and CD to pin 4. A 256 MB microSD card was inserted into the adapter. After this, the file system software was ready for testing.

### **9.1.3 VEML7700**

To test the hardware functionality of the VEML7700 light sensor, it was wired up the sensor to the ESP32-C6 using a breadboard and properly connected it by pairing the 3V output to the Vin, ground, and SDA and SCL lines to their respective GPIO pins (21 and 22). After wiring, it was confirmed that it worked properly with a power LED showing on the light sensor. Also, through software testing, it was confirmed that the SDA and SCL lines were properly connected by running some code and ensuring the proper transfer of data through flashing.

### **9.1.4 TCA9548A I2C Multiplexer**

To test the TCA9548A to see if it was properly hooked up in terms of hardware, there was a similar strategy used to test as the VEML7700 light sensor. It was hooked up to the ESP32-C6 with its Vin to the 3V output from the microcontroller and the grounds connected. Also, the data transfer was tested by hooking up the SDA and SCL to GPIO 21 and 22 and then connecting two sensors to the multiplexer to ports 2 and 3.

### **9.1.5 Motors**

Two servo motors are attached to a 3D printed L piece, figure 8.7, to have precise rotation of reflector on x and y axis. Step per cycle limited to 2 to increase precision as rotation speed is not required. The last servo motor will attach to the sensor PCB to rotated up and down as take in input from sensor. The angle of rotation for x motor is  $270^\circ$ , y motor is  $90^\circ$ , and z motor is  $120^\circ$ . Stepper motor is used for the w axis, which attach to a plate at base to rotate the whole structure. Rotation expected to be rotated  $270^\circ$  with assistance from a wheel hub and a gear box for smooth transition and torque on rotation.

### **9.1.6 Antenna**

The ESP32-C6 development boards have a built-in antenna and no external antenna connector. With modifications to the board however, the antenna connection can be exposed, and an external antenna may be soldered on in replacement. For the module alone on the custom PCB, a complicated modification and breaking the built-in antenna is not needed, simply connecting the external antenna to the IPEX connector is sufficient.

### 9.1.7 PCB Simulation

The PCBs' designs were improved through several theoretical testing. A test run on Fadstad circuits to identify the design for LED indicator with 4.7V and 3V Zenner diodes. Simulation of TI Webench on 3.3V and 5V regulators shown a consistent level off in voltage after 3ms with an input of 12V and output as expected.

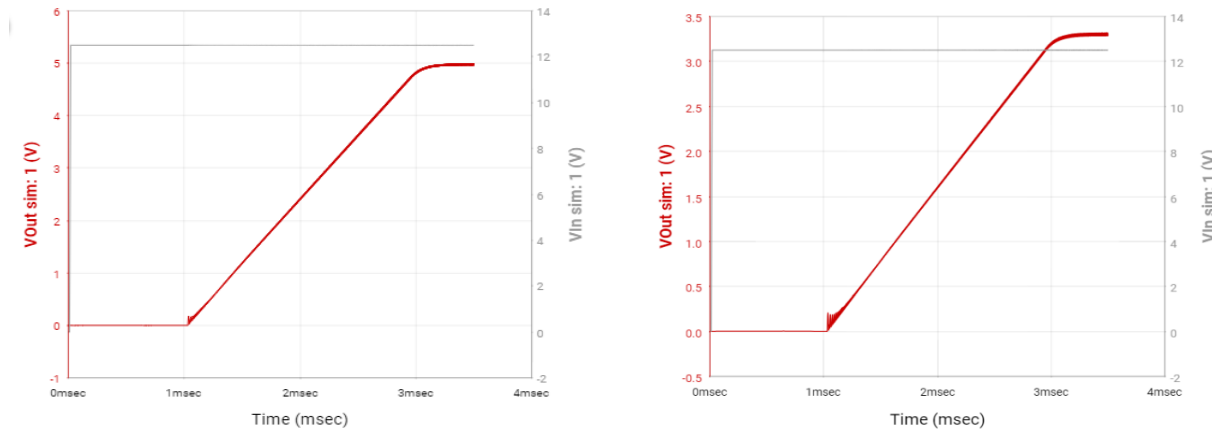


*Figure 9.1. TI Webench Regulators Simulations*

### 9.1.8 Charge Controller

The charge controller was powered through a DC power supply to verify its function. There was initially an issue with over-voltage protection, in which the charge controller would enter over-voltage protection mode over 13V, despite our LiFePo battery coming out of the box at 13.08V. Thus, the charge controller would not properly operate with the battery. After manipulating the settings on the charge controller and configuring it specifically for LiFePo batteries, the charge controller operated as expected. The charger controller performs well under load, maintaining both the battery charge and supplying the other regulators with a consistent 12V.

### 9.1.9 Solar Panel

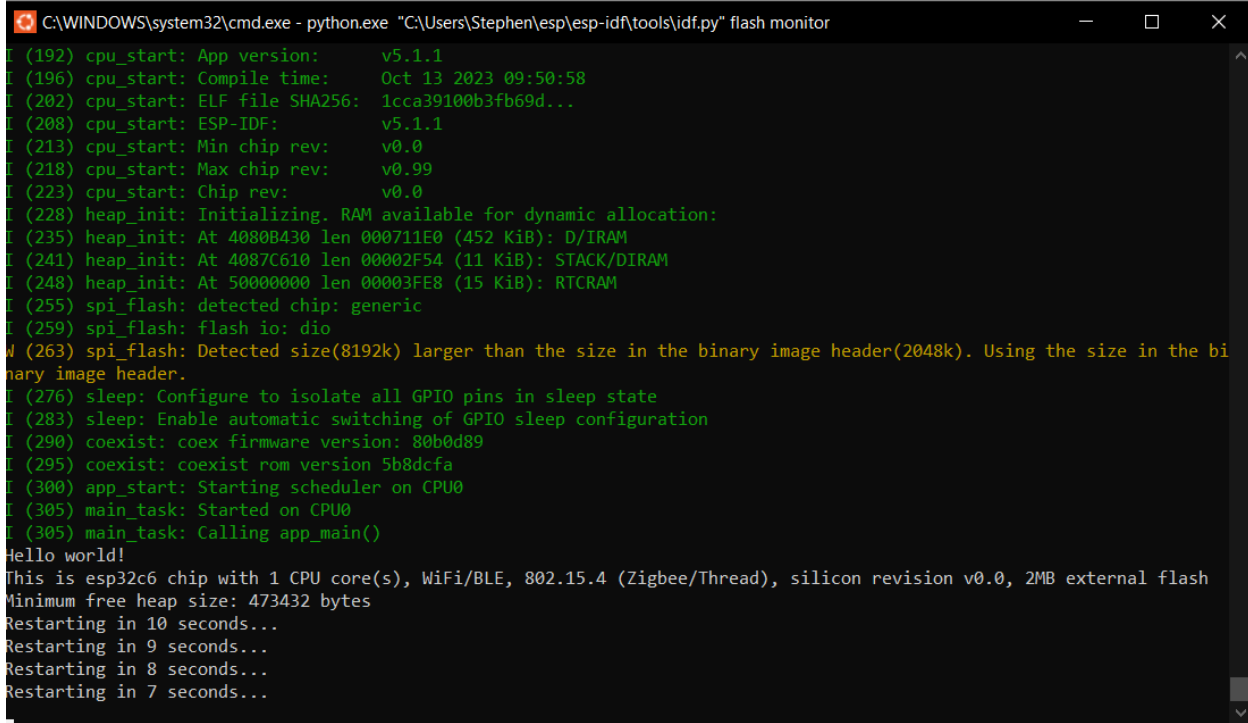
The solar panel was tested outdoors during day-light hours. The resulting voltage was 24V as measured with a multi-meter. This is the expected value from the specified panel. Further testing at a different time, revealed an open circuit voltage of 21V and a short circuit current of 2.9A. This is inline with the ratings of the panel and prove that the panel can produce more than 30W under load.

## 9.2 Software Testing

### 9.2.1 ESP32-C6

For the ESP32-C6, we started by cloning the appropriate GitHub repository onto our local devices to set up our environment. Most of us used some type of terminal (Ubuntu, Command Prompt, Windows Powershell) to run ESP-IDF, which is the framework used to build and run projects using the microcontroller.

Once we set up our environments, we started by running some of the example code given to us by Espressif to run code on our devices. This included a few small programs such as “hello\_world.c” and “blink.c” which wrote Hello World to the terminal while flashing and blinks the LED light on the breakout board respectively. Below are some screenshots of the code running on our devices.



```
C:\WINDOWS\system32\cmd.exe - python.exe "C:\Users\Stephen\esp\esp-idf\tools\idf.py" flash monitor
I (192) cpu_start: App version:      v5.1.1
I (196) cpu_start: Compile time:    Oct 13 2023 09:50:58
I (202) cpu_start: ELF file SHA256: 1cca39100b3fb69d...
I (208) cpu_start: ESP-IDF:         v5.1.1
I (213) cpu_start: Min chip rev:   v0.0
I (218) cpu_start: Max chip rev:   v0.99
I (223) cpu_start: Chip rev:      v0.0
I (228) heap_init: Initializing. RAM available for dynamic allocation:
I (235) heap_init: At 4080B430 len 000711E0 (452 KiB): D/IRAM
I (241) heap_init: At 4087C610 len 00002F54 (11 KiB): STACK/DIRAM
I (248) heap_init: At 50000000 len 00003FE8 (15 KiB): RTCRAM
I (255) spi_flash: detected chip: generic
I (259) spi_flash: flash io: dio
W (263) spi_flash: Detected size(8192k) larger than the size in the binary image header(2048k). Using the size in the binary image header.
I (276) sleep: Configure to isolate all GPIO pins in sleep state
I (283) sleep: Enable automatic switching of GPIO sleep configuration
I (290) coexist: coex firmware version: 80b0d89
I (295) coexist: coexist rom version 5b8dcfa
I (300) app_start: Starting scheduler on CPU0
I (305) main_task: Started on CPU0
I (305) main_task: Calling app_main()
Hello world!
This is esp32c6 chip with 1 CPU core(s), WiFi/BLE, 802.15.4 (Zigbee/Thread), silicon revision v0.0, 2MB external flash
Minimum free heap size: 473432 bytes
Restarting in 10 seconds...
Restarting in 9 seconds...
Restarting in 8 seconds...
Restarting in 7 seconds...
```

**Figure 9.2.** Flashing of hello\_world.c example program  
by Author

```
C:\WINDOWS\system32\cmd.exe - python.exe "C:\Users\Stephen\esp\esp-idf\tools\idf.py" flash monitor
I (187) cpu_start: Min chip rev: v0.0
I (192) cpu_start: Max chip rev: v0.99
I (197) cpu_start: Chip rev: v0.0
I (202) heap_init: Initializing. RAM available for dynamic allocation:
I (209) heap_init: At 4080C1E0 len 00070430 (449 KiB): D/IRAM
I (215) heap_init: At 4087C610 len 00002F54 (11 KiB): STACK/DIRAM
I (222) heap_init: At 50000000 len 00003FE8 (15 KiB): RTCRAM
I (229) spi_flash: detected chip: generic
I (233) spi_flash: flash io: dio
W (237) spi_flash: Detected size(8192k) larger than the size in the binary image header(2048k). Using the size in the binary image header.
I (250) sleep: Configure to isolate all GPIO pins in sleep state
I (257) sleep: Enable automatic switching of GPIO sleep configuration
I (264) coexist: coex firmware version: 80b0d89
I (269) coexist: coexist rom version 5b8dcfa
I (274) app_start: Starting scheduler on CPU0
I (279) main_task: Started on CPU0
I (279) main_task: Calling app_main()
I (279) example: Example configured to blink addressable LED!
I (289) gpio: GPIO[8]| InputEn: 0| OutputEn: 1| OpenDrain: 0| Pullup: 1| Pulldown: 0| Intr:0
I (299) example: Turning the LED OFF!
I (1299) example: Turning the LED ON!
I (2299) example: Turning the LED OFF!
I (3299) example: Turning the LED ON!
I (4299) example: Turning the LED OFF!
I (5299) example: Turning the LED ON!
I (6299) example: Turning the LED OFF!
I (7299) example: Turning the LED ON!
I (8299) example: Turning the LED OFF!
```

*Figure 9.3. Flashing of blink.c example program*

*by Author*

From this point, we started working on different peripherals to run using the ESP32-C6 and began running some example codes to ensure new parts can run on the environments that we have installed.

### 9.2.2 MicroSD card adapter

To test that the microSD card and its adapter were functioning properly, the menuconfig and sdspi code included with ESP-IDF were the most useful. The menuconfig allowed for easily configuring the SPI pin layout and confirming that the connections were correct, in a terminal GUI. After everything was ready, sdspi could be flashed successfully. When checking the storage system of the microSD card after running the software, NIHAO.TXT could be found using Windows File Explorer. This confirms that formatting the microSD card, file input and file output are functioning correctly.

### 9.2.3 VEML7700

For the VEML7700 light sensor, the first job was to determine how the code was going to be run in an effective manner. After some research, an open-source GitHub repository was found created by Kristijan Grozdanovski that created a driver for the VEML7700 that was used to build and run the light sensor that could read the ambient light sensor (ALS) as well as the white light within ESP-IDF. For this project, only the ambient light readings will be used. After making some changes to the files to link them to the environment, the code was successfully flashed to the monitor to show some of those default values in a room. These values are measured in lux, and the code is shown in a screenshot below.

```
C:\WINDOWS\system32\cmd.exe - python.exe "C:\Users\Stephen\esp\esp-idf\tools\idf.py" flash monitor
VEML7700 measured White 421.1280 lux or 39.1241 fc
VEML7700 measured ALS 343.5696 lux or 31.9186 fc
VEML7700 measured White 421.0632 lux or 39.1180 fc
VEML7700 measured ALS 343.7568 lux or 31.9360 fc
VEML7700 measured White 421.1928 lux or 39.1301 fc
VEML7700 measured ALS 343.6128 lux or 31.9227 fc
VEML7700 measured White 421.1280 lux or 39.1241 fc
VEML7700 measured ALS 343.7424 lux or 31.9347 fc
VEML7700 measured White 421.2360 lux or 39.1341 fc
VEML7700 measured ALS 343.9152 lux or 31.9508 fc
VEML7700 measured White 421.4880 lux or 39.1575 fc
VEML7700 measured ALS 343.6920 lux or 31.9300 fc
VEML7700 measured White 421.2072 lux or 39.1314 fc
VEML7700 measured ALS 343.5480 lux or 31.9166 fc
VEML7700 measured White 421.0992 lux or 39.1214 fc
VEML7700 measured ALS 342.9936 lux or 31.8651 fc
VEML7700 measured White 420.1920 lux or 39.0371 fc
VEML7700 measured ALS 350.7768 lux or 32.5882 fc
VEML7700 measured White 431.6256 lux or 40.0993 fc
```

**Figure 9.4.** Flashing of VEML7700 ALS

by Author

#### 9.2.4 TCA9548A I2C Multiplexer

For the TCA9548A, the whole purpose of it is to easily connect multiple sensors to the ESP32-C6 at the same time utilizing I2C with only two GPIO pins. The light sensors utilized did not offer configurable I2C addresses, and the sensors all had the same address. A Mux was implemented to be able to individually communicate with each light sensor, by multiplexing which sensor was being communicated with before requesting information from the sensor. With 5 sensors placed on the sensor board, an 8-channel Mux was used.

#### 9.2.5 Motors

Implemented I2C protocol bus to test multiple servo motors with servo motor's driver, PCA9685 break out board. Each servo motors run at a different angles and rotation at 2 steps interval and the pulse width of 1.5ms. Based on the inputs of each sensor, rotation of x, y, and z-axis servo motor. The master run on the address of 0x40 then distribute to three slave servo motors at each distinct address. The step is reduced to 1 per cycles as the minimum angle different when rotating the reflector.

A stepper motor driver break-out board, DRV8834 used to test stepper motor Nema23. ESP internal clock of 81MHz is too fast when implemented, hence a delay used to hold the stepper's rotation between pulses. Pulse width declared in microsecond to drive the stepper motor. Additionally, the amperage drawn from Nema 23 is larger than the rating of DRV8834. TB9095 development board operate Nema23 as expected.

## 9.2.6 Antenna

To test the built-in antenna on the ESP32-C6 as well as any newly connected antennas to the IPEX slot, the various pieces of Zigbee example code included in ESP-IDF were useful. The ESP-Zigbee-SDK was also essential for testing. Many example programs from ESP-Zigbee-SDK were useful and flashing them to the board was done with ESP-IDF, mainly the HA\_on\_off\_light program. Using two ESP32-C6 processors with this program flashed was able to show us that communication was working. This program makes it so one device acts as the coordinator and the other device acts as the end device. By pushing the button on the coordinator you can see actions happening on the end device, which in this case is turning the LED on and off. This is further verified by the monitor command on the command line which shows exactly how the devices are linking up through the network and when signals are sent and received.

## 9.2.7 Use of Interrupts

The most effective strategy for this system to save power and become more efficient was to use interrupts in the code. To do this, the light sensor code from the VEML7700 and TCA9548A to create a similar program that read values but on a timer interrupt. For faster testing, we decided to use a 5 second software timer to test our interrupt code and used libraries given by the ESP-IDF such as esp\_intr\_alloc.h and esp\_timer.h to set up a software timer.

## 9.2.8 Integration of Systems

After testing all these pieces of software individually, it was imperative to merge them all together to make one system.

### 9.2.8.1 Integration of the Servo Motor with the Sensors

The first step taken to merge these components was having the servo motor for the sensor arm to adjust to the lux taken in from the sensor. The sensor arm has a vertical range of motion of 90 degrees, so the software needs to take that into account. To convert this into step sizes, the range was found when calibrating the sensor on the arm to be between step sizes 495, which is horizontal, to step size 765, which is vertical. To move the motorized arm dependent on the sensors, there needed to be an algorithm that tested the values of the sensors against each other to determine where to move the servo. The servo only controls the vertical movement of the sensor board, so the algorithm that was made goes through the following steps:

1. Creating two variables, the average of the top two sensors divided by the average of the bottom two sensors named servo\_spin\_down and the average of the of the bottom two sensors divided by the average of the top two sensors named servo\_spin\_up
2. When a variable is below 0.8, that means the values are too far apart and the motorized arm needs to be adjusted
3. Take the inverse of the value that is below 0.8, which will come up with a value in servo steps that the arm needs to spin
4. If the value is above 20, set it back to 20 or else the arm will overcompensate the adjustment
5. Add the value of the adjustment to the previous value if the servo is spinning up or subtract the value of the adjustment to the previous value if the servo is spinning down

- If the new value would exceed the maximum range or fall below the minimum range, set it to the maximum or minimum respectfully

With this algorithm, the arm can effectively adjust the arm in a dynamic manner that takes the values of the sensors to test them against each other to move the motor in a productive manner.

#### ***9.2.8.2 Integration of the Stepper Motor with the Sensors***

Like the servo motor, the base of the tower needs to be adjusted so the sensors can track the sun in a horizontal manner. The base of the tower has a full range of 360 degrees, or 5760 step sizes, and can move either clockwise or counterclockwise. To create an algorithm, some similar steps were taken from the vertical movement of the servo to move the base with the stepper to account for the horizontal tracking of the sun. The steps of the algorithm or given below

- Creating two variables, the average of the left two sensors divided by the average of the right two sensors named stepper\_spin\_counterclockwise and the average of the of the right two sensors divided by the average of the left two sensors named stepper\_spin\_clockwise
- When a variable is below 0.9, that means the values are too far apart and the motorized arm needs to be adjusted
- Take the inverse of the value that is below 0.9 and take it to the eighth power to adjust the value in an effective manner
- If the value is above 300, set it back to 300 or else the base will overcompensate the adjustment
- Spin the motor counterclockwise or clockwise with this respective value since the stepper does not need a previous value to adjust from

With this algorithm, the base can spin in 360 degrees continuously and with a dynamic manner based on the values taken by the sensors which moves the stepper motor in an effective manner.

#### ***9.2.8.3 Integration of the Servo Motor for the Vertical Movement of the Mirror***

The next step of the process is to move the mirror to reflect the light of the sun to the target. Based on Snell's law of reflection, we need to vertically position the mirror halfway between the target and the light source to accurately reflect light. In the vertical position, this means we need to translate the position of the servo from the sensor arms and correlate it to the vertical mirror arm. This was done by first doing a scaling operation to convert the steps of the sensor servo to the vertical mirror servo which is given by the following equation, where  $v_m$  is the vertical step size of the mirror motor and  $v_s$  is the step size of the sensor motor:

$$v_m = \frac{(v_s - 495)(400 - 600)}{765 - 495} + 600$$

Then, this value is averaged by the vertical position of the target to move the mirror to the halfway position between the two vertical positions. If the halfway point were beyond the vertical ranges of the step sizes for the mirrors, the mirror would only move to the maximum or minimum range, which would reduce the accuracy of the mirror, but would ensure no damage done to the structural integrity of the base of the tower or motors.

#### **9.2.8.4 Integration of the Servo Motor for the Horizontal Movement of the Mirror**

Like the vertical position of the mirror, the horizontal position of the mirror must follow Snell's law of reflection to position the mirror halfway between the horizontal position of the sun and target to reflect light accurately. This is more difficult with the stepper motor because it doesn't hold previous values of the step and can move in a full 360-degree motion. Due to this and the fact that our range of the mirror is cut off from the sensor arm, the mirror can only effectively direct light to the right of our tower.

For our algorithm to direct light, we decided to set the stepper value to be 0 after every movement and to add, or subtract depending on the direction, the step size to the horizontal positioning of the target so the mirror can reflect light accurately according to the movement of the base. The first step of this is to determine the values needed to create a range of 180 degrees of horizontal reflectivity. To do this, the mirror only needs 90 degrees of motion because of the principal of Snell's law of reflectivity. Based on this concept, the values will need to be scaled to create an effective positioning of the mirror. The scaling operation is shown in the equation below where  $h_m$  is the horizontal step size of the mirror servo and  $h_t$  is the halfway point of the horizontal position of the target:

$$h_m = \frac{h_t(300 - 510)}{1440} + 510$$

This will scale the value to point the mirror at the position to put it in the hallway point between the two targets. If the halfway point were beyond the horizontal ranges of the step sizes for the mirrors, the mirror would only move to the maximum or minimum range, which would reduce the accuracy of the mirror, but would ensure no damage done to the structural integrity of the base of the tower or motors.

#### **9.2.8.4 Integration of Zigbee to the Changing of Targets**

To show the use of the mesh network in the project with the Zigbee communication protocols using the communication beacon, we decided to use the tower as a receiver of the Zigbee signal and change the target for the mirror to reflect light. In the code, we have the targets saved as values in an array, and when the target is changed through the received signal, the target will be toggled to the new value in the by changing the array index. This allows for real time changing of targets using the mesh network and show the integration of both towers in the overall system.

## **Chapter 10 - Administrative Content**

### **10.1 Budget**

The budget provided for this project is limited to \$750. This limit is set by FSI and not by UCF or self-imposed. The goal of this project is to keep all costs within the \$750 provided by FSI to minimize personal costs from group members.

Higher cost items, such as motors, microcontrollers, the frame, batteries, and solar panels, have been allocated a larger portion of the budget. Lower cost items such as regulators and sensors are

allocated a smaller portion of the budget. Note the \$750 budget includes multiple iterations, meaning the Bill of Materials must include room for spending on replacement or exchanged parts.

**Table 10.1.** The Budget allocation for the various parts of the project

Sub-System	Budget
PSU and Solar	\$ 150.00
Frame/Reflector	\$ 200.00
PCBs and Electrical	\$ 100.00
<b>Total</b>	<b>\$ 450.00</b>

Seen from the table above, this project is underbudget. This enables more margin for error, such as part replacement, and the iterative design process to take place without significant financial repercussions.

## 10.2 Bill of Materials

**Table 10.2.** An Itemized Bill of Materials

Component	Name	Price	Quantity
<b><u>Mechanical</u></b>			
<b>Mirror</b>	0.032" x 24" x 24", 3003-H14 Aluminum Sheet	\$28.86	1
<b><u>Electrical</u></b>			
<b>Battery</b>	Howell Energy hw-4f7	32.99	1
<b>Motor w</b>	Nema 23	\$30.73	1
<b>Motor x-y-z</b>	9.5-11kg*cm Servo Motor	\$17.59	3
<b>Charge Controller/BMS</b>	Smaraad SR11004	\$39.99	1
<b>Solar Panel</b>	RNG-50D-SS	\$49.99	1
<b>Microcontroller</b>	ESP32-C6-DEVKITC-1-N8	\$9.00	1
<b>External Antenna</b>	Wlaniot 2.4G	\$17.98	2
<b>MicroSD card</b>	5251	\$4.50	2
<b>MicroSD card breakout board+</b>	254	\$7.50	1
<b><u>PCB</u></b>			
<b>Microcontroller for PCB</b>	ESP32-C6-WROOM-1U	\$3.48	1
<b>Stepper Motor Controller</b>	DRV8833PW	\$2.84	1
<b>Servos Motor Controller</b>	PCA9685PW,112	\$2.64	1
<b>3.3V Regulator</b>	TPS54JA20	\$1.50	1
<b>5V Regulator</b>	TPS54JA20	\$1.50	1

<b>USB-A Connector</b>	2057-USB-AP-S-RA-SMT-ND	\$0.55	3
<b>Sensor-MUX</b>	TCA9548APWR	\$1.78	1
<b>Sensor</b>	VEML7700	\$1.88	5
<b>USB-to-UART Bridge Controller</b>	CP2102N-A02-GQFN28	\$4.07	1
<b>MicroSD Socket</b>	1660	\$1.95	1
<b>Misc.</b>	Resistors, Capacitors, Inductr, Jumpers, Etc.....	~\$20.00	
<b>Total</b>		<b>\$459.69</b>	

### 10.3 Distribution of Worktable

Below is the distribution of worktable detailing the assigned tasks to the group members. The responsibility of each system is distributed to specific members; however, each system relies on other member's systems. Collaboration is present among the group members at every level of this project to ensure these systems are designed in a manner that they fit other system's requirements. This ensures that all members are aware of and involved in the design and implementation of systems, regardless of if they are directly responsible for it or not.

*Table 10.3. The distribution of worktable.*

<b>Electrical Engineering</b>	<b>Responsibilities</b>
Alexandre Fiset	PSU Design and Implementation
	PCB Design
	MPPT Tracking Implementation
	Administrative Documentation
<b>Computer Engineering</b>	<b>Responsibilities</b>
Binh Pham	Reflector Technology and Design
	Motor and Motor Controls
	Vectoring Technology
	Project Lead
	Positioning and Vectoring Algorithm
<b>Computer Engineering</b>	<b>Responsibilities</b>
Pedro Kasprzykowski	MCU Selection and Implementation
	Software Design and Implementation
	Antenna and Communications
	Website Design and Management
<b>Computer Engineering</b>	<b>Responsibilities</b>
Stephen Martin	Sensor Selection and Implementation
	MCU Selection and Implementation

	Positioning and Vectoring Algorithm
	Software Design and Implementation

## 10.4 Milestones

Multiple events and meeting are required to create a good dynamic between members and a successful project. First, new members are recruited, and project's topics discussion held in the first week of senior design I to kick start the project with sufficient information:

**Table 10.4.** Project Initialization Milestone

Project Initialization				
Start Date	Planned Date	Required End Date	Task	Description
08/21/2023	08/21/2023	08/21/2023	Recruiting	Members recruited: Alexandre Fiset (EE), Pedro Kasprzykowski (CpE), Stephen Martin (CpE), Binh Pham (CPE)
08/22/2023	08/29/2023	08/29/2023	Brainstorming	Meeting to discuss potential projects
08/30/2023	08/30/2023	08/30/2023	Sponsor Meeting	Discuss idea with sponsor.
08/28/2023	09/04/2023	09/15/2023	Initial Document	First 10 pages of Divide and Conquer
08/28/2023	10/28/2023	11/03/2023	60-Page Milestone	First half of the Document
08/28/2023	12/01/2023	12/05/2023	Final Document	Final Document of SD I

**Table 10.5.** Project Fabrication Milestone

Project Fabrication				
Start Date	Planned Date	Required End Date	Task	Description
08/28/2023	09/28/2023	09/28/2023	Components Selection	Making a tentative BOM with core component
09/13/2023	10/29/2023	12/05/2023	System Design	Making overall schematic for the project
10/29/2023	12/01/2023	12/05/2023	System Testing	Testing individual component and compatibility
10/29/2023	11/15/2023	1/15/2024	PCB Design	Design PCBs and have them ordered
01/15/2024	02/28/2024	3/15/2024	PCB Testing	Receive and test the PCBs
03/05/2024	04/05/2024	04/15/2024	Prototype Completion	Have a deliverable, tested, final product

Various tasks are overlap as expecting due to the nature of the project. This milestone is a guideline for reference as a successful project.

## **Chapter 11 - Conclusion**

In conclusion, the ASTROCOM project, developed in collaboration with NASA's Artemis missions and the Florida Space Institute (FSI), represents a significant leap forward in lunar exploration capabilities. As outlined in the executive summary, the primary objective of ASTROCOM is to address the challenge of permanently shaded regions near the Moon's south pole, hindering the efficient use of solar-powered assets. The solution devised by the University of Central Florida's engineering students involves a sophisticated network of towers designed to transmit power and information wirelessly within and around these challenging lunar craters.

The two main components of the ASTROCOM system, the Heliostat Tower and the Communication Beacon, work in harmony to overcome the limitations posed by the lunar environment. The Heliostat Tower utilizes a reflector to redirect sunlight into shaded areas, enabling the illumination of these regions and providing power to solar assets. Simultaneously, the tower acts as a communication hub, forming a telecommunication network to facilitate data transfer between different components of the system. On the other hand, the portable Communication Beacon, deployed by lunar rovers, establishes a network between the rover and the fixed Heliostat Tower, ensuring seamless communication over obstacles and varied terrains.

The innovative design of ASTROCOM allows for adaptability and sustainability in lunar exploration. The Heliostat Tower serves as a fixed infrastructure, capable of sustaining itself for long-term usage. In contrast, the Communication Beacon adds a dynamic element, allowing for temporary network establishment during rover missions and subsequent retrieval, recharge, and reuse. This combination of fixed and portable elements maximizes the system's efficiency and versatility.

The integration of these towers with a rover, as part of a comprehensive exploration system, marks a pioneering approach to lunar research. The collaboration between the ASTROCOM components enables the exploration of previously untouched areas on the Moon, particularly those in permanently shaded craters. The successful implementation of this system is crucial not only for the Artemis missions but also as a steppingstone for future Martian missions, using the Moon as a testbed for evolving technologies.

This document serves as a comprehensive record of the ASTROCOM's design process, covering fundamental theories, technologies, part selection, implementation, limitations, and administrative aspects. The meticulous planning and execution of this project, coupled with the innovative solutions devised by the University of Central Florida's engineering students, affirm that we are on track for the successful deployment and operation of ASTROCOM. As we move forward, the insights gained from this project will undoubtedly contribute to the advancement of lunar exploration and space exploration technologies.

## Appendix A - Copyright Permissions' Requested

Photodiodes (Figure 3.14)

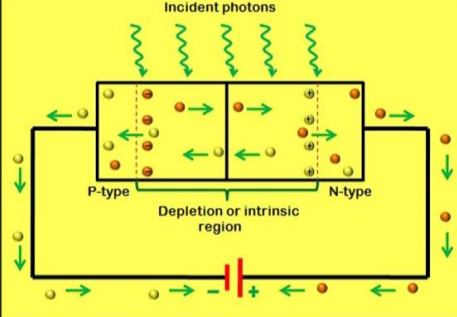
SM Stephen Martin <st322653@ucf.edu>  
10:27 AM

To: admin@electronicshub.org

Good morning,

I am a student at the University of Central Florida (UCF) and I am working on a Senior Design project with some other classmates and we are building a heliostat light reflection tower and communication tower for a set of rovers. We would like to receive permission for some diagrams and images from your website: <https://www.electronicshub.org/photodiode-working-characteristics-applications/>. Our report will be published on the UCF website (<https://www.ece.ucf.edu/seniordesign/index.php>) upon completion.

We are hoping to obtain the following images:



Thanks,  
Stephen Martin

Phototransistors (Figure 3.15)

Permission to use Copyright Diagram in Educational Paper

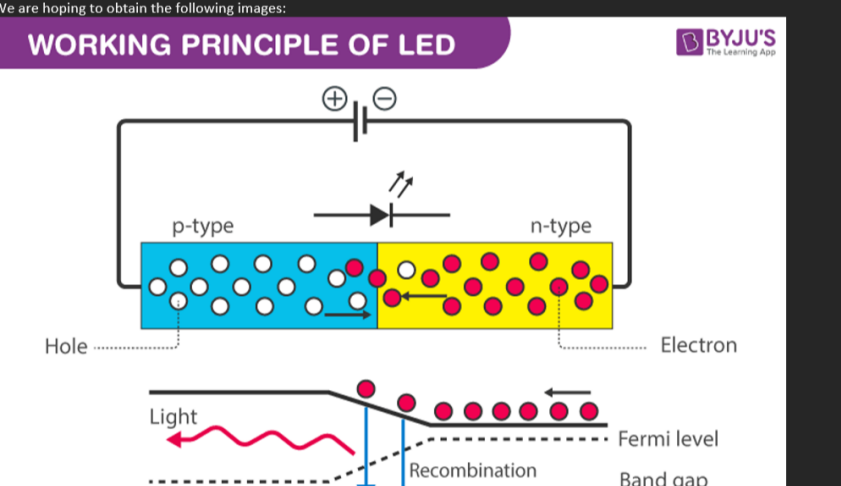
SM Stephen Martin <st322653@ucf.edu>  
10:18 AM

To: queries@byjus.com

Good morning,

I am a student at the University of Central Florida (UCF) and I am working on a Senior Design project with some other classmates and we are building a heliostat light reflection tower and communication tower for a set of rovers. We would like to receive permission for some diagrams and images from your website: <https://byjus.com/physics/light-emitting-diode/>. Our report will be published on the UCF website (<https://www.ece.ucf.edu/seniordesign/index.php>) upon completion.

We are hoping to obtain the following images:



## CMOS (Figure 3.16)

SM Stephen Martin <st322653@ucf.edu>  
10:19 AM

To: learnelectronicswithme@gmail.com

Good morning,

I am a student at the University of Central Florida (UCF) and I am working on a Senior Design project with some other classmates and we are building a heliostat light reflection tower and communication tower for a set of rovers. We would like to receive permission for some diagrams and images from your website: <https://www.learnelectronicswithme.com/p/contact-us.html>. Our report will be published on the UCF website (<https://www.ece.ucf.edu/seniordesign/index.php>) upon completion.

We are hoping to obtain the following images:

The diagram illustrates a CMOS inverter circuit. It consists of two complementary metal-oxide-semiconductor (CMOS) transistors: an NMOS transistor on the left and a PMOS transistor on the right, sharing a common P-substrate. The NMOS transistor has its source terminal (S) connected to ground, its drain terminal (D) connected to the output node, and its gate terminal (G) connected to the input node. The PMOS transistor has its source terminal (S) connected to VDD, its drain terminal (D) connected to the output node, and its gate terminal (G) connected to the input node. The output node of the inverter is connected to the input node of the next stage through a resistor. The input signal is labeled 'IN' and the output signal is labeled 'OUT'.

Thanks,  
Stephen Martin

## LED (Figure 3.17)

Your Name (required)  
Stephen Martin

Your Email (required)  
st322653@ucf.edu

Subject  
Permission to use Copyright Diagram in Educational Paper

Your Message

Good morning,

I am a student at the University of Central Florida (UCF) and I am working on a Senior Design project with some other classmates and we are building a heliostat light reflection tower and communication tower for a set of rovers. We would like to receive permission for some diagrams and images from your website: <https://electronicsdesk.com/phototransistor.html>. Our report will be published on the UCF website (<https://www.ece.ucf.edu/seniordesign/index.php>) upon completion.

We are hoping to obtain the following images:

## I2C (Figures 4.1, 4.2, 4.3)

## CONTACT US

If you have any questions or are interested in advertising and sponsorship opportunities on Circuit Basics, please contact us by filling out the form below:

Stephen Martin

st322653

Good morning,

I am a student at the University of Central Florida (UCF) and I am working on a Senior Design project with some other classmates and we are building a heliostat light reflection tower and communication tower for a set of rovers. We would like to receive permission for some diagrams and images from your website: <https://www.circuitbasics.com/basics-of-the-i2c-communication-protocol/>. Our report will be published on the UCF website (<https://www.ece.ucf.edu/seniordesign/index.php>) upon completion.

I have read, understand, and agree to the Privacy Policy

SEND

## Antenna

### How can we help?\*

To whomever it may concern,  
I and my group are requesting permission to use the images in  
the datasheet for the PC140 antenna for our capstone project  
documentation, which is using the same antenna.  
Best,  
Group 14

- I consent to the storing, processing, transfer of my personal data as outlined in the [Taoglas privacy notice](#) to receive marketing communications regarding Taoglas products, services, and events.
- In order to fulfil your request Taoglas needs to store, process, and transfer your personal data as outlined in the [Taoglas privacy notice](#). By continuing, I consent to the storing, processing, and transfer of my personal data as outlined above in order for Taoglas to respond to my enquiry. \*

Submit

Figure 9.1. Requested

The screenshot shows a Now Support chat window. At the top, there's a header with the Now Support logo and a message 'Agent has joined.' Below the header, a message from a user (labeled A) reads: 'Thank you for contacting TI Customer Support. I will assist you today. 感谢您联络德州仪器客户支持中心，很高兴为您服务' (Thank you for contacting TI Customer Support. I will assist you today. Thank you). The message was sent '1m ago'. Below this, a message from the support agent reads: 'Good Evening; I am a student at the University of Central Florida. Recently, our senior design group have utilized your webbench service to create some Regulators and ran simulation for them. We would kindly request your permission to used some of the data in our documentation. I hope you can help us with this inquiry. We would really appreciate your help. Thank you.' This message was sent 'just now'. To the right of the messages, there are two graphs titled 'Volt sim 1 (V)' and 'Volt sim 2 (V)', both plotted against 'Time (msec)' from 0 to 4. The first graph shows a red curve starting at 0V, rising to about 11V between 2.5 and 3.5 msec. The second graph shows a red curve starting at approximately -0.3V, rising to about 13V between 2.5 and 3.5 msec. A dark blue box labeled 'The data in question are:' is positioned above the graphs.

Figure 4.5. Requested

The screenshot shows an email draft. The 'To' field is set to 'communications@nema.org' and the 'Cc' field is empty. The subject line is 'Request of Image Usage' and the draft was saved at 8:39 PM. The body of the email starts with 'Good Evening,' followed by a message from a student named Binh Pham: 'My name is Binh Pham, and I am a student at the University of Central Florida. My team and I are currently working on a project for my senior design project.' Below this, Binh writes: 'My team and I were hoping to obtain permission to reproduce the following image(s) in our project documentation relating to research on our project as attached. The images are from one of your documentations: NEMA Standards Publication ICS 20-2009 (R2015). We appreciate your help.' The email concludes with 'Thank you,' and is signed off by 'Binh Pham'. An attachment is shown as a graph with four curves labeled A, B, C, and D. The vertical axis ranges from 200 to 280, and the horizontal axis shows time points. Curve D is a red line starting at ~275 and decreasing. Curve A is a red line starting at ~200 and peaking at ~275. Curve C is a blue line starting at ~200 and peaking at ~220. Curve B is a green line starting at ~200 and peaking at ~210.

Figure 3.9. Requested

To asgonzal@ing.uc3m.es X Bcc

Cc

Image Usage Permission Request Draft saved at 8:44 PM

Good Evening, Dr. Alberto Sánchez-González,

My name is Binh Pham, and I am a University of Central Florida student. My team and I are currently working on a project for my senior design project.

We were hoping to obtain permission to reproduce the following image in our project documentation relating to research on our project as attached. The image is from one of your research documents "Reflections between heliostats: Model to detect alignment errors". We appreciate your help.

Thank you,

Binh Pham



Figure 3.8. Requested

To mcnulty@jlab.org X Bcc

Cc

Image Usage Request Draft saved at 8:47 PM

Good Evening, Dr. Dustin McNulty,

My name is Binh Pham, and I am a University of Central Florida student. My team and I are currently working on a project for my senior design project.

We were hoping to obtain permission to reproduce the following image in our project documentation relating to research on our project as attached. The image is from one of your lab documents "Reflectivity Measurements". We appreciate your help.

Thank you,

Binh Pham

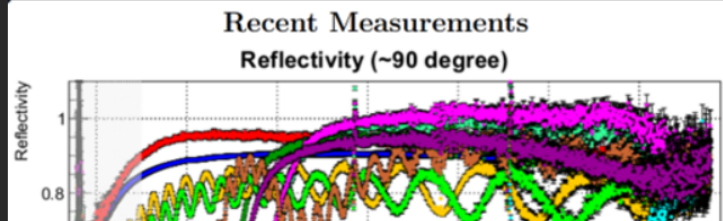


Figure 3.7. Requested

To ali\_02us@yahoo.com X Bcc

Cc

Images Usage Request Draft saved at 8:50 PM

Good Evening, Dr. A. Ibrahim,

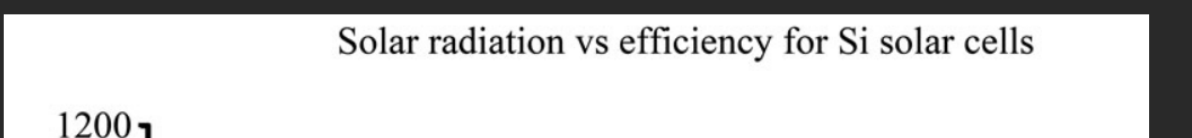
My name is Binh Pham, and I am a University of Central Florida student. My team and I are currently working on a project for my senior design project.

We were hoping to obtain permission to reproduce the following image in our project documentation relating to research on our project as attached. The image is from one of your research paper "Analysis of Electrical Characteristics of Photovoltaic Single Crystal Silicon Solar Cells at Outdoor Measurements". We appreciate your help.

Thank you,

Binh Pham

Solar radiation vs efficiency for Si solar cells



Figures 3.12., 3.13 Requested

To info@moons.com.cn X Bcc

Cc

Add a subject Draft saved at 9:04 PM

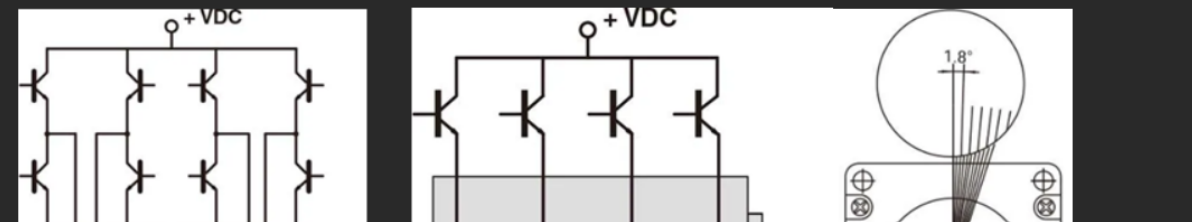
Good Evening,

My name is Binh Pham, and I am a student at the University of Central Florida. My team and I are currently working on a project for my senior design project.

My team and I were hoping to obtain permission to reproduce the following image(s) in our project documentation relating to research on our project as attached. The images are from one of your documentations: Step Motor – Basic Structure & Operation. We appreciate your help

Thank you,

Binh Pham



## Appendix B - Copyright Permissions' Granted

Photodiodes (Figure 3.14)

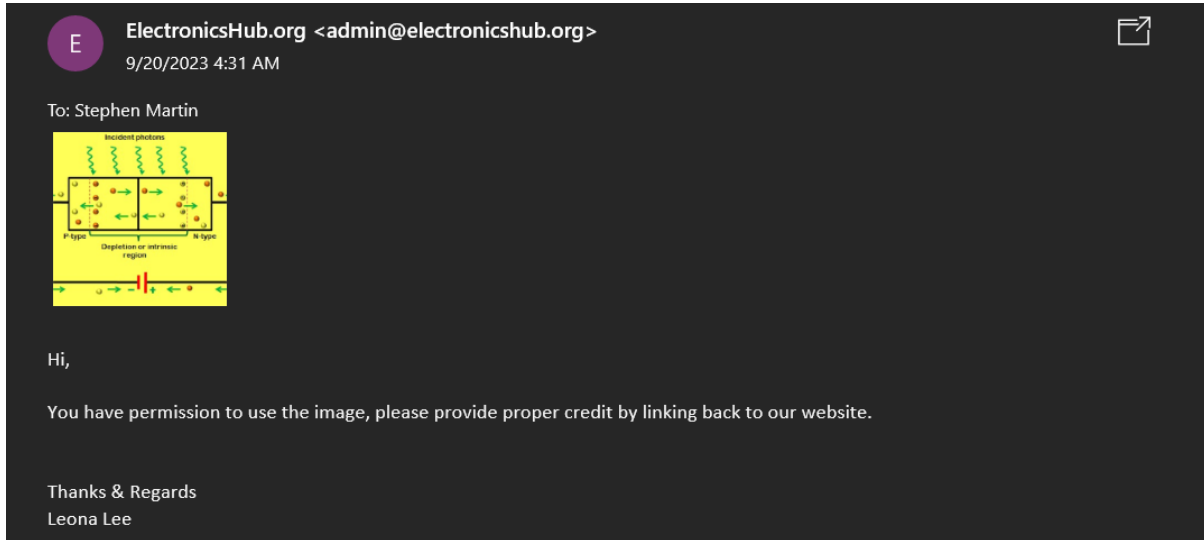
An email from ElectronicsHub.org (admin@electronicshub.org) dated 9/20/2023 4:31 AM. The subject is "Photodiodes (Figure 3.14)". The message body contains a diagram of a photodiode showing incident photons hitting the P-type region, creating electron-hole pairs which diffuse across a depletion or intrinsic region to the N-type region, generating a voltage. Below the diagram, the text reads: "Hi, You have permission to use the image, please provide proper credit by linking back to our website." At the bottom, it says "Thanks & Regards, Leona Lee".

Figure 3.9. ACcepted

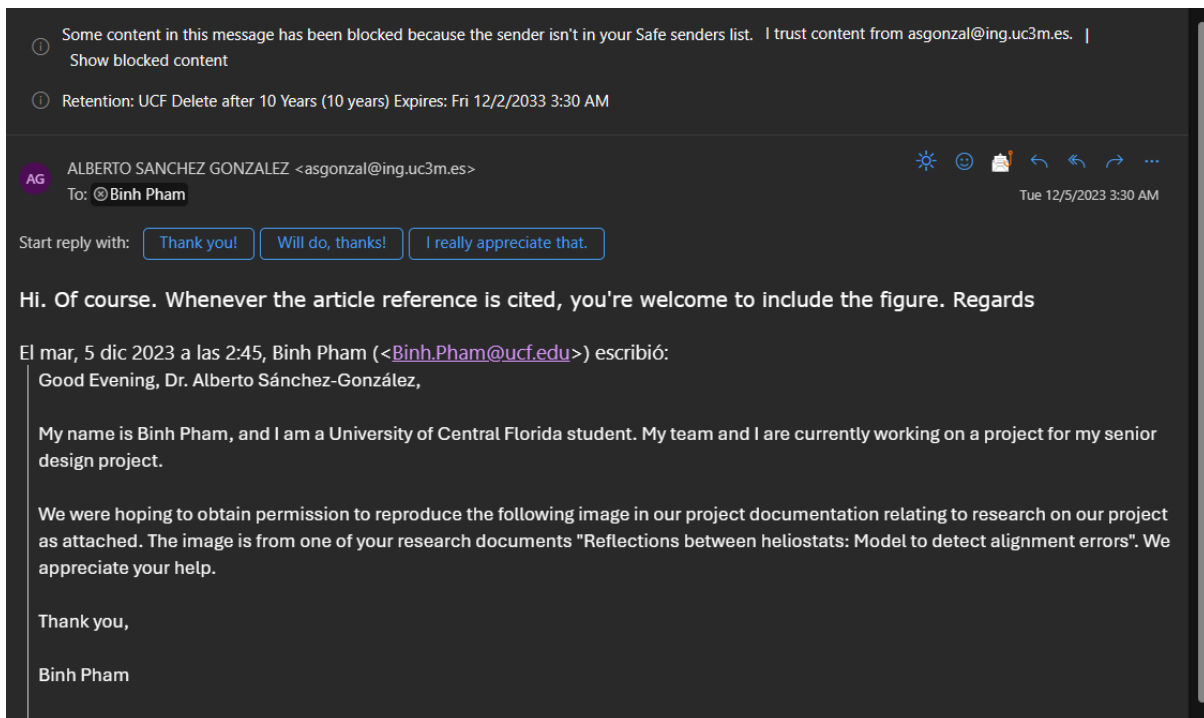
An email exchange between ALBERTO SANCHEZ GONZALEZ (asgonzal@ing.uc3m.es) and Binh Pham. The email from Binh Pham is dated Tue 12/5/2023 3:30 AM. It starts with "Hi. Of course. Whenever the article reference is cited, you're welcome to include the figure. Regards". Binh then asks if he can reproduce the image in his project documentation. Alberto replies with "Good Evening, Dr. Alberto Sánchez-González," and provides a detailed response about his team's work on a senior design project. He expresses appreciation for the help and signs off with "Thank you, Binh Pham".

Figure 9.1. Accepted

 TI Customer Support <support@ti.com>  
to me ▾

2023-12-05 07:25:33 CST - Jejomar Ildefonso

Hi Binh,

Thank you for contacting TI Customer Support and for choosing our products as part of your solution. This is to acknowledge the support request that you have raised.

The TI Webench Power Designer is part of TI online services that can be utilized by our customers. You can use the design provided that you agree to the [Texas Instruments Online Terms of Use](#) of these tools and services.

Please let me know if you have additional questions.

If my answer resolves your query, please click on "Accept Solution" on case number **CS2112083** on your TI Customer Support Portal. Otherwise if you have additional clarifications or concerns, please click on "Reject Solution" or reply to this message.

We would also appreciate if you could participate in a quick survey after your support request is closed. Please take a moment to give your valuable feedback on your support experience.

Documents are open access with proper citations:

Figure 3.5. Accepted

## Evaluation of reflectivity of metal parts by a thermo-camera



Open access

Download

[Text \(PDF, 764.5Kb\)](#)

Rights / license

In Copyright - Non-Commercial Use Permitted

Permanent link

<https://doi.org/10.3929/ethz-a-006206911>

Publication status

published

Book title

InfraMation 2010 proceedings

Pages / Article No.

475 - 486

Author

Sárosi, Zoltán  
Knapp, Wolfgang  
Kunz, Andreas

Show all +

Date

2010

Figure 3.6. Accepted

OPEN ACCESS

## Solar Spectrum Conversion for Photovoltaics Using Nanoparticles

WRITTEN BY

W.G.J.H.M. van Sark, A. Meijerink and R.E.I. Schropp

Submitted: 25 November 2011, Published: 16 March 2012

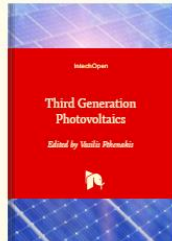
DOI: 10.5772/39213

FROM THE EDITED VOLUME

### Third Generation Photovoltaics

Edited by Vasilis Fthenakis

[Book Details](#) | [Order Print](#)



## Appendix C - References

- Ada, Lady. “TSL2561 Luminosity Sensor.” *Adafruit Learning System*, 29 July 2012, learn.adafruit.com/tsl2561?view=all.
- Ada, Lady. “TSL2561 Luminosity Sensor.” *Electronic Components Distributor - Mouser Electronics*, 1 Dec. 2022, www.mouser.com/datasheet/2/737/tsl2561-932888.pdf.
- Administrator. “BH1750 Ambient Light Sensor with Arduino.” *ElectronicsHub*, 12 Oct. 2021, www.electronicshub.org/bh1750-ambient-light-sensor/.
- Akrour, Lahcene, et al. “Arduino with BH1750 Ambient Light Sensor.” *Random Nerd Tutorials*, 11 Mar. 2022, randomnerdtutorials.com/arduino-bh1750-ambient-light-sensor/.
- Aksinasi, Rachel. “Photos Show What Life Looks like in One of the Darkest Places on Earth after Residents Built a System of Mirrors to Mimic the Sun.” *Insider*, 24 Jan. 2020, https://www.insider.com/what-life-is-like-in-rjukan-norway-2018-11. Accessed 6 Aug. 2023.
- “All about the I2C Standard & Protocol.” *Circuit Crush*, 30 June 2021, https://www.circuitcrush.com/i2c-tutorial/
- “Ambient Light Tinyshield.” *TinyCircuits*, tinycircuits.com/products/ambient-light-tinyshield. Accessed July 2023.
- “AP3216C.” *PDF.Com*, [www.datasheet-pdf.com/PDF/AP3216C-Datasheet-LITE-ON-1016217](http://www.datasheet-pdf.com/PDF/AP3216C-Datasheet-LITE-ON-1016217). Accessed July 2023.
- “Arduino Mkr Wan 1310.” *Arduino Online Shop*, store-usa.arduino.cc/products/arduino-mkr-wan-1310?selectedStore=us. Accessed 24 Nov. 2023.
- “Arduino MKR WIFI 1010.” *Arduino Online Shop*, store-usa.arduino.cc/products/arduino-mkr-wifi-1010?selectedStore=us. Accessed 24 Nov. 2023.
- Barrera, T. P. (2023). *Spacecraft Lithium-Ion Battery Power Systems*. Wiley.
- Battery University. (n.d.). Retrieved from <https://batteryuniversity.com/article/bu-107-comparison-table-of-secondary-batteries>
- “Bluetooth Technology Overview.” *Bluetooth® Technology Website*, www.bluetooth.com/learn-about-bluetooth/tech-overview/. Accessed 24 Nov. 2023.
- “Buy A Raspberry Pi Zero 2 W.” *Raspberry Pi*, www.raspberrypi.com/products/raspberry-pi-zero-2-w/. Accessed 24 Nov. 2023.
- “CC1352R.” *CC1352R Data Sheet, Product Information and Support / TI.Com*, www.ti.com/product/CC1352R#order-quality. Accessed 24 Nov. 2023.

“CC2650.” *CC2650 Data Sheet, Product Information and Support / TI.Com*, www.ti.com/product/CC2650#product-details. Accessed 24 Nov. 2023.

“Complementary Technologies: Lorawan and Bluetooth Whitepaper.” *LoRa Alliance*, resources.lora-alliance.org/home/complementary-technologies-lorawan-and-bluetooth-whitepaper. Accessed 24 Nov. 2023.

“Customize TPS54JA20RWW - 10V-15V to 3.30V @ 7A.” *Power Designer*, webench.ti.com/power-designer/switching-regulator/customize/5. Accessed 4 Dec. 2023.

Dahale, S., Das, A., Pindoriya, N. M., & Rajendran, S. (2017). *An overview of DC-DC converter topologies and controls in DC microgrid*. Pune: IEEE.

“Different Wi-Fi Protocols and Data Rates.” *Intel*, Intel, www.intel.com/content/www/us/en/support/articles/000005725/wireless/legacy-intel-wireless-products.html. Accessed 24 Nov. 2023.

Doyle, Aine. *Taoglas*, Taoglas, 6 Feb. 2012, cdn.taoglas.com/datasheets/FXP70.07.0053A.pdf.

Dunlop, J. P. (1997). *Batteries and Charge Control in Stand-Alone Photovoltaic Systems: Fundamentals and Application*. Florida Solar Energy Center.

“ESP32-Devkitc.” *ESP32-DevKitC Board I* Espressif, www.espressif.com/en/products/devkits/esp32-devkitc. Accessed 24 Nov. 2023.

Flowers, T. a. (2023). *Chemistry (OPENSTAX)*. LibreTexts.

Gardner, Jonathan P. “Mirrors Webb/NASA.” NASA, NASA, 15 Feb. 2016, webb.nasa.gov/content/observatory/ote/mirrors/index.html#:~:text=A%20telescope's%20sensitivity%2C%20or%20how,before%20been%20launched%20into%20space.

Garcia, M. (2021, February 1). *Spacewalkers Complete Multi-Year Effort to Upgrade Space Station Batteries*. Retrieved from NASA: https://www.nasa.gov/feature/spacewalkers-complete-multi-year-effort-to-upgrade-space-station-batteries

Grozdanovski, Kristijan. “VEML7700 Light Sensor Driver for ESP-IDF.” *GitHub*, 31 July 2022, github.com/kgrozdanovski/veml7700-esp-idf.

Halpert, S. a. (1986). *The NASA Aerospace Battery Safety Handbook*. Pasadena: NASA.

Hanna, Katie Terrell, and John Burke. “What Is Frequency-Hopping Spread Spectrum (FHSS)?” *TechTarget*, TechTarget, 27 July 2021, www.techtarget.com/searchnetworking/definition/frequency-hopping-spread-spectrum.

*HyperLink Wireless Embedded 2.4 GHz Omni-Directional PCB Antenna Model ...*, L-com, Inc, www.l-com.com/Images/Downloadables/Datasheets/ds\_HG2402PU-UFL.pdf. Accessed 24 Nov. 2023.

Ibrahim, A. “Analysis of electrical characteristics of photovoltaic single crystal silicon solar cells at outdoor measurements.” *Smart Grid and Renewable Energy*, vol. 02, no. 02, 2011, pp. 169–175, <https://doi.org/10.4236/sgre.2011.22020>.

“Informational Guide to Electrical Industrial Topics.” *NEMA Standards Publication ICS 20-2009 (R2015)*, National Electrical Manufacturers Association, Rosslyn, VA, 2009, pp. 1–30.

Leon, N. J. (2004, January). *Lithion-ion Power System for Small Satellites*. Retrieved from NASA - Space Technology 5: <https://www.jpl.nasa.gov/nmp/st5/TECHNOLOGY/battery.html>

Mahoney, E. (2022, August 18). *Moon's South Pole is Full of Mystery, Science, Intrigue*. Retrieved from NASA: Moon's South Pole is Full of Mystery, Science, Intrigue

Mark. “2.4 GHz vs 5 Ghz WIFI Frequency Spectrum.” *Study CCNA*, 31 Dec. 2022, [study-ccna.com/2-4-ghz-vs-5-ghz-wifi-frequency-spectrum/](http://study-ccna.com/2-4-ghz-vs-5-ghz-wifi-frequency-spectrum/).

McNulty, Dustin. Idaho State University, 2016, *Reflectivity Measurements*.

“Microwave Encyclopedia.” *Microwave and RF Information for Engineers / Microwave Calculators, Encyclopedia, Discussion Forum*, www.microwaves101.com/. Accessed 24 Nov. 2023.

Mohammadmehdi Seyedmahmoudian, S. M. (2013). Analytical Modeling of Partially Shaded Photovoltaic Systems. *Energies*.

Mulligan, Geoff. “The 6LoWPAN Architecture: Proceedings of the 4th Workshop on Embedded Networked Sensors.” *ACM Conferences*, 1 June 2007, [dl.acm.org/doi/10.1145/1278972.1278992](https://dl.acm.org/doi/10.1145/1278972.1278992).

National Renewable Energy Laboratory. (n.d.). *Best Research-Cell Efficiency Chart*. Retrieved from NREL: <https://www.nrel.gov/pv/cell-efficiency.html>

Olsson. “6LoWPAN Demystified .” *Texas Instruments*, www.ti.com/lit/wp/swry013/swry013.pdf. Accessed 24 Nov. 2023.

“Optimizing Current Consumption in Bluetooth Low Energy Devices.” *Optimizing Current Consumption in Bluetooth Low Energy Devices - v2.13 - Bluetooth API Documentation* Silicon Labs, docs.silabs.com/bluetooth/2.13/general/system-and-performance/optimizing-current-consumption-in-bluetooth-low-energy-devices. Accessed 24 Nov. 2023.

P. Glaser, F. S. (2014). Illumination conditions at the lunar south pole using high resolution. *Icarus*.

peppe8o. "Raspberry Pi Pico W Power Consumption (MA) and How to Reduce It." *Peppe8o*, 20 Jan. 2023, [peppe8o.com/raspberry-pi-pico-w-power-consumption/](http://peppe8o.com/raspberry-pi-pico-w-power-consumption/).

"Phototransistor : Construction, Circuit Diagram & Its Applications." *ElProCus*, 17 Feb. 2021, [www.elprocus.com/phototransistor-basics-circuit-diagram-advantages-applications/#:~:text=A%20phototransistor%20activates%20once%20the,well%20as%20changed%20into%20voltage](http://www.elprocus.com/phototransistor-basics-circuit-diagram-advantages-applications/#:~:text=A%20phototransistor%20activates%20once%20the,well%20as%20changed%20into%20voltage).

"Product Document." *TSL2572 Light-to-Digital Converter*, AMS, 30 Nov. 2022, [ams.com/documents/20143/36005/TSL2572\\_DS000178\\_5-00.pdf](http://ams.com/documents/20143/36005/TSL2572_DS000178_5-00.pdf).

"Proximity and Ambient Light Sensing (ALS) Module." *Stmicroelectronics*, Mar. 2016, [www.st.com/resource/en/datasheet/vl6180x.pdf](http://www.st.com/resource/en/datasheet/vl6180x.pdf).

"Raspberry Pi 4 Model B Specifications." *Raspberry Pi*, [www.raspberrypi.com/products/raspberry-pi-4-model-b/specifications/](http://www.raspberrypi.com/products/raspberry-pi-4-model-b/specifications/). Accessed 24 Nov. 2023.

*Raspberry Pi Documentation*, [www.raspberrypi.com/documentation/microcontrollers/rp2040.html](http://www.raspberrypi.com/documentation/microcontrollers/rp2040.html). Accessed 24 Nov. 2023.

Rembor, Kattni. "Adafruit VEML7700 Ambient Light Sensor." *Adafruit Learning System*, 26 May 2022, [learn.adafruit.com/adafruit-veml7700](http://learn.adafruit.com/adafruit-veml7700).

Rini, Nicholas. "Benefits of Object-Oriented Programming in Java." *Developer.Com*, 18 May 2023, [www.developer.com/java/oop-benefits/](http://www.developer.com/java/oop-benefits/).

Robmilne.ca, and Instructables. "Heliostat Offset Mirror Algorithm." *Instructables*, Instructables, 6 Dec. 2021, [www.instructables.com/Heliostat-Offset-Mirror-Algorithm/](http://www.instructables.com/Heliostat-Offset-Mirror-Algorithm/).

"RP2040 Thing plus Hookup Guide." *RP2040 Thing Plus Hookup Guide - SparkFun Learn*, [learn.sparkfun.com/tutorials/rp2040-thing-plus-hookup-guide/hardware-overview](http://learn.sparkfun.com/tutorials/rp2040-thing-plus-hookup-guide/hardware-overview). Accessed 24 Nov. 2023.

Sánchez-González, Alberto, and Julius Yellowhair. "Reflections between Heliostats: Model to detect alignment errors." *Solar Energy*, vol. 201, 13 Mar. 2020, pp. 373–386, <https://doi.org/10.1016/j.solener.2020.03.005>.

Sárosi, Zoltán, et al. "Evaluation of Reflectivity of Metal Parts by a Thermo-Camera." *InfraMation 2010 Proceedings*, ETH Zurich, IWF, Zurich, NV, 2010, pp. 475–486.

Schaefer, Falk-Moritz, et al. "Energy Consumption of 6LoWPAN and Zigbee in Home Automation Networks." *IEEE*, IEEE, 2013, [ieeexplore.ieee.org/document/6686463](http://ieeexplore.ieee.org/document/6686463).

"SI1145/46/47 Data Sheet." *Adafruit Industries*, Silicon Laboratories, 2013, [cdn-shop.adafruit.com/datasheets/SI1145-46-47.pdf](http://cdn-shop.adafruit.com/datasheets/SI1145-46-47.pdf).

Siepert, Bryan. "Adafruit BH1750 Ambient Light Sensor." *Adafruit Industries*, 24 Aug. 2023, <cdn-learn.adafruit.com/downloads/pdf/adafruit-bh1750-ambient-light-sensor.pdf>.

Sinha, Ashwini Kumar, and Vinay Minj. "Photodiode Basics, Working and Its Applications: EFY." *Electronics For You*, 19 Oct. 2020, <www.electronicsforu.com/technology-trends/learn-electronics/photodiode-working-applications>.

"Specifications Download Request." CSA, <csa-iot.org/developer-resource/specifications-download-request/>. Accessed 24 Nov. 2023.

Staff, Embedded. "Catching the Z-Wave." *Embedded.Com*, 2 Oct. 2006, <www.embedded.com/catching-the-z-wave/>.

Staff, Embedded. "Manipulating Hardware with C." *Embedded.Com*, 2 Feb. 2022, <www.embedded.com/manipulating-hardware-with-c/#:~:text=C%20is%20the%20language%20of,easy%20access%20to%20the%20hardware>.

"Step Motor – Basic Structure & Operation." *Moving In Better Ways!*, Moon Industry, <www.moonsindustries.com/article/basic-structure-and-operating-principle-of-stepper-motor>. Accessed 4 Dec. 2023.

Teja, Ravi. "What Is a Photodiode? Working, V-I Characteristics, Applications." *ElectronicsHub*, 8 Sept. 2021, <www.electronicshub.org/photodiode-working-characteristics-applications/>.

"Trello Makes It Easier for Teams to Manage Projects and Tasks." *Trello*, <trello.com/tour>. Accessed July 2023.

"TSL2561 Ambient Light Sensor - Light-to-Digital Converter." *Ams*, <ams.com/en/tsl2561#tab/applications>. Accessed July 2023.

"Understanding Bluetooth Range." *Bluetooth® Technology Website*, <www.bluetooth.com/learn-about-bluetooth/key-attributes/range/>. Accessed 24 Nov. 2023.

Van, W.G.J.H.M., et al. "Solar spectrum conversion for photovoltaics using nanoparticles." *Third Generation Photovoltaics*, 16 Mar. 2012, <https://doi.org/10.5772/39213>.

*VEML7700*, Vishay Semiconductors, 28 Apr. 2022, <www.vishay.com/docs/84286/veml7700.pdf>.

"VSWR vs. Returned Power Cheat Sheet - A.H. Systems." *A.H. Systems*, A.H. systems, <www.ahsystems.com/notes/VSWR-cheat-sheet.pdf>. Accessed 24 Nov. 2023.

"Wave Open Source Specification." *Z-Wave Alliance*, 9 Nov. 2023, <z-wavealliance.org/development-resources-overview/specification-for-developers/>.

“What Are Lora® and Lorawan®?” *LoRa Developer Portal*, lora-developers.semtech.com/documentation/tech-papers-and-guides/lora-and-lorawan/. Accessed 24 Nov. 2023.

“What Is C Programming?” *Simplilearn.Com*, Simplilearn, 13 Feb. 2023, www.simplilearn.com/c-programming-article.

“What Is CMOS?” *IONOS Digital Guide*, IONOS, 8 Dec. 2021, www.ionos.com/digitalguide/server/know-how/what-is-cmos/#:~:text=How%20does%20it%20work%3F,turned%20off%20and%20vice%20versa.

“What Is Github? A Beginner’s Introduction to Github.” *Kinsta*, 13 Dec. 2022, kinsta.com/knowledgebase/what-is-github/.

“What Is Java?” *IBM*, www.ibm.com/topics/java. Accessed July 2023.

“What Is Jira?: How to Use Jira Testing Software Tool: Simplilearn.” *Simplilearn.Com*, Simplilearn, 24 July 2023, www.simplilearn.com/tutorials/jira/what-is-jira-and-how-to-use-jira-testing-software.

“What Is Led? - Definition, Working, Properties, Uses, Advantages.” *BYJUS*, BYJU’S, 1 Dec. 2022, byjus.com/physics/light-emitting-diode/.

“What Is Lorawan® Specification.” *LoRa Alliance®*, 19 Nov. 2022, lora-alliance.org/about-lorawan/.

“Wi-Fi & Lorawan® Deployment Synergies.” *LoRa Alliance*, resources.lora-alliance.org/smart-cities/wi-fi-lorawan-deployment-synergies. Accessed 24 Nov. 2023.

“What Is Python Used for? A Beginner’s Guide.” *Coursera*, 15 June 2023, www.coursera.org/articles/what-is-python-used-for-a-beginners-guide-to-using-python.

Yang, Zengxu, and C. Hwa Chang. “6LoWPAN Overview and Implementations - EWSN.” *EWSN*, www.ewsn.org/file-repository/ewsn2019/357\_361\_yang1.pdf. Accessed 24 Nov. 2023.

“Z-Wave Security - Silicon Labs.” *Z-Wave Security - Silicon Labs*, 17 Aug. 2022, www.silabs.com/wireless/z-wave/specification/security.

“ZigBee Specification FAQ.” *ZigBee Alliance*, web.archive.org/web/20130627172453/www.zigbee.org/Specifications/ZigBee/FAQ.aspx. Accessed 24 Nov. 2023.

“Zigbee vs. 6LoWPAN for Sensor Networks.” *Laird Connectivity*, www.lairdconnect.com/resources/white-papers/zigbee-vs-6lowpan-for-sensor-networks. Accessed 24 Nov. 2023.

## Appendix D - Codes

“astrocom.c” full integration of all components flashed onto MCU PCB:

```
// YOU NEED TO DISABLE WATCHDOG TIMER IN MENUCONFIG TO RUN THIS CODE
// Component config -> ESP System settings -> Disable Task Watchdog Timer

// includes Vishay VEML7700 Light Sensor driver for integration with ESP-IDF
framework by Kristijan Grozdanovski
// Copyright (c) 2022, Kristijan Grozdanovski

#include <stdio.h>
#include <math.h>
#include "driver/i2c.h"
#include "veml7700.h"
#include "esp_log.h"
#include "driver/gpio.h"
#include "esp_intr_alloc.h"
#include "esp_timer.h"
// zigbee libraries
#include "freertos/FreeRTOS.h"
#include "freertos/task.h"
#include "managed_components/espressif_esp-zigbee-
lib/include/ha/esp_zigbee_ha_standard.h"
#include "managed_components/espressif_esp-zigbee-lib/include/esp_zb_light.h"
#include "nvs_flash.h"

#define I2C_MASTER_SCL_IO 10          // GPIO for sensor I2C clock
#define I2C_MASTER_SDA_IO 11          // GPIO for sensor I2C data
#define I2C_MASTER_NUM I2C_NUM_0
#define TCA9548_ADDR 0x71
//-----
-----
#define USBC_PIN GPIO_NUM_12 // Define GPIO pin 12
#define USBA_PIN GPIO_NUM_1 // Define GPIO pin 1
#define STEP_PIN GPIO_NUM_22      // CLK pin 22
#define DIR_PIN GPIO_NUM_23      // DIR pin 23

// PCA9685 I2C address
#define PCA9685_ADDR    0x40

// Registers
#define PCA9685_MODE1    0x00
#define PCA9685_PRESCALE 0xFE
```

```

#define LED0_ON_L      0x06
#define LED0_ON_H      0x07
#define LED0_OFF_L     0x08
#define LED0_OFF_H     0x09

#define SERVO_NUM       3

// I2C Configuration
#define I2C_PORT        0
#define I2C_FREQ_HZ    20000 // 20kHz

// Configuration for servo motors
#define SERVO_FREQ_HZ   50
#define SERVO_MIN_US    500
#define SERVO_MAX_US   2500
#define SERVO_MIN_AN    90
#define SERVO_MAX_AN   360

// global variables to store sensor and mirror values
float angle_spin = 0.0;
float save_value = 0.0;
float angle_val = 0.0;

int target_num = 0; // target number
int dir = 1; // direction of stepper

// global variables to store stepper values
float current_stepper_val = 0.0;
float stepper_save_value = 0.0;
float stepper_val_new = 0.0;

// target location arrays
float target_val_servo[] = {600,450};
float target_val_stepper[] = {0,720};

// function prototype for slow servo spin
void set_servo_angle_loop(float new_value, float current_value, int channel);

//-----ZIGBEE-----
/*
 * @note Make sure set idf.py menuconfig in zigbee component as zigbee end
device!
*/
#if !defined ZB_ED_ROLE

```

```

#error Define ZB_ED_ROLE in idf.py menuconfig to compile light (End Device)
source code.
#endif

// manufacturer info
char modelid[] = {11, 'E', 'S', 'P', '3', '2', 'C', '6', '.', 'E', 'n', 'd'};
char manufname[] = {9, 'E', 's', 'p', 'r', 'e', 's', 'i', 'f'};

static const char *TAG = "ASTROCOM";
/********************* Define functions ********************/
static void bdb_start_top_level_commissioning_cb(uint8_t mode_mask)
{
    ESP_ERROR_CHECK(esp_zb_bdb_start_top_level_commissioning(mode_mask));
}

void attr_cb(uint8_t status, uint8_t endpoint, uint16_t cluster_id, uint16_t
attr_id, void *new_value)
{
    if (cluster_id == ESP_ZB_ZCL_CLUSTER_ID_ON_OFF) {
        uint8_t value = *(uint8_t *)new_value;
        if (attr_id == ESP_ZB_ZCL_ATTR_ON_OFF_ON_OFF_ID) {
            /* implemented light on/off control */
            if (!target_num)
            {
                target_num++;
                ESP_LOGI(TAG, "set to target 0");
                gpio_set_level(20, 1);
            }
            else if (target_num)
            {
                target_num--;
                ESP_LOGI(TAG, "set to target 1");
                gpio_set_level(20, 0);
            }
            light_driver_set_power((bool)value);
        }
    } else {
        /* Implement some actions if needed when other cluster changed */
        ESP_LOGI(TAG, "cluster:0x%x, attribute:0x%x changed ", cluster_id,
attr_id);
    }
}

void esp_zb_app_signal_handler(esp_zb_app_signal_t *signal_struct)
{

```

```

        uint32_t *p_sg_p      = signal_struct->p_app_signal;
        esp_err_t err_status = signal_struct->esp_err_status;
        esp_zb_app_signal_type_t sig_type = *p_sg_p;
        switch (sig_type) {
            case ESP_ZB_ZDO_SIGNAL_SKIP_STARTUP:
                ESP_LOGI(TAG, "Zigbee stack initialized");
                esp_zb_bdb_start_top_level_commissioning(ESP_ZB_BDB_MODE_INITIALIZATION);
                break;
            case ESP_ZB_BDB_SIGNAL_DEVICE_FIRST_START:
            case ESP_ZB_BDB_SIGNAL_DEVICE_REBOOT:
                if (err_status == ESP_OK) {
                    ESP_LOGI(TAG, "Start network steering");
                    esp_zb_bdb_start_top_level_commissioning(ESP_ZB_BDB_MODE_NETWORK_STEE-
RING);
                } else {
                    /* commissioning failed */
                    ESP_LOGW(TAG, "Failed to initialize Zigbee stack (status: %d)",
err_status);
                }
                break;
            case ESP_ZB_BDB_SIGNAL_STEERING:
                if (err_status == ESP_OK) {
                    esp_zb_ieee_addr_t extended_pan_id;
                    esp_zb_get_extended_pan_id(extended_pan_id);
                    ESP_LOGI(TAG, "Joined network successfully (Extended PAN ID:
%02x:%02x:%02x:%02x:%02x:%02x:%02x:%02x, PAN ID: 0x%04hx, Channel:%d)",
extended_pan_id[7], extended_pan_id[6], extended_pan_id[5],
extended_pan_id[4], extended_pan_id[3], extended_pan_id[2], extended_pan_id[1],
extended_pan_id[0],
esp_zb_get_pan_id(), esp_zb_get_current_channel());
                } else {
                    ESP_LOGI(TAG, "Network steering was not successful (status: %d)",
err_status);
                    esp_zb_scheduler_alarm((esp_zb_callback_t)bdb_start_top_level_commiss-
ioning_cb, ESP_ZB_BDB_MODE_NETWORK_STEERING, 1000);
                }
                break;
            default:
                ESP_LOGI(TAG, "ZDO signal: %d, status: %d", sig_type, err_status);
                break;
        }
    }

    static void esp_zb_task(void *pvParameters)

```

```

{
    /* initialize Zigbee stack with Zigbee end-device config */
    esp_zb_cfg_t zb_nwk_cfg = ESP_ZB_ZED_CONFIG();
    esp_zb_init(&zb_nwk_cfg);
    /* set the on-off light device config */
    esp_zb_on_off_light_cfg_t light_cfg = ESP_ZB_DEFAULT_ON_OFF_LIGHT_CONFIG();
    esp_zb_ep_list_t *esp_zb_on_off_light_ep =
esp_zb_on_off_light_ep_create(HA_ESP_LIGHT_ENDPOINT, &light_cfg);
    // make cluster + send info
    esp_zb_attribute_list_t *esp_zb_basic_cluster =
esp_zb_zcl_attr_list_create(ESP_ZB_ZCL_CLUSTER_ID_BASIC);
    esp_zb_basic_cluster_add_attr(esp_zb_basic_cluster,
ESP_ZB_ZCL_ATTR_BASIC_MODEL_IDENTIFIER_ID, &modelid[0]);
    esp_zb_basic_cluster_add_attr(esp_zb_basic_cluster,
ESP_ZB_ZCL_ATTR_BASIC_MANUFACTURER_NAME_ID, &manufname[0]);
    //
    esp_zb_device_register(esp_zb_on_off_light_ep);
    esp_zb_device_add_set_attr_value_cb(attr_cb);
    esp_zb_set_primary_network_channel_set(ESP_ZB_PRIMARY_CHANNEL_MASK);
    ESP_ERROR_CHECK(esp_zb_start(false));
    esp_zb_main_loop_iteration();
}
//-----END OF ZIGBEE-----
-----

//-----SERVO MUX FUNCTIONS-----
-----

void pca9685_write_byte(i2c_port_t i2c_num, uint8_t reg_addr, uint8_t data) {
    i2c_cmd_handle_t cmd = i2c_cmd_link_create();
    i2c_master_start(cmd);
    i2c_master_write_byte(cmd, (PCA9685_ADDR << 1) | I2C_MASTER_WRITE, true);
    i2c_master_write_byte(cmd, reg_addr, true);
    i2c_master_write_byte(cmd, data, true);
    i2c_master_stop(cmd);
    i2c_master_cmd_begin(i2c_num, cmd, pdMS_TO_TICKS(1000));
    i2c_cmd_link_delete(cmd);
}

void pca9685_set_pwm(i2c_port_t i2c_num, uint8_t channel, uint16_t on_time,
uint16_t off_time) {
    uint8_t reg_addr = LED0_ON_L + 4 * channel;
    uint8_t on_l = on_time & 0xFF;
    uint8_t on_h = (on_time >> 8) & 0x0F;
    uint8_t off_l = off_time & 0xFF;
    uint8_t off_h = (off_time >> 8) & 0x0F;
}

```

```

    pca9685_write_byte(i2c_num, reg_addr, on_l);
    pca9685_write_byte(i2c_num, reg_addr + 1, on_h);
    pca9685_write_byte(i2c_num, reg_addr + 2, off_l);
    pca9685_write_byte(i2c_num, reg_addr + 3, off_h);

}

void pca9685_init(i2c_port_t i2c_num) {
    pca9685_write_byte(i2c_num, PCA9685_MODE1, 0x00); // Reset PCA9685

    // Set PWM frequency
    uint8_t prescale_val = (uint8_t)(25000000 / (4096 * SERVO_FREQ_HZ) - 1);
    pca9685_write_byte(i2c_num, PCA9685_PRESCALE, prescale_val);

    // Restart PCA9685
    pca9685_write_byte(i2c_num, PCA9685_MODE1, 0xA1);
    vTaskDelay(pdMS_TO_TICKS(5)); // Delay at least 500us after restart

    // Set all channels off initially
    for (int i = 0; i < SERVO_NUM; i++) {
        pca9685_set_pwm(i2c_num, i, 0, 0);
    }
}

//-----END OF SERVO MUX FUNCTIONS-----
-----

//-----SERVO CTL FUNCTIONS-----
-----

void set_servo_angle(i2c_port_t i2c_num, uint8_t channel, double angle) {
    // Calculate pulse length
    uint16_t pulse = (uint16_t)(SERVO_MIN_US + (angle / 180.0) * (SERVO_MAX_US - SERVO_MIN_US));
    uint16_t pwm_val = (uint16_t)(pulse * 4096 / 20000); // 20ms (50Hz) period
for servos

    // Set PWM for the servo channel
    pca9685_set_pwm(i2c_num, channel, 0, pwm_val);
}

void set_servo_angle_loop(float new_value, float current_value, int channel)
{
    if(new_value < current_value)
    {
        for(int i=current_value; i>=new_value; i--){

```

```

        set_servo_angle(I2C_PORT, channel, i);
        vTaskDelay(pdMS_TO_TICKS(30));
    }
}
else if(new_value > current_value)
{
    for(int i=current_value; i<=new_value; i++){
        set_servo_angle(I2C_PORT, channel, i);
        vTaskDelay(pdMS_TO_TICKS(30));
    }
}
//-----END OF SERVO CTL FUNCTIONS-----
-----

//-----  

// timer interrupt handler prototype
void timer_isr(void* arg);

// structure of light sensor
typedef struct {
    veml7700_handle_t dev;
    double lux;
    double fc;
} VEML_Data;

// I2C init function
void i2c_master_init() {
    i2c_config_t conf;
    conf.mode = I2C_MODE_MASTER;
    conf.sda_io_num = I2C_MASTER_SDA_IO;
    conf.sda_pullup_en = GPIO_PULLUP_ENABLE;
    conf.scl_io_num = I2C_MASTER_SCL_IO;
    conf.scl_pullup_en = GPIO_PULLUP_ENABLE;
    conf.master.clk_speed = I2C_FREQ_HZ; // 100 kHz clock speed
    conf.clk_flags = 0;
    i2c_param_config(I2C_MASTER_NUM, &conf);
    i2c_driver_install(I2C_MASTER_NUM, conf.mode, 0, 0, 0);
}

// sensor mux channel select
void select_channel(uint8_t channel) {
    uint8_t cmd = 1 << channel;
    i2c_cmd_handle_t cmd_handle = i2c_cmd_link_create();
    i2c_master_start(cmd_handle);
}

```

```

    i2c_master_write_byte(cmd_handle, (TCA9548_ADDR << 1) | I2C_MASTER_WRITE,
true);
    i2c_master_write_byte(cmd_handle, cmd, true);
    i2c_master_stop(cmd_handle);
    i2c_master_cmd_begin(I2C_MASTER_NUM, cmd_handle, 1000 / portTICK_PERIOD_MS);
}

// sensor init function
void initialize_veml_device(VEML_Data *data, int channel) {
    esp_err_t init_result = veml7700_initialize(&(data->dev), I2C_MASTER_NUM);
    if (init_result != ESP_OK) {
        ESP_LOGE("VEML7700", "Failed to initialize VEML7700 (Channel %d). Result: %d\n", channel, init_result);
    }
    else{
        ESP_LOGI("VEML7700", "Successfully initialized VEML7700 (Channel %d). Result: %d\n", channel, init_result);
    }
}
//-----
//Set stepper task
void stepper_task(float val) {
    esp_rom_gpio_pad_select_gpio(STEP_PIN);           //selecting CLK pin
    esp_rom_gpio_pad_select_gpio(DIR_PIN);           //selecting DIR pin
    gpio_set_direction(STEP_PIN, GPIO_MODE_OUTPUT);   //set CLK pin to output
    gpio_set_direction(DIR_PIN, GPIO_MODE_OUTPUT);   //set DIR pin to output
    //Pull USBC pin up to switch on power to Servos
    esp_rom_gpio_pad_select_gpio(USBC_PIN);
    gpio_set_direction(USBC_PIN, GPIO_MODE_OUTPUT);
    //gpio_set_pull_mode(USBC_PIN, GPIO_PULLUP_ONLY);
    gpio_set_level(USBC_PIN,1);
    val = 1.0/val;
    printf("val after inverse is %.4f\n\n", val);
    val = pow(val,8); // set to 8th power to adjust accurately to sensor values
    // if above 200 reset to 200
    if(val >= 200)
    {
        val = 200;
    }
    current_stepper_val = 0.0;
    ESP_LOGI(TAG, "old horiz value of target is %.4f", target_val_stepper[0]);
    target_val_stepper[0] = ((dir*val) + target_val_stepper[0]);
    ESP_LOGI(TAG, "new horiz value of target is %.4f", target_val_stepper[0]);
    target_val_stepper[1] = ((dir*val) + target_val_stepper[1]);
}

```

```

printf("\n\nstep size is %.4f\n\n", val);
for (int i = 0; i < val; i++) { // 200 steps for one revolution
    gpio_set_level(STEP_PIN, 1);
    vTaskDelay(pdMS_TO_TICKS(10)); // Adjust delay
    gpio_set_level(STEP_PIN, 0);
    vTaskDelay(pdMS_TO_TICKS(10)); // Adjust delay
}
vTaskDelay(pdMS_TO_TICKS(200)); // Delay between rotations

esp_rom_gpio_pad_select_gpio(USBA_PIN);
gpio_set_direction(USBA_PIN, GPIO_MODE_OUTPUT);
gpio_set_level(USBA_PIN, 1);

return;
}

// main function
void app_main() {
    esp_rom_gpio_pad_select_gpio(USBA_PIN);
    gpio_set_direction(USBA_PIN, GPIO_MODE_OUTPUT);
    gpio_set_level(USBA_PIN, 1); // power switch **sensor**

    gpio_reset_pin(USBC_PIN);
    esp_rom_gpio_pad_select_gpio(20);
    gpio_set_direction(20, GPIO_MODE_OUTPUT);

    i2c_master_init();
    pca9685_init(I2C_PORT);
    printf("ESP32 Initialized for I2C.\n");

    //-----ZIGBEE-----
    esp_zb_platform_config_t config = {
        .radio_config = ESP_ZB_DEFAULT_RADIO_CONFIG(),
        .host_config = ESP_ZB_DEFAULT_HOST_CONFIG(),
    };
    ESP_ERROR_CHECK(nvs_flash_init());
    /* load Zigbee light_bulb platform config to initialization */
    ESP_ERROR_CHECK(esp_zb_platform_config(&config));
    /* hardware related and device init */
    light_driver_init(0);
    //-----ZIGBEE-----

    VEML_Data veml_devices[] = {
        { .dev = NULL, .lux = 0, .fc = 0 }, // Data for channel 0 (index 0)

```

```

{ .dev = NULL, .lux = 0, .fc = 0 }, // Data for channel 1 (index 1)
{ .dev = NULL, .lux = 0, .fc = 0 }, // Data for channel 2 (index 2)
{ .dev = NULL, .lux = 0, .fc = 0 }, // Data for channel 3 (index 3)
{ .dev = NULL, .lux = 0, .fc = 0 }, // Data for channel 4 (index 4)
};

int num_veml_devices = sizeof(veml_devices) / sizeof(VEML_Data);

for (int i = 0; i < num_veml_devices; i++) { // Start from index 0
    select_channel(i); // Channel index starts from 0
    initialize_veml_device(&veml_devices[i], i); // Initialize VEML device
}

// Initialize timer
esp_timer_create_args_t timer_args = {
    .callback = timer_isr,
    .name = "software_timer",
    .arg = &veml_devices
};
esp_timer_handle_t software_timer;
esp_timer_create(&timer_args, &software_timer);

//ZIGBEE-----
xTaskCreate(esp_zb_task, "Zigbee_main", 4096, NULL, 5, NULL);
//ZIGBEE-----


//-----STARTING VALS FOR MOTORS-----
save_value = 600;
set_servo_angle_loop(600,495, 0);
ESP_LOGI(TAG, "set sensor servo to 600");

set_servo_angle_loop(510, 510, 1);
set_servo_angle_loop(600, 600, 2);
ESP_LOGI(TAG, "set mirror horizontal servo to 520 and vertical to 600");
vTaskDelay(pdMS_TO_TICKS(1000));

set_servo_angle_loop(459, 510, 1);
set_servo_angle_loop(450, 600, 2);
ESP_LOGI(TAG, "set mirror horizontal servo to 459 and vertical to 450");
vTaskDelay(pdMS_TO_TICKS(2000));
//-----STARTING VALS FOR MOTORS-----


// Start timer
esp_timer_start_periodic(software_timer, 5000000); // 5s timer

```

```

// infinite loop
while (1) {

}

// interrupt handler
void timer_isr(void* arg) {
    printf("Software interrupt timer ISR\n");
    VEML_Data* veml_devices = (VEML_Data*)arg;
    for (int i = 0; i < 5; i++) { // Start from index 0
        select_channel(i); // Channel index starts from 0
        printf("Channel %d on the TCA9548 is now open.\n", i);

        // Read VEML data
        if (veml_devices[i].dev != NULL) {
            double lux = 0, fc = 0;
            esp_err_t read_result =
veml7700_read_als_lux_auto(veml_devices[i].dev, &lux);
            if (read_result == ESP_OK) {
                fc = lux * LUX_FC_COEFFICIENT;
                veml_devices[i].lux = lux;
                veml_devices[i].fc = fc;
                printf("Sensor %d (Channel %d) - ALS: %0.4f lux, %0.4f fc\n", i,
i, lux, fc);
            } else {
                ESP_LOGE("VEML7700", "Failed to read data from VEML7700 (Channel
%d). Result: %d\n", i, read_result);
            }
        } else {
            ESP_LOGE("VEML7700", "VEML7700 device not initialized for Channel
%d\n", i);
        }
    }

    // calculate ratios of sensor
    float servo_spin_down = (((veml_devices[0].lux + veml_devices[3].lux)/2) /
((veml_devices[1].lux + veml_devices[2].lux)/2)); // ratio for down movement
    float servo_spin_up = (((veml_devices[1].lux + veml_devices[2].lux)/2) /
((veml_devices[0].lux + veml_devices[3].lux)/2)); // ratio for up movement
    float stepper_spin_clockwise = (((veml_devices[2].lux +
veml_devices[3].lux)/2) / ((veml_devices[0].lux + veml_devices[1].lux)/2)); // ratio for clkwise stepper
}

```

```

float stepper_spin_counterclockwise = (((veml_devices[0].lux +
veml_devices[1].lux)/2) / ((veml_devices[2].lux + veml_devices[3].lux)/2)); //  

ratio for cntrclkwise stepper  

float servo_spin_down_inv = 1/servo_spin_down; // inverse of down  

float servo_spin_up_inv = 1/servo_spin_up; // inverse of up  

if(servo_spin_down_inv > 20) // reset to 20 if bigger  

    servo_spin_down_inv = 20;  

if(servo_spin_up_inv > 20) // reset to 20 if bigger  

    servo_spin_up_inv = 20;  
  

printf("\n\n");
if(stepper_spin_counterclockwise < 1)
{
    printf("counterclockwise is %.4f\n", stepper_spin_counterclockwise);
}
if(stepper_spin_clockwise < 1)
{
    printf("clockwise is %.4f\n", stepper_spin_clockwise);
}  
  

if(servo_spin_down < 0.8) // sensor needs to be moved down
{
    printf("Servo value is %.4f\n", servo_spin_down);
    if((save_value - servo_spin_down_inv) < 495)
    {
        printf("hit max range at 495, horizontal\n");
        angle_spin = 495;
    }
    else{
        angle_spin = save_value - servo_spin_down_inv;
    }
    printf("setting servo step to %.4f\n\n", angle_spin);
    printf("\n\nservo begins spinning\n");
    set_servo_angle_loop(angle_spin, save_value, 0);
    printf("servo done spinning\n\n");
    vTaskDelay(pdMS_TO_TICKS(1000));
}
else if(servo_spin_up < 0.8) // sensor needs to be moved up
{
    printf("Servo value is %.4f\n", servo_spin_up);
    if((save_value + servo_spin_up_inv) > 765)
    {
        printf("hit max range at 765, vertical\n");
        angle_spin = 765;
    }
}

```

```

    }
else
{
    angle_spin = save_value + servo_spin_up_inv;
}
printf("setting servo step to %.4f\n\n", angle_spin);
printf("\n\nservo begins spinning\n");
set_servo_angle_loop(angle_spin, save_value, 0);
printf("servo done spinning\n\n");
vTaskDelay(pdMS_TO_TICKS(1000));
}

if(stepper_spin_clockwise < 0.9) // stepper needs to be moved clockwise
{
    printf("clockwise is %.4f\n", stepper_spin_clockwise);
    gpio_set_level(DIR_PIN, 1); // Set direction 1 clockwise
    ESP_LOGI(TAG, "dir is %d-----", dir);
    if(dir < 0)
    {
        dir *= -1;
        ESP_LOGI(TAG, "dir changes");
    }
    printf("\n\nstepper begins spinning\n");
    stepper_task(stepper_spin_clockwise);
    printf("stepper done spinning\n\n");
}
else if(stepper_spin_counterclockwise < 0.9) // stepper needs to be moved
counterclockwise
{
    printf("counterclockwise is %.4f\n", stepper_spin_counterclockwise);
    gpio_set_level(DIR_PIN, 0); // Set direction 0 counterclockwise
    ESP_LOGI(TAG, "dir is %d-----", dir);
    if(dir != -1)
    {
        dir *= -1;
        ESP_LOGI(TAG, "dir changes");
    }
    printf("\n\nstepper begins spinning\n");
    stepper_task(stepper_spin_counterclockwise);
    printf("stepper done spinning\n\n");
}

printf("angle val is %.4f\n\n", angle_val);

// scale vertical movement of sensor position to mirror

```

```

float new_servo_exchange = (((angle_spin - 495)*(400-600))/(765-495)) + 600;
float old_servo_exchange = (((save_value - 495)*(400-600))/(765-495)) + 600;

// set values to half of target and sensor range
float servo_vertical_pos_new = (new_servo_exchange +
target_val_servo[target_num])/2;
float servo_vertical_pos_old = (old_servo_exchange +
target_val_servo[target_num])/2;

ESP_LOGI(TAG, "target val servo is %.4f", target_val_servo[target_num]);

// if past furthest range reset
if(servo_vertical_pos_new > 600)
{
    servo_vertical_pos_new = 600;
    servo_vertical_pos_old = 600;
    ESP_LOGI(TAG, "GOT PAST 600");
}

// move mirror with servo function
set_servo_angle_loop(servo_vertical_pos_new, servo_vertical_pos_old, 2);
ESP_LOGI(TAG, "set servo to %.4f", servo_vertical_pos_new);

// new stepper value is half of the target, since sensor is always at 0
stepper_val_new = target_val_stepper[target_num]/2;

// scale values to mirror range
float scaled_stepper_val_new = ((stepper_val_new*(300-510))/1440) + 510;
float scaled_stepper_val_old = ((stepper_save_value*(300-510))/1440) + 510;

// if past max range reset to max range
if(scaled_stepper_val_new > 510)
{
    scaled_stepper_val_new = 510;
    scaled_stepper_val_old = 510;
    ESP_LOGI(TAG, "GOT PAST 510");
}
ESP_LOGI(TAG, "horizontal mirror servo set from %.4f to %.4f",
scaled_stepper_val_old, scaled_stepper_val_new);

// move mirror with servo function
set_servo_angle_loop(scaled_stepper_val_new, scaled_stepper_val_old, 1);

```

```

    // save old values of servos
    stepper_save_value = stepper_val_new;
    save_value = angle_spin;
}s

```

“esp\_ha\_customized\_switch.c” for communication box:

```

#include "esp_ha_customized_switch.h"
#include "esp_check.h"
#include "esp_err.h"
#include "esp_log.h"
#include "nvs_flash.h"
#include "string.h"
#include "freertos/FreeRTOS.h"
#include "freertos/task.h"
#include "zcl/esp_zigbee_zcl_common.h"

// idf.py menuconfig allows you to define what the device is.
// In this case it is defined as an end device.
#if !defined ZB_ED_ROLE
#error Define ZB_ED_ROLE in idf.py menuconfig to compile light switch (End
Device) source code.
#endif

// manufacturer info
char modelid[] = {13, 'E', 'S', 'P', '3', '2', 'C', '6', '.', 'L', 'i', 'g', 'h',
't'};
char manufname[] = {9, 'E', 's', 'p', 'r', 'e', 's', 's', 'i', 'f'};

// Tag for log messages
static const char *TAG = "ESP_HA_ON_OFF_SWITCH";

// Defining the button that toggles the switch and the control it is connected
to, as a pair
static switch_func_pair_t button_func_pair[] = {
    {GPIO_INPUT_IO_TOGGLE_SWITCH, SWITCH_ONOFF_TOGGLE_CONTROL}
};

typedef struct light_bulb_device_params_s {
    esp_zb_ieee_addr_t ieee_addr;
    uint8_t endpoint;
    uint16_t short_addr;
} light_bulb_device_params_t;

```

```

typedef struct zdo_info_ctx_s {
    uint8_t endpoint;
    uint16_t short_addr;
} zdo_info_user_ctx_t;

/* remote device struct for recording and managing node info */
light_bulb_device_params_t on_off_light;

static void esp_zb_buttons_handler(switch_func_pair_t *button_func_pair)
{
    switch (button_func_pair->func) {
    case SWITCH_ONOFF_TOGGLE_CONTROL: {
        /* send on-off toggle command to remote device */
        esp_zb_zcl_on_off_cmd_t cmd_req;
        cmd_req.zcl_basic_cmd.dst_addr_u.addr_short = on_off_light.short_addr;
        cmd_req.zcl_basic_cmd.dst_endpoint = on_off_light.endpoint;
        cmd_req.zcl_basic_cmd.src_endpoint = HA_ONOFF_SWITCH_ENDPOINT;
        cmd_req.address_mode = ESP_ZB_APSS_ADDR_MODE_16_ENDP_PRESENT;
        cmd_req.on_off_cmd_id = ESP_ZB_ZCL_CMD_ON_OFF_TOGGLE_ID;
        ESP_EARLY_LOGI(TAG, "Send 'on_off toggle' command to address(0x%x)
endpoint(%d)", on_off_light.short_addr, on_off_light.endpoint);
        esp_zb_zcl_on_off_cmd_req(&cmd_req);
    } break;
    default:
        break;
    }
}

static void bdb_start_top_level_commissioning_cb(uint8_t mode_mask)
{
    ESP_ERROR_CHECK(esp_zb_bdb_start_top_level_commissioning(mode_mask));
}

static void bind_cb(esp_zb_zdp_status_t zdo_status, void *user_ctx)
{
    if (zdo_status == ESP_ZB_ZDP_STATUS_SUCCESS) {
        ESP_LOGI(TAG, "Bind response from address(0x%x), endpoint(%d) with
status(%d)", ((zdo_info_user_ctx_t *)user_ctx)->short_addr,
        ((zdo_info_user_ctx_t *)user_ctx)->endpoint, zdo_status);
        /* configure report attribute command */
        esp_zb_zcl_config_report_cmd_t report_cmd;
        bool report_change = 0;
        report_cmd.zcl_basic_cmd.dst_addr_u.addr_short = on_off_light.short_addr;
        report_cmd.zcl_basic_cmd.dst_endpoint = on_off_light.endpoint;
    }
}

```

```

report_cmd.zcl_basic_cmd.src_endpoint = HA_ONOFF_SWITCH_ENDPOINT;
report_cmd.address_mode = ESP_ZBAPSADDRMODE16ENDP_PRESENT;
report_cmd.clusterID = ESP_ZBZCLCLUSTERIDONOFF;

esp_zb_zcl_config_report_record_t records[] = {
    {ESP_ZB_ZCL_CMD_DIRECTION_TO_SRV, ESP_ZB_ZCL_ATTR_ON_OFF_ON_OFF_ID,
ESP_ZB_ZCL_ATTR_TYPE_BOOL, 0, 30, &report_change}};
    report_cmd.record_number = sizeof(records) /
sizeof(esp_zb_zcl_config_report_record_t);
    report_cmd.record_field = records;

esp_zb_zcl_config_report_cmd_req(&report_cmd);
}

}

static void ieee_cb(esp_zb_zdp_status_t zdo_status, esp_zb_ieee_addr_t ieee_addr,
void *user_ctx)
{
    if (zdo_status == ESP_ZB_ZDP_STATUS_SUCCESS) {
        memcpy(&(on_off_light.ieee_addr), ieee_addr, sizeof(esp_zb_ieee_addr_t));
        ESP_LOGI(TAG, "IEEE address: %02x.%02x.%02x.%02x.%02x.%02x.%02x",
            ieee_addr[7], ieee_addr[6], ieee_addr[5], ieee_addr[4],
            ieee_addr[3], ieee_addr[2], ieee_addr[1], ieee_addr[0]);
        /* bind the on-off light to on-off switch */
        esp_zb_zdo_bind_req_param_t bind_req;
        memcpy(&(bind_req.src_address), on_off_light.ieee_addr,
sizeof(esp_zb_ieee_addr_t));
        bind_req.src_endp = on_off_light.endpoint;
        bind_req.cluster_id = ESP_ZB_ZCL_CLUSTER_ID_ON_OFF;
        bind_req.dst_addr_mode = ESP_ZB_ZDO_BIND_DST_ADDR_MODE_64_BIT_EXTENDED;
        esp_zb_get_long_address(bind_req.dst_address_u.addr_long);
        bind_req.dst_endp = HA_ONOFF_SWITCH_ENDPOINT;
        bind_req.req_dst_addr = on_off_light.short_addr;
        static zdo_info_user_ctx_t test_info_ctx;
        test_info_ctx.endpoint = HA_ONOFF_SWITCH_ENDPOINT;
        test_info_ctx.short_addr = on_off_light.short_addr;
        esp_zb_zdo_device_bind_req(&bind_req, bind_cb, (void *) &
(test_info_ctx));
    }
}

static void ep_cb(esp_zb_zdp_status_t zdo_status, uint8_t ep_count, uint8_t
*ep_id_list, void *user_ctx)
{
    if (zdo_status == ESP_ZB_ZDP_STATUS_SUCCESS) {

```

```

        ESP_LOGI(TAG, "Active endpoint response: status(%d) and endpoint
count(%d)", zdo_status, ep_count);
        for (int i = 0; i < ep_count; i++) {
            ESP_LOGI(TAG, "Endpoint ID List: %d", ep_id_list[i]);
        }
    }
}

static void simple_desc_cb(esp_zb_zdp_status_t zdo_status,
esp_zb_af_simple_desc_1_1_t *simple_desc, void *user_ctx)
{
    if (zdo_status == ESP_ZB_ZDP_STATUS_SUCCESS) {
        ESP_LOGI(TAG, "Simple desc resposne: status(%d), device_id(%d),
app_version(%d), profile_id(0x%08x), endpoint_ID(%d)", zdo_status,
simple_desc->app_device_id, simple_desc->app_device_version,
simple_desc->app_profile_id, simple_desc->endpoint);

        for (int i = 0; i < (simple_desc->app_input_cluster_count + simple_desc-
>app_output_cluster_count); i++) {
            ESP_LOGI(TAG, "Cluster ID list: 0x%08x", *(simple_desc-
>app_cluster_list + i));
        }
    }
}

static void user_find_cb(esp_zb_zdp_status_t zdo_status, uint16_t addr, uint8_t
endpoint, void *user_ctx)
{
    if (zdo_status == ESP_ZB_ZDP_STATUS_SUCCESS) {
        ESP_LOGI(TAG, "Match desc response: status(%d), address(0x%08x),
endpoint(%d)", zdo_status, addr, endpoint);
        /* save into remote device record structure for future use */
        on_off_light.endpoint = endpoint;
        on_off_light.short_addr = addr;
        /* find the active endpoint */
        esp_zb_zdo_active_ep_req_param_t active_ep_req;
        active_ep_req.addr_of_interest = on_off_light.short_addr;
        esp_zb_zdo_active_ep_req(&active_ep_req, ep_cb, NULL);
        /* get the node simple descriptor */
        esp_zb_zdo_simple_desc_req_param_t simple_desc_req;
        simple_desc_req.addr_of_interest = addr;
        simple_desc_req.endpoint = endpoint;
        esp_zb_zdo_simple_desc_req(&simple_desc_req, simple_desc_cb, NULL);
        /* get the light ieee address */
        esp_zb_zdo_ieee_addr_req_param_t ieee_req;

```

```

        ieee_req.addr_of_interest = on_off_light.short_addr;
        ieee_req.dst_nwk_addr = on_off_light.short_addr;
        ieee_req.request_type = 0;
        ieee_req.start_index = 0;
        esp_zb_zdo_ieee_addr_req(&ieee_req, ieee_cb, NULL);
        esp_zb_zcl_read_attr_cmd_t read_req;
        uint16_t attributes[] = {ESP_ZB_ZCL_ATTR_ON_OFF_ON_OFF_ID};
        read_req.address_mode = ESP_ZBAPS_MODE_16_ENDP_PRESENT;
        read_req.attr_number = sizeof(attributes) / sizeof(uint16_t);
        read_req.attr_field = attributes;
        read_req.clusterID = ESP_ZB_ZCL_CLUSTER_ID_ON_OFF;
        read_req.zcl_basic_cmd.dst_endpoint = on_off_light.endpoint;
        read_req.zcl_basic_cmd.src_endpoint = HA_ONOFF_SWITCH_ENDPOINT;
        read_req.zcl_basic_cmd.dst_addr_u.addr_short = on_off_light.short_addr;
        esp_zb_zcl_read_attr_cmd_req(&read_req);
    }
}

void esp_zb_app_signal_handler(esp_zb_app_signal_t *signal_struct)
{
    uint32_t *p_sg_p      = signal_struct->p_app_signal;
    esp_err_t err_status = signal_struct->esp_err_status;
    esp_zb_app_signal_type_t sig_type = *p_sg_p;
    esp_zb_zdo_signal_leave_params_t *leave_params = NULL;
    switch (sig_type) {
        case ESP_ZB_BDB_SIGNAL_DEVICE_FIRST_START:
        case ESP_ZB_BDB_SIGNAL_DEVICE_REBOOT:
        case ESP_ZB_BDB_SIGNAL_STEERING:
            if (err_status != ESP_OK) {
                ESP_LOGW(TAG, "Stack %s failure with %s status",
steering",esp_zb_zdo_signal_to_string(sig_type), esp_err_to_name(err_status));
                esp_zb_scheduler_alarm((esp_zb_callback_t)bdb_start_top_level_commissioning_cb, ESP_ZB_BDB_MODE_NETWORK_STEERING, 1000);
            } else {
                /* device auto start successfully and on a formed network */
                esp_zb_ieee_addr_t extended_pan_id;
                esp_zb_get_extended_pan_id(extended_pan_id);
                ESP_LOGI(TAG, "Joined network successfully (Extended PAN
ID: %02x:%02x:%02x:%02x:%02x:%02x, PAN ID: 0x%04hx, Channel:%d, Short
Address: 0x%04hx)",
extended_pan_id[7], extended_pan_id[6], extended_pan_id[5],
extended_pan_id[4], extended_pan_id[3], extended_pan_id[2], extended_pan_id[1],
extended_pan_id[0],

```

```

        esp_zb_get_pan_id(), esp_zb_get_current_channel(),
esp_zb_get_short_address();
    esp_zb_zdo_match_desc_req_param_t find_req;
    find_req.addr_of_interest = 0x0000;
    find_req.dst_nwk_addr = 0x0000;
    /* find the match on-off light device */
    esp_zb_zdo_find_on_off_light(&find_req, user_find_cb, NULL);
}
break;
case ESP_ZB_ZDO_SIGNAL_LEAVE:
    leave_params = (esp_zb_zdo_signal_leave_params_t
*)esp_zb_app_signal_get_params(p_sg_p);
    if (leave_params->leave_type == ESP_ZB_NWK_LEAVE_TYPE_RESET) {
        ESP_LOGI(TAG, "Reset device");
    }
    break;
default:
    ESP_LOGI(TAG, "ZDO signal: %s (0x%x), status: %s",
esp_zb_zdo_signal_to_string(sig_type), sig_type,
esp_err_to_name(err_status));
    break;
}
}

static esp_err_t zb_attribute_reporting_handler(const
esp_zb_zcl_report_attr_message_t *message)
{
    ESP_RETURN_ON_FALSE(message, ESP_FAIL, TAG, "Empty message");
    ESP_RETURN_ON_FALSE(message->status == ESP_ZB_ZCL_STATUS_SUCCESS,
ESP_ERR_INVALID_ARG, TAG, "Received message: error status(%d)",
message->status);
    ESP_LOGI(TAG, "Received report from address(0x%x) src endpoint(%d) to dst
endpoint(%d) cluster(0x%x)", message->src_address.u.short_addr,
message->src_endpoint, message->dst_endpoint, message->cluster);
    ESP_LOGI(TAG, "Received report information: attribute(0x%x), type(0x%x),
value(%d)\n", message->attribute.id, message->attribute.data.type,
message->attribute.data.value ? *(uint8_t *)message-
>attribute.data.value : 0);
    return ESP_OK;
}

static esp_err_t zb_read_attr_resp_handler(const
esp_zb_zcl_cmd_read_attr_resp_message_t *message)
{

```

```

ESP_RETURN_ON_FALSE(message, ESP_FAIL, TAG, "Empty message");
ESP_RETURN_ON_FALSE(message->info.status == ESP_ZB_ZCL_STATUS_SUCCESS,
ESP_ERR_INVALID_ARG, TAG, "Received message: error status(%d)",
                     message->info.status);

esp_zb_zcl_read_attr_resp_variable_t *variable = message->variables;
while (variable) {
    ESP_LOGI(TAG, "Read attribute response: status(%d), cluster(0x%x),
attribute(0x%x), type(0x%x), value(%d)", variable->status,
             message->info.cluster, variable->attribute.id, variable-
             >attribute.data.type,
             variable->attribute.data.value ? *(uint8_t *)variable-
             >attribute.data.value : 0);
    variable = variable->next;
}

return ESP_OK;
}

static esp_err_t zb_configure_report_resp_handler(const
esp_zb_zcl_cmd_config_report_resp_message_t *message)
{
    ESP_RETURN_ON_FALSE(message, ESP_FAIL, TAG, "Empty message");
    ESP_RETURN_ON_FALSE(message->info.status == ESP_ZB_ZCL_STATUS_SUCCESS,
ESP_ERR_INVALID_ARG, TAG, "Received message: error status(%d)",
                     message->info.status);

    esp_zb_zcl_config_report_resp_variable_t *variable = message->variables;
    while (variable) {
        ESP_LOGI(TAG, "Configure report response: status(%d), cluster(0x%x),
attribute(0x%x)", message->info.status, message->info.cluster,
                 variable->attribute_id);
        variable = variable->next;
    }

    return ESP_OK;
}

static esp_err_t zb_action_handler(esp_zb_core_action_callback_id_t callback_id,
const void *message)
{
    esp_err_t ret = ESP_OK;
    switch (callback_id) {
        case ESP_ZB_CORE_REPORT_ATTR_CB_ID:

```

```

        ret = zb_attribute_reporting_handler((esp_zb_zcl_report_attr_message_t
*)message);
        break;
    case ESP_ZB_CORE_CMD_READ_ATTR_RESP_CB_ID:
        ret = zb_read_attr_resp_handler((esp_zb_zcl_cmd_read_attr_resp_message_t
*)message);
        break;
    case ESP_ZB_CORE_CMD_REPORT_CONFIG_RESP_CB_ID:
        ret =
zb_configure_report_resp_handler((esp_zb_zcl_cmd_config_report_resp_message_t
*)message);
        break;
    default:
        ESP_LOGW(TAG, "Receive Zigbee action(0x%02x) callback", callback_id);
        break;
    }
    return ret;
}

static void esp_zb_task(void *pvParameters)
{
    /* initialize Zigbee stack */
    esp_zb_cfg_t zb_nwk_cfg = ESP_ZB_ZED_CONFIG();
    esp_zb_init(&zb_nwk_cfg);
    //esp_zb_set_network_channel(23);
    uint8_t test_attr;
    test_attr = 0;
    /* basic cluster create with fully customized */
    esp_zb_attribute_list_t *esp_zb_basic_cluster =
esp_zb_zcl_attr_list_create(ESP_ZB_ZCL_CLUSTER_ID_BASIC);
    esp_zb_basic_cluster_add_attr(esp_zb_basic_cluster,
ESP_ZB_ZCL_ATTR_BASIC_ZCL_VERSION_ID, &test_attr);
    esp_zb_basic_cluster_add_attr(esp_zb_basic_cluster,
ESP_ZB_ZCL_ATTR_BASIC_POWER_SOURCE_ID, &test_attr);
    // send info
    esp_zb_basic_cluster_add_attr(esp_zb_basic_cluster,
ESP_ZB_ZCL_ATTR_BASIC_MODEL_IDENTIFIER_ID, &modelid[0]);
    esp_zb_basic_cluster_add_attr(esp_zb_basic_cluster,
ESP_ZB_ZCL_ATTR_BASIC_MANUFACTURER_NAME_ID, &manufname[0]);
    esp_zb_cluster_update_attr(esp_zb_basic_cluster,
ESP_ZB_ZCL_ATTR_BASIC_ZCL_VERSION_ID, &test_attr);
    /* identify cluster create with fully customized */
    esp_zb_attribute_list_t *esp_zb_identify_cluster =
esp_zb_zcl_attr_list_create(ESP_ZB_ZCL_CLUSTER_ID_IDENTIFY);

```

```

    esp_zb_identify_cluster_add_attr(esp_zb_identify_cluster,
ESP_ZB_ZCL_ATTR_IDENTIFY_IDENTIFY_TIME_ID, &test_attr);
    /* create client role of the cluster */
    esp_zb_attribute_list_t *esp_zb_on_off_client_cluster =
esp_zb_zcl_attr_list_create(ESP_ZB_ZCL_CLUSTER_ID_ON_OFF);
    esp_zb_attribute_list_t *esp_zb_identify_client_cluster =
esp_zb_zcl_attr_list_create(ESP_ZB_ZCL_CLUSTER_ID_IDENTIFY);
    /* server role */
    esp_zb_on_off_cluster_cfg_t on_off_cfg;
    on_off_cfg.on_off = ESP_ZB_ZCL_ON_OFF_ON_OFF_DEFAULT_VALUE;
    esp_zb_attribute_list_t *esp_zb_on_off_cluster =
esp_zb_on_off_cluster_create(&on_off_cfg);
    /* create cluster lists for this endpoint */
    esp_zb_cluster_list_t *esp_zb_cluster_list =
esp_zb_zcl_cluster_list_create();
    esp_zb_cluster_list_add_basic_cluster(esp_zb_cluster_list,
esp_zb_basic_cluster, ESP_ZB_ZCL_CLUSTER_SERVER_ROLE);
    esp_zb_cluster_list_add_identify_cluster(esp_zb_cluster_list,
esp_zb_identify_cluster, ESP_ZB_ZCL_CLUSTER_SERVER_ROLE);
    esp_zb_cluster_list_add_on_off_cluster(esp_zb_cluster_list,
esp_zb_on_off_client_cluster, ESP_ZB_ZCL_CLUSTER_CLIENT_ROLE);
    esp_zb_cluster_list_add_on_off_cluster(esp_zb_cluster_list,
esp_zb_on_off_cluster, ESP_ZB_ZCL_CLUSTER_SERVER_ROLE);
    esp_zb_cluster_list_add_identify_cluster(esp_zb_cluster_list,
esp_zb_identify_client_cluster, ESP_ZB_ZCL_CLUSTER_CLIENT_ROLE);

    esp_zb_ep_list_t *esp_zb_ep_list = esp_zb_ep_list_create();
    esp_zb_ep_list_add_ep(esp_zb_ep_list, esp_zb_cluster_list,
HA_ONOFF_SWITCH_ENDPOINT, ESP_ZB_AF_HA_PROFILE_ID,
ESP_ZB_HA_ON_OFF_SWITCH_DEVICE_ID);
    esp_zb_device_register(esp_zb_ep_list);
    esp_zb_core_action_handler_register(zb_action_handler);
    esp_zb_set_primary_network_channel_set(ESP_ZB_PRIMARY_CHANNEL_MASK);
    esp_zb_set_secondary_network_channel_set(ESP_ZB_SECONDARY_CHANNEL_MASK);
    ESP_ERROR_CHECK(esp_zb_start(true));
    esp_zb_main_loop_iteration();
}

void app_main(void)
{
    esp_zb_platform_config_t config = {
        .radio_config = ESP_ZB_DEFAULT_RADIO_CONFIG(),
        .host_config = ESP_ZB_DEFAULT_HOST_CONFIG(),
    };
    ESP_ERROR_CHECK(nvs_flash_init());
}

```

```
ESP_ERROR_CHECK(esp_zb_platform_config(&config));
switch_driver_init(button_func_pair, PAIR_SIZE(button_func_pair),
esp_zb_buttons_handler);
xTaskCreate(esp_zb_task, "Zigbee_main", 4096, NULL, 5, NULL);
}
```